WETTABILITY ALTERATION OF CARBONATE ROCKS TO ALLEVIATE CONDENSATE BLOCKAGE AROUND GAS-CONDENSATE WELLS

By

Jalal Fahimpour

BSc., MSc.

Submitted for the degree of **Doctor of Philosophy** in

Petroleum Engineering

Heriot-Watt University
School of Energy, Geoscience, Infrastructure and Society
Institute of Petroleum Engineering
Edinburgh, UK

March 2015

ABSTRACT

Over the recent decades, gas-condensate reservoirs have attracted increasing attention from many energy suppliers around the globe. The production and improved recovery techniques to extract more hydrocarbons from these reservoirs are still a demanding and challenging subject. Two unique and complex effects that prevail in gas/condensate flow behaviour near the wellbore are: i) negative inertia, decrease in relative permeability with increasing velocity and ii) positive coupling, increase in relative permeability with increasing velocity/decreasing IFT.

When pressure near the wellbore falls below the dew-point the wetting condensate that drops out can block the gas flow paths. The water blockage can also cause severe productivity losses. In the last decade, wettability alteration of the reservoir rocks from liquid- to intermediate-gas wet conditions, using appropriate liquid-repellent chemicals, has been proposed as a new solution to mitigate the liquid hold-up around the wellbore on a relatively permanent basis compared to other common remedial techniques, e.g. solvent injection and hydraulic fracturing stimulation. Despite relatively considerable number of investigations in the literature dedicated to application of such chemical treatments in gas-condensate systems, there are still serious and important questions about the reliability of the results. That is, in all these investigations, conventional gas/oil fluids and/or procedures and conditions not representative of gas condensate reservoirs have been employed.

The research work presented in this thesis is devoted to providing a better understanding of the application of such chemical treatments in gas-condensate systems and address the crucial limitations and benefits associated with this stimulation technique. The investigations performed are also aimed at finding appropriate wettability modifiers for carbonate rocks, which compared to sandstones, have received less attention. The current research study can be divided into three main parts.

In the first part, results of initial screening tests performed to identify an optimized treatment solution for carbonate minerals are discussed. The conventional fluid systems

such as decane-nitrogen are employed for this purpose. Initially, the static contact angle data are used to examine the performance of fifteen fluorinated chemicals, out of which four liquid-repellent agents have been short listed. The brine compatibility, spontaneous imbibition and unsteady-state displacements tests are then employed to investigate the impact of a number of important parameters including: chemical concentration, chemical particle size, solvent type, temperature, rock permeability and brine salinity. The final treatment solution developed in this part, i.e an anionic fluorosurfactant carried with methanol, is further evaluated to understand its impact on improving the fluids mobility as well as its durability.

In the second part of this thesis, the performance of the optimized wettability modifier developed in the first part, is evaluated in presence of gas-condensate fluids. For this purpose, initially high pressure (and in few cases high temperature) contact angle measurements using synthetic binary- and multi-component gas-condensate mixtures are conducted. These tests, for the first time, reveal that the wetting characteristic of the treated carbonate surface is significantly dependent on the interfacial tension and molecular composition of the system. That is, by increasing the interfacial tension and/or number of carbon atoms in the system the contact angle increases. The generality of these new findings are further confirmed by performing a number of unsteady-state displacement tests. The ultimate effect of the wettability alteration is finally quantified by measuring series of steady-state relative permeability data points under various IFT and velocity conditions. The new findings demonstrate that chemical treatment performance is significantly affected by the thermodynamic and flow conditions of the gas-condensate system.

In the final part of this work, a simulation exercise is carried out to complement the experimental results and provide better practical understanding of application of this chemical treatment technique. Here, a number of single-parameter simulations are initially performed, which in particular look into the favourable performance of chemical treatment versus solvent injection, water- versus alcohol-based solution and chemical treatment in mature fields with large condensate banks. In the second section of this part, the simultaneous impacts of five important parameters on well productivity are scrutinized employing statistical approaches. The five selected parameters are treatment radius, treatment uniformity, improvement factor of relative permeability, permeability damage and treatment durability. Accordingly, a Matlab-based computer programme is developed to facilitate the simulation of 1080 multi-parameter simulations using a full-factorial experimental design. The relationship between the

parameters and their impact on treatment performance are then analysed using the fitted linear response surface models. It is demonstrated that the kr improvement factor has the largest positive impact on CT performance. On the other hand, permeability damage (PD) is the only negative parameter with a significant adverse impact on the CT performance. In summary, the new findings from the study provide valuable insights into the practical application of chemical treatment and offer useful guidelines on designing more effective wettability modifiers.

DEDICATION

To my wonderful wife, *Saeideh*,
whose endless love keeps me alive

&

To my beautiful daughter, *Tarannom*,
whose sweet smile brightens up my life

ACKNOWLEDGEMENTS

I would like to first express my special appreciation and thanks to my principal supervisor, Professor Mahmoud Jamiolahmady, his tremendous guidance and unconditional support were constantly with me during this study. I have really enjoyed working with him and benefited greatly from his thoughtful and intelligent supervision. His genuine commitment and enthusiasm to do research and work have always been inspiring to me. I would also like to extend my sincere thanks to my co-supervisor, Professor Mehran Sohrabi, for his valuable guidance and patience throughout this research work.

I am also extremely thankful to Shaun Ireland, Kamran Ahmed, Pantelis Tsolis, Adam Sisson, Colin Flockhart, Jack Irvine and Jim Allison, who kindly provided the technical help and support in the laboratory with the experimental setups.

I wish to thank Dr. Romain Severac from DuPont, for generously supplying the chemical products and giving constructive guidance and help during this research project. His contribution has been instrumental in development of the successful chemical treatment achieved in this work.

I would also like to specially acknowledge the financial support of the Iranian Ministry of Science, Research and Technology and also Heriot-Watt University from my study at IPE.

Many thanks to my thesis examiners Prof. Eric Mackay and Prof. Christopher Brown, I was very much benefited by their valuable suggestions and constructive corrections to my work, which tremendously helped me to improve in various aspects.

Furthermore, I would like to express my deepest appreciation to all friends and colleagues at IPE who provided me the possibility to enjoy my time in Edinburgh and complete this work. My special thanks go to Alireza Emadi, Mobeen Fatemi, John Mills, Amir Farzaneh, Lili Xue, Fuyong Wang, Rasoul Nazari, Heron Gachuz and Shinsuke Ohshita for their support and being good company.

Finally, my sincerest gratitude goes to my loving wife, Saeideh Sabahati, who is always standing by me with all her heart and mind. Undoubtedly, without her endless support, encouragement and patience this work would not have come to fruition.

LIST OF PUBLICATIONS

Conference Papers

- Fahimpour, J., Jamiolahmady, M., (2014). "*Practical Guidelines on Application of Chemical Treatment in Gas-Condensate Reservoirs: Impact of Gas-Condensate Composition and Interfacial Tension".* DEVEX European Production and Development Conference, Aberdeen, 7-8 May 2014.

- Fahimpour, J., Jamiolahmady, M., Sohrabi, M., Mills, J., (2013). "*Dependency of Wettability Alteration on Hydrocarbon Composition and Interfacial Tension in Gas/Condensate Systems".* SPE 164802, EAGE Annual Conference & Exhibition incorporating SPE Europec, London, UK, 10–13 June 2013.

- Fahimpour, J., Jamiolahmady, M., Sohrabi, M., (2012). "*A Combined Experimental and Theoretical Investigation on Application of Wettability Modifiers in Gas-Condensate Reservoirs".* SPE 159807, SPE Annual Technical Conference and Exhibition, San Antonio, Texas, USA, 8-10 October 2012.

- Fahimpour, J., Jamiolahmady, M., Severac, R., Sohrabi, M., (2012). "*Performance of Fluorochemicals on Wettability Alteration of Carbonate Rocks to Alleviate Condensate/Water Banking*". International Symposium of the Society of Core Analysts (SCA), Aberdeen, UK, 27-30 August, 2012.

- Fahimpour, J., Jamiolahmady, M., Severac, R., Sohrabi, M., (2012). "*Optimization of Fluorinated Wettability Modifiers for Gas-Condensate Carbonate Reservoirs*". SPE 154522, EAGE Annual Conference & Exhibition incorporating SPE Europec, Copenhagen, Denmark, 4–7 June 2012.

Journal Papers

- Fahimpour, J., Jamiolahmady, M., Nazari-Moghaddam, R.,. (2015). "*An Improved Understanding of Performance of Wettability Alteration for Condensate Banking Removal under Steady-State Flow Conditions*". SPE Journal, Submitted.

- Fahimpour, J., Jamiolahmady, M.,. (2015). "*Optimization of Fluorinated Wettability Modifiers for Gas-Condensate Carbonate Reservoirs".* SPE Journal, SPE-154522-PA.

- Fahimpour, J., Jamiolahmady, M.,. (2014). "*Impact of Gas-Condensate Composition and Interfacial Tension on Oil-repellency Strength of Wettability Modifiers".* Energy and Fuels, 2014, 28 (11), 6714–6722.

TABLE OF CONTENTS

LIST OF FIGURES

LIST OF TABLES

LIST OF SYMBOLS

Nomenclature

A	core cross section area
D	diameter of the core sample
f_g	gas fractional flow
k	absolute permeability
k_r	relative permeability
k_{rb}	base relative permeability
k_{rc}	condensate relative permeability
k_{rg}	gas relative permeability
k_{rm}	miscible relative permeability
L	length of the core sample
M	molecular weight
Nc	capillary number
P	pressure
Q_c	condensate volumetric flow rate
Q_g	gas volumetric flow rate
R	gas constant
Re	Reynolds number
S	spreading coefficient
Sg	gas saturation
S_{wi}	initial water saturation
T	temperature
v_{ag}	actual pore velocity of gas
W	mass flow rate
Z	gas compressibility factor

Greek Letters

ϕ	porosity
σ	interfacial tension
ρ	density

θ	contact angle
β_g	two-phase gas beta-factor
β_d	single-phase (dry) beta-factor
β	inertial factor (non-Darcy or Forchheimer coefficient)
v	Darcy velocity
μ	viscosity
∇P	pressure gradient

Abbreviations

BD	Baker-Dolomite carbonate rock
C-61	Capstone FS-61 anionic fluorosurfactant
CCE	constant composition expansion,
CGR	condensate to gas flow rate ratio
CS	chemical solution
CT	chemical treatment
CVD	constant volume depletion
DIW	deionised water
DP	differential pressure
DSA	drop shape analysis setup
EtOH	ethanol
GOR	gas-to-liquid ratio
GPG	gas production gain
HPHT	high pressure-high temperature
HSB	high-salinity brine
IFT	interfacial tension
ILRSM	linear response surface model with interaction terms
IPA	isopropyl alcohol
kr-IF	relative permeability improvement factor
LRSM	linear response surface model without interaction terms
LSB	low-salinity brine
MeOH	methanol
PD	permeability damage
PV	pore volume
SI	solvent injection
SS-kr	steady-state relative permeability

STB	stock tank barrel
TC	Texas-Cream carbonate rock
TR	treatment radius
USS	unsteady-state
Z-610	Zonyl FS-610 anionic fluorosurfactant

1 INTRODUCTION

1.1 INTRODUCTION

During the recent decades, underground gas as well as conventional oil deposits have been the focus of attention to respond to global demand for more energy resources on a more sustainable and eco-friendly basis (Wang and Economides 2009). Gas, compared to oil, reservoirs are usually found in deep formations at such high pressures and temperatures that the new technological advances have made them easier to extract. The light liquid condensates associated with the wet and retrograde gases are also very lucrative for refinery purposes, compared to crude oils, as they can easily be turned into high-value finished products.

Retrograde condensation, i.e. liquid drop-out from the gaseous phase soon after the bottom-hole pressure drops below the dew-point, is a unique characteristic of gas-condensate reservoirs, distinguishing them from other types of gas reserves (Danesh 1998). The coexistence of gas and condensate within the individual pores moving together at low interfacial tensions (IFT) and high velocities complicates the dynamic flow behaviours of the existing phases in the vicinity of the wellbore (Asar and Handy 1988, Danesh et al. 1994, Jamiolahmady et al. 2000, Jamiolahmady et al. 2003). Contrary to the observed reductions in gas effective permeability at high flowing velocities due to non-Darcy or inertial effects, the increase in the gas and condensate relative permeabilities with increasing velocity (known as positive coupling effect) has also been reported for these low-IFT condensing systems (Danesh et al. 1994, Blom et al. 1997). As a well-established fact, the competition between the capillary and viscous forces (correlated through the definition of the capillary number, $Nc=v\mu/\sigma$) plays an important part in fluid interactions and their resulting mobilities in such systems (Henderson et al. 1997, Jamiolahmady et al. 2009). The sophisticated but strictly speaking demanding steady-state displacement techniques are essentially required to

capture such unique features pertaining to gas-condensate fluids (Henderson et al. 2000).

1.2 PROBLEM STATEMENT

As the production from a gas-condensate well continues, when the pressure drops below the dew-point, the condensate phase continues to drop out of the gas phase in the reservoir. The low mobility of the condensate due to its strong tendency to wet the rock surface, compared to gas, holds up the condensate within the pores and hence restricts the gas from flowing freely. Such condensate build-up, reported even for lean gases with a maximum liquid dropout of about 2% (Afidick et al. 1994), can severely decline the production and even kill the well. Beside condensate, the water from the aquifer or drilling fluids can also aggravate the issue of near-wellbore liquid-blockage in gas-condensate reservoirs. The main preventive or remedial techniques commonly deployed in the industry to cope with such liquid, especially condensate, blocking issues are: solvent or alcohol stimulation, horizontal well drilling, hydraulic fracturing and dry-gas recycling (e.g. Jones et al. 1998, Dehane and Tiab 2000, Al-Anazi et al. 2005). These methods, despite their positive potentials to mitigate the liquid blockages and improve the well productivity, are not always economical and furthermore their performances are not long-lasting as the re-deposition of the condensate is inevitable in many of these cases.

For the last several years, wettability alteration using chemical treatment (CT) technique has been proposed as a standalone or a hand-in-hand solution to the aforementioned techniques to tackle the liquid-blockage problems in gas-condensate systems with relatively permanent benefits (Li and Firoozabadi 2000, Kumar et al. 2006). This method involves delivering oil- and water-repellent agents to the region around the wellbore using a carrier solvent, altering the formation wetting state from preferential liquid- to intermediate gas-wet conditions. The adsorption of the surface active chemicals on the rock substrate, reduces the surface energy of the minerals, hence renders them liquid-repellent. As a result, the capillary forces are diminished and less liquid is held in the pores and the fluids mobilities are improved.

There are a large number of experimental investigations in the literature dedicated to such chemical treatments, all of which suffer from lack of an in-depth and thorough understanding of the essential issues regarding the application of this method in gas-condensate systems. Many of these studies have only been limited to using conventional fluids rather than more complex gas-condensate fluid samples (e.g. Al-Anazi et al.

2007, Fahes and Firoozabadi 2007). Moreover, the few cases, which have employed the gas-condensate fluids, do not follow the correct procedures that capture the real flow behaviours of condensing systems (e.g. Bang et al. 2010). Such shortcomings are discussed in more details in Chapters 5 and 6 of this thesis.

1.3 THESIS OUTLINE

In a systematic approach, the work presented in this thesis concentrates on the wettability alteration of reservoir rocks for gas-condensate fluids. The investigations are specifically focused on the performance of wettability modifiers with respect to the condensate-banking removal, however their application for the water blockage issues is also to some extend addressed throughout this work. The corresponding studies mainly aimed to find appropriate wettability modifiers for carbonate minerals, which compared to sandstone rock types, have received less attention. Here, it should be mentioned that the "carbonate" terminology, which is regularly used throughout this thesis, is only reflecting the mineralogy and composition of the rock samples that have been used in this work, whereas the nature of the fracture networks existing in the carbonate reservoirs are not considered. In other words, the limestone and dolomite carbonate outcrops that have been used in this study have almost homogenous porosity and permeability distributions without any distinct behaviour representative of heterogeneous fractured rocks.

At the beginning of this work, initially a number of static (i.e. contact angle, brine stability) and dynamic (i.e. spontaneous imbibition, unsteady-state displacement) experiments using conventional fluids, which are much simpler and more straightforward compared to tests dealing with the complex condensing fluids, were performed. The performance of the final optimized treatment solution was then evaluated for the gas-condensate fluid samples conducting series of contact angle, unsteady state and steady-state flow tests using more sophisticated set-up and procedures. The experimental results were further complemented with a comprehensive simulation exercise exploring the impact of several parameters on the treatment performance. The results from this study will shed light on the positive and negative aspects of application of the chemical treatment for field trials. It will be shown that from the standpoint of the complex thermodynamic behaviour of gas-condensate systems, the wettability alteration, contrary to the understandings of some sectors of the industry, can not always be considered as an effective method to alleviate the condensate blockage issues.

The main body of this thesis is structured based on the following chapters.

Chapter 2 starts with a short introduction to the importance and role of gas-condensate resources in the world's energy supply. In the first part of this chapter, the main thermodynamic properties of such fluid systems are described. The unique flow characteristics of condensing fluids, known as positive coupling and negative inertia, associated with the IFT and velocity effects are then discussed and the available experimental methods and empirical correlations to capture and model these effects are explained. The second part of this chapter concentrates on the condensate/water blockage issues impairing the productivity of many gas-condensate wells. The commonly used solutions to deal with such problems, e.g. solvent injection and hydraulic-fracturing stimulation, are discussed. Then the basic concept of the chemical treatment technique is introduced followed by a comprehensive literature review on all previous investigations carried out on this subject. Finally the main shortcomings of the previous studies and the principal reasons behind the current work are discussed.

In Chapter 3 first, the main experimental facilities and their essential components used over the course of experiments conducted in this study, are described. The main instruments deployed here are the High-Pressure High-Temperature (HPHT) drop shape analysis setup (DSA), chemical treatment oven, free imbibition setup and unsteady-state and steady-state core flood rigs. In the second part of this chapter, the general standard procedures used in this work to prepare the rock and fluid samples, set up various elements of the tests and carry out the corresponding experiments are extensively explained.

Chapter 4 presents the results of the investigations performed, using conventional screening tests, in order to optimize an appropriate treatment solution. The overall performances of fifteen fluorinated repellent agents with different ionic functionalities used in this work are initially discussed. It is shown that the anionic and to lesser extent non-ionic chemicals are the most effective wettability modifiers for the carbonate minerals. The results of the contact angle measurements, free imbibition and unsteady-state displacement tests, all carried out using conventional fluid systems, are then discussed for four selected fluorochemicals. The impact of the chemical's active ingredient in the solution, type of solvent, temperature, chemical's delivery method and brine impurities on the wettability alteration process are comprehensively investigated. It will also be shown that whilst the existence of the chemical's large aggregates can impair the rock permeability, adjusting the polarity of the solution by adding alcohols and/or filtration of the chemical's large particles before displacing through the core can

remediate this problem. The last part of this chapter is dedicated to the overall performance of the final optimized treatment solution obtained in this work, i.e. 2 wt% anionic fluorosurfactant (C-61) diluted in methanol. The effectiveness of the treatment in presence of low- and high-salinity brines and its durability against the gas flow are discussed. A new method of combining the anionic with non-ionic chemicals is then proposed serving to enhance the stability of the anionic part in the brine. This chapter ends with an evaluation of the water-repellency strength of the treated surface versus various brine compositions through measuring some contact angle data.

Chapter 5 is dedicated to the contact angle measurements conducted in this work using various mixtures of synthetic gas-condensate fluids. To the best of the author's knowledge this is the first time that such measurements have been carried out. The fluid properties of the binary- and multi-component mixtures employed for these tests are first described. The results of the measured contact angles using binary-mixtures of C1-nC10, C1-nC6 and C1-nC4 at various pressures (or interfacial tensions) and at ambient temperature are then presented. In addition, limited contact angle data using C1-nC10 at 50 and 100°C are also discussed demonstrating the minimal impact of temperature on the measured contact angle data. Through these measurements, it will be demonstrated that the interfacial tension and molecular composition of the gas-condensate mixture have crucial impacts on the wetting tendency of the liquid condensate on the treated carbonate substrate. The second part of this chapter presents the results of the measured contact angles using multi-component mixtures of C1-nC5-nC8-nC10 (and –nC15) at low- and high-IFT limits of 1 and 10 mN/m. It will be demonstrated that similar to binary-mixtures, the presence of the heavy-end components in the fluid composition (e.g. nC15) strongly favours preserving the oil-wetting characteristic of the treated surface. This chapter concludes with series of unsteady-state flow tests performed using different binary gas-condensate mixtures at 20 and 100°C, results of which are shown to be in close agreement with those observed during the contact angle measurements.

Chapter 6 presents the results of series of sophisticated steady-state relative permeability (k_r) measurements carried out in this work on a Baker-Dolomite carbonate core sample before and after the proposed wettability alteration process. The main grounds for selection of the gas-condensate mixture, i.e. C1-nC10, and the corresponding thermodynamic and flow conditions of the tests are discussed in this chapter. The core treatment procedure and the required steps followed to measure each steady-state data point are also explained. The results of a number of unsteady-state tests are then discussed, which were aimed to confirm the effectiveness of the

wettability alteration process. The rest of this chapter focuses on the interpretation of the steady-state experiments, two of which conducted at the high IFTs of 10.8 and 2.7 mN/m and one at the low IFT of 0.77 mN/m under single- and multiple-velocity conditions, respectively. The results, consistent with the contact angle measurements and unsteady-state displacement tests presented in Chapter 5, show that the improvement of the relative permeabilities owing to the rock altered wettability diminishes as IFT decreases.

Chapter 7 of this thesis includes the results of a comprehensive simulation exercise on the application of chemical treatment in gas-condensate reservoirs. The general description of the synthetic reservoir model including well, rock and fluid properties are initially explained. The approach followed to analyse the results is then discussed. The first part of this simulation exercise, evaluates the impact of a number of parameters pertinent to the application of chemical stimulation individually. The topics covered are: the performance of the alcohol-based versus water-based solutions, the benefits of the chemical treatment over solvent (alcohol) stimulation and the feasibility of using chemical treatment in mature gas fields. The effect of three single parameters including k_r improvement factor, treatment durability and permeability damage are also investigated. The second part of this exercise presents the results of a statistical approach adopted to understand the simultaneous impact of five important parameters on the treatment performance. These parameters are treatment radius, treatment uniformity, improvement factor of relative permeabilities, permeability damage and treatment durability. A wide range of variation of these parameters is considered. A full-factorial experimental design is then employed to sample total of 1080 simulation cases. The simulations are conducted using a developed Matlab-based computer program that automatically reads input data file, links different stages of simulations, carried out using the Eclipse 100 Black-oil simulator, and stores output data. The linear response surface models with and without interaction terms are finally fitted to the simulation outputs, to express the relationship between the parameters and their level of importance on the chemical treatment performance.

Chapter 8 summarizes the main conclusions drawn from this research study. The implications of the new important findings from this work for practical field applications are also discussed. The chapter is concluded with some recommendations for future work in this area.

1.4 REFERENCES

1. Afidick, D., N. J. Kaczorowski and S. Bette (1994). Production Performance of a Retrograde Gas Reservoir: A Case Study of the Arun Field. SPE 28749, SPE Asia Pacific Oil and Gas Conference, 7-10 November, Melbourne, Australia.

2. Al-Anazi, H. A., J. G. Walker, G. A. Pope, M. M. Sharma and D. F. Hackney (2005). "A Successful Methanol Treatment in a Gas/condensate Reservoir: Field Application." SPE Production & Facilities 20(1): 60 - 69.

3. Al-Anazi, H. A., J. Xiao, A. A. Al-Eidan, I. M. Buhidma, M. S. Ahmed, M. Al-Faifi and W. J. Assiri (2007). Gas Productivity Enhancement by Wettability Alteration of Gas-Condensate Reservoirs. SPE-107493-MS, European Formation Damage Conference, 30 May-1 June, Scheveningen, The Netherlands.

4. Asar, H. and L. L. Handy (1988). "Influence of Interfacial Tension on Gas/Oil Relative Permeability in a Gas-Condensate System." SPE Reservoir Engineering 3(01): 257-264.

5. Bang, V., G. A. Pope, M. M. Sharma, J. R. J. Baran and Ahmadi (2010). "A New Solution To Restore Productivity of Gas Wells With Condensate and Water Blocks." SPE Reservoir Evaluation & Engineering 13 (2): 323-331.

6. Blom, S. M. P., J. Hagoort and D. P. N. Soetekouw (1997). Relative Permeability at Near-Critical Conditions. SPE Annual Technical Conference and Exhibition, 5-8 October, San Antonio, Texas, Society of Petroleum Engineers.

7. Danesh, A. (1998). "PVT and Phase Behaviour of Petroleum Reservoir Fluids." Elsevier Science and Technology Books.

8. Danesh, A., M. Kahazam, G. D. Henderson, D. H. Tehrani and J. M. Peden (1994). Gas Condensate Recovery Studies. DTI Improved Oil Recovery and Research Dissemination Seminar, London.

9. Dehane, A. and D. Tiab (2000). Performance of Horizontal Wells in Gas Condensate Reservoirs, Djebel Bissa Field, Algeria. SPE/AAPG Western Regional Meeting, 19-22 June, Long Beach, California.

10. Fahes, M. M. and A. Firoozabadi (2007). "Wettability Alteration to Intermediate Gas-Wetting in Gas-Condensate Reservoirs at High Temperatures." SPE Journal 12(4): pp. 397-407.

11. Henderson, G. D., A. Danesh, B. Al-kharusi and D. Tehrani (2000). "Generating reliable gas condensate relative permeability data used to develop a correlation with capillary number." Journal of Petroleum Science and Engineering 25(1–2): 13.

12. Henderson, G. D., A. Danesh, D. H. Tehrani and J. M. Peden (1997). "The effect of velocity and interfacial tension on relative permeability of gas condensate fluids in the wellbore region." Journal of Petroleum Science and Engineering 17(3–4): 265-273.

13. Jamiolahmady, M., A. Danesh, D. H. Tehrani and D. B. Duncan (2000). "A Mechanistic Model of Gas-Condensate Flow in Pores." Transport in Porous Media 41(1): 17-46.

14. Jamiolahmady, M., A. Danesh, D. H. Tehrani and D. B. Duncan (2003). "Positive Effect of Flow Velocity on Gas–Condensate Relative Permeability: Network Modelling and Comparison with Experimental Results." Transport in Porous Media 52(2): 159-183.

15. Jamiolahmady, M., M. Sohrabi, S. Ireland and P. Ghahri (2009). "A generalized correlation for predicting gas–condensate relative permeability at near wellbore conditions." Journal of Petroleum Science and Engineering 66(3–4): 98-110.

16. Jones, A. T., M. S. Al Salhi, S. M. Al Shidl, M. England and R. Pongratz (1998). Multiple Hydraulic Fracturing of Deep Gas-Condensate Wells in Oman. SPE-49100-MS, SPE Annual Technical Conference and Exhibition, 27-30 September, New Orleans, Louisiana, Society of Petroleum Engineers.

17. Kumar, V., G. A. Pope and M. M. Sharma (2006). Improving the Gas and Condensate Relative Permeability Using Chemical Treatments. SPE-100529-MS, SPE Gas Technology Symposium, 15-17 May, Calgary, Alberta, Canada.

18. Li, K. and A. Firoozabadi (2000). "Experimental Study of Wettability Alteration to Preferential Gas-Wetting in Porous Media and Its Effects." SPE Reservoir Evaluation & Engineering 3(2): 139 - 149.

19. Wang, X. and M. Economides (2009). Advanced Natural Gas Engineering, Gulf Publishing Company, Houston, Texas.

2 GAS-CONDENSATE RESERVOIRS

2.1 INTRODUCTION

Depletion of conventional oil reservoirs over the last century and increasing global demand for more energy resources have turned the attention of many energy suppliers to gas reservoirs over the recent decades. Gas, compared to oil and coal, burns cleaner, more efficiently and with less potentially harmful by-products for the environment (Wang and Economides 2009). Retrograde condensate, owing to existence of intermediate hydrocarbons in its composition, is also a valuable feed for oil refineries. For these reasons and also because of new advances in drilling and production technologies, making the hard-to-reach formations profitable, there has been a considerable growth in new gas fields exploration, development and production activities. About 23% of the total world energy supply is now provided by natural gas and as **Figure 2.1** depicts this share would certainly increase, playing a key role in the future of expanding the world's energy supply (IEA 2011).

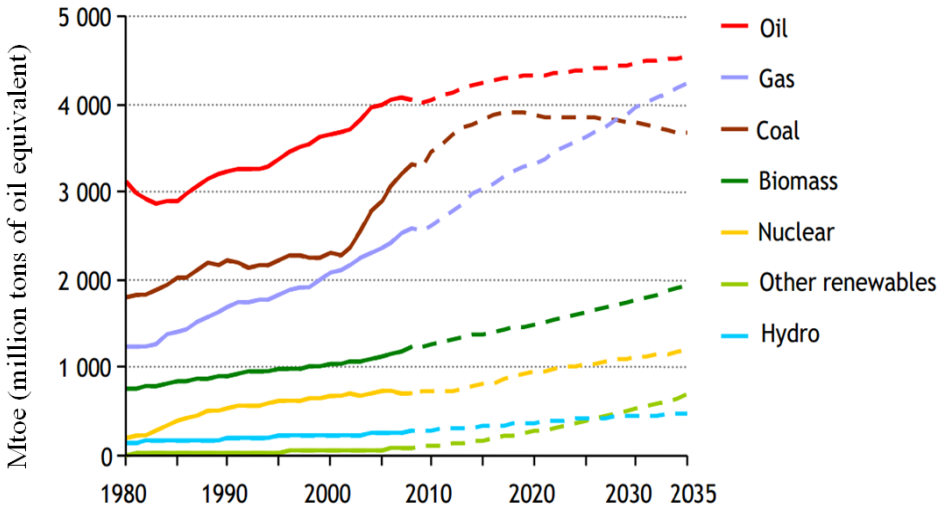

Figure 2.1: World primary energy demand by fuel (Source: IEA, world energy outlook, report 2011).

2.2 GAS-CONDENSATE PHASE BEHAVIOUR AND CHARACTERISTICS

A gas reservoir, depending on its thermodynamic condition and fluid composition, can be classified as dry-gas, wet-gas or gas-condensate. Dry gases are predominantly composed of methane and non-hydrocarbons, e.g. N_2 and CO_2, and remain single phase from reservoir to the surface conditions (point A in **Figure 2.2**). A wet-gas fluid, however, contains other light hydrocarbons in addition to methane, hence, produces some condensate at the surface. The presence of heavier hydrocarbons in gas-condensate fluids causes the retrograde condensation to occur within the reservoir, especially around the wellbore, when the pressure falls below the dew-point (Danesh 1998). Point B in **Figure 2.2** shows a typical gas-condensate fluid with temperature of the reservoir being between the critical point and the cricondentherm.

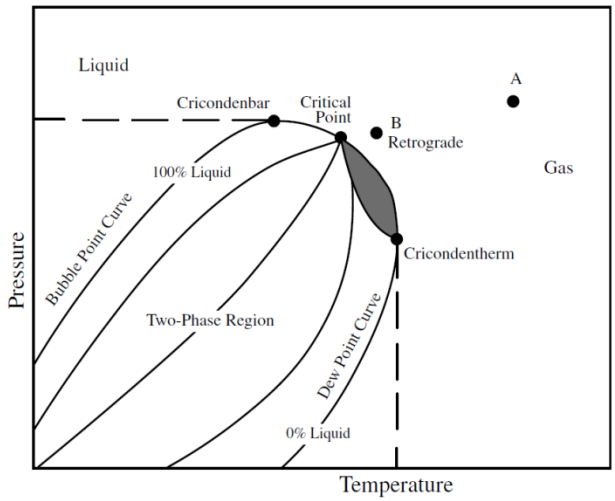

Figure 2.2: Phase diagram of a hydrocarbon reservoir fluid.

A gas-condensate fluid is mainly composed of methane with decreasing amounts of ethane and propane and smaller amounts of butane, pentane, hexane, and heptane and heavier hydrocarbons (Thornton 1946). **Table 2.1** shows the molar composition of both gas and condensate portions of a typical gas-condensate fluid.

From a compositional standpoint, the heptanes plus concentration of a gas-condensate fluid is generally less than 12.5 mole%, as those with higher portions of that are almost always in the liquid phase in the reservoir (Moses 1986). Condensate, compared to crude oil, is light-coloured. It contains a large fraction of volatile petroleum components and its API gravity ranges from 40° to 60°. The gas-to-liquid ratios (GOR) of wells producing gas-condensate usually range between 3000 to 150,000

SCF/STB, whereas for practical purposes a well with GOR of above 50,000 can be treated as a wet gas (Kilgren 1966, Danesh 1998).

Table 2.1: The percentage composition of a typical gas-condensate fluid (Thornton 1946).

	Reservoir Fluid (Mole %)	Gas (Mole %)	Condensate (Mole %)
Methane	87.07	91.32	----
Ethane	4.39	4.43	----
Propane	2.29	2.12	1.41
Butanes	1.74	1.36	5.71
Pentanes	0.83	0.42	8.11
Hexanes	0.6	0.15	10.46
Heptanes and heavier	3.08	0.2	74.31
Total	100	100	100

Complex phase behaviour of gas-condensate fluids necessitates careful attention when sampling and conducting PVT tests. The common separator sampling method, used in oil reservoirs, by collecting the liquid and gas samples at the surface and recombining them, is dubious for gas-condensate wells due to possible risk of loss of liquid content in the reservoir or production tubulars. Downhole sampling techniques can yield representative gas-condensate samples as long as the wellbore flowing pressure is above the dew-point. Over the last decade, the modern formation testers, such as the Modular Formation Dynamics Tester (MDT), have provided an opportunity to acquire more representative in situ fluid samples by pressing a probe into the borehole wall and withdrawing the fluids directly from the formation (Li Fan. 2005).

The two most common tests conducted on a gas-condensate fluid sample at the reservoir temperature are the constant composition expansion, CCE, and the constant volume depletion, CVD tests (Danesh 1998). The CCE test is carried out by incrementally expanding the cell volume to lower fluid pressure while the total composition remains constant. In the CVD test, however, the cell volume returns to its original value at the end of each pressure stage by expelling the excess gas from it at constant pressure. **Figure 2.3** (left picture) shows the percentage of condensate dropout versus pressure corresponding to CVD and CCE tests performed on a gas-condensate fluid sample from the North Sea. The liquid dropout behaviour of a gas-condensate fluid depends strongly on the richness of the gas, i.e. the presence of heavy compounds in the fluid composition (**Figure 2.3**, right picture). The CCE test can be more representative of the fluid behaviour within the condensate ring, where the mixture

composition remains almost constant as the condensate flows with the gas under quasi-steady state conditions. The CVD test, on the other hand, simulates the behaviour of the fluids in the reservoir bulk, where the condensate is minimally dropped out, hence it can be assumed to be immobile (Danesh 1998).

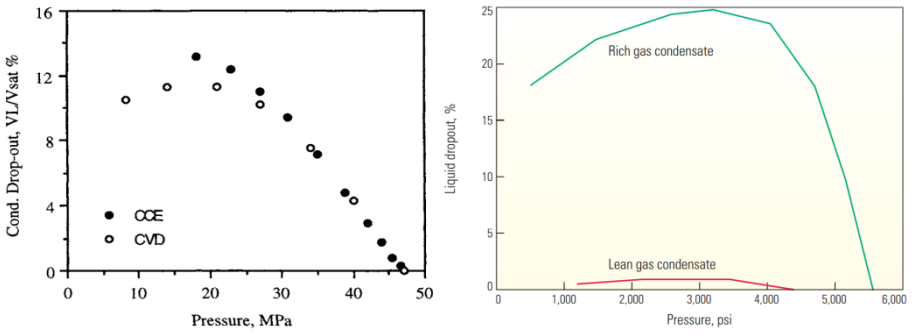

(a) (b)

Figure 2.3: PVT tests used for gas-condensate fluids characterization; (a) liquid drop-out behaviour of the North Sea gas-condensate at 394 K in CCE (constant composition expansion) and CVD (constant volume depletion) tests and (b) The impact of gas richness on condensate drop-out as pressure falls below the dew point.

2.3 IFT AND VELOCITY EFFECTS

The traditional Darcy's equation, expressing a linear relationship between the pressure drop and flow rate, is principally used for estimating the mobility of the fluids in the reservoir bulk, where the velocity is low and capillary forces are more dominant. In the vicinity of the wellbore, however, the deviation from Darcy's law occurs due to high velocities of the fluids, referred to as the inertial effect, especially considered for gases. Forchheimer (1901) was first to propose an appropriate nonlinear relationship for the flow at such conditions:

$$\nabla P = \frac{\mu}{k k_r} v + \beta \rho |v| v \qquad \text{Equation 2.1}$$

where ∇P is the pressure gradient, μ and ρ are the fluid's viscosity and density, respectively, k is the rock absolute permeability, k_r is the fluid relative permeability, v is the Darcy velocity and β is the coefficient of inertial flow resistance, also known as non-Darcy or Forchheimer coefficient.

This equation turns into the familiar Darcy's equation as velocity approaches zero. It is noted that from the perspective of conventional Darcy's flow theory, the effective permeability reduces with increasing velocity when the inertia becomes important.

There have been significant theoretical and experimental investigations on finding appropriate empirical correlations for the β-factor as a function of rock properties (Katz 1962, Geertsma 1974, Narayanaswamy et al. 1998). The Geertsma equation, which benefits from consistent dimensions, for dry cores is:

$$\beta = (4.85 \times 10^4) k^{-0.5} \emptyset^{-5.5} \qquad \text{Equation 2.2}$$

where β is the inertial factor (ft^{-1}), k is the absolute permeability (mD) and ϕ is the porosity (fraction).

The improvement of gas and oil relative permeabilities with decreasing interfacial tension in low IFT systems, such as flow regions adjacent to a gas-condensate well, is a well-established phenomenon (Bardon and Longeron 1980, Asar and Handy 1988, Henderson et al. 1997). In low-IFT condensing fluid systems, contrary to the conventional non-Darcy flow type mentioned above, the increase in relative permeability with velocity, known as positive rate effect, has also been observed. This was first reported by Danesh et al. (1994) and was confirmed by a number of other researchers thereafter (Ali et al. 1997, Blom et al. 1997). This unique behaviour has been attributed to the different distributions and flow of gas and oil phases in conventional and gas-condensate systems. That is, flow in conventional gas-oil systems is based on the channel flow concept, in which the non-wetting gas invades the largest accessible pores whilst the oil flows through the smaller ones. In a condensing system, however, both gas and condensate exist, owing to in-situ condensation process, and flow together in a single pore space (Henderson et al. 1998). The efficient hydraulic continuity of condensate throughout the pores is attributed to the highly conductive layer of condensate film present everywhere. The simultaneous flow of condensate and the gas within individual pores is the next unique characteristic of these low IFT systems. At such conditions, the gas passage is intermittently blocked as the condensate evolves in the pore throats and subsequently reopens when continuous viscous flow of gas breaks the capillary barrier. This mechanism, observed through micromodel experiments (Jamiolahmady et al. 2000) and captured by pore network modelling (Jamiolahmady et al. 2003), has been invoked to account for the positive rate effect at low-IFT condensing systems. The positive velocity dependency, however, diminishes gradually towards high IFT values, as capillary forces become stronger and gas and

condensate flow through the pore spaces separately, which resembles the conventional flow behaviour (Jamiolahmady et al. 2003).

2.4 MEASUREMENT AND MODELING OF RELATIVE PERMEABILITY

It is believed that the two-phase flow of gas and condensate in the vicinity of the wellbore is mainly governed by the interactions between viscous, capillary and inertial forces. As discussed earlier, the relative permeability of condensing fluids improves as velocity increases and/or IFT decreases. This phenomenon, which is more dominant at higher condensate saturations, is known as positive coupling effect. At low condensate saturations, however, the decrease in relative permeability has been reported as velocity is increased (Henderson et al. 2001). This later observation is attributed to the dominant effect of inertia (non-Darcy flow) over positive coupling. Accurate experimental design and procedures are demanded in order to capture these essential flow features, i.e. IFT and velocity effects associated with condensing fluids. Representative k_r models are also needed to be developed for reliable well deliverability calculations.

Use of unsteady-state displacements has been shown to minimize the effect of positive coupling (Henderson et al. 2000). Steady-state (Henderson et al. 1997, Henderson et al. 1998) and pseudosteady-state (Asar and Handy 1988, Mott et al. 2000) tests have been deployed instead, to measure more representative gas and condensate relative permeabilities under the prevalent conditions of the near wellbore region. During the steady-state measurements, the core, initially saturated with gas-condensate mixture above the dew-point, is depleted to the test pressure corresponding to the desired IFT value whereby the condensate phase is primarily distributed in the core by condensation. The equilibrium gas and condensate phases are subsequently injected into the core at a selected CGR (condensate to gas ratio) value until the steady-state conditions (equal CGRs at the core inlet and outlet) are established. The injection rate of both phases is then increased in several steps under the constant selected CGR. The same procedures are also repeated at different CGR values to provide k_r data covering a wide range of condensate saturations. In the pseudosteady-state method the single phase gas mixture, maintained at a pressure above the dew-point, is injected into the core while the core downstream pressure is fixed at a pressure below the dew-point. This method gives one single relative permeability point corresponding to the outlet fractional flow fixed at the outlet pressure.

Figure 2.4 depicts the combined effects of negative inertia and positive coupling on the measured gas (k_{rg}) and condensate (k_{rc}) relative permeabilities of Clashach

sandstone outcrop core sample (L=66 cm, D=5 cm, k=546 mD, ϕ=0.18) under steady-state conditions using binary C1-nC4 fluid mixture at IFT of 0.78 mNm/m (Henderson et al. 2000). There is a significant reduction in k_{rg} (**Figure 2.4a**) at the lowest condensate saturation, i.e. 0%, when velocity increases, due to inertia. As the condensate saturation increases the positive coupling effect becomes active and competes with the negative inertia. As a result, the k_{rg} curves at various velocities converge at condensate saturation of around 30%, after which the positive coupling dominates the flow and gas relative permeability continually increases with velocity. The corresponding measured k_{rc} curves (**Figure 2.4b**) demonstrates the minimal effect of inertia on condensate relative permeability at lower condensate saturations, whilst the positive coupling becomes evident at higher saturations of above approximately 40%.

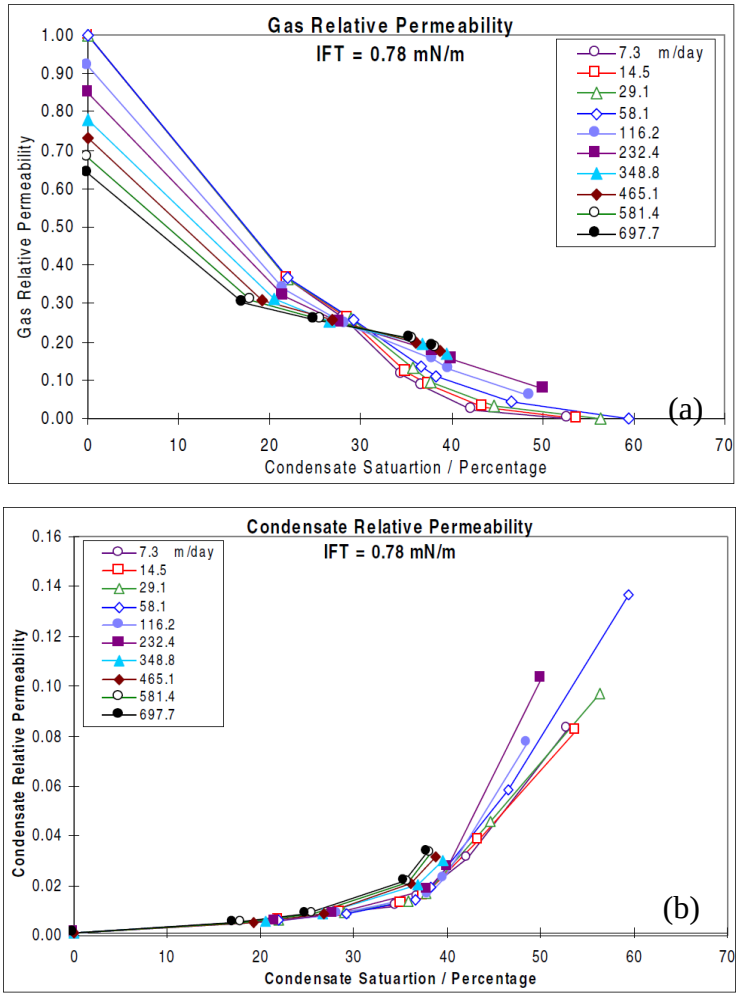

Figure 2.4: Gas (a) and condensate (b) relative permeability curves of Clashach sandstone outcrop core sample (k=546 mD, ϕ=0.18) measured experimentally using steady-state technique, demonstrating the positive coupling and negative inertial effects on k_r data (Henderson et al. 2000).

There are several empirical correlations in the literature developed accounting for the effects of coupling and inertia at near wellbore conditions (Blom and Hagoort 1998, Whitson et al. 1999, Henderson et al. 2000, Jamiolahmady et al. 2009). All these models estimate the effect of coupling and inertia separately through different formulations, which are later incorporated into the general form of **Equation 2.1**. It is a well-established fact that the inertia principally dominates the gas phase mobility, whereas its impact on the condensate flow is minimal (Henderson et al. 2000). The availability of the two-phase inertial-factor correlations for gas in the literature is mostly limited to the gas-water systems or those extended from single-phase data (Frederick and Graves 1994, Narayanaswamy et al. 1998). One of the most commonly used correlations in the commercial reservoir simulators for two-phase gas beta-factor (β_g) has the following form:

$$\beta_{\mathrm{g}} = \beta_d S_{\mathrm{g}}^{c} \left(k_{\mathrm{rg}}\right)^{d} \qquad \text{Equation 2.3}$$

where β_d is the single-phase (dry) beta-factor, Sg is the gas saturation and k_{rg} is gas relative permeability. The exponents in this equation, *c* and *d*, are also the core specific constants determined experimentally.

To model the effect of coupling on k_r data, the most common approach, favoured by many investigators (Coats 1980, Henderson et al. 1996, Whitson et al. 1999), is to interpolate the relative permeability between the immiscible (base) and miscible curves through a correlating function dependent on capillary number (Nc). The general form of the formulation used in many studies is:

$$k_{ri} = f(N_c) k_{rbi} + \left(1 - f(N_c)\right) k_{rmi} \qquad \text{Equation 2.4}$$

where, k_{rb} and k_{rm} are the base and miscible relative permeability curves, respectively, and subscript (*i*) refers to gas or condensate phases.

There are several formulations defined for capillary number, expressing the ratio of viscous to capillary forces, among which the following equations have received more attention:

$$N_c = \frac{v_g \mu_g}{\sigma_{gc}} \qquad \text{Equation 2.5}$$

$$N_c' = \frac{k|\nabla P|}{\sigma \emptyset} \qquad \text{Equation 2.6}$$

In the above formulations σ refers to the interfacial tension between gas and condensate phases.

The base relative permeability (k_{rb}) curve in **Equation 2.4** is measured at low velocity and high IFT conditions whereby it becomes independent of capillary number (Nc) and the effect of coupling diminishes. The miscible curve is assumed to be typical straight lines, end points of which are adjusted according to the residual gas saturation varying with capillary number (e.g. see Henderson et al. 2000).

There are two general approaches that use **Equation 2.4** to obtain k_r data for gas-condensate near-wellbore region. These include: 1- using saturation-based correlations (Blom and Hagoort 1998, Henderson et al. 2000) and 2- treating k_r as a function of relative permeability ratios, e.g. k_{rg}/k_{rc} (Whitson et al. 1999) or $k_{rg}/(k_{rg}+k_{rc})$ (Jamiolahmady et al. 2009). The advantage of the second approach is that it eliminates the need for development of separate formulations for each phase, i.e. k_{rg} and k_{rc} are related to each other through k_r-ratio parameter. The relative permeablity ratio can also be readily obtained from the fluid composition and pressure data under steady-state conditions prevailing at the near wellbore region. That is, using Darcy's law for two-phase flow and after applying some mathematical manipulations the following equation is obtained:

$$\frac{k_{rg}}{k_{rg} + k_{rc}} = \frac{\mu_g f_g}{\mu_g f_g + \mu_c (1 - f_g)} \qquad \text{Equation 2.7}$$

where f_g is the gas fractional flow proportional to the ratio of gas to the total gas plus condensate volumetric flow rates, i.e. $f_g = \frac{Q_g}{Q_g + Q_c}$.

Furthermore, expressing the relative permeability data as a function of k_r-ratio provides more reliable correlation for various rock types, which according to their different characteristics (pore size distribution) could bear different phase saturations at

similar (fractional) flow conditions (Jamiolahmady et al. 2009). Based on this theory, they proposed a generalized correlation using either universal parameters (applicable to all rocks) or those available from routinely measured petrophysical rock properties (i.e. k, ϕ and β_d), which could satisfactorily predict gas and condensate k_r data for a wide range of rock types. Jamiolahmady et al. (2009) have also identified that the base IFT and Nc for a wide range of rock types are 3 mNm^{-1} and 1E−7, respectively.

2.5 CONDENSATE AND WATER BLOCKING

Well productivity of many gas and gas-condensate reservoirs can suffer considerably from reduced gas mobility due to capillary hold-up and accumulation of liquid phases, i.e. condensate and water, around the wellbore. A significant productivity loss of 50% in the Arun field has been attributed to the accumulation of dropped out condensate from a fairly lean gas, with a maximum liquid dropout of 1.1% (Afidick et al. 1994). A sharp decline in the gas production rate from a tight reservoir in the Cal Canal field was also noticed soon after the well bottom-hole pressure fell below the dew point. The presence of liquid hydrocarbon and that of water in the vicinity of wellbore were considered as the main parameters restricting the production from this reservoir to only 10% of original Gas In Place (Engineer 1985). A large number of theoretical and experimental studies have been devoted to understanding, modelling and predicting the condensate accumulation and its associated impaired well productivity (O'Dell et al. 1967, Fussell 1973, Jones and Raghavan 1988), in particular in the presence of capillary number and inertial effects (Henderson et al. 1993, Fevang et al. 1996, Blom and Hagoort 1998, Mott 2002).

Having employed a numerical method, Blom and Hagoort (1998) studied the impact of condensate drop-out on productivity impairment of a gas-condensate well producing under different near wellbore conditions whereby inertial and/or coupling effects were dominant. Their results, obtained for steady-state radial flow, demonstrated that the condensate build-up in gas-condensate systems exaggerates the inertial pressure losses compared to that in dry gas reservoirs. Furthermore, they highlighted that the well impairment due to two-phase flow can be grossly overestimated if the dependence of relative permeability on capillary number (i.e. coupling effect) is ignored. **Figure 2.5,** displaying the well inflow performance at varying flow rates, summarizes the results of their study.

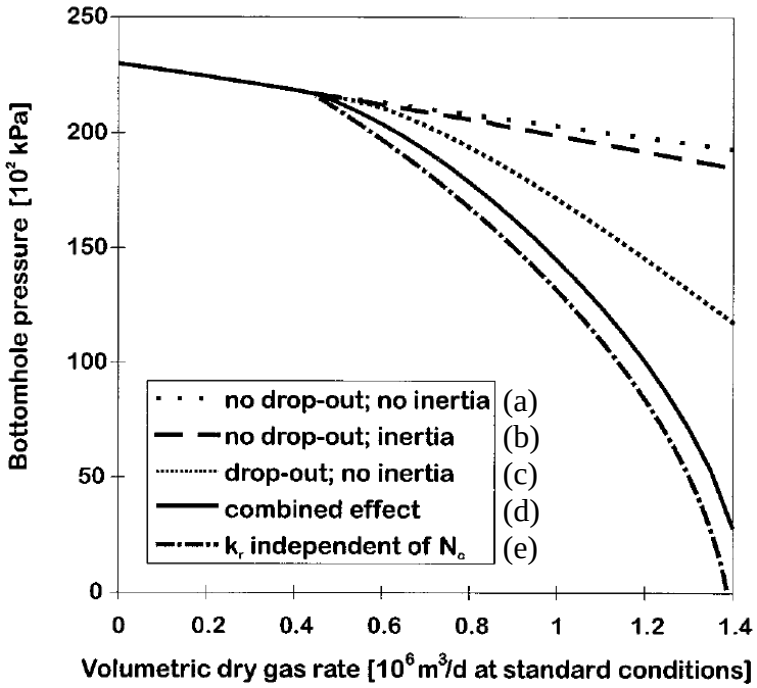

Figure 2.5: Well bottom hole pressure at varying gas flow rates estimated for: a) single-phase (dry gas) flow without inertial effect (Darcy flow), b) single-phase flow with inertial effect (non-Darcy flow), c) two-phase (gas-condensate) flow without inertia and with coupling (Nc-dependent k_r) effect, d) two-phase flow with combined inertia and coupling effects and e) two-phase flow with inertia and without coupling effects, (Blom and Hagoort 1998).

2.6 COMMON TECHNIQUES TO IMPROVE WELL PRODUCTIVITY

Water and especially condensate blocking near the wellbore region, not only reduce the formation capability to produce gas, but also cause a considerable amount of valuable condensate components to be trapped underground. For several decades, there have been a number of improved recovery techniques practiced in the industry to improve the productivity of gas-condensate wells. These methods, aiming at either preventing/delaying the condensate formation or removing/bypassing condensate bank, are briefly explained in the following sections.

2.6.1 Gas Recycling

Strictly speaking, maintaining the reservoir pressure above the dew-point by gas recycling is the most conventional (Foran and Dixon 1939, Sänger et al. 1994) and the most effective scenario (Adel et al. 2006) to extract most of the gas and condensate content of the reservoir. Nonetheless, it is not always an economical solution. Dry-gas

recycling in the Sleipner field in the Norwegian North Sea was implemented with the twofold purposes of minimizing the rate of the reservoir pressure decline and revaporizing the dropped out condensate, which increased the condensate recovery to 81% compared to 56% predicted according to a hypothetical natural depletion scheme, **Figure 2.6** (Eikeland and Hansen 2009). The experimental investigations have also shown the viability of injecting nitrogen, methane (Sanger and Hagoort 1998, Al-Anazi et al. 2004) and propane (Jamaluddin et al. 2001) into the reservoir to vaporize the condensate and restore the effective gas permeability.

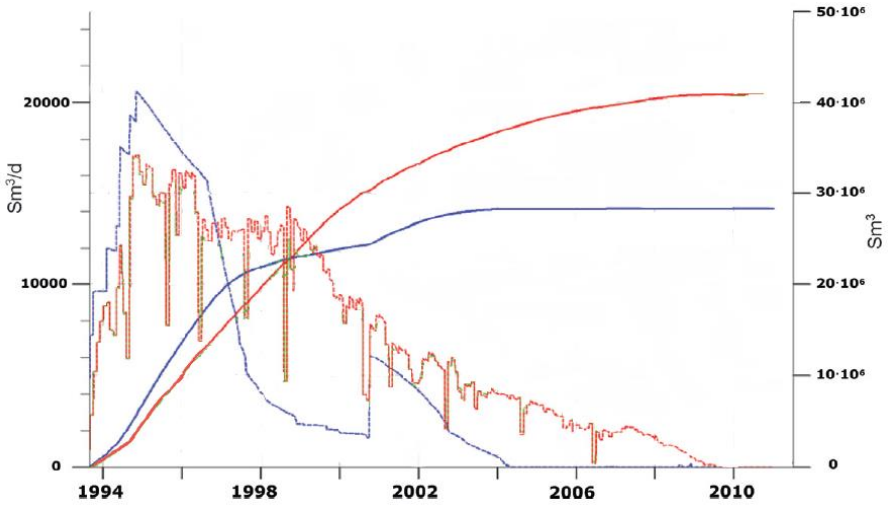

Figure 2.6: Daily and cumulative condensate production from Sleipner field for two cases of actual dry-gas reinjection (red) and hypothetical pure pressure depletion (blue) (Eikeland and Hansen 2009).

2.6.2 Horizontal/Deviated Well Drilling

Penetrating the hydrocarbon formations by drilling horizontal and deviated wells has been widely used to enhance the productivity of many oil and gas reservoirs (Joshi 1991). Reaching larger reservoir contacts in horizontal wells can noticeably minimize the resulting pressure drawdowns, by three to five times, compared to that of the vertical wells for the similar flow rates. This in turn, would delay the condensate deposition in the vicinity of a gas-condensate well, hence leading to higher well deliverability (Marir and Tiab 2006, Jamiolahmady and Danesh 2007). The simulation studies on a history matched model of Djebel Bissa field (Dehane and Tiab 2000) demonstrated that the condensate production of a horizontal well compared to that of a conventional vertical well can be improved by a factor of three (**Figure 2.7**).

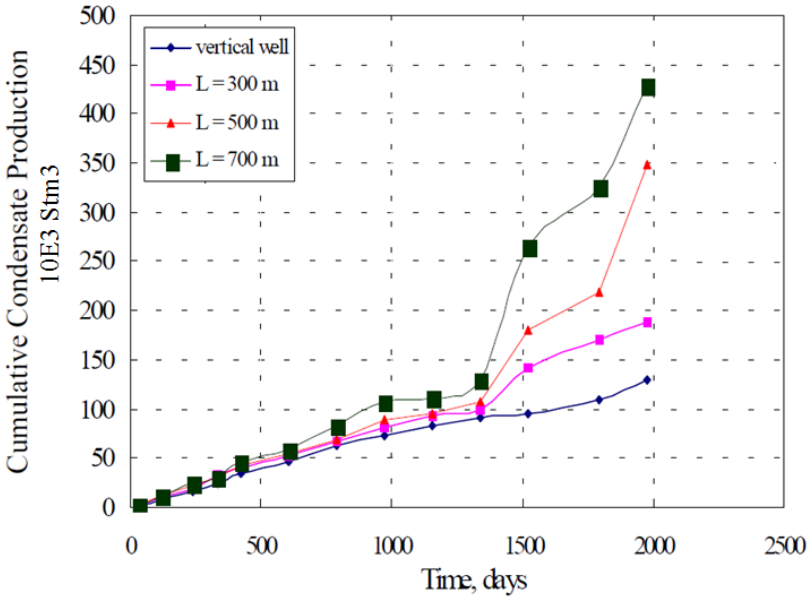

Figure 2.7: Comparison between condensate production in vertical and horizontal wells with varying horizontal well length (Dehane and Tiab 2000).

2.6.3 Hydraulic Fracturing

Producing wells drilled in the low-permeability rocks are principally treated by inducing hydraulic fractures, increasing the connectivity of the wellbore with the formation. This in fact, increases the effective apparent radius of the wellbore and therefore improves its productivity. In gas-condensate wells, however, in addition to this primary advantage, the fracturing stimulation reduces the pressure drawdown and thus less liquid drop-out and blocking occurs (Carlson and Myer 1995, Kroemer et al. 1997, Jones et al. 1998). The performance of the fractured well is primarily governed by the reservoir heterogeneity, fracture length and conductivity (Settari et al. 1996). The single-well model simulations by Hashemi and Gringarten (2005) demonstrated that the productivity of a vertical well producing below the dew point can be increased by 50-80%, dependent on the fracture length, when fracturing treatment was employed (**Figure 2.8**).

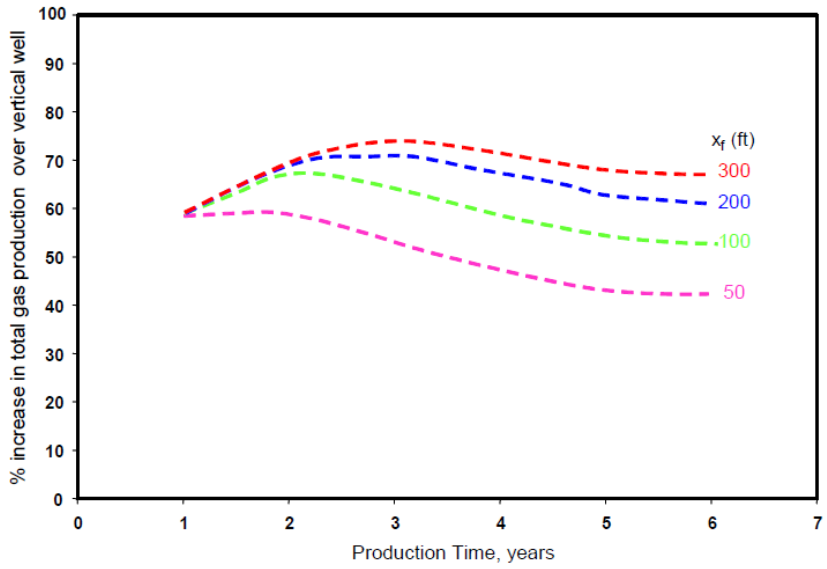

Figure 2.8: Relative increase in cumulative gas production for fractured vertical wells with different fracture half-length (x_f) compared to a vertical well under two-phase conditions (below P_{dew}) (Hashemi and Gringarten 2005).

2.6.4 Solvent Injection

Removal of the condensate and water blocks hold up around the wellbore by injecting appropriate solvents have shown promising results to restore the effective permeability. Pure alcohol and alcohol blends, such as methanol and isopropanol, and other solvents like inhibited diesel or a combination of them aided with the surfactants as IFT modifiers have been employed to stimulate the production from gas condensate wells (Eakin et al. 1965, Du et al. 2000, Garzon et al. 2006). A successful methanol treatment has been reported in the Hatter's Pond field, in which the gas and condensate production was increased by a factor of two over the first four months and 50% thereafter, **Figure 2.9** (Al-Anazi et al. 2005).

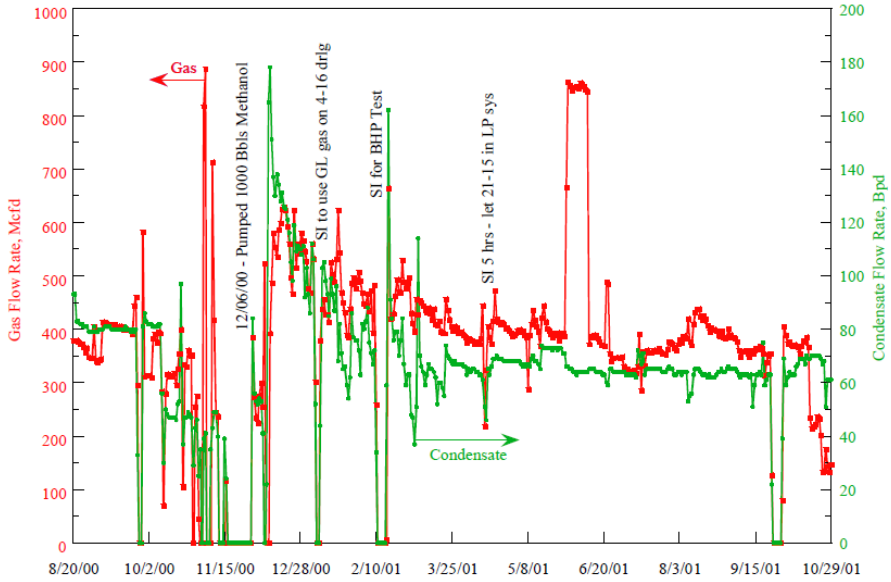

Figure 2.9: Gas and condensate production rates for Hatter's Pond field before and after the methanol injection (Al-Anazi et al. 2005).

2.7 CHEMICAL TREATMENT

The application of all of the above-mentioned methods used to mitigate the liquid blockage issues may or may not be economic on a long-term basis. The gas recycling despite yielding the maximum condensate recovery can be restricted due to economic deficiencies. In horizontal drilling and hydraulic fracturing scenarios, although the condensate deposition is delayed, the condensate bank eventually evolves and restricts the flow soon after the bottom hole pressure reaches the dew-point. In solvent injection the re-deposition of the condensate liquid is also unavoidable after a short time following the initial cleaning up.

Over the past decade, modification of the reservoir rock wettability from liquid- to intermediate gas-wet, associated with an improvement in the liquid and gas mobilities, has attracted the attention of many researchers dealing with the liquid-blockage issues. In this method, a chemical solution carrying liquid-repellent agents is injected into the producing well, invading a few meters around the wellbore. The adsorption of the chemical on the mineral surfaces, rendering it less liquid-wet, is believed to remediate the consequent liquid blockages on a potentially permanent basis, something which differentiates it from other common remedial techniques. The application of this method, known as chemical treatment or wettability alteration, is the main focus of this research study. The following is a summary of the previous research investigations carried out on this subject in the literature.

2.7.1 Literature Review on Chemical Treatment

The early work of Buckley and Leverett (1942) stressed the importance of capillary forces (rigorously associated with the wetting state of the rock) on the fluid displacement in oil-bearing sands during water flooding. Since then, there have been numerous studies dedicated to wettability effects on fluid interactions and displacement mechanisms in the porous media (Wagner and Leach 1959, Anderson 1987, Morrow 1990), many of which dealt with the oil/water/rock systems. Wagner and Leach (1959) studied the improvement of the oil recovery by reversing the wettability of the cores from oil-wet to water-wet through altering the pH or salinity of the displacing water phase. Froning and Leach (1967) presented the results of wettability alteration flooding in Gallup sandstone and Clearfork limestone reservoirs using sulphide and carbonate-phosphate chemical agents, respectively. A delay in the water breakthrough and a reduced water-oil ratio thereafter was observed, resulting in additional oil of about 10% to be recovered. Penny et al. (1983) published results of a technique employed in several fields in the United Sates to increase the flow efficiency of fractured gas wells. Their method involved using a non-wetting agent in the proppant laden fluid, to render both porous matrix and proppant gas-wet. An increase of 50-80% in the load water recoveries (fracturing fluid) compared to the 10-15% for the routine treatments and as a result 2-3 fold higher production rates were reported.

The application of wettability alteration for liquid-blockage issues in gas-condensate systems was first proposed by Li and Firoozabadi (2000), where they changed the wettability of sandstone and chalk substrates (**Figure 2.10**) to neutral-wet, using two fluoropolymers. The experiments that they performed were, however, not representative of gas-condensate fluids as an air-decane system was used. Furthermore, both rock treatments and flow tests were conducted at room temperature, i.e. 20°C. Their work was later extended to higher temperatures up to 90°C by Tang and Firoozabadi (2003), whilst conventional nC10 and nC14 (representative of oil) and distilled water dissolved with 0.2% NaCl (representative of brine) were employed to perform spontaneous imbibition and unsteady-state displacement tests. Fahes and Firoozabadi (2007) discovered the ineffectiveness of the aforementioned two chemicals at 140°C. Accordingly, they employed a chemical solution of fluoroaliphatic silyl ether monomer diluted in an ethanol-water solvent to reach an effective wettability alteration at 140°C on two Berea and reservoir sandstone cores when conventional oil/gas systems were used.

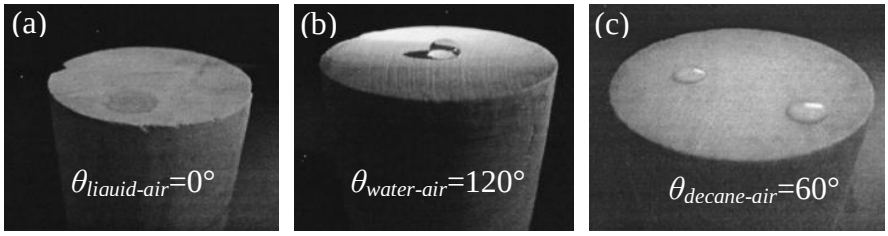

Figure 2.10: Liquid droplets on the surface of the air-saturated chalk before (a) and after (b and c) the wettability alteration (Li and Firoozabadi 2000).

Adibhatla et al. (2006) studied the effect of different surfactant solutions on the wettability of carbonate (calcite and marble) and silica (mica and silica wafer) mineral surfaces at room temperature. They concluded that among the tested fluorosilanes, increasing the number of fluoro groups, promotes the solid substrate towards less water-wet conditions. The addition of field brine to the chemical solution caused the formation of gel and suspensions inside the solution, affecting the chemical adsorption. They also found out that at chemical concentrations well above the CMC (critical micellar concentration) value, the risk of formation of bilayers increases, which adversely affects the chemicals' water-repellency performance.

Al-Anazi et al. (2007) used different fluorosurfactants and silanes to alter the wettability of carbonate and sandstone substrates. Treatment volume, aging time, core permeability and temperature were the factors that affected the treatment performance. They used an ESEM (environmental scanning electron microscope) technique to demonstrate the magnitude of the wettability alteration at the micro pore scale (**Figure 2.11**).

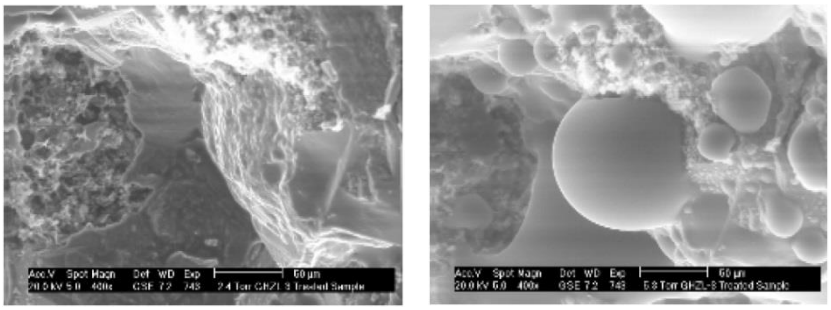

Figure 2.11: Pore scale water-repellency achieved after treating a sandstone core, the ESEM images above illustrate the treated pore minerals before (a) and after (b) water condensation (Al-Anazi et al. 2007).

Panga et al. (2006) investigated the application of a number of surfactants and fluoropolymers delivered by alcohol-brine mixtures into sandstone rocks for prevention of water-blockage in gas wells at high temperatures, e.g. 126°C. Their experimental

results revealed that the possible formation damage due to chemical adsorption, between 10 and 50%, can adversely increase the capillary pressures prompting higher water retention within the pores. In an effective treatment, on the other hand, they showed that injected gas into the treated core can mobilize the resident brine at lower pressure gradients and displace higher volume of it from the core.

Noh and Firoozabadi (2008) investigated the effect of wettability on the high-velocity (inertia) coefficient. Their measurements showed that when the rock wettability was altered from liquid- to intermediate gas-wet conditions, the two-phase inertial factor by liquid saturation increase was reduced by almost one order of magnitude.

Wu and Firoozabadi (2010) studied the effect of initial brine saturation, e.g. NaCl and CaCl2, on wettability alteration of sandstone rocks. They showed that whilst the resident salts can have an adverse effect on the treatment performance, pretreating the rock by displacement of brine with water and then nitrogen can improve the treatment by clearing more adsorption sites for the chemical molecules.

Kumar et al. (2006) reported an effective chemical treatment for outcrop (permeability between 200-500 mD) and reservoir (permeability between 10-70 mD) sandstone cores using a non-ionic surfactant carried by the methanol-water solvent. They employed a pseudo-steady state method to measure the relative permeabilities before and after the treatment using different synthetic gas-condensate mixtures over a temperature range of 145 to 275°F. Their experiments were conducted for capillary numbers in the order of 10^{-6} to 10^{-4} at the gas/oil interfacial tensions of about 4-5 dynes/cm. The k_r improvement factors between 1.5 to 3 were obtained (**Figure 2.12**). Bang et al. (2008) extended this work to make the chemical solution compatible with brine by replacing the solvent with a glycol-alcohol mixture. They also employed this chemical solution for treatment of the sand-filled propped fractures of the sandstone core samples, initially suffering from 90% reduction in gas mobility due to the condensate blockage. The proppant treatments improved the fracture conductivity by a factor of 1.5 to 2.5. Butler et al. (2009) used the aforementioned chemical solution for a field trial to improve the uneconomic productivity of a well located in the Lower Morrow sandstone reservoir in Oklahoma, suffering from the liquid blockage. About a four-fold increase in gas as well as condensate production was reported over the first six months production period after the treatment. Ahmadi et al. (2011) later continued these studies to develop an effective treatment solution for carbonate reservoirs. They used an amine pre-flush to coat the rock surface with a thin layer of multifunctional polymer.

This effectively strengthened the bonding of the chemical to the mineral surface and hence, improved the durability of the treatment.

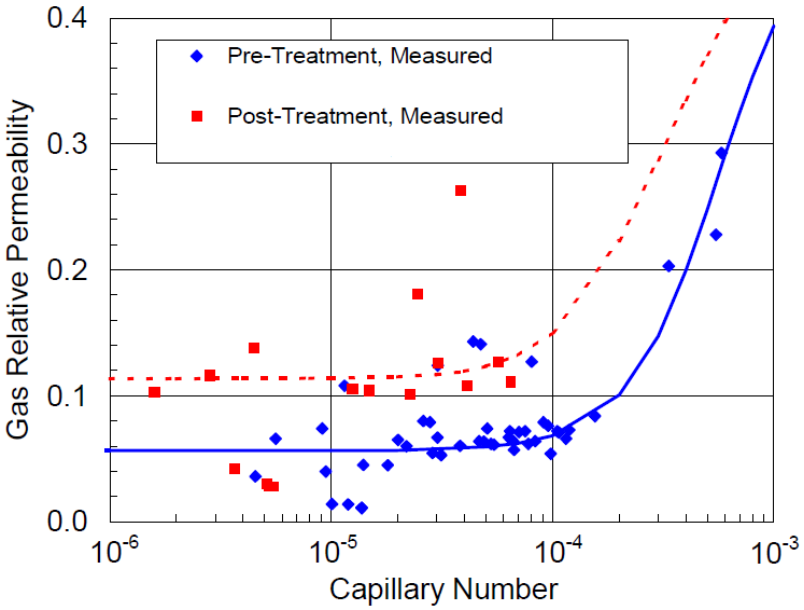

Figure 2.12: Comparison of relative permeability curves before and after wettability alteration using gas condensate fluids in pseudo-steady state measurements (Kumar et al. 2006) .

Zheng and Rao (2011) studied the dynamic behaviour of the condensate drop settled on an oil-wet quartz substrate during the injection of an anionic surfactant carried with brine at HPHT conditions. Their observations demonstrated that the primarily positive spreading coefficient for the oil (e.g. 34) turned into significantly smaller values (e.g. 10) after the surfactant injection, showing the weak oil-wet state of the surface.

Al Ghamdi et al. (2013) reported the results of a field trial of the chemical treatment in one of the Saudi Arabian sandstone gas reservoirs with a severe condensate banking issue. The treatment involved injecting a pre-flush solvent and then 900 barrels of the treatment solution (a non-ionic fluorinated surfactant dissolved in isopropyl alcohol) into the well, which was displaced in the formation using nitrogen. After 12 hours shut-in time, a second nitrogen overflush was carried out to propagate the chemical solution further in the formation, allowing larger area around the wellbore to be treated. After another 12-hour soaking period the well was brought back on production. As a result of the treatment, a sustainable improvement in the well productivity was observed over the first six months (**Figure 2.13**). That is, gas and condensate rates were improved by 75% and 300%, respectively, after the treatment. An increase in FWHP (flowing wellhead pressure) by 90% for the same choke size as that used before the treatment was also

noticed. However, no data were reported after this initial six-month post-treatment period to confirm the durability of treatment over a longer production period.

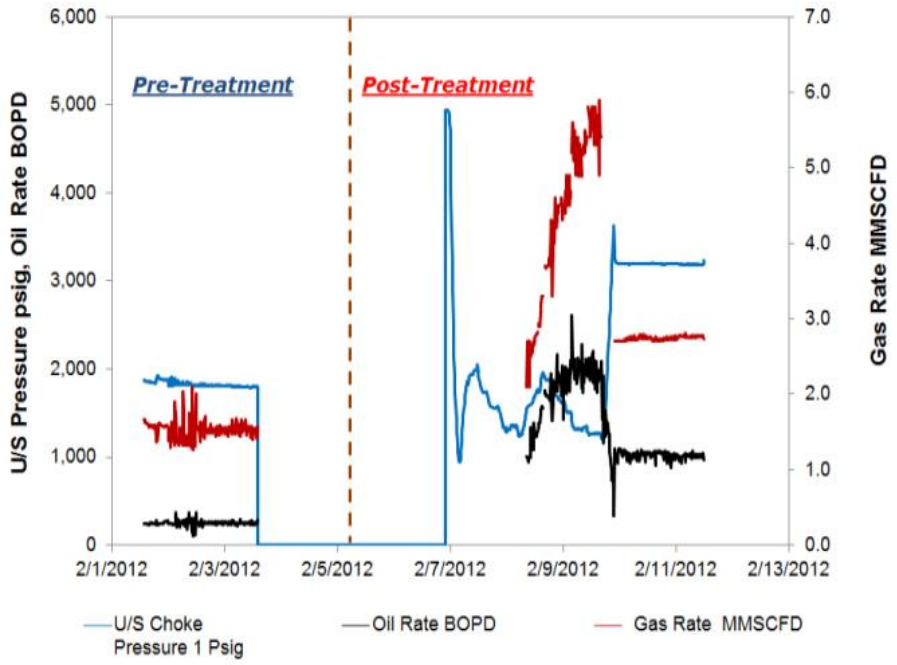

Figure 2.13: Field trial of chemical treatment in a gas-condensate well in Saudi Arabia (Al Ghamdi et al. 2013).

As discussed earlier (Section 2.3), it should be noted that the fluid interactions and displacement regimes in gas-condensate reservoirs are prominently governed by thermodynamic (e.g. interfacial tension between gas and condensate) and flow (e.g. velocity) conditions of the system. It was also highlighted that selecting representative fluids (e.g. low-IFT gas-condensate samples) and employing accurate experimental procedures (e.g. steady-state technique) are crucial to properly simulate the fluid flow in such complex systems (See Section 2.4). Despite these facts, it is noted that all reported studies on chemical treatment discussed above lack a profound and thorough understanding of the application of such a technique in gas-condensate systems. The main body of these investigations are limited to using conventional gas/oil fluids, and furthermore, those that deal with the condensing fluids lack correct and reliable procedures. That is, in all available studies in the literature conventional oil and gas fluids, e.g. decane/air (e.g. Fahes and Firoozabadi 2007, Ahmadi et al. 2011), have been employed to measure the static contact angles and hence assess the oil-repellency

strength of the chemicals used. These results, however, have been considered to be (controversially) applicable to gas-condensate systems. There are also a few cases (e.g. Kumar et al. 2006, Bang et al. 2008), which have deployed the pseudo-steady state technique using gas-condensate fluids to quantify the level of improvement in relative permeabilities due to wettability alteration. These experiments, however, have been limited to IFTs above 4 mN/m, whereas as discussed in Section 2.4 the unique velocity effects observed in condensing systems becomes evident at IFTs below 3 mN/m (Jamiolahmady et al. 2009). Furthermore, it should be noted that the pseudo-steady state technique used in these studies would not thoroughly simulate the flow behaviour pertaining to near wellbore gas-condensate wells, where the steady state conditions dominates the flow. Such shortcomings existing in all previous studies would leave the application of their results for gas-condensate systems open to important criticisms. Further detailed discussions about these shortcomings are presented in Chapters 5 and 6 of this thesis. It should be mentioned that, there are also unofficial reports of use of chemicals similar to those mentioned in the above studies that have resulted in very short term well productivity improvement, which can raise further serious questions on the generality of results reported in the literature.

The major part of the studies reported on the application of chemical treatment has been devoted to finding effective chemical agents for sandstone rock types (e.g. Li and Firoozabadi 2000, Kumar et al. 2006, Panga et al. 2006, Al-Anazi et al. 2007, Butler et al. 2009, Zheng and Rao 2011, Al Ghamdi et al. 2013), whilst there are only a few investigations carried out for carbonate minerals (e.g. Adibhatla et al. 2006, Ahmadi et al. 2011). The research study presented in this thesis, first of all, is dedicated to find appropriate wettability modifiers for carbonate rock types, which compared to sandstones, have received less attention. Furthermore, to gain a better understanding of the performance of such wettability modifiers at conditions more representative of gas-condensate reservoirs, a series of experimental and simulation studies have been performed through appropriate and systematic approaches. The new findings from this research work stress some important limitations and benefits associated with chemical treatment and offer valuable guidelines for practical field applications.

2.8 REFERRENCES

1. Adel, H., D. Tiab and T. Zhu (2006). Effect of Gas Recycling on the Enhancement of Condensate Recovery, Case Study: Hassi R'Mel South Field, Algeria. International Oil Conference and Exhibition in Mexico, 31 August-2 September, Cancun, Mexico.

2. Adibhatla, B., K. K. Mohanty, P. Berger and C. Lee (2006). "Effect of surfactants on wettability of near-wellbore regions of gas reservoirs." Journal of Petroleum Science and Engineering 52(1–4): 227-236.

3. Afidick, D., N. J. Kaczorowski and S. Bette (1994). Production Performance of a Retrograde Gas Reservoir: A Case Study of the Arun Field. SPE 28749, SPE Asia Pacific Oil and Gas Conference, 7-10 November, Melbourne, Australia.

4. Ahmadi, M., M. M. Sharma, G. Pope, D. E. Torres, C. A. McCulley and H. Linnemeyer (2011). "Chemical Treatment To Mitigate Condensate and Water Blocking in Gas Wells in Carbonate Reservoirs." SPE Production & Operations 26(1): 67-74.

5. Al-Anazi, H. A., M. M. Sharma and G. A. Pope (2004). Revaporization of Condensate with Methane Flood. SPE Annual Technical Conference and Exhibition, 26-29 September, Houston, Texas.

6. Al-Anazi, H. A., J. G. Walker, G. A. Pope, M. M. Sharma and D. F. Hackney (2005). "A Successful Methanol Treatment in a Gas/condensate Reservoir: Field Application." SPE Production & Facilities 20(1): 60 - 69.

7. Al-Anazi, H. A., J. Xiao, A. A. Al-Eidan, I. M. Buhidma, M. S. Ahmed, M. Al-Faifi and W. J. Assiri (2007). Gas Productivity Enhancement by Wettability Alteration of Gas-Condensate Reservoirs. SPE-107493-MS, European Formation Damage Conference, 30 May-1 June, Scheveningen, The Netherlands.

8. Al Ghamdi, B. N., B. H. Al-Malki, A. Al-Kanaan, Z. Rahim and H. D. Al-Anazi (2013). Field Implementation of Condensate Bank Removal Using Chemical Treatment. IPTC-16545-MS, International Petroleum Technology Conference, 26-28 March, Beijing, China.

9. Ali, J. K., P. J. McGauley and C. J. Wilson (1997). The Effects of High-Velocity Flow and PVT Changes Near the Wellbore on Condensate Well Performance. SPE Annual Technical Conference and Exhibition, 5-8 October, San Antonio, Texas, Society of Petroleum Engineers.

10. Anderson, W. G. (1987). "Wettability Literature Survey-Part 6: The Effects of Wettability on Waterflooding." Journal of Petroleum Technology 39(12): 1605 - 1622.

11. Asar, H. and L. L. Handy (1988). "Influence of Interfacial Tension on Gas/Oil Relative Permeability in a Gas-Condensate System." SPE Reservoir Engineering 3(01): 257-264.

12. Bang, V. S. S., G. A. Pope, M. M. Sharma, J. Jimmie R. Baran and M. Ahmadi (2008). A New Solution to Restore Productivity of Gas Wells With Condensate and Water Blocks. SPE-116711-MS, SPE Annual Technical Conference and Exhibition. Denver, Colorado, USA, Society of Petroleum Engineers.

13. Bang, V. S. S., C. Yuan, G. A. Pope, M. M. Sharma, J. R. Baran, Jr., J. Skildum and H. C. Linnemeyer (2008). Improving Productivity of Hydraulically Fractured Gas Condensate Wells by Chemical Treatment. OTC-19599-MS, Offshore Technology Conference, 5-8 May, Houston, Texas, USA.

14. Bardon, C. and D. G. Longeron (1980). "Influence of Very Low Interfacial Tensions on Relative Permeability." Society of Petroleum Engineers Journal 20(05): 11.

15. Blom, S. M. P. and J. Hagoort (1998). "The Combined Effect of Near-Critical Relative Permeability and Non-Darcy Flow on Well Impairment by Condensate Drop Out." 1: 421-429.

16. Blom, S. M. P., J. Hagoort and D. P. N. Soetekouw (1997). Relative Permeability at Near-Critical Conditions. SPE Annual Technical Conference and Exhibition, 5-8 October, San Antonio, Texas, Society of Petroleum Engineers.

17. Buckley, S. E. and M. C. Leverett (1942). "Mechanism of Fluid Displacement in Sands." Transactions of the AIME 146(1): 107 - 116.

18. Butler, M., J. B. Trueblood, G. A. Pope, M. M. Sharma, J. R. Baran, Jr. and D. Johnson (2009). A Field Demonstration of a New Chemical Stimulation Treatment for Fluid-Blocked Gas Wells. SPE-125077-MS, SPE Annual Technical Conference and Exhibition, 4-7 October, New Orleans, Louisiana.

19. Carlson, M. R. M. and J. W. G. J. Myer (1995). The Effects Of Retrograde Liquid Condensation On Single Well Productivity Determined Via Direct (Compositional) Modelling Of A Hydraulic Fracture In A Low Permeability Reservoir. SPE-29561-MS, Low Permeability Reservoirs Symposium, 19-22 March, Denver, Colorado, Society of Petroleum Engineers.

20. Coats, K. H. (1980). "An Equation of State Compositional Model." Society of Petroleum Engineers Journal 20(05): 363 - 376.

21. Danesh, A. (1998). "PVT and Phase Behaviour of Petroleum Reservoir Fluids." Elsevier Science and Technology Books.

22. Dehane, A. and D. Tiab (2000). Performance of Horizontal Wells in Gas Condensate Reservoirs, Djebel Bissa Field, Algeria. SPE/AAPG Western Regional Meeting, 19-22 June, Long Beach, California.

23. Du, L., J. G. Walker, G. A. Pope, M. M. Sharma and P. Wang (2000). Use of Solvents To Improve the Productivity of Gas Condensate Wells. SPE-62935-MS, SPE Annual Technical Conference and Exhibition, 1-4 October, Dallas, Texas.

24. Eakin, J. L., J. S. Miller and W. E. Eckard (1965). Removal of Water Blocks from Gas-producing Formations. API-65-026, Drilling and Production Practice, 1 January, New York, New York.

25. Eikeland, K. M. and H. Hansen (2009). "Dry Gas Reinjection in a Strong Waterdrive Gas-Condensate Field Increases Condensate Recovery—Case Study: The Sleipner Øst Ty Field, South Viking Graben, Norwegian North Sea." SPE Reservoir Evaluation & Engineering 12(2): 281 - 296.

26. Engineer, R. (1985). Cal Canal Field, California: Case History of a Tight and Abnormally Pressured Gas Condensate Reservoir. SPE-13650-MS, SPE California Regional Meeting, 27-29 March, Bakersfield, California.

27. Fahes, M. M. and A. Firoozabadi (2007). "Wettability Alteration to Intermediate Gas-Wetting in Gas-Condensate Reservoirs at High Temperatures." SPE Journal 12(4): 397-407.

28. Fevang, Ø., C. H. Whitson and (1996). "Modeling Gas-Condensate Well Deliverability." SPE Reservoir Engineering Journal 11 (4): 221-230.

29. Foran, E. V. and P. C. Dixon (1939). Condensate Wells-Completion and Recycling Operations. API-39-340, Drilling and Production Practice, 1 January, New York, New York, American Petroleum Institute.

30. Frederick, D. C., Jr. and R. M. Graves (1994). New Correlations To Predict Non-Darcy Flow Coefficients at Immobile and Mobile Water Saturation, Society of Petroleum Engineers.

31. Froning, H. R. and R. O. Leach (1967). "Determination of Chemical Requirements and Applicability Of Wettability Alteration Flooding." Journal of Petroleum Technology 19(6): 839 - 843.

32. Fussell, D. D. (1973). "Single-Well Performance Predictions for Gas Condensate Reservoirs " Journal of Petroleum Technology 25(7): 860-870.

33. Garzon, F. O., H. Anazi, J. A. Leal Jauregui and M. Al-Faifi (2006). Laboratory and Field Trial Results of Condensate Banking Removal in Retrograde Gas Reservoirs: Case History. SPE-102558-MS, SPE Annual Technical Conference and Exhibition, 24-27 September, San Antonio, Texas, USA, Society of Petroleum Engineers.

34. Geertsma, J. (1974). "Estimating the Coefficient of Inertial Resistance in Fluid Flow Through Porous Media." 14(05): 6.

35. Hashemi, A. and A. C. Gringarten (2005). Comparison of Well Productivity Between Vertical, Horizontal and Hydraulically Fractured Wells in Gas-Condensate Reservoirs. SPE-94178-MS, SPE Europec/EAGE Annual Conference, 13-16 June, Madrid, Spain.

36. Henderson, G. D., A. Danesh, B. Al-kharusi and D. Tehrani (2000). "Generating reliable gas condensate relative permeability data used to develop a correlation with capillary number." Journal of Petroleum Science and Engineering 25(1–2): 13.

37. Henderson, G. D., A. Danesh and D. H. Tehrani (2001). "Effect of positive rate sensitivity and inertia on gas condensate relative permeability at high velocity." Petroleum Geoscience 7: 6.

38. Henderson, G. D., A. Danesh, D. H. Tehrani and B. Al-Kharusi (2000). The Relative Significance of Positive Coupling and Inertial Effects on Gas Condensate Relative Permeabilities at High Velocity. SPE Annual Technical Conference and Exhibition. 1-4 October, Dallas, Texas, Society of Petroleum Engineers.

39. Henderson, G. D., A. Danesh, D. H. Tehrani, S. Al-Shaidi and J. M. Peden (1998). "Measurement and Correlation of Gas Condensate Relative Permeability by the Steady-State Method." SPE Reservoir Evaluation & Engineering 1(2): 134-140.

40. Henderson, G. D., A. Danesh, D. H. Tehrani, S. Al-Shaldi and J. M. Peden (1996). "Measurement and Correlation of Gas Condensate Relative Permeability by the Steady-State Method." SPE Journal: 191 - 202.

41. Henderson, G. D., A. Danesh, D. H. Tehrani and J. M. Peden (1997). "The effect of velocity and interfacial tension on relative permeability of gas condensate fluids in the wellbore region." Journal of Petroleum Science and Engineering 17(3–4): 265-273.

42. Henderson, G. D., A. Danesh, D. H. Tehrani, J. M. Peden and (1993). "An Investigation Into the Processes Governing Flow and Recovery in Different Flow Regimes Present in Gas Condensate Reservoirs." Paper SPE 26661 presented at the SPE Annual Technical Conference and Exhibition, 3-6 October, Houston, Texas.

43. IEA (International Energy Agency), "World Energy Outlook" report 2011, (http://www.iea.org/).

44. Jamaluddin, A. K. M., S. Ye, J. Thomas, apos, D. Cruz and J. Nighswander (2001). Experimental and Theoretical Assessment of Using Propane to Remediate Liquid Buildup in Condensate Reservoirs. PE-71526-MS, SPE Annual Technical Conference and Exhibition, 30 September-3 October, New Orleans, Louisiana.

45. Jamiolahmady, M. and A. Danesh (2007). Comparison of Vertical, Slanted, and Horizontal Wells Productivity in Layered Gas-Condensate Reservoirs. EUROPEC/EAGE Conference and Exhibition, 11-14 June, London, U.K.

46. Jamiolahmady, M., A. Danesh, D. H. Tehrani and D. B. Duncan (2000). "A Mechanistic Model of Gas-Condensate Flow in Pores." Transport in Porous Media 41(1): 17-46.

47. Jamiolahmady, M., A. Danesh, D. H. Tehrani and D. B. Duncan (2003). "Positive Effect of Flow Velocity on Gas–Condensate Relative Permeability: Network Modelling and Comparison with Experimental Results." Transport in Porous Media 52(2): 159-183.

48. Jamiolahmady, M., M. Sohrabi, S. Ireland and P. Ghahri (2009). "A generalized correlation for predicting gas–condensate relative permeability at near wellbore conditions." Journal of Petroleum Science and Engineering 66(3–4): 98-110.

49. Jones, A. T., M. S. Al Salhi, S. M. Al Shidl, M. England and R. Pongratz (1998). Multiple Hydraulic Fracturing of Deep Gas-Condensate Wells in Oman. SPE-49100-MS, SPE Annual Technical Conference and Exhibition, 27-30 September, New Orleans, Louisiana, Society of Petroleum Engineers.

50. Jones, J. R. and R. Raghavan (1988). "Interpretation of Flowing Well Response in Gas-Condensate Wells." SPE Formation Evaluation 3(3): 578 - 594.

51. Joshi, S. D. (1991). Horizontal Well Technology, PennWell Publishing Company.

52. Katz, M. R. T. K. H. C. D. L. (1962). "The Effect of Turbulence on Flow of Natural Gas Through Porous Reservoirs." Journal of Petroleum Technology 14(07): 7.

53. Kilgren, K. H. (1966). "Phase Behavior of a High-Pressure Condensate Reservoir Fluid." Journal of Petroleum Technology 18(08): 1001-1005.

54. Kroemer, E., I. S. Abou-Sayed, D. K. Babu and M. F. Cohen (1997). Compositional Simulation of Well Performance for Fractured and Multiple Fractured Horizontal Wells in Stratified Gas Condensate Reservoirs. SPE Reservoir Simulation Symposium, 8-11 June, Dallas, Texas.

55. Kumar, V., G. A. Pope and M. M. Sharma (2006). Improving the Gas and Condensate Relative Permeability Using Chemical Treatments. SPE-100529-MS, SPE Gas Technology Symposium, 15-17 May, Calgary, Alberta, Canada.

56. Kumar, V., G. A. Pope and M. M. Sharma (2006). Improving the Gas and Condensate Relative Permeability Using Chemical Treatments. SPE Gas Technology Symposium. Calgary, Alberta, Canada, Society of Petroleum Engineers.

57. Li Fan., B. W. H., A. Jamaluddin, J. Kamath, R. Mott, G.A. Pope, A. Shandrygin, C.H. Withson (2005). "Understanding Gas-Condensate Reservoirs." Oilfield Review, Schlumberger 17(4): 14.

58. Li, K. and A. Firoozabadi (2000). "Experimental Study of Wettability Alteration to Preferential Gas-Wetting in Porous Media and Its Effects." SPE Reservoir Evaluation & Engineering 3(2): 139 - 149.

59. Marir, B. and D. Tiab (2006). Performance of Horizontal Wells in Gas Condensate Reservoirs: Hassi R'Mel Field, Algeria (Russian). SPE Russian Oil and Gas Technical Conference and Exhibition, 3-6 October, Moscow, Russia.

60. Morrow, N. R. (1990). "Wettability and Its Effect on Oil Recovery." Journal of Petroleum Technology 42(12): 1476 - 1484.

61. Moses, P. L. (1986). "Engineering Applications of Phase Behavior of Crude Oil and Condensate Systems " Journal of Petroleum Technology 38(07): 9.

62. Mott, R. (2002). "Engineering Calculations of Gas Condensate Well Productivity" Paper SPE 77551 presented at the AnnualTechnical Conference and Exhibition, 29 September-2 October 2002, San Antonio, Texas.

63. Mott, R. E., A. S. Cable and M. C. Spearing (2000). "Measurements of Relative Permeabilities for Calculating Gas-Condensate Well Deliverability." SPE Reservoir Evaluation & Engineering 3(6): 473 - 479.

64. Narayanaswamy, G., M. M. Sharma and G. A. Pope (1998). Effect of Heterogeneity on the Non-Darcy Flow Coefficient. SPE Gas Technology Symposium, 15-18 March, Calgary, Alberta, Canada, Society of Petroleum Engineers.

65. Noh, M. H. and A. Firoozabadi (2008). "Effect of Wettability on High-Velocity Coefficient in Two-Phase Gas/Liquid Flow." SPE Journal 13(3): 298-304.

66. O'Dell, H. G., T. O. Co.; and R. N. Miller (1967). "Successfully Cycling a Low-Permeability, High-Yield Gas Condensate Reservoir." Journal of Petroleum Technology 19(1): 41-47.

67. Panga, M. K. R., Y. S. Ooi, P. L. Koh, K. S. Chan, P. G. Enkababian, P. Cheneviere and M. M. Samuel (2006). Wettability Alteration for Water Block Prevention in High Temperature Gas Wells. SPE-100182-MS, SPE Europec/EAGE Annual Conference and Exhibition, 12-15 June, Vienna, Austria.

68. Penny, G. S., M. W. Conway and J. E. Briscoe (1983). Enhanced Load Water-Recovery Technique Improves Stimulation Results. SPE-12149-MS, SPE Annual Technical Conference and Exhibition, 5-8 October, San Francisco, California.

69. Sänger, P. J., H. K. Bjørnstad and J. Hagoort (1994). Nitrogen Injection Into Stratified Gas-Condensate Reservoirs. SPE-28941-MS, SPE Annual Technical Conference and Exhibition, 25-28 September, New Orleans, Louisiana.

70. Sanger, P. J. and J. Hagoort (1998). "Recovery of gas-condensate by nitrogen injection compared with methane injection." SPE Journal 3(1): 26-33.

71. Settari, A., R. C. Bachman, K. A. Hovem and S. G. Paulsen (1996). "Productivity of Fractured Gas Condensate Wells - A Case Study of the Smorbukk Field." SPE Reservoir Engineering 11(4): 236 - 244.

72. Tang, G.-Q. and A. Firoozabadi (2003). "Wettability Alteration to Intermediate Gas-Wetting in Porous Media at Elevated Temperatures." Transport in Porous Media 52(2): 185-211.

73. Thornton, O. F. (1946). Gas-Condensate Reservoirs-A Review, American Petroleum Institute.

74. Wagner, O. R. and R. O. Leach (1959). "Improving Oil Displacement Efficiency by Wettability Adjustment." Transactions of the AIME 216(1): 65 - 72.

75. Wang, X. and M. Economides (2009). Advanced Natural Gas Engineering, Gulf Publishing Company, Houston, Texas.

76. Whitson, C. H., Ø. Fevang and A. Sævareid (1999). Gas Condensate Relative Permeability for Well Calculations, Society of Petroleum Engineers.

77. Wu, S. and Firoozabadi, A. 2010. Effect of Salinity on Wettability Alteration to Intermediate Gas-Wetting. SPE Reservoir Evaluation & Engineering, 13 (2): 228-245.

78. Zheng, Y. and D. N. Rao (2011). Experimental Study of Spreading and Wettability Effects by Surfactants in Condensate Reservoirs at Reservoir Conditions. SPE-141016-MS, . SPE International Symposium on Oilfield Chemistry, 11-13 April, The Woodlands, Texas, USA.

3 EXPERIMENTAL EQUIPMENT AND PROCEDURES

3.1 EXPERIMENTAL EQUIPMENT

The general specifications of the main experimental rigs used in this work are explained in this chapter. This includes a brief description of their essential components.

3.1.1 Pumps

Quizix Pumps

Two types of Quizix high pressure syringe pumps are present for handling the chemical solution, brine and hydrocarbon mixtures during the core treatments and displacement tests. These positive displacement metering pumps include Quizix Q5000, with the maximum pressure and flow rate of 5000 psi and 2020 cc/hr, and Quizix Q6000, with the maximum pressure and flow rate of 10000 psi and 24000 cc/hr, incorporated into the USS and SS core flood facilities, respectively.

DBR Pumps

Two mechanical DBR pumps, having twin-cylinders, each 1 litter, with positive displacements, are in the SS core flood rig, administering the flow of oil (condensate) around the system. The maximum pressure and flow rate corresponding to these pumps are 10000 psi and 1000 cc/hr, respectively.

Vacuum Pump

A vacuum pump is usually used to remove the air from the fluid accumulators and mixing cells, before transferring the desired samples into them. This prevents the airborne contaminations of the fluid mixture. The water, decane and brine solutions are also degassed using this vacuum pump, before contact angle measurements and imbibition tests. The Edwards vacuum pump used in this work has the capability of creating an ultimate vacuum of 2×10^{-3} mbar.

3.1.2 Gas Booster

To pressurize the gas, used for the experiments, a gas booster from Sprague Products, which is a piston-type, air-operated booster, is used. This booster with 100 psi driving air is able to produce a maximum outlet pressure of 10300 psi.

3.1.3 Fluid Accumulators

High-pressure cylinders, including Proserv and Alva type, are used to store and inject the chemical solutions, brines and hydrocarbon mixtures at low and high temperatures. The cylinders can tolerate the high temperatures up to 160°C with a working pressure of 10,000 psi. Each of these storage cylinders utilises a piston, behind which there is water connected to a pump that is used to inject or withdraw the desired fluid sample at the front side of the piston. Cylinder volumes range from 300cc to 1 litre. The wetted parts of the cylinders are Stainless Steel, Titanium or Hastelloy, depending on the fluid type delivered with them.

3.1.4 Electronic Balance

There is a fine precision-high resolution Sartorius Cubis balance that was used for preparing the chemical and brine solutions in required proportions. Cubis balance can measure a maximum weight of 1010 g with a precision of 0.001 g. The electronic balance has a user-friendly interface and can be connected to a computer to log and store the data. This feature was used to record the corresponding data of the imbibition tests performed in this study.

3.1.5 Gas Meter

In the laboratory, a digital gasometer from Chandler Engineering is used to measure the produced atmospheric gas from the core during the USS displacement tests. It consists of two chambers with a volume of 1000 and 2000 cm^3, which can be used separately or in series to provide the maximum capacity of 3000 cm^3. Each chamber contains a floating piston, whose position is monitored by the dual digital volume meters which are calibrated in cubic centimetres. The gasometer can work up to a maximum pressure of about 2 psi and provides the digital readings with an accuracy of 0.2%.

3.1.6 Pressure Transducers

Quartzdyne digital pressure transducers are used to read the fluid pressure at the core inlet and outlet during displacement tests and subsequently to calculate the pressure drop across the core. The Quartzdyne transducer utilises quartz crystal sensor elements,

providing high stability and fine resolution for reading the pressure. The deployed pressure transducers for this work were customized to precisely sensor the pressure values with an accuracy of 0.01 psi with the maximum working pressure and temperature of 10000 psi and 150°C, respectively.

3.1.7 Back Pressure Regulator

In order to perform the core displacement test under pressure, during the USS tests, while the produced volumes of gas and oil are collected and recorded at atmospheric conditions, a back pressure regulator (BPR) is at the core outlet. The BPR has a PTFE diaphragm at its centre, above which the desired test pressure is applied using the N2 gas cell connected to a pump. The fluids consequently flow at high pressures until they reach the BPR outlet, where the effluent is at atmospheric pressure. The BPR used here had a maximum working pressure and temperature of 10,000 psi and 350°F, respectively.

3.1.8 Ovens

The wettability alteration of either small rock substrates or larger core samples at low, e.g. 65°C, and high, e.g. 130°C, temperatures, are conducted in a controlled air bath, Binder heating oven. The Binder oven utilises an electronically controlled preheating chamber, having a temperature range from 5°C to 300°C, with an accuracy of one degree. It should be mentioned that the SS-kr tests were also conducted inside another air-bath system, working at a constant temperature of 38°C.

3.1.9 Core Holders

The core treatments and the subsequent USS displacement tests in this work were conducted on 1 and 1.5" carbonate core plugs with a maximum length of 10 cm. The Vinci hydrostatic core holder made of stainless steel was used to load and test such core samples. This core holder has a length of 40 cm and can work at a maximum pressure and temperature of 770 bar and 200°C, respectively. In addition, the 2" stainless-steel core holder holding up to 1-meter long core samples was employed to perform the steady-state k_r measurements on a carbonate core sample with L=30 cm and D=1".

3.1.10 DSA (Drop Shape Analysis)

The DSA 100 from KRUSS-Eurotechnica that was customised for the purpose of this project is used for characterizing the surface treatments, i.e. static contact angles, at both ambient and high pressure-high temperature (HPHT) conditions, using the sessile drop

method. The interfacial tensions between gas and condensate samples can also be measured, employing the pendant drop technique. With DSA, it is possible to perform the measurements under extreme pressure of 7500 psi and temperature of 150°C. DSA utilises a general camera and illumination system, which are mounted together on a stand-alone frame so it is feasible to be used with both ambient and high-pressure modules. DSA is a software-controlled apparatus, which allows the user to carry out the main parts of the test such as imaging and data acquisition and evaluation from a desktop. In addition, there are a number of other tasks such as sample positioning, dosing and adjusting the image resolution and illumination that can be performed either manually or by the software.

The ambient module of DSA, shown in **Figure 3.1**, consists of a sample stage with movable legs in x and y directions, used to centre the rock surface with respect to the needle above it. The needle, mounted on a vertical stand, can subsequently move upward and downward to an appropriate distance (1-2 mm) from the substrate, where the liquid sample is deposited.

The main part of the HPHT module of DSA is a 30cc view chamber, equipped with two high-pressure optical windows, a pressure transducer, a thermometer and a number of relevant fittings used for the test fluids to be transferred into or withdrawn from the cell. The fluid samples can be injected and pressurized using either two screw-piston hand pumps provided with DSA or external set of Quizix pumps. An electrical heating jacket, fixed round the optical chamber, is used to maintain the test temperature at the desired constant value. In order to facilitate making and employing the gas condensate fluid samples in-place at high pressure and temperature conditions, DSA has also been equipped with two custom-designed 600cc and 300cc fluid accumulators fitted with heating jackets. **Figure 3.2** depicts the overall schematic of the HPHT module of DSA. Using DSA it is feasible to measure the contact angles and surface tensions in a range from 0 to 180° and 0.01 to 1000 mNm^{-1}, with a resolution of 0.1° and 0.01 mNm^{-1}, respectively.

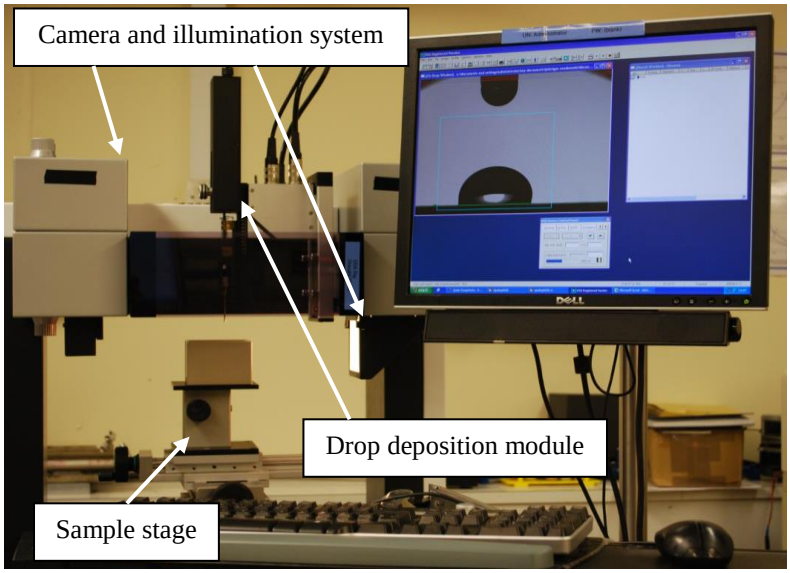

Figure 3.1: Ambient module of the drop shape analysis (DSA) setup used for contact angle measurements on treated rock substrates at atmospheric conditions.

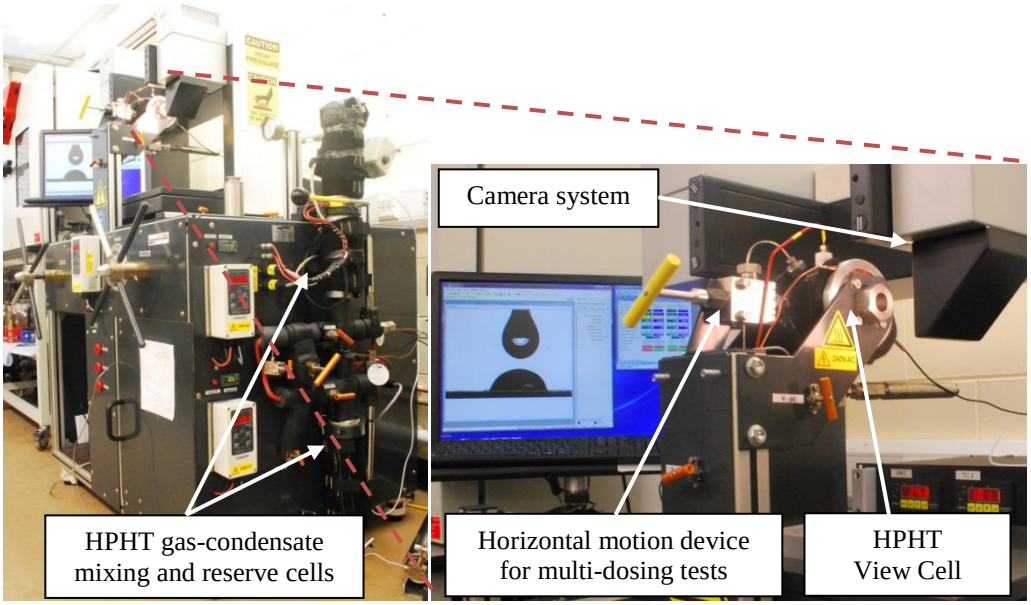

Figure 3.2: Custom-designed high pressure-high temperature module of the drop shape analysis (DSA) setup equipped with HPHT mixing cells for making and employing gas condensate fluid mixtures in place.

3.1.11 Unsteady-State Core Flood Rig

The unsteady-state (USS) core flood rig is assembled inside the Binder oven. In this work, this rig was mainly used for treating the carbonate core samples and conducting the unsteady-state displacements at ambient or high temperatures. The USS setup utilises a set of Quizix pumps, four piston cells, one core holder, two pressure transducers, one BPR and one Gasometer. **Figure 3.3** depicts a schematic of the USS

setup including the main parts. Four 300 cc piston cells have been allocated to the oil, gas, chemical solution (or brine) and N2 gas, among which oil and gas cells are used during the displacement tests and N2 cell creates the essential pressure for BPR. The pressure transducers at the core inlet and outlet read the flowing pressure during the displacement. These data are continuously received via a computer programme, called LabVIEW, where it stores and plots the core inlet, outlet and differential pressure data versus injection time during the test.

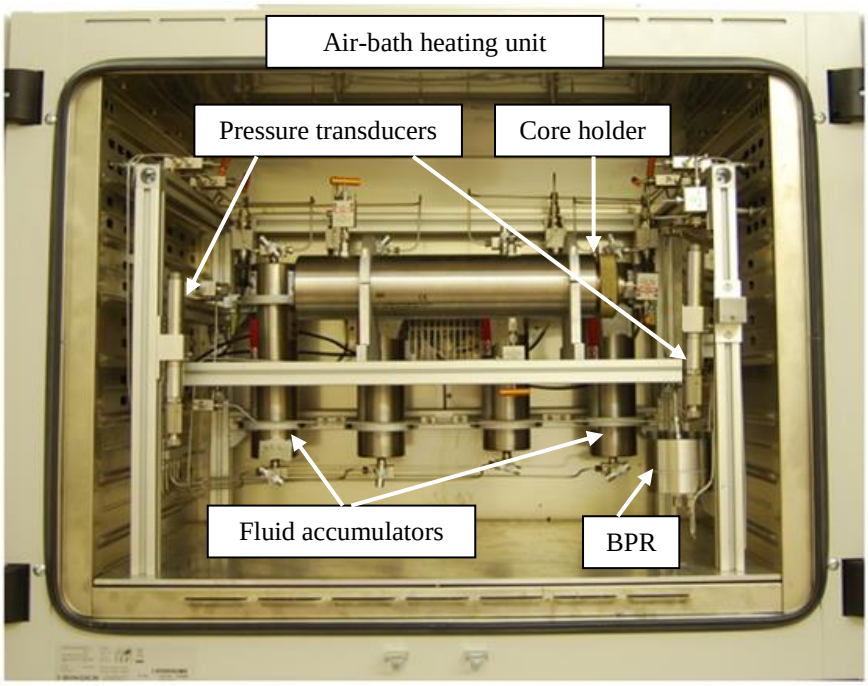

Figure 3.3: High pressure-high temperature core flooding setup used to perform unsteady-state displacement and chemical treatments tests.

3.1.12 Steady-State Core Flood Rig

The steady-state (SS) core flood rig, shown in **Figure 3.4**, is a unique and sophisticated setup, which has been designed in-house at Heriot-Watt University, especially dedicated to measure steady-state gas-condensate k_r data at near wellbore conditions, where the high velocities and low IFT conditions are predominant.

The main parts of SS core flood facility includes two condensate cells, two gas cells, two sets of DBR pumps connected to condensate and gas cells, a set of Quizix pump for gas, rotating core holder, high-pressure sight-glass and pressure transducers.

Figure 3.5 depicts a general schematic of SS core flood rig, showing its main components and the relevant connections between them. All these parts have been

accommodated inside a heating chamber, usually kept at 38°C, to carry out the experiments at stabilized temperature.

Positive displacement DBR pumps are used to circulate the condensate, and if required gas, around the flow system at low velocities. On the other hand, Quizix pumps, consisting of three pistons each with a volume of 550 cm^3, hasvebeen incorporated into the core facility to store the equilibrium gas and inject it at high velocities through the core. The configuration of these three pistons allows continual injection of gas through the core, as the injection and receiving pistons automatically switch direction at the end of their stroke while the third one operates in a mode, which ensures minimal spike in the differential pressure when switching occurs. The high rate Quizix pump can be automatically isolated from the flow system, allowing the low rate DBR pump to measure the relative permeability.

The pumps used to circulate the fluid have a resolution of 0.01 cm^3; with the volumes of fluid displaced into the core being checked independently using linear transducers also with a resolution of 0.01 cm^3.

Figure 3.4: Gas-condensate core flood rig used for steady-state relative permeability measurements.

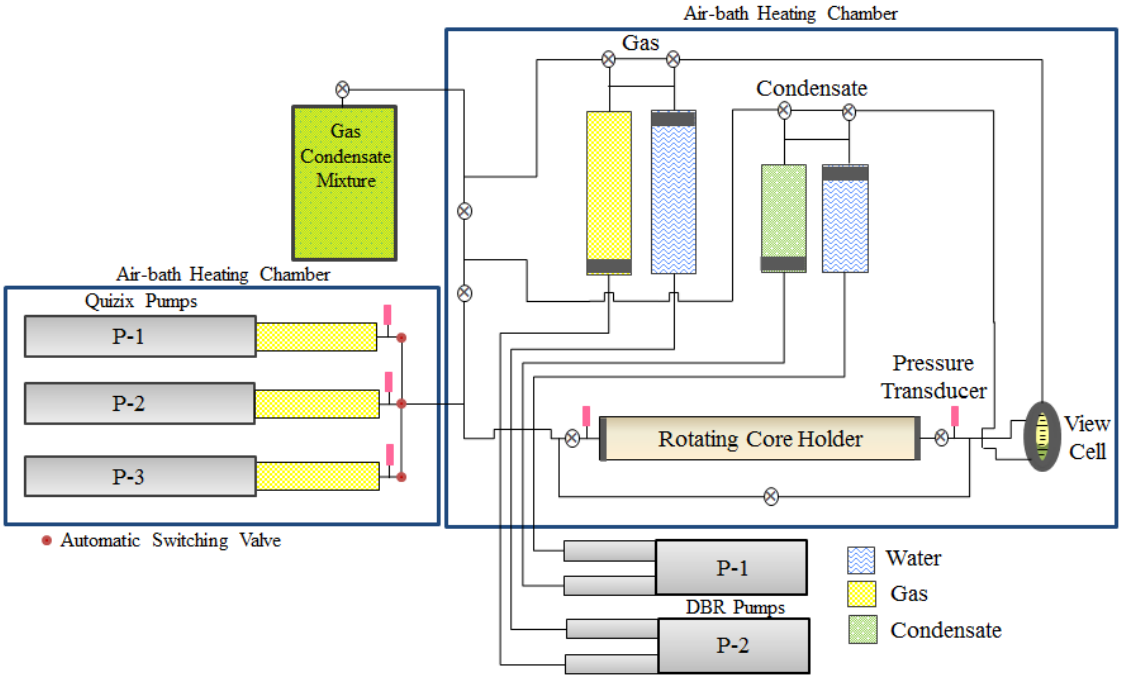

Figure 3.5: The schematic of the steady-state core flood rig used to measure gas condensate relative permeability at high velocity and low IFT conditions.

3.1.13 Carbonate Rock Samples

Two types of carbonate outcrop rocks, Texas Cream (TC) and Baker Dolomite (BD), were used during this work studying the performance of fluorochemicals on carbonate minerals. TC composes of 99% dolomite and BD has 98% calcite as the main element of its mineralogy. **Figure 3.6** depicts the BD and TC core plugs and substrates used in this study to perform the flow tests and contact angle measurements. **Figure 3.7** shows oil (decane) and water (deionized water) drops on TC and BD substrates at their untreated virgin state. As it is evident both liquids demonstrate zero contact angles ($\theta_{liquid/gas}$=0°) on both substrates, i.e. liquid drops quickly imbibe into the rock surface, showing the intrinsically preferential liquid-wetting conditions of these minerals.

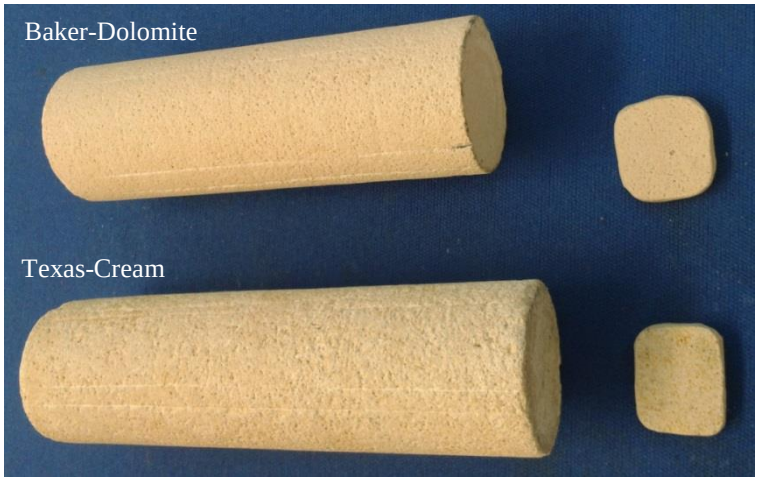

Figure 3.6: The core plugs and substrates of two outcrop carbonate minerals, Baker-Dolomite (top) and Texas-Cream (bottom), used in this study.

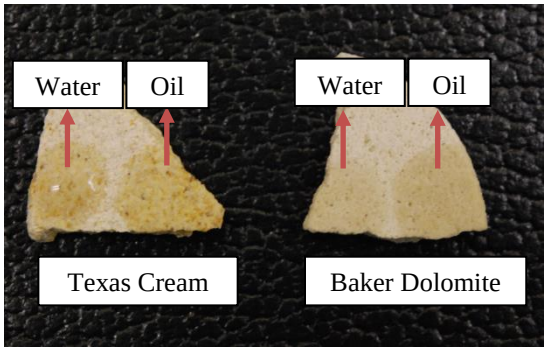

Figure 3.7: Water (deionized water) and oil (decane) drops on carbonate Texas-Cream (left) and Baker-Dolomite (right) substrates, demonstrating the intrinsically preferential liquid-wetting conditions of these minerals.

3.2 EXPERIMENTAL PROCEDURES

The general experimental procedures, used to set up and carry out the main experiments in this work, are explained in the following sections. This includes the preliminary steps required to prepare the rock and fluid samples plus the stages followed to perform the experiments.

3.2.1 Preparation of Rock Samples

Carbonate Substrates

The carbonate substrates were trimmed as small thin sections (about 2 mm thick) off the outcrop rock samples by using a slitting saw. The surfaces of the required samples were polished and smoothed using a specific tool called a Dremel. The carbonate substrates were then thoroughly washed by soaking in methanol or toluene/methanol solvents at 60°C for 8 hours after which they were dried out in an oven at 100°C. For further details

about the reasons for the methods used for preparation and cleaning of the rock samples and their significance for the rock wetting characteristics refer to Appendix B, at the end of this thesis.

Core Samples

The carbonate core samples were drilled from the outcrop blocks using a core cutter machine. The samples were then washed by either using a Soxhlet method using methanol at 65°C or flushing adequate pore volumes of methanol solvent through the core, loaded in a core holder. The former method was mainly used for shorter core plugs. The samples were finally dried inside an oven at 100°C.

3.2.2 Porosity Measurement

In this study the core effective pore volume was measured by employing the helium porosity method. According to this, the core pore volume was measured for four to five successive times and the average value was used to calculate the porosity. These measurements were carried out at laboratory temperature and a confining pressure of 500 psi for the core pressure of about 100 psi. The volume of the core attachments were also calculated separately either volumetrically by measuring their dimensions or using the helium method.

3.2.3 Permeability Measurement

The single phase absolute permeability of the core to the gas, during the displacement tests, was measured using nitrogen or a gas mixture. Accordingly, the single phase gas was flowed through the core at a constant flow rate from 100 to 2000 cc/hr and the stabilised differential pressure at each rate was used to calculate the absolute permeability using Darcy's law.

3.2.4 Preparation of Fluid Mixtures

The standard procedure for preparing the C1-nC10 binary-mixture with a molar composition of 96.5%-3.5% at 38°C, used in the gas-condensate SS-kr measurements, is explained here. Similar procedure applies to all other fluid mixtures used in this study. To prepare the fluid mixture, the 6 litres mixing cell is initially filled with water, at room temperature, while the piston and its relevant perforated mixer are set at the top-end of the cell. The vacuum is then applied on the top-side of the cell for two hours, ensuring no air is trapped in the system. Subsequently, 2500 cc of water is discharged from the cell by injecting methane gas into it, followed by pressurizing the cell to 5600

psi, using a booster pump connected to the methane cylinder. Next, the cell temperature is raised using a temperature-controlled heating jacket set on 38°C. When temperature is stabilised, the cell pressure, increases slightly due to gas expansion at 38°C, which is adjusted at 5600 psi by bleeding the cell of excess methane slowly. Finally, 247.2 cc decane, accumulated and pressurized at 5750 psi in a separate piston cell at room temperature, i.e. 20°C, is transferred into the mixing cell by opening the top-valve on the cell slightly and injecting decane at very low rate while the injection pressure is maintained constant at 5750 psi. Following this, the water-side of the cell is connected to a pump to adjust and maintain the mixture pressure at 5600 psi. The two fluid components, i.e. C1 and nC10, are then fully mixed by flipping the mixing cell around for a period of time until the temperature of the system is stabilised at 38°C, resulting in no further change in mixture pressure.

3.2.5 Wettability Alteration Process

Treatment of Rock Substrates

In this work, to treat the carbonate substrate, the clean rock sample were soaked in the prepared chemical solution (about 30 cc) and pressurized at 400 psi using a piston cell, at the desired temperature, e.g. 90 and 130°C, for 18 hours, preferably overnight. The pressure was applied to prevent the solution reaching its boiling point at elevated temperatures. It should be noted that the whole setup requires about five hours to be heated up and stabilized at the desired temperature. Moreover, the preliminary screening tests performed in this study demonstrated that the treatment process, i.e. adsorption of chemical molecules on the rock surface, is accomplished within the initial three to four hours of immersing the rock substrate inside the chemical solution after temperature is stabilized. However, to ensure a complete treatment has occurred, the treatment process lengthened to 18 hours. As the treatment was concluded, the rock samples were removed from the solution and dried inside the oven at 100°C for at least two hours, after which the contact angle measurements were carried out using DSA apparatus.

Treatment of Core Samples

In this study all core treatments were conducted at high temperature of 130°C. For this purpose, the clean core sample was initially fitted inside a rubber sleeve using special silicon tapes resistant to very high temperatures. The wrapped core was then loaded in the core holder and the whole setup was positioned horizontally inside the oven. The desired chemical solution and nitrogen gas were also transferred into the corresponding

accumulators before raising the temperature. The confining pressure of 1500 psi was then applied on the core using water. Subsequently, the N2 cell was opened to the core and all its corresponding attachments, while the BPR (back pressure regulator) at the core outlet was set at 1000 psi. The whole setup, at this stage, was pressure tested for any possible leakages. The temperature was then increased in 20°C incremental stages (each of which took about 4 hours to be stabilized) until reach the target temperature of 130°C. This was to prevent the core overburden and other relevant fluid cells from being over-pressurized and fail due to sudden and uncontrolled expansion of the fluids. The chemical solution cell was finally opened to the core and approximately 20 to 30 PVs of chemical solution was injected at a constant flow rate of 4 cc/hr, unless otherwise stated. This was followed by an additional 18 hrs soaking time, ensuring a complete interaction between the chemical molecules and the rock surface has occurred. The unabsorbed chemicals were eventually displaced from the core by injecting N_2 gas, mimicking the back-flow stage of chemical solution from the well subsequent to chemical injection. The core was then loaded off the core holder and dried inside the oven at 100°C, before being used in the post-treatment displacement/imbibition tests.

3.2.6 Contact Angle Measurements

Ambient Conditions

The preliminary evaluations on the performance of each fluorochemical agent were carried out by measuring the deionised-water (DIW) and decane (oil) contact angles on the treated substrates at ambient conditions. For this purpose the ambient module of the drop shape analysis apparatus (DSA) was employed. To perform the contact angle measurements, the treated substrate is positioned and balanced horizontally on the centre of DSA sample stage where the liquid-sample syringe is mounted vertically above it on the DSA framework. The syringe is then shifted downward to a very close (within 1-2 mm) distance to the rock surface and about 5 µl of the liquid sample, i.e. oil or water, is injected through the needle, until attached to the rock surface. The needle is subsequently shifted upward until the deposited liquid sample is detached from the needle tip and forms a sessile drop on the substrate. In this work, the DSA polynomial or tangent method-2, which adapts a curve to the left and right regions of the three-phase contact point of liquid/gas/rock system, irrespective of the drop shape symmetry, was employed to calculate the corresponding contact angles (for further details on available techniques for calculation of contact angle and the mathematical physics behind these models refer to Appendix A at the end of this thesis). Accordingly, the

average of the right and left angles was reported as the final contact angle value here. The experimental error pertinent to this measurement procedure is about 5°. The stability (permanency) of the contact angles was also evaluated by assessing the behavior of the oil or water drops on the treated surface for a period of 15 minutes. As a result, if the contact angle was almost constant within this period it was considered as a stable contact angle. An unstable contact angle, on the other hand, was referred to a case with a substantial reduction in the initial measured value of contact angle with time, in which the sample drops imbibed into the rock surface slowly.

High Pressure-High Temperature Conditions

To scrutinize the performance of wettability modifiers in more representative conditions of hydrocarbon systems, contact angle measurements were performed at high pressures and in few cases at high temperatures as well, using synthetic gas-condensate fluids. This was achieved by deploying the high-pressure high-temperature (HPHT) module of the DSA setup, depicted in **Figure 3.2**. To carry out such a test, the treated carbonate substrate was horizontally centred inside the DSA high-pressure optical cell (or chamber), with a PTFE/Hasteloy capillary needle (having outside diameter of 1/16 or 1/32 inches) which was used to deposit the condensate droplet on the rock surface from above. The cell temperature was then raised to the test temperature in incremental stages. When the conditions were stabilized, the chamber was first purged of the air through the outlet valve by injecting the methane gas into it slowly. It was then pressurized to the desired test pressure using methane. Pre-pressurizing of the cell with methane was essential to maintain the desired gas-mixture (embedding fluid) in-phase and prevent its condensation due to sudden exposure to the atmospheric pressure. The gas-mixture, reserved in an accumulator at desired test pressure and temperature, was finally injected into the chamber, displacing the existing methane inside it. To ensure the chamber was fully saturated with gas sample, the equilibrated gas-mixture was injected for more than three times the chamber volume (i.e. 30cc).

To conduct the contact angle measurement, the condensate mixture was injected through the needle slowly (0.5 cc/hr), until it detached from the needle and formed a sessile drop on the substrate. The angle formed at the three-phase line between the condensate/gas/rock system was then measured and tracked versus time to evaluate its stability. Similar to ambient tests, tangent method-2 was used to calculate the corresponding contact angles. It should be mentioned that the image analysis of the condensate pendent drop, right before being detached from the needle, was also used to

measure the interfacial tension between gas and condensate phases. This was performed by fitting the Young-Laplace equation to the droplet profile using the DSA software.

3.2.7 Brine Compatibility Tests

The stability of the chemical molecules in brine media was examined through visual observation of the phase behaviour of the chemical agent after combining the chemical solution with brine by a weight ratio of 1:1 at room (20°C) and 90°C temperatures. Various brine compositions such as low-salinity (e.g., 0.8% NaCl + 0.2% $CaCl_2$) and high-salinity (e.g., 8% NaCl + 2% $CaCl_2$) brines were used. The solutions were consequently checked for any undesired sign of chemical precipitation, coagulation or suspension, showing the instability of the chemical particles in presence of brine ions.

3.2.8 Spontaneous Imbibition Tests

In order to perform the spontaneous imbibition test, the dry core sample (before and after the treatment) was suspended vertically from a support, standing on a digital balance. The weight of the whole setup on the balance was then reset to zero and subsequently the bottom end of the core plug, by about 3 cm, was immersed in the liquid sample, i.e. DIW or nC10, held in a glass beaker. **Figure 3.8** depicts the schematic of the setup used here. As the rock sample touched the liquid surface, the amount of the liquid imbibed into the rock was recorded versus time until reached a plateau, at which the imbibition curve was accomplished.

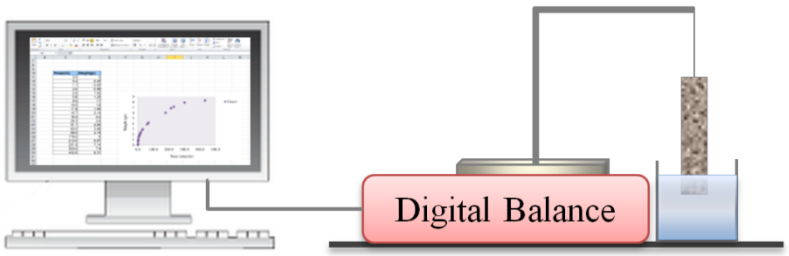

Figure 3.8: The schematic of the setup used for spontaneous imbibition tests.

3.2.9 Unsteady-state Displacement Tests

The majority of displacement tests in this work were performed using N2/nC10 and N2/DIW fluid systems. However, in a few cases, hydrocarbon mixtures such as C1/nC10 and C1/nC4 were also used. Here, the standard procedures to perform the unsteady-state (USS) test for a gas/oil system in general, which practically apply to all fluid systems used in this study, are explained. It should also be mentioned that to

simplify the experimental procedures, all USS tests were conducted at room temperature, i.e. 20°C, except one which was carried out at 100°C.

To carry out an unsteady-state displacement test, the clean and dry core is initially saturated and pressurized with the methane gas at the test pressure to prevent condensation from occurring, if the gas-mixture is exposed to the core at atmospheric pressure in the first place. The original gas-mixture is then injected through the core slowly (e.g. 5 cc/hr) for several PVs to displace the resident methane. It should be mentioned that the absolute permeability of the core to dry methane and gas-mixture is also measured at the end of these two stages. The core is then isolated from the system and the oil cell is opened to the by-pass line, to measure its solution-gas content before injecting into the core. For this purpose, the volume of the produced oil, after passing through the BPR, is recorded in a graduated cylinder, while its released gas is transferred into a volumetric gasometer. Having shut the by-pass line, the oil cell is opened to the core and oil is injected at a constant flow rate of 100, 20 or 10 cc/hr to displace the gas inside the core. The differential pressures (DPs) across the core during the displacement tests before and after the treatment are finally compared to evaluate the performance of the chemical on altering the rock wettability. That is, the lower differential pressure after the treatment, the more effective wettability alteration and better oil mobility. The production data along with the DPs are also used in a number of cases to estimate the k_r data corresponding to pre- and post-treatment conditions using Sendra optimizer software. Having the flow test accomplished, the core is flushed with N2 to displace the remaining oil and gas phases, after which it is dried inside the oven completely. It should be highlighted that to have consistent and comparable results, the pre- and post-treatment displacement tests are necessary to be conducted at similar initial conditions, i.e. clean and dry core.

Here, it should be mentioned that all displacement tests with N2/DIW were conducted with non-equilibrated fluids at atmospheric conditions, i.e. core outlet pressure was 14.7 psi. In a number of N2/nC10 displacement tests and all those performed with hydrocarbon mixtures, equilibrated fluids at high pressure conditions were employed in order to minimize the impact of nC10 solubility in the gas phase. It should be noted that performing the test at atmospheric outlet pressure simplifies the test procedure but it is believed that the results could be affected by the compression of gas. However, considering that similar pre- and post- treatment tests are compared, the

resultant impact is believed to be minimal. This was confirmed when a selected number of similar tests were performed at outlet flowing pressure of 14.7 and 1000 psi.

3.2.10 Steady-state Displacement Tests

In this work, the gas-condensate core flood rig was used to measure the steady-state relative permeability (SS-kr) data on a carbonate core sample before and after the wettability alteration. Here, a general description of the experimental procedures followed to perform such steady-state k_r measurements is given, the full details of which will be discussed in Chapter 6.

First, it should be mentioned that all steps corresponding to SS-kr tests in this study were conducted at a temperature of 38°C. To commence a SS test, the dry core is initially saturated with the methane gas at the required test pressure. The core single-phase inertial factor is also measured at this stage by injecting the methane gas through the core at various velocities, to estimate the gas permeability reduction due to inertia. Subsequently, the single-phase gas-condensate mixture, e.g. C1-nC10 used here, is injected into the methane-saturated core, at approximately 500 psi above the dew-point pressure, until the methane is completely removed from the system and the differential pressure across the core became stable. The whole setup pressure is next depleted to the dew-point pressure, by retracting the gas cell at a rate of ~10 psi/min initially, until 50 psi above the dew-point, at which the depletion rate is reduced to about 1 psi/min. The dew-point is witnessed when a condensate mist is observed in the sight-glass, resulting in a condensate layer to be deposited with time. The system pressure is further decreased to the desired test pressure (according to the selected IFT conditions) slowly, during which the initial condensate film is distributed everywhere within the pores. The core is then isolated from the system and subsequently the gas and dropped out condensate phases are circulated between the fluid accumulators for several times through the sight-glass, allowing the fluid components to reach the thermodynamic equilibrium conditions. The equilibrium is achieved when no further changes in the gas and condensate volumes are identified in two successive mixes. The gas and condensate phases are separated and stored in the individual gas and oil cells during this mixing process.

The test corresponding to each pressure (or IFT) value starts at the lowest selected condensate to gas flow rate ratio (CGR). To establish the steady-state flow at a selected value of CGR (volume condensate/volume gas), the equilibrium gas and condensate are injected simultaneously through the core at the required flow rates, until the differential

pressure across the core and the fractional flow of gas and condensate at the core outlet and condensate level in the sight glass are stabilised. The test is continued by increasing the gas and condensate flow rates (velocities), simultaneously to keep CGR constant. After completion of this, this step is repeated at the next CGR. The fluids are also thoroughly mixed between each two successive CGRs. This together with condensate volume collected at the end of the test are used to calculate the condensate saturation within the core using material balance for this closed system. Performing the tests at various flowing velocities is required to capture the effect of inertia and coupling on the relative permeability data. After measuring SS-kr at an IFT, all the condensate within the core is stripped and collected (together with condensate in all other parts of the rig) for the saturation calculation purpose. Having the whole set of k_r data accomplished for the first selected pressure or IFT conditions, the pressure of the system including the core and relevant oil and gas cells are raised to a pressure above the dew-point, i.e. single-phase gas. Following this, the fluid components are thoroughly mixed by circulating the fluid mixture through the sight-glass for several times. The core pressure is then depleted to the next desired pressure and all steps explained above are repeated accordingly.

4 OPTIMIZATION OF TREATMENT SOLUTION USING CONVENTIONAL FLUID SYSTEMS

4.1 INTRODUCTION

Wettability is one of the main driving factors governing the distribution of fluids in porous media, hence influencing the mobility of flowing phases. Surface thermodynamic properties of solid, e.g. rock, and surrounding fluids, e.g. gas and oil, are the key controlling parameters determining the wetting state of a system. In a solid/liquid/gas system, high energy surfaces render the spreading of the liquid on the solid, while the low energy surfaces exhibit a partial wetting characteristic with respect to the liquid phase (Whalen 1973). In the following, some important concepts about the wetting characteristics of solid substances and importance of contact angle and surface tension phenomena are presented, while further technical details about these parameters are discussed in Appendix A and Appendix B, at the end of this thesis.

The tendency of a liquid (*l*) to spread on a rock surface in the presence of a gas phase (*g*) is usually described by the spreading coefficient (*S*), which can be related to the surface forces (σ) between each pair of three phases at the triple contact line (**Figure 4.1**):

$$S = \sigma_{sg} - \left(\sigma_{sl} + \sigma_{lg}\right) \qquad \text{Equation 4.1}$$

A complete spreading or perfect wetting of the rock surface by the liquid phase occurs when the spreading coefficient is either positive or zero (de Gennes 1985, Danesh et al. 1988). The liquid phase, on the other hand, forms a droplet or partially wets the surface when the spreading coefficient is negative (Rowlinson and Widom 1982, Araujo et al. 2001).

The solid, liquid and gas system, with defined surface tension values, is considered to be in thermodynamic equilibrium when chemical equilibrium (chemical potential matching for each component present) and thermal equilibrium (temperature matching) between liquid and gas exist (Bonn et al. 2009). At such conditions, the relation between contact angle (θ) (**Figure 4.1**) and three phase surface tensions is given by Young's equation (Young 1805):

$$\sigma_{sg} = \sigma_{sl} + \sigma_{lg}\cos\theta \qquad \text{Equation 4.2}$$

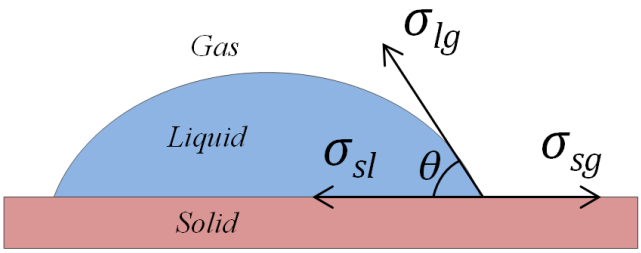

Figure 4.1: Partial wetting of a solid surface by a liquid droplet in presence of the gas phase at equilibrium conditions.

The concept of contact angle is important as one of the main wettability criteria in a system (Fowkes 1964). Accordingly, the tendency of the liquid to spread increases as θ decreases. It should be noted that the contact angle is a macroscopic quantity which together with the surface tension parameters (σ_{sg}, σ_{sl} *and* σ_{lg}) describe adequately the energy content of the interfaces (de Gennes 1985). As **Figure 4.2** depicts, three wettability states of completely-wet, partially-wet and completely-dry, can be considered for a solid/liquid/gas system, with the latter one rarely observed naturally. There have been many experimental and theoretical investigations studying the impact of rock wettability, i.e. contact angle, on wetting and non-wetting phase relative permeabilities (Owens and Archer 1971, McCaffery and Bennion 1974, Bradford et al. 1997).

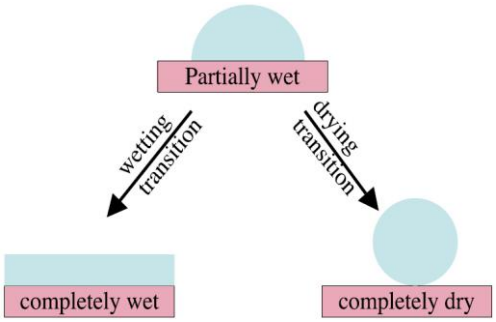

Figure 4.2: Different liquid wetting states of a solid surface.

As mentioned above, whilst the high energy surface of a solid causes the liquid phase to wet out its substrate, modification of the solid's surface energy can minimize the liquid penetration, i.e. makes the surface partially wet. For several decades fluorochemicals have been recognized (the advent of fluorinated organic chemicals is back to 1940's) as one of the most effective chemical agents altering the liquids and solids surface energy, wettability and surface activity (Jarvis and Zisman 1965). Zisman (1964), who is one of the most remarkable surface chemists of his time, states "Because of their low surface energies, fluorinated solids have the most nonwettable and nonadhesive surfaces known". Fluorochemical finishes have been used extensively in textiles as non-wetting and anti-stain agents (Hubbell 2009). Low cohesive forces inherent in fluorochemicals enable them to create low surface energy barriers. Fluorinated repellent agents are exceptionally capable of repelling both water and oil, whereas repellents with silicone or hydrocarbons repel only water. The molecular structures of two fluorinated chemical compounds are depicted in **Figure 4.3**. A fluorochemical molecule consists of two parts including fluorinated part and non-fluorinated part. The fluorinated part, called the perfluoroalkyl group, comprises of carbon atoms linked together, forming the core of the molecule, which is surrounded by the fluorine atoms forming a sheath. This creates the fluorinated tail of the chemical, which has to be oriented outward to produce an effective low surface energy barrier.

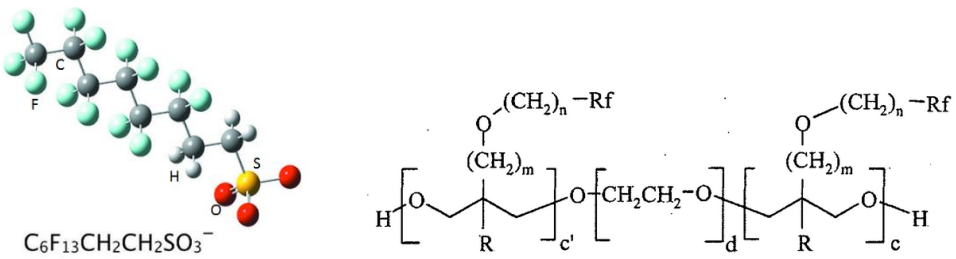

Figure 4.3: The molecular structure of a fluorosurfactant (left) and fluoropolymer (right).

Research studies (Jarvis and Zisman 1965) have shown that as the number of fluorine atoms attached to the carbon atoms increases and they are packed closer together, the chemical repellency improves. The non-fluorinated part of the chemical, known as the polar head, on the other hand, forms a backbone to the fluorochemical, anchoring it to the solid surface, hence making it more durable. A fluorochemical can be anionic, cationic, non-ionic or amphoteric according to the ionic functionality of its head moiety. The chemical's head group administrates its solubility and compatibility with other fluids and its interaction with the formation minerals. **Figure 4.4** depicts a schematic of the fluorinated molecules of a surfactant attached to a solid surface.

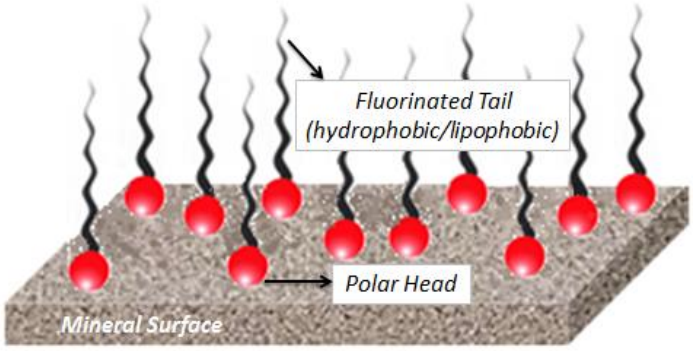

Figure 4.4: Fluorochemical adsorption on the rock substrate brings it to a water and oil-repellent state.

4.2 SCREENING TESTS ON CHEMICALS

Fluorochemicals for enhanced oil recovery purposes have a long established history but their applications for alleviation of condensate banking have received attention only recently. This is because for the latter much lower surface energies are to be achieved to alter the rock wettability from strongly liquid-wetting to intermediate gas-wetting conditions whilst for the former the solid surface wettability characteristics for different liquids (i.e. oil and water) are altered. Furthermore, fluid phase behaviour and flow of gas-condensate systems have been well recognized, both experimentally and theoretically, to be unique but complex compared to conventional gas-oil systems. In Chapter 2 of this thesis the main complications in dealing with such reservoirs were discussed. Working with gas-condensate systems and obtaining reliable experimental results is a demanding and laborious task accordingly. On the other hand, there are various variables influencing the performance of a chemical, such as chemical concentration, type of solvent, temperature, type of mineral and etc., which all have to be carefully scrutinized to reach an optimum treatment solution. For such reasons, initial investigations (on the performance of each chemical) were primarily confined to

using conventional gas-oil fluids, e.g. Air-nC10, N2-nC10 and N2-H2O, rather than more complex gas-condensate ones, eliminating the costly and time-consuming experiments associated with condensing systems. These initial screening tests include: contact angle measurements, spontaneous imbibition tests, unsteady-state displacement tests and brine compatibility tests. Contact angle measurements were the first stage among all screening tests, from which the impact of chemical concentration, solvent composition, temperature and mineralogy on the wettability alteration process were investigated. It should also be mentioned that the ultimate performance of the optimized chemical solutions, achieved through the screening tests, was finally evaluated for more realistic conditions of gas-condensate systems as discussed in Chapters 5 and 6.

4.2.1 Chemicals Selection Criteria

The main aim of chemical treatment is to alter the rock wettability from strongly liquid-wetting to intermediate gas-wetting conditions, verified principally through apparent change in contact angle values. Considering that typically reservoir rocks are preferentially liquid-wet (in presence of the gas phase) in their virgin state (i.e. θ=0º), the contact angle attained after the chemical adsorption on the surface should be 90º or above to achieve an effective altered wettability conditions. Furthermore, there are several other important factors that from the reservoir engineering point of view need careful attention for design and application of such wettability modifiers in field scales. Following are the main criteria to be considered.

High Temperature Formations

Gas-condensate fluids are typically found in deep formations with high temperatures ranging between 100 and 200ºC. The thermodynamic interactions between the chemical molecules and charged minerals are highly influenced by the reservoir conditions, in particular temperature. The chemical's reaction rate and its magnitude hence should be carefully assessed for each specific condition. The chemical agents should also be able to sustain their functionalities at high-temperature conditions. In this work, the author initially explored the chemical performance at low temperature conditions of 65ºC (and in some cases 90ºC) and then after obtaining favourable results, high-temperature treatments at 130ºC were carried out.

Alcohol-Based Solvents

The fluorochemical molecules form the core structure of a treatment solution and are responsible for creating favourite water/oil repellent sites on the rock surface. Beyond

this, the type and composition of the chemical solvent, known as carrier fluid, has also a crucial role on the treatment performance. The carrier solvent in fact governs the chemical delivery and interaction with the rock surface during the injection as well as its clean-up efficiency during the post-treatment production period.

Fluorochemicals are mostly water-soluble, with some soluble in oil-based solvents as well. Alcohol-based solvents, which are pure alcohols, alcohol blends or alcohol/water mixtures, can also be used as an alternative carrier fluid. Although alcohol-based, compared to water-based, fluids are less favourable solvents for surface finishes due to safety and environmental considerations, from a reservoir engineering point of view they are the most desirable carrier solvents for field applications because: 1- alcohol-based solvents minimise the adverse effect of chemical solution back-flow during after-treatment production period owing to their high volatility and mobility, 2- alcohol as the carrier fluid can efficiently wash out the resident fluids such as brine and condensate, accumulated around the wellbore, hence provides sufficient adsorption sites for chemical molecules and 3- it is believed that the size of the chemical aggregates (i.e. collection of several chemical particles attached together to reach more stability in the solution) is smaller in alcohol-based solvents, because of the lower polarity of alcohols compared to water, hence less permeability impairment of the porous rock is anticipated.

Formation Permeability Damage

To achieve an effective and long-lasting wettability alteration, it is essential to have strong and robust chemical bonds between the wettability modifier molecules and the mineral surface. Increasing the fluorine content of a fluorinated compound would serve this purpose by intensifying the chemical reaction with the surface. This, however, enlarges the size of the chemical aggregates existing in the solution. Chemicals with large particles or those that overreact with the surface can impair the rock permeability unfavourably. An effective chemical adsorption is the one that causes minimum/zero permeability damage.

Formation Resident Brine

A hydrocarbon formation typically contains brine, which is either interstitial connate water, entrapped in the pore spaces of sediments during their deposition, or water conning from a bottom-layer aquifer, risen towards the well perforations. The salinity and pH of the brine strongly affect the surface charge of the rock mineral, which in turn would influence the adsorption of surfactant molecules on the rock surface (Stumm and

Morgan 1970, Leja 1982). Moreover, dissociated ions in brine can cause the chemical to salt out. That is, salt ions attract the solvent (e.g. water) molecules and as a result the interactions between chemical molecules become stronger than solvent-solute interactions. Consequently, the chemical molecules coagulate by forming hydrophobic interactions with each other. Such incompatibility between treatment solution and resident brine results in poor chemical performance and also precipitation of chemical particles, which in turn can severely damage the reservoir rock permeability.

Environmental Considerations

The fluorochemical solutions have two key portions: fluorinated chemical and carrier solvent. There are potential health and safety concerns inherent in both parts. PFOS (perfluorooctane sulfonate), PFOA (perfluorooctanoic acid), PFHxS (perfluorohexane sulfonate) and their associated compounds are persistent (do not break down) and toxic chemicals with proven detrimental impacts on environment and humans health. There are also environmental and safety issues associated with the carrier solvents, e.g. some alcohols like methanol, injected under the ground. In recent years, the introduction of shorter perfluoroalkyl chain compounds against the typical C8 (or longer) ones, used in the past, has considerably fulfilled the government and industry desires for PFOA-free products. Accordingly, fluorochemical products based on the short-chain technology, using 6 or less fluorinated carbon atoms, have little tendency to bio-degrade in the environment and furthermore their by-products can faster break down than PFOA.

4.3 FLUORINATED WETTABILITY MODIFIERS

Fluorochemical agents used in this research programme as wettability modifiers were sourced from DuPont de Numerous, an American chemical company considered as one of the major and leading manufacturers of the fluorinated chemicals in the globe. A wide range of Zonyl® and Capstone® products, i.e. commercial names for DuPont surfactant and repellent agents, were employed in line with the extensive investigations carried out for finding effective wettability modifiers for carbonate minerals.

The investigations were initially started on Zonyl® type chemicals, followed by recently developed Capstone® fluorochemicals repellent agents. DuPont has developed this new line of surface protection products based on sustainable short-chain technology ($F(CF_2)_nCH_2CH_2$–, where n=6 or shorter) that deliver superior performance, supported by extensive health and safety testing. That is, they cannot break down and degrade to degradation products harmful to the environment and human life. Furthermore, the corresponding potentially degradation products have a favorable environmental profile

with low absorption, rapid bioelimination, low toxicity and do not bioconcentrate or bioaccumulate. Capstone® repellent and surfactant products have been designed in accordance with the goals of U.S. EPA 2010/15 PFOA stewardship program aligned with the direction of global regulatory, costumers and the markets needs. Capstone® chemicals are currently replacing all previous Zonyl® products.

In total, the performances of fifteen different fluorinated chemicals were evaluated in a series of screening experiments. The following is a list of these chemicals describing their main properties and specifications. It should be noted that the suggested use rates and appropriate solvents for these chemicals, mentioned below, are based on their available technical data sheets from DuPont, whereas such information are subject to change according to the chemical's performance observed during screening tests.

***Zonyl 210*:** Solvent-based non-ionic acrylic fluorinated co-polymer, composed of 25% solid and 75% Isopar H, suggested use rate: 1.5-2.5% active ingredient diluted in hydrocarbons (e.g. Heptane) or alcohol/hydrocarbon mixtures (80/20).

***Zonyl 225*:** Solvent-based non-ionic acrylic fluorinated co-polymer, composed of 25% solid and 75% Butylacetate, suggested use rate: 1.5-2.5% active ingredient diluted in hydrocarbons or alcohol/hydrocarbon mixtures.

***Zonyl 8740*:** Water-based cationic perfluroalkyl methacrylic copolymer, composed of 30% polymeric fluoroadditive and 70% water, suggested use rate: 1-5% active ingredient diluted in water or alcohol-based solvents.

***Zonyl FSG*:** Solvent-based non-ionic Flourinated methacrylate polymer, composed of 40% fluorosurfactant and 60% Isopar H, suggested use rate: 0.1-0.5% active ingredient.

***Zonyl FS-610*:** Water-based anionic phosphate fluorosurfactant, composed of 22% fluorosurfactant and 78% water, suggested use rate: 0.05-0.2% active ingredient.

***Capstone FS-61*:** Water-based dispersion of anionic fluorosurfactant, composed of 13-15% solids in water, suggested use rate: 0.005-0.5% active ingredient.

***Capstone FS-84*:** Aqueous dispersion of cationic fluorinated acrylic copolymer, composed of 25% solids in water, suggested use rate: 0.5% active ingredient.

***Capstone FS-65*:** Water-soluble non-ionic (slightly anionic) fluorosurfactant, composed of 25% solids in 75% water, suggested use rate: 0.01-0.5% active ingredient.

***Capstone FS-30*:** Water-soluble ethoxylated nonionic fluorosurfactant, composed of 25% solids in 75% water, suggested use rate: 0.01-0.1% active ingredient.

***Capstone FS-31*:** Aqueous or solvent-based non-ionic fluorosurfactant, composed of 25% solids in 75% water, suggested use rate: 0.01-0.1% active ingredient.

***Capstone FS-34*:** Water-soluble ethoxylated nonionic fluorosurfactant, composed of 25% solids in 75% water, suggested use rate: 0.01-0.1% active ingredient.

***Capstone FS-22*:** Solvent-borne nonionic fluorosurfactant (partially fluorinated acrylic copolymer), composed of 30% solids in methyl isobutyl ketone, soluble >5% in diesel fuel, mineral spirits, butyl acetate, n-heptane, toluene, xylene.

***Capstone FS-64*:** Water-soluble anionic fluorosurfactant, composed of 15% solids in 85% water, suggested use rate: 0.01-0.1% active ingredient.

***Capstone FS-82*:** Aqueous dispersion of a cationic fluorinated acrylic copolymer, composed of 25% solids in water, suggested use rate: 0.2-1% active ingredient

***TLF 10696*:** Water-based amphoteric fluorinated polymer with 30% solid content.

4.3.1 Chemicals Overall Performance

Many studies on the reservoir rock chemistry have verified that the surface charge of silica (e.g. sandstone rocks) and calcite (e.g. carbonate rocks) in water is positive at low pH, while it becomes negative at higher pH values. Accordingly, the silica surface becomes negatively charged when pH increases above 2 to 3.7 and calcite stays positively charged before pH exceeds to about 8 to 9.5 (Anderson 1986). Therefore, at neutral pH, the carbonate minerals remain positively charged, hence both anionic and nonionic surfactants can potentially bond with the carbonate surface, altering its wettability. The cationic compounds, on the other hand, would make stronger interactions with the negatively charged sandstone surfaces. In this study four different ionic groups, i.e. non-ionic, anionic, cationic and amphoteric, of fluorinated chemicals were used to identify their impacts on the carbonate minerals.

As stated above, both anionic and non-ionic compounds are potential wettability modifiers for carbonate minerals. Furthermore, non-ionic chemical agents possess considerably better sustainability in the brine medium among all ionic functionality groups. This explains why the majority of the chemicals tested here, i.e. eight out of fifteen, were selected from non-ionic repellents, as listed above.

As mentioned earlier, prior to any other experiment, contact angle measurement tests were carried out on treated carbonate substrates using various chemical compositions with varying chemical concentration and solvent. The observed contact angles provided a quick and apparent image of the chemical's overall oil- and water-repellency strength.

A good level of oil/water repellency is considered for chemical solutions with measured contact angle of 90º or above ($\theta \geq 90^{o}$), as per **Table 4.1**. As the main intention of this research programme was to seek out effective wettability modifiers for both water blockage and condensate banking issues, the chemical is considered appropriate when it delivers both water and oil repellencies to the carbonate substrate together. Whilst the majority of the chemicals from different ionic groups showed effective water repellencies, only two anionic (Zonyl FS-610 and Capstone FS-61) and two non-ionic (Zonyl 225 and Capstone FS-65) chemicals provided promising oil, as well as water, repellencies . This was also in agreement with the general understanding about the positively charged surfaces of the carbonate minerals and their inherent tendency to bond with anionic and non-ionic compounds. For the sake of simplicity, the chemicals mentioned above are hereafter abbreviated as Z-610, C-61, Z-225 and C-65, respectively. Here it should be mentioned that C-61 is the alternative Capstone-type fluorosurfactant to Z-610. The results of the screening tests performed on these chemicals are discussed in the following sections.

Table 4.1: The performance of four different groups of fluorinated wettability modifiers on carbonate substrates.

Chemical Type	No.	Product Name	Solvents	Oil Repellency	Water Repellency
Non-ionic	1	Capstone FS-65	DIW	✓	✓
	2	Zonyl 225	Heptane, Heptane/IPA (1:3)	✓	✓
	3	Zonyl 210	Heptane	✗	✓
	4	Capstone FS-22	Heptane, IPA	✗	✓
	5	Zonyl FSG	Heptane	✗	✓
	6	Capstone FS-30	DIW , MeOH , IPA	✗	✗
	7	Capstone FS-34	DIW , MeOH , IPA	✗	✗
	8	Capstone FS-31	DIW , MeOH , IPA	✗	✗
Anionic	9	Capstone FS-61	DIW/IPA (3:1) , MeOH	✓	✓
	10	Zonyl FS-610	DIW	✓	✓
	11	Capstone FS-64	DIW , MeOH	✗	✗
Cationic	12	Zonyl 8740	DIW/IPA (1:3)	✗	✓
	13	Capstone FS-84	DIW	✗	✓
	14	Capstone FS-82	DIW	✗	✓
Amphoteric	15	TLF 10696	DIW, MeOH, EtOH	✗	✗

4.4 PERFORMANCE OF Z-225

4.4.1 Contact Angle Measurements

The contact angle measurements were conducted with the aim of evaluating the impact of temperature, treatment duration and chemical solution (CS) composition on the treatment. Texas Cream carbonate substrates were used for these series of tests.

Table 4.2 shows the results of different treatments performed using this chemical. In Tests #1 and #2, both treatments with 1.5 and 3 wt% chemical diluted in Heptane almost showed similar results, i.e. $\theta_{C10\text{-}air}$=96-97° and $\theta_{DIW\text{-}air}$=141-145°. However, tracking the contact angles over a period of time (e.g. 20 minutes) demonstrated that using 3 wt% Z-225 results in noticeably more stable contact angles than low-concentrated solution with 1.5 wt% Z-225. That is, in 1.5 wt% treatment case $\theta_{C10\text{-}air}$ reduced substantially from its initial value of 96° to 14° within 20 minutes, whereas in 3 wt% case, θ only reduced to 86° over the same period. **Figure 4.5** depicts the deposited decane drops on both treated substrates versus time.

Tests #3 and #4 were both performed at 90°C but with two different soaking time of 6 and 18 hours. This was to examine the impact of the treatment duration on the wettability alteration process and to verify whether the 18 hours treatment time, used as a code of practice in these treatments, was sufficient to achieve the maximum chemical performance. Almost similar $\theta_{C10\text{-}air}$ of 95° and 98° were observed for 6 and 18 hrs treatments respectively, with the difference to be minimal and within the experimental error of the contact angle measurement tests, i.e. ±5°.

Tests #5 and #6 were conducted at 130 and 190°C, aiming at investigating the impact of high temperatures on the treatment. Contact angles of 93° and 84° were obtained for the C10-air system, respectively. The slight reduction in contact angles compared to low-temperature treatments at 65 and 90°C can be related to the increased level of the chemical solubility in solution at higher temperatures, resulting in lesser interactions between the chemical molecules and the rock surface and therefore lower oil-repellency strength of the surface.

Two additional experiments, Tests #7 and #8, were also carried out using two alcohol-based solvents, i.e. Heptane+IPA and Heptane+EtOH, both mixed with a weight ratio of 1:3, at 130°C. Whilst the level of water repellency was preserved, a slight reduction in oil repellency was observed for both alcohol-base solvents (i.e. $\theta_{C10\text{-}air}$=84°). Generally speaking, alcohols tend to decrease the CMC (critical micelle concentration) of the surfactants, which in turn can increase the solubility of the

surfactant molecules inside the solution. This can reduce the interaction between the chemical molecules and the charged minerals and subsequently, causes lesser extent of liquid repellency. This trend, i.e. the reduction of the chemical liquid-repellency by adding alcohol proportions to the solution, was also observed, even to a greater extent, for other chemical compounds used in this work as discussed in the following sections.

Table 4.2: Contact angle measurements on treated Texas Cream carbonate substrate using Z-225, investigating the impact of chemical solution composition, temperature and treatment duration on wettability alteration.

Test No.	Chemical Solid Percent (wt%)	Solvent	Treatment Temperature (°C)	Treatment Duration (hr)	C10/Air Conatct Angle (Degree)	DIW/Air Conatct Angle (Degree)
1	1.5	Heptane	65	18	96	145
2	3	Heptane	65	18	97	141
3	3	Heptane	90	6	95	-
4	3	Heptane	90	18	98	-
5	3	Heptane	130	18	93	-
6	3	Heptane	190	18	84	144
7	3	Heptane+IPA (1:3)	130	18	84	142
8	3	Heptane+EtOH (1:3)	130	18	84	145

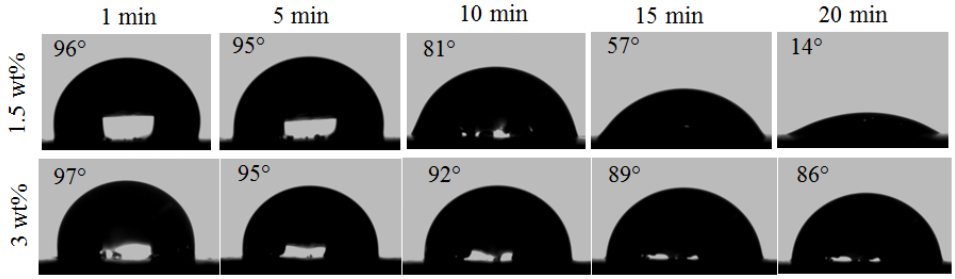

Figure 4.5: Decane contact angles measured on treated carbonate substrate using two different concentrations of 1.5 and 3 wt% Z-225 diluted in Heptane at 65°C at different time periods, demonstrating sustainable oil-repellency achieved by high-concentrated solution (i.e. 3 wt%).

4.4.2 Spontaneous Imbibition Tests

Considering that 3 wt% Z-225+Heptane showed better performance compared to other chemical solutions at high temperatures, observed over the course of contact angle measurements, it was decided to further investigate the performance of this chemical solution on treated cores. Before treatment process, pre-treatment free imbibition tests

were performed using nC10 and DIW. These tests were conducted on Texas-Cream core TC1. **Table 4.3** shows the properties of this core and other carbonate cores used in this work to perform screening tests. To treat the core, the dry sample was evacuated and saturated with chemical solution and then aged for 18 hrs at 130°C. Post-treatment imbibition tests were then conducted and compared with those measured before the treatment as shown in **Figure 4.6**. A significant decrease in the total amount of water imbibed into the core is evident after the treatment, demonstrating an effective wettability alteration process with respect to the water phase. On the other hand, whilst the oil imbibition rate has declined to some extent after the wettability alteration, the final amounts of the oil imbibed into the core are similar before and after the treatment. These observations demonstrate that the chemical solution (and/or the treatment method as discussed later for chemical Z-610) has probably not been effective to alter the rock wettability with respect to the oil phase, despite the promising results of contact angle measurements. This chemical was not further tested due to environmental considerations about the Zonyl products. That is, future tests were performed with the new type of Capstone fluorochemicals with more ecological friendly characteristics.

Table 4.3: Rock properties of carbonate cores (1″ diameter) used during the course of screening tests.

Core Index	Length (cm)	K (md)	Ø (%)	Chemicals Used
TC1	4.7	-	22	Z-225
TC2	9.0	10.8	29	Z-610
TC3	8.8	9.7	25	Z-610
TC4	8.8	10	30	C-65
TC5	8.8	10	30	C-61
TC6	7.1	14	27	C-61
BD18	7.9	122	26	C-61
BD14a	7.9	58	21	C-61
BD14b	6.3	92	27	C-61

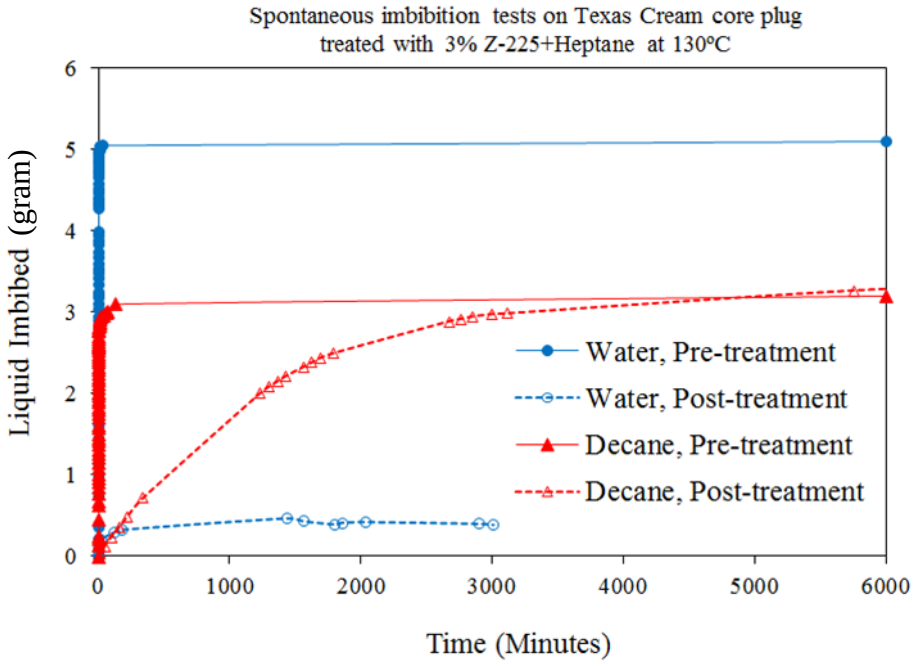

Figure 4.6: Pre- and Post-treatment spontaneous imbibition tests with DIW and nC10 on treated carbonate core (TC1) by using 3 wt% Z-225+Heptane at 130°C.

4.5 PERFORMANCE OF Z-610

Z-610 is an anionic fluorosurfactant, which is primarily a water-based chemical but can also be dissolved in water/alcohol mixtures. Z-610 is expected to make strong water- and oil-repellent bonds with the carbonate minerals because of its anionic functionality.

4.5.1 Effect of Solvent Composition

Contact angle measurements, like those mentioned for Z-225, were performed using various concentrations of chemical Z-610, diluted in its basic solvent, i.e. DIW. The results proved 0.5 wt% of this fluorosurfactant is able to bring satisfactory level of liquid-repellency to the rock surface at 130°C, i.e. $\theta_{C10\text{-}air}$=115° and $\theta_{DIW\text{-}air}$=139°. Because alcohol-based solvents are more favourable carrier fluids than water-based ones, their potential in delivering this anionic chemical was also investigated. **Figure 4.7** shows a number of these tests conducted using DIW/IPA or DIW/EtOH solvent mixtures. Overall, Z-610 showed poor oil-repellency when delivered by a water/alcohol mixture, whilst its good water-repellency characteristic was preserved in many cases similar to that of water-based solvent. The lesser extent of oil-repellency with alcohol-based solvents compared to that of water-based one was related to the reduced level of chemical adsorption on the rock surface due to its higher molecular activity in alcohols. The alcohol type and its proportion inside the solution affect the extent of this

behaviour. Since alcohol-based solvents showed poor oil-repellency, it was decided to concentrate studies on water-based solutions.

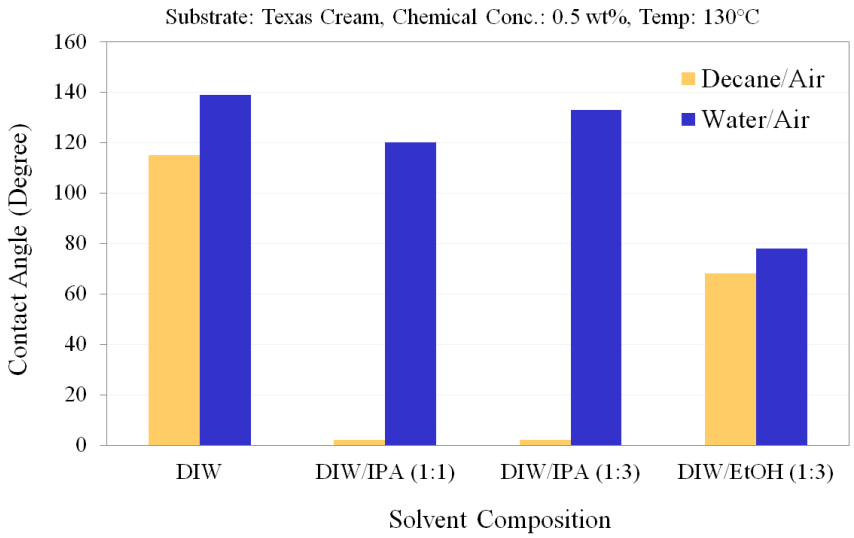

Figure 4.7: Effect of solvent composition on the performance of anionic chemical Z-610 on wettability alteration of carbonate rock at 130°C.

4.5.2 Treatment at Elevated Temperatures

To evaluate the stability and effectiveness of Z-610 wettability modifier at harsh realistic reservoir conditions, two treatments, using 0.5 wt% Z-610+DIW, at elevated temperatures of 160 and 190°C, were conducted. Promising C10-air and DIW-air contact angles like those measured at 130°C were obtained. However, as **Figure 4.8** depicts, an undesirable layer of chemical was precipitated on the rock surface in both cases. It is likely that increasing the temperature has intensified the reactions between the polar head group of the chemical and the positively charged surfaces of the carbonate mineral.

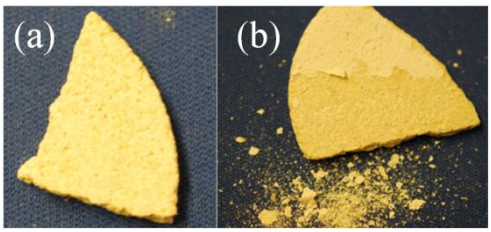

Figure 4.8: Texas-Cream carbonate substrates treated by 0.5wt% anionic chemical Z-610 diluted in DIW at different temperatures of: a) 130°C and b) 160 and 190°C. A deposited layer of chemical is evident on the treated rocks for case (b).

4.5.3 Brine Compatibility Test

These tests were performed by combining 1 wt% Z-610+DIW with different brine solutions at a weight ratio of 1:1. It is noted that at this mixing ratio, the final chemical concentration in solution becomes 0.5 wt%. **Figure 4.9** and **Figure 4.10** depict the phase behaviour of the chemical agent inside the solution for different brine compositions at 20°C (room) and 90°C temperatures. As **Figure 4.9** shows, whilst chemical Z-610 showed acceptable compatibility with 1% NaCl brine, increasing the NaCl concentration to 10% caused the instability and coagulation of chemical particles. CaCl2 brine showed more adverse effect, compared to NaCl, as the chemical severely coagulated even at low concentration of 1 wt%. The chemical instability was also observed at low- and high-salinity NaCl/CaCl2 brines. Almost similar phase behaviours, albeit to a lesser extent, were also observed at 90°C. That is, the chemical precipitation was evident but its amount was less at this higher temperature, demonstrating the increased level of chemical solubility inside the solution. These observations underline the importance of the type of salt components and moreover their concentrations in the formation brine composition on the stability and therefore performance of such fluorinated chemicals.

The performance of the 1 wt% Z-610+DIW chemical solution contaminated with 1% NaCl brine, with a weight ratio of 1:1, was also evaluated by performing contact angle measurements on the treated carbonate substrate at 130°C. Acceptable level of wettability alteration resulting in contact angles of $\theta_{C10\text{-}air}$=87° and $\theta_{DIW\text{-}air}$=134° were obtained, showing the preserved level of chemical effectiveness in a solution contaminated with this brine.

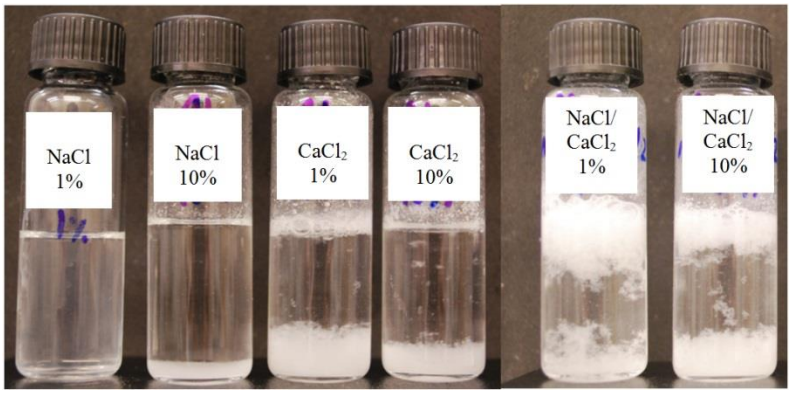

Figure 4.9: Brine compatibility tests performed on anionic chemical Z-610 (1wt%+DIW) after contamination (with a weight ratio of 1:1) with different types of brines at room (20°C) temperature.

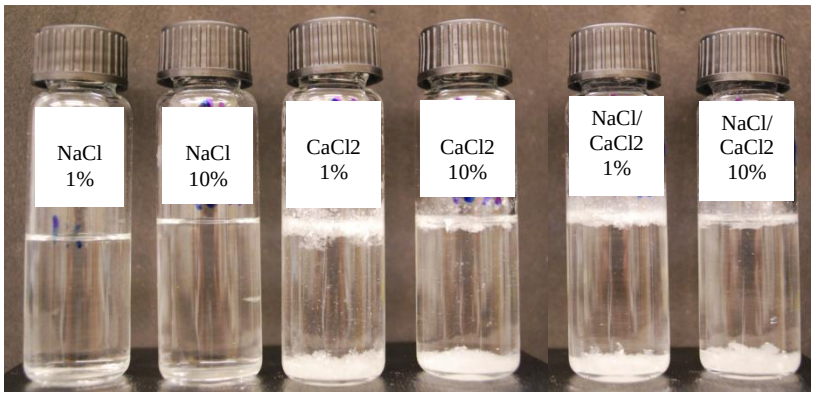

Figure 4.10: Brine compatibility tests performed on anionic chemical Z-610 (1wt%+DIW) after contamination (with a weight ratio of 1:1) with different types of brines at 90°C.

4.5.4 Core Treatments

The optimum treatment solution of 0.5 wt% Z-610+DIW was used to treat TC2 carbonate core at 130°C. Here to examine the effect of chemical delivery method and volume of injected chemical on treatment performance, two different methods were investigated: 1- the evacuated core was saturated with 1 PV chemical solution and then aged for 18 hrs at 130°C and 2- approximately 10 PVs of chemical solution were injected through the core with a constant flow rate of 20 cc/hr at 130°C and then the core was aged for extra 18 hrs in the solution. The remaining chemicals in both cases were displaced by N2 at the end of treatment and the core was dried for subsequent imbibition and displacement tests. It should be noted that TC2 was initially treated by the first method and following an unsuccessful treatment, as discussed later, was re-treated with the second procedure.

Imbibition and Displacement Tests

Figure 4.11 and **Figure 4.12** show the spontaneous free imbibition and unsteady-state displacement tests, respectively, carried out on TC2 before and after each treatment. The water imbibition tests (**Figure 4.11**) demonstrate that the rock wettability has been significantly altered with respect to the water phase following the first treatment procedure (method-1). However, the oil imbibition curves before and after the first treatment show minimal difference and follow almost similar trends. This implies method-1 has delivered insufficient amount of chemical onto the rock surface to effectively render it oil-repellent. The trends of the differential pressures during the displacement tests by decane (**Figure 4.12**) are also consistent with this observation. On

the other hand, exposing the rock surface to considerably larger amount of chemical agents by injecting 10 PVs CS through the core, i.e. method-2, demonstrated a promising level of oil-repellency. Both imbibition and displacement tests after the second treatment, strongly confirm this fact (**Figure 4.11** and **Figure 4.12**).

To confirm the previous findings and evaluate the potential of Z-610 anionic chemical on improving the oil mobility, it was decided to conduct new series of USS displacement tests using equilibrated nC10/N2 at 1000 psi to eliminate the component exchange between non-equilibrated nC10 and N2 phases, which might have happened during the previous tests performed on TC2. Accordingly, another carbonate core (TC3) was treated using method-2. **Figure 4.13** shows the differential pressures corresponding to pre- and post-treatment conditions during these displacement tests. An average oil saturation of about 0.79 at the stabilized conditions, when the pressure drops reached a plateau, was obtained for both untreated and treated cases using a material balance calculation. Subsequently, the end-point oil relative permeability before and after the treatment was estimated to be 0.17 and 0.27, respectively, using Darcy's law. This verifies the improvement of end-point k_{ro} almost by a factor of 1.6 as a result of wettability alteration. Absolute permeability measurements also demonstrated no sign of permeability damage after the treatment. Z-610, Zonyl-type fluorinated chemical, was later phased out for further investigations, as DuPont replaced it with a more eco-friendly Capstone FS-61 fluorosurfactant.

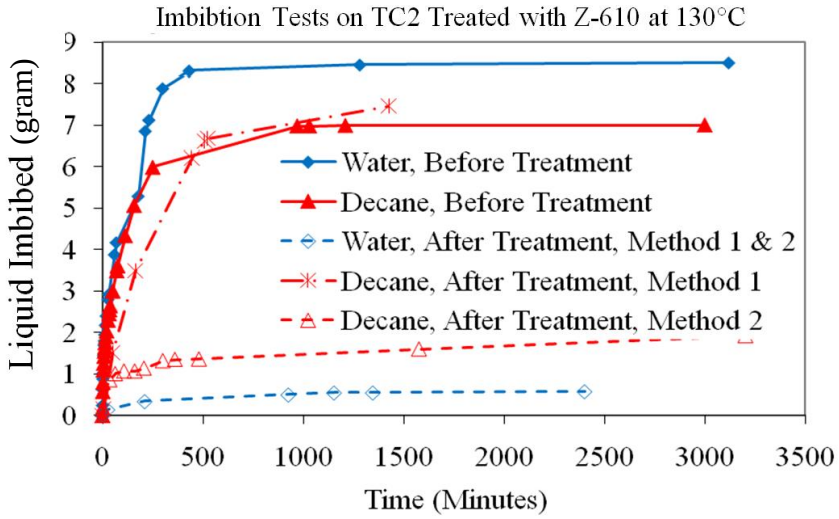

Figure 4.11: Spontaneous imbibition tests before and after treatment for the TC2 carbonate core treated by 0.5 wt% anionic chemical Z-610+DIW at 130°C using two treatment methods: 1-saturating core by 1 PV chemical solution and 2- injecting 10 PVs chemical solution through the core.

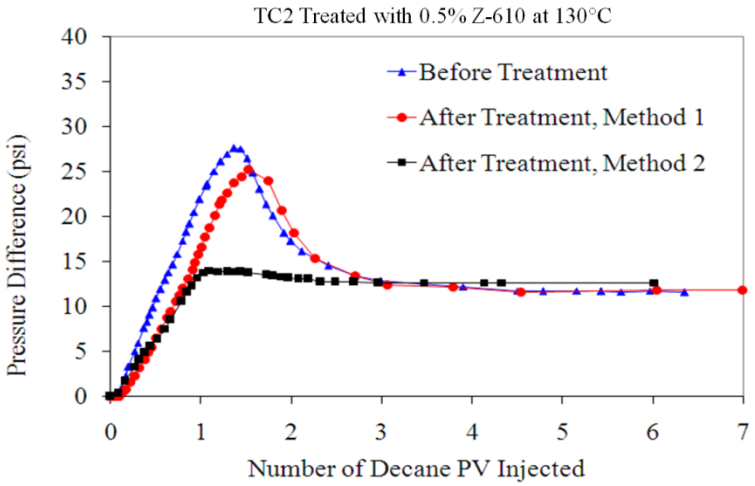

Figure 4.12: Differential pressures during unsteady-state injection of non-equilibrated nC10 into the TC2 carbonate core (100% saturated with N2, outlet pressure=14.7 psi) before and after treatment by 0.5 wt% Z-610+DIW at 130°C using two treatment method: 1-saturating core by 1 PV chemical solution and 2- injecting 10 PVs chemical solution through the core.

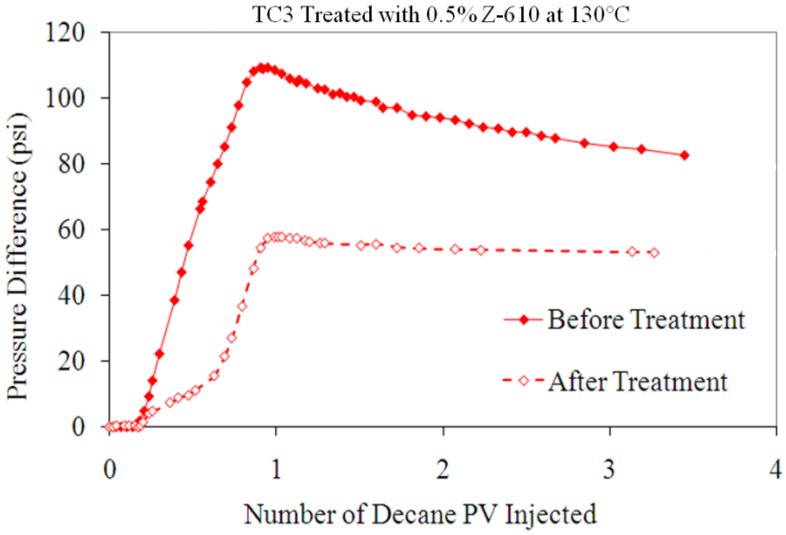

Figure 4.13: Differential pressures during unsteady-state injection of equilibrated C10 (with N2) with a flow rate of 20 cc/hr into the TC3 core (100% saturated with N2, outlet pressure=1000 psi) before and after treatment by 0.5 wt% Z-610+DIW at 130°C.

4.6 PERFORMANCE OF C-65

C-65 is a water-soluble fluorosurfactant. It has mainly non-ionic functionality with a slightly anionic structure as a part of its formulation. It was believed that the non-ionic group would deliver good stability in brine media and the anionic head, on the other hand, can provide effective interactions with the positively charged carbonate minerals.

4.6.1 Chemical Concentration versus Temperature

Contact angle measurements were conducted at various chemical concentrations at two low- and high-temperature limits. **Figure 4.14** and **Figure 4.15** show the corresponding contact angles measured on the treated substrates at 65 and 130°C, respectively. In all treatments the chemical agent was diluted in DIW, as its basic aqueous solvent. It should be noted that the treatments were unpromising when the chemical was delivered in alcohol or combined water/alcohol solvents.

From **Figure 4.14** it is noted that whilst the non-ionic chemical effectively repels the water phase at low concentration of 0.1 wt% ($\theta_{DIW\text{-}air}$ = 120°) at 65°C, it is ineffective with respect to the oil phase. Increasing the chemical concentration to 0.5 wt% provides acceptable level of oil- as well as water-repellency (second test in **Figure 4.14**). However, at higher concentration of 1 wt% of the chemical agent it is noted that the water-repellency deteriorates while chemical still provides promising level of oil-repellency. Performing similar experiments at 130°C (**Figure 4.15**) showed almost the same trend of contact angles as those observed at 65°C. However, at this higher temperature the carbonate substrate became both water- and oil-repellent at 0.1 wt% while water-repellency deteriorated at concentrations above 0.1 wt%. These observations, first of all, show that at higher chemical concentrations the water-repellency abates, which can be attributed to the possible formation of surfactant bilayers on the rock surface. This increase, however, is in favour of increasing the oil-repellency strength of the chemical. The temperature, on the other hand, accelerates the chemical adsorption on the rock surface, making it more effective at lower, more desirable, concentration limits.

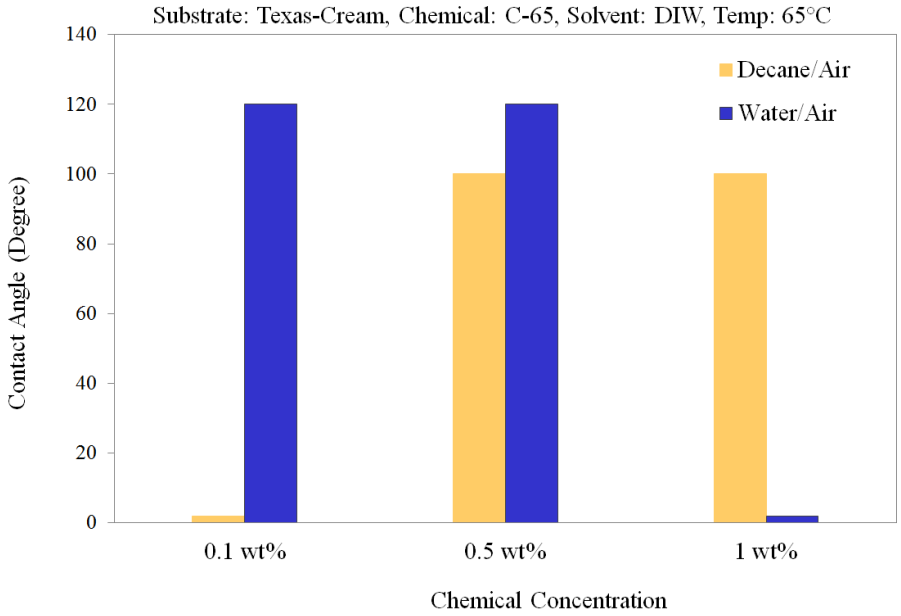

Figure 4.14: Effect of non-ionic chemical (C-65) concentration on wettability alteration of carbonate substrate at 65°C.

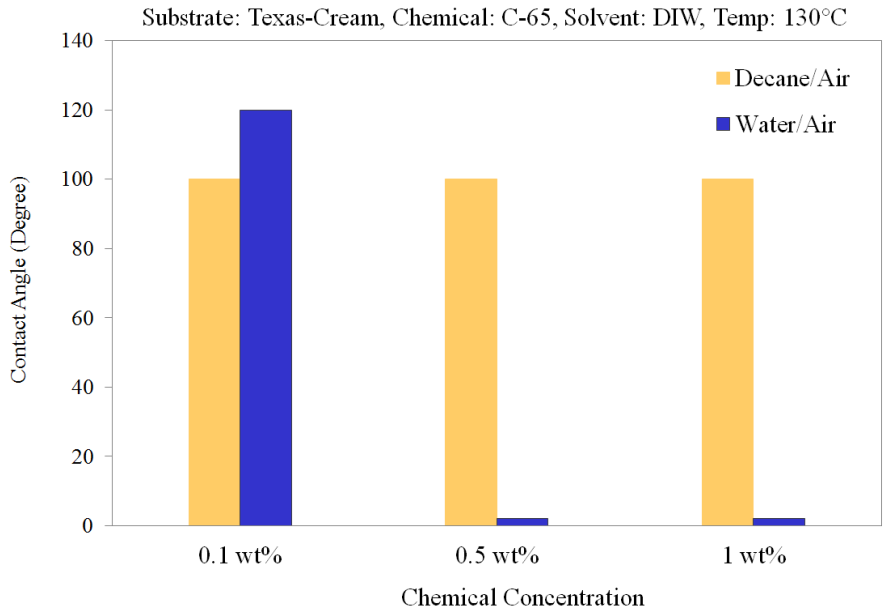

Figure 4.15: Effect of the non-ionic chemical (C-65) concentration on wettability alteration of carbonate substrate at 130°C.

4.6.2 Effect of Brine on Chemical Performance

Chemical C-65 owing to its non-ionic head group showed satisfactory level of stability in low- and high-salinity brines (i.e. 1 and 10wt% NaCl+CaCl2) at different chemical concentrations. **Figure 4.16** and **Figure 4.17** depict the phase behaviour of 0.1 and 0.5 wt% of C-65 dissolved in a solution of DIW+brine (1:1) at two temperatures of 20°C and 90°C, respectively. It is noted that there is no sign of chemical precipitation/suspension observed at both levels of chemical concentrations, albeit more

opaque solutions were noticed at higher fractions of the chemical's active ingredient, i.e. 0.5 wt%, at room temperature. The solutions, however, became more transparent, i.e. chemical solubility increased, as the temperature was raised to 90°C.

To examine the impact of brine on wettability alteration process, 0.2 wt% C-65+DIW mixed with 10 wt% NaCl/CaCl2 brine (with a weight ratio of 1:1) was also tested at 130°C. Accordingly, $\theta_{C10\text{-}air}$ of 100° was obtained after the treatment. However, water-repellency of the chemical was deteriorated, i.e. $\theta_{DIW\text{-}air}$=0°, compared to the free-brine solution treatment (first test in **Figure 4.15**). It is likely that the existence of brine ions in the solution and their affinity to attach to the solvent molecules, has caused more chemical moieties to be free and bond with the mineral surface. As was mentioned before, excessive adsorbed layer of chemical molecules (formation of bilayers) on the rock surface would reduce the chemical's water-repellency strength, whereas its oil-repellency increases.

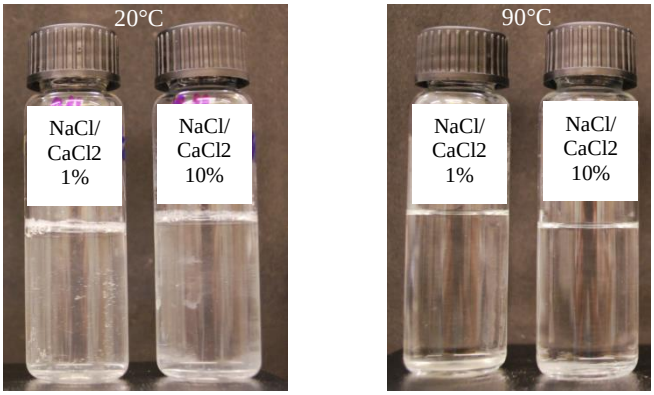

Figure 4.16: Brine compatibility tests performed on non-ionic chemical C-65 (0.2wt%+DIW) after contamination (with a weight ratio of 1:1) with two different brines at 20°C (left) and 90°C (right).

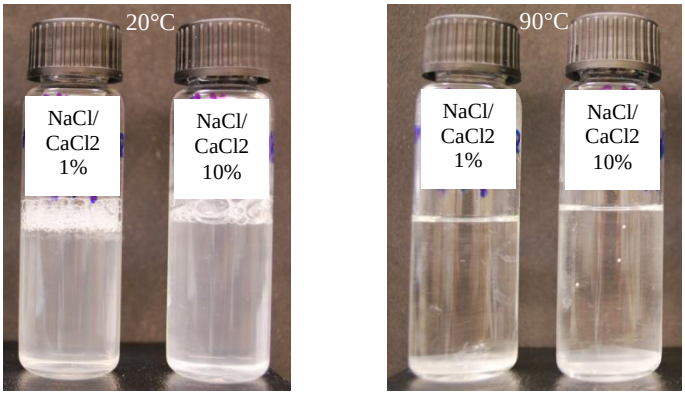

Figure 4.17: Brine compatibility tests performed on non-ionic chemical C-65 (1wt%+DIW) after contamination (with a weight ratio of 1:1) with two different brines at 20°C (left) and 90°C (right).

4.6.3 Core Treatments

Following the contact angle measurements, 0.1 wt% surfactant C-65 diluted in DIW was selected as the optimum treatment solution, providing satisfactory levels of oil- and water-repellency at 130°C. Accordingly, this treatment solution was selected to treat a Texas-Cream core plug by injecting 10 PVs of CS at a flow rate of 20 cc/hr into the core at 130°C. The post-treatment differential pressures during the unsteady-state displacement tests were to some extent above those of the pre-treatment case, demonstrating the rock permeability impairment during the injection of chemical solution. Careful examination of the rock surface showed that the damage has only occurred at the core inlet face, in which a precipitated layer of chemicals was observed. This was confirmed when the rock permeability restored to its original value after trimming a thin layer (about 3 mm) off the core inlet-face.

It was hypothesized that perhaps long-lasting retention of the chemical solution in the core, especially at the upstream conditions, while injecting at the low rate of 20 cc/hr, has caused the excessive adsorption of the chemical at the core inlet face. Accordingly, to minimize the retention time, in another test performed on the TC4 core sample, the chemical injection rate was increased by a factor of 10 to 200 cc/hr. Similar plugging issue was also observed for this case. **Figure 4.18** and **Figure 4.19** depict the corresponding imbibition and displacement tests performed on TC4 before and after the treatment. The minimal difference between the imbibition curves shows a negligible change in wettability following the treatment. Moreover, the undesirable increase in the measured differential pressure after treatment proves that the core permeability has reduced due to damage by chemical injection (**Figure 4.19**).

In fact, since the head groups in non-ionic surfactants have weak polarity, fluorinated tails have more tendencies to attach together and aggregate in order to provide stronger polar heads, making them more soluble in the high-polar solvent, i.e. water. The resultant large chemical micelles or aggregates (the collection of the surfactant molecules) dispersed inside the solution can potentially be deposited at the core inlet face causing its blockage. Following this hypothesis, the particle size of chemical C-65 diluted in DIW at different concentrations was measured using a light scattering technique. **Table 4.4** tabulates these measurements. It is noted that the average size of aggregates for 0.1 wt% of C-65 in DIW is 243 nm. On the other hand, according to the centrifuge Pc measurements, it was realized that about 30% of the total pore volume in Texas-Cream rock consists of pores with a radius less than 250 nm. **Figure 4.20** shows

the pore size distribution (PSD) of Texas-Cream and Baker-Dolomite carbonate rocks estimated from capillary pressure data obtained from centrifuge tests. Comparing the pore size distribution of Texas-Cream rock and the particle size distribution of chemical C-65 can provide a simple explanation for the issue of plugging by large chemical particles, particularly at the core inlet face. It is believed that decreasing or optimizing the polarity of the water by adding co-solvents such as alcohols to the carrier fluid composition can minimize the number and size of the chemical aggregates inside the solution, hence less plugging issue is expected. The optimization of the non-ionic treatment solution in this direction was carried out. However, as mentioned previously in section 4.6.1, zero contact angles were obtained when chemical C-65 was delivered with non-aqueous solvents. In the next section, presenting the results for anionic chemical C-61, it is discussed that employing a filtration method to separate the chemical large aggregates from the solution provides an effective technique to eliminate such plugging issues.

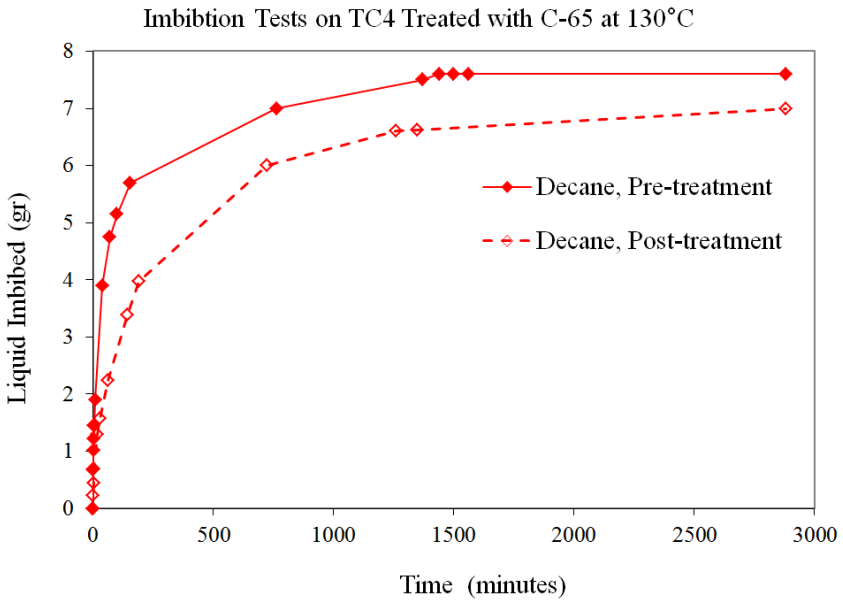

Figure 4.18: Spontaneous imbibition tests before and after the treatment performed on the TC4 carbonate core sample treated by 0.1 wt% non-ionic chemical C-65+DIW at 130°C.

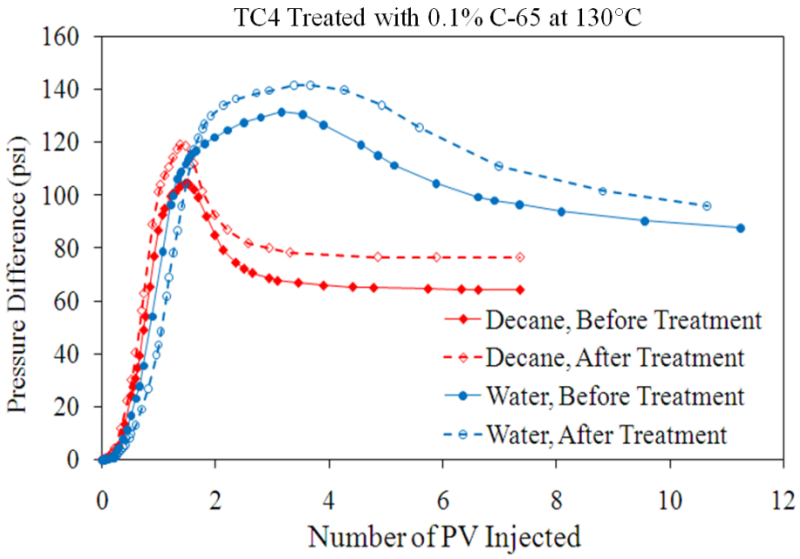

Figure 4.19: Differential pressures during unsteady-state injection of non-equilibrated C10 at a flow rate of 100 cc/hr into the TC4 carbonate core sample (100% saturated with N2, outlet pressure=14.7 psia) before and after the treatment (using 0.1 wt% nonionic chemical C-65+DIW at 130°C).

Table 4.4: Particle size and distribution, measured, in the DuPont laboratory, right after the preparation of the solution, for different concentrations of chemical C-65 in DIW.

Concentration (Active ingredient) (%)	0.01		0.05		0.1		0.5	
Non-ionic Fluorosurfactant C-65	Average Size (nm)	Distribution	Average Size (nm)	Distribution	Average Size (nm)	Distribution	Average Size (nm)	Distribution
	158.2	0.227	256.2	0.024	243.0	0.097	246	0.045

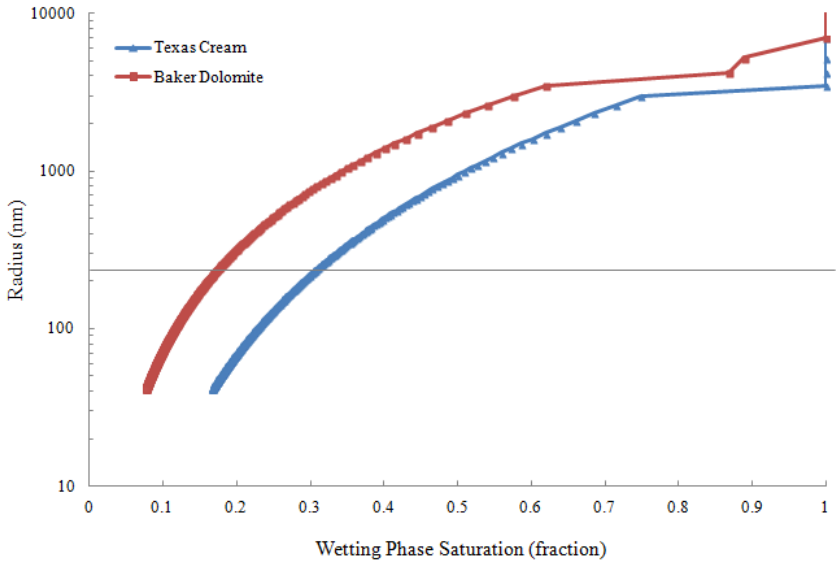

Figure 4.20: Pore size distribution of Texas-Cream and Baker-Dolomite carbonate rocks estimated from capillary pressure data obtained from centrifuge tests.

4.7 PERFORMANCE OF C-61

C-61 is an anionic phosphate fluorosurfactant. This chemical is a water-based dispersion with a yellow liquid appearance and has a pH of 7-9 and specific gravity of 1.1. The screening tests and subsequent optimizations performed on C-61 chemical solutions that lead to development of an effective wettability alteration process, are explained in the following sections. Two types of low (Texas-Cream) and high (Baker-Dolomite) permeability carbonate rocks were used in these investigations. **Table 4.3** summarises the basic properties of the core samples used in these experiments.

4.7.1 Water-based Solvent

The first series of contact angle measurements for C-61 was conducted for various concentrations of this chemical diluted in its basic carrier solvent, i.e. water. **Figure 4.21** depicts the deposited water and oil drops on Texas-Cream substrate treated with 0.005, 0.05 and 0.5 wt% C-61+DIW at 130°C. The corresponding magnified pictures of water and oil drops on the treated substrate taken by DSA software has also been shown in **Figure 4.22**. **Figure 4.23** represents all measured contact angles on treated substrates at various concentrations. Similar contact angles of $\theta_{C10\text{-}air}$=100° and $\theta_{DIW\text{-}air}$ =140° were obtained for all ranges of concentrations from 0.005 to 0.5 wt%, demonstrating high potential of C-61 for wettability alteration purposes even with low-concentrated solutions. However, at concentrations of 0.01 and 0.05 wt% a white precipitated layer of the chemical was observed on the rock substrate. This was attributed to the excessive adsorption of the surfactant molecules onto the surface. The precipitation seemed more severe at higher concentrations of 0.1 and 0.5 wt%. **Figure 4.24** shows the physical state of the treated substrate with the pertinent precipitated layer at different concentrations. These observations disfavour delivering chemical C-61 with water whereby the potential impairment of the rock permeability can occur.

From a practical point of view, and as mentioned before, water as a carrier fluid is a poor solvent to displace the reservoir resident fluids (e.g. brine and oil) accumulated around the wellbore that would create appropriate adsorption sites for the chemical molecules. It can also adversely affect well productivity during the post-treatment production (back-flow) period, due to its low-mobility ratio compared to gas and condensate. It is believed that increasing the solubility of the surfactant molecules in the solvent by adding a co-solvent such as alcohol to the solution can control the reaction rate between chemical and mineral surface. This was investigated by diluting 0.1 wt% chemical C-61 in two mixtures of DIW and IPA with weight ratios of 1:3 and 3:1.

Figure 4.25 shows the results of the corresponding contact angle measurements, using these carrier solvent blends. It was noted that the presence of IPA in solvent composition can effectively eliminate the undesired chemical layer deposited on the surface. However, using DIW/IPA with a weight ratio of 1:3 significantly reduced the chemical oil-repellency at both low (65°C) and high (130°C) temperatures (Test #1 in **Figure 4.25**). Reducing the alcohol proportion in the solution from 75% to 25% restored the chemical performance at low temperatures (Test #2 in **Figure 4.25**), but was still ineffective to repel the oil at 130°C (Test #3 in **Figure 4.25**). The effect of increasing the chemical concentration from 0.1% to 0.5% in two solvent mixtures of DIW/IPA is shown in **Figure 4.26**. Increasing chemical concentration improved the effectiveness of DIW/IPA (1:3) solution at 65°C (Test #1 in **Figure 4.26**). However, at 130°C, it was found out that only DIW/IPA (3:1) could result in an effective wettability alteration process (Test #3 in **Figure 4.26**). These exercises were aimed at adjusting the chemical interaction with the rock surface by optimising the proportion of alcohol in the carrier solution. However, it was revealed that the chemical concentration needs to be optimized according to the temperature as well as the proportion of alcohol in the mixture.

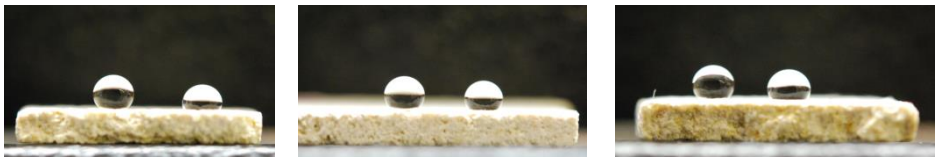

Figure 4.21: Water (left droplet) and decane (right droplet) drops on Texas-Cream substrates treated by 0.005, 0.05 and 0.5 wt% chemical C-61+DIW at 130°C, respectively from left to right, respectively.

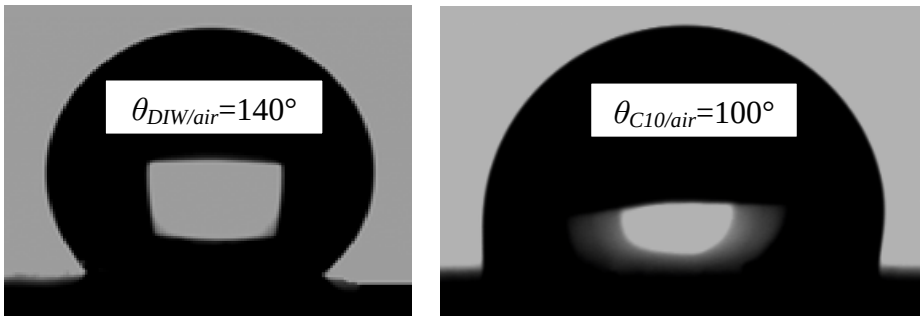

Figure 4.22: Measured contact angles of water (left) and decane (right) drops on Texas-Cream substrate treated by 0.5 wt% C-61+DIW using DSA apparatus.

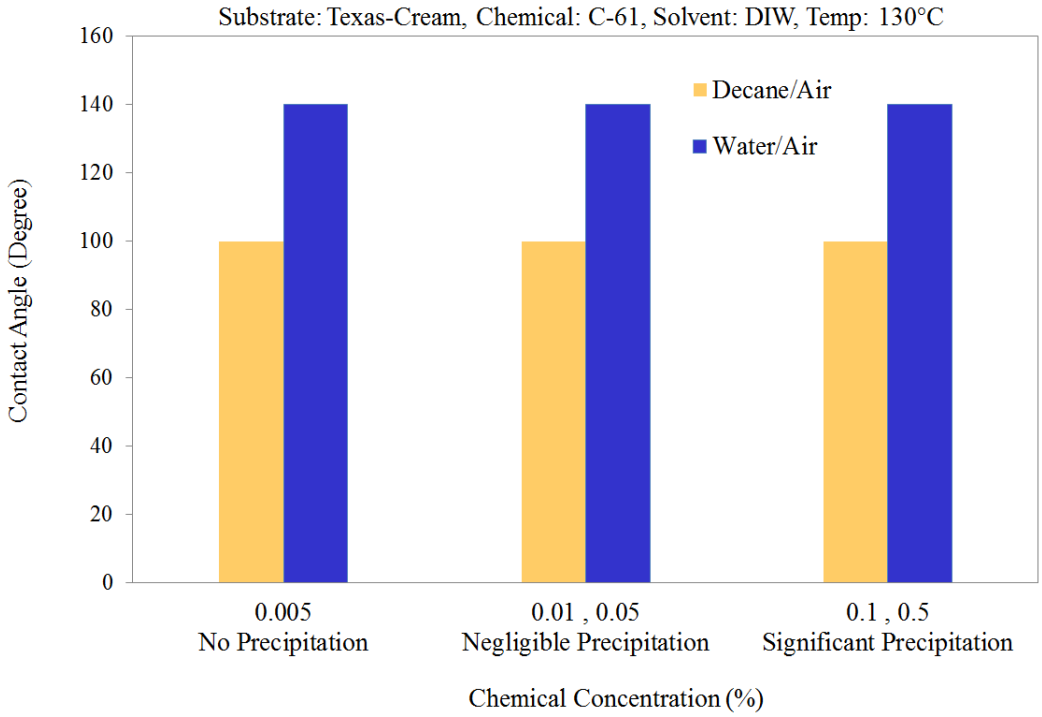

Figure 4.23: Decane and water contact angles measured on the carbonate substrate treated by chemical C-61 diluted in water-based solvent.

Figure 4.24: Texas-Cream substrates treated by 0.005, 0.05 and 0.5 wt% C-61+DIW at 130°C, from left to right, respectively, showing the physical state of the rock surface after the treatment. A white precipitated layer of chemical is evident on the rock surfaces treated with 0.05 and 0.5 wt% concentrated solutions.

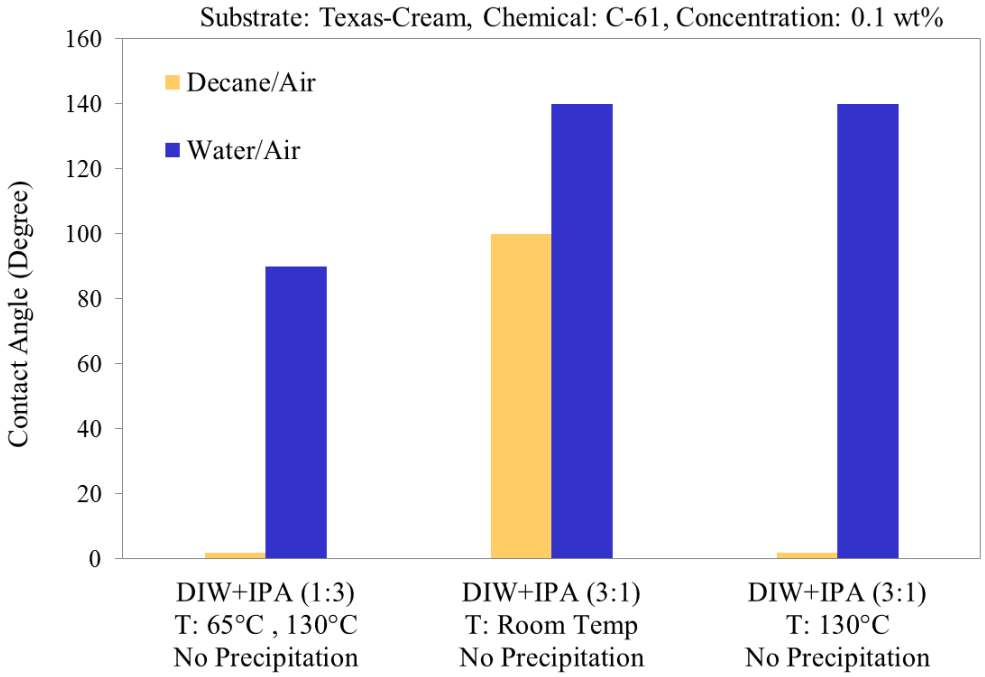

Figure 4.25: Effect of adding co-solvent (IPA) to the water-based solution (at two proportions) on wettability alteration of carbonate substrate using 0.1 wt% C-61 at different temperatures.

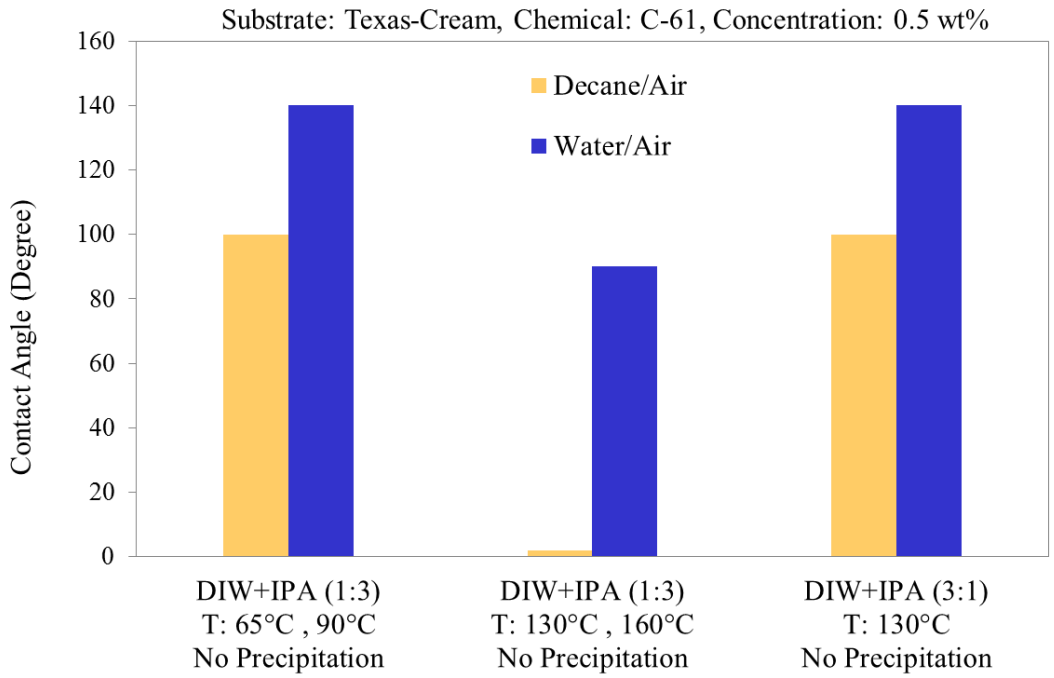

Figure 4.26: Effect of adding co-solvent (IPA) to the water-based solution (at two proportions) on wettability alteration of carbonate substrate using 0.5 wt% C-61 at different temperatures.

Core Treatment with Water-based Solvent

The optimum treatment solution, providing satisfactory oil- and water-repellencies at 130°C without precipitation, i.e. 0.5% C-61+DIW/IPA (3:1), was used to treat the TC5 core sample. **Figure 4.27** shows the recorded differential pressure (DP) across the core during displacement tests conducted before and after the treatment. In these experiments, DIW was injected at a flow rate of 100 cc/hr into the core initially saturated with N2 gas. Differential pressure during the post-treatment displacement was stabilised at a level substantially above that of the pre-treatment experiment, showing considerable rock permeability damage has occurred. Trimming about 0.8 cm off the core inlet face restored the rock permeability to that of the pre-treatment conditions (**Figure 4.27**). The observations demonstrated the possibility of plugging issue due to deposition or filtration of chemical's large aggregates at the core inlet face, similar to what happened in the case of core treatment with C-65 chemical solution (section 4.6.3)

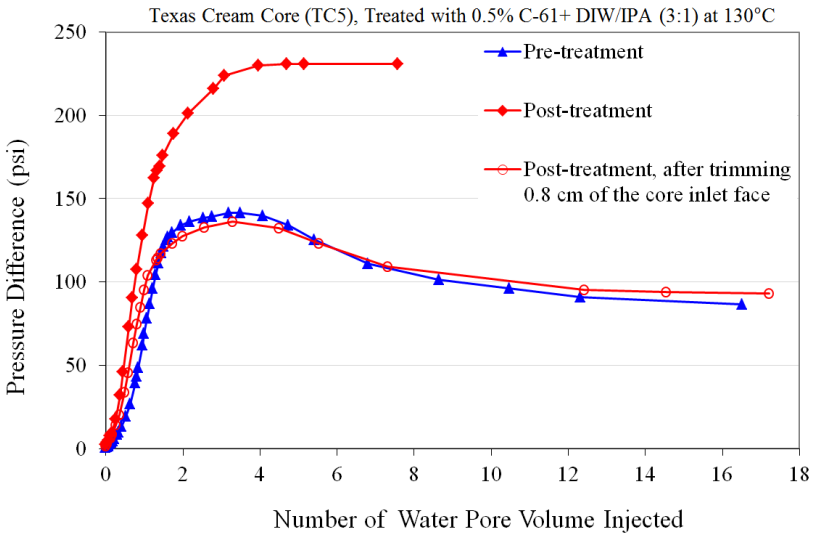

Figure 4.27: Differential pressure during unsteady-state injection of water (not-equilibrated with resident N_2) at a flow rate of 100 cc/hr into the TC5 core sample 100% saturated with N_2, outlet pressure=14.7 psia, core treated with the C-61water-based solution.

4.7.2 Alcohol-based Solvent

It is believed that using alcohols as a co-solvent for chemicals, in addition to its impact on the chemical's activity in the solution and hence its adsorption on the rock surface, as discussed above (section 4.7.1), would result in formation of smaller aggregates compared to those in water, owing to the alcohol's low polarity. Considering this hypothesis and following the plugging issue observed with the C-61 when treatment

was carried by the water-based (DIW/IPA, 3:1) solvent, it was decided to scrutinize the performance of alcohol-based solvents in delivering C-61 repellent agent. Accordingly, new series of contact angle measurements, shown in **Figure 4.28**, were conducted aiming at finding an appropriate alcohol-based solvent for C-61. Methanol-based solvents, i.e. MeOH and MeOH/IPA (3:1) (Test #2 in **Figure 4.28**), among all fluids tested here, showed an effective performance at 130°C, providing $\theta_{C10\text{-}air}$=100° and $\theta_{DIW\text{-}air}$ =120°. As described later, light scattering tests also confirmed the existence of smaller particle sizes in methanol compared to that in water. It should be noted that all other tested alcohol-based solvents, such as DIW+EtOH, IPA or EtOH resulted in identical or smaller C10-air contact angles compared to those obtained by the methanol-based solvent. Moreover, the methanol-based solvent was the only carrier fluid that resulted in stable contact angles with respect to both oil and water phases. That is, the initial contact angles, observed right after depositing the liquid drop on the substrate, were almost stationary within the 15 minutes assessment period. In **Figure 4.28**, the initial values of unstable contact angles are illustrated by light columns. For instance, the treated substrate using chemical C-61 delivered with DIW+EtOH solvent initially showed $\theta_{C10\text{-}air}$=70° and $\theta_{DIW\text{-}air}$ =100°, whereas both values decreased to about zero by time.

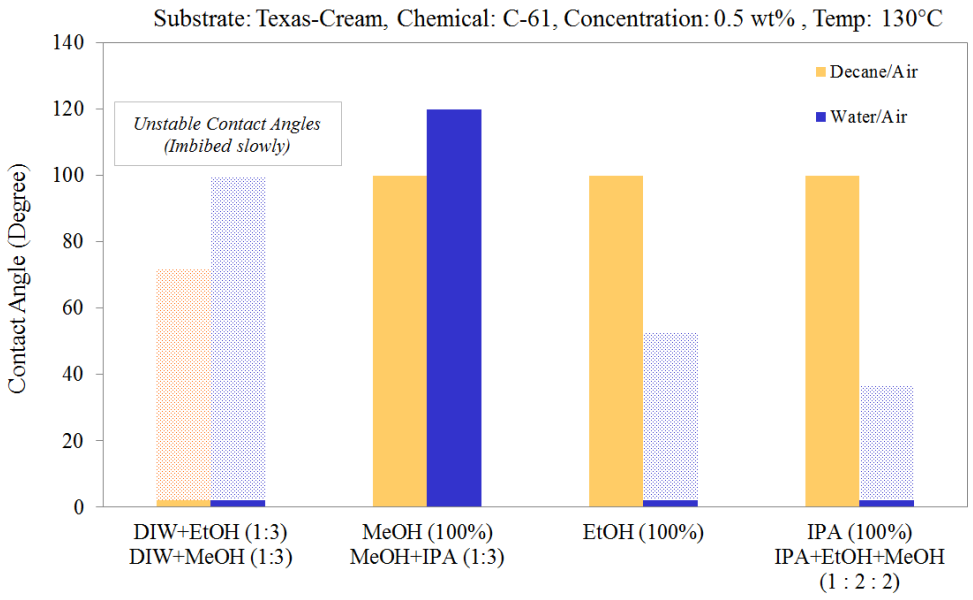

Figure 4.28: Screening contact angle measurements on Texas-Cream carbonate substrates treated by 0.5 wt% anionic chemical C-61 diluted in various alcohol-based solvents.

Core Treatment with Alcohol-based Solvent

Following the new contact angle measurements using alcohol-based solvents, 0.5 wt% C-61+MeOH was used to treat the TC6 core sample by injecting 20 PVs of CS at a flow rate of 40 cc/hr. Results of tests using this alcohol-based solvent showed noticeably lesser plugging issue compared to that observed for the water-based solution used for TC5, albeit the amount of damage was still considerable. Similar to the previous case, trimming about 0.4 cm off the core inlet face restored the rock permeability to its original value. **Figure 4.29** shows these results for displacement tests by DIW. Similar behaviour was also observed for displacements using C10.

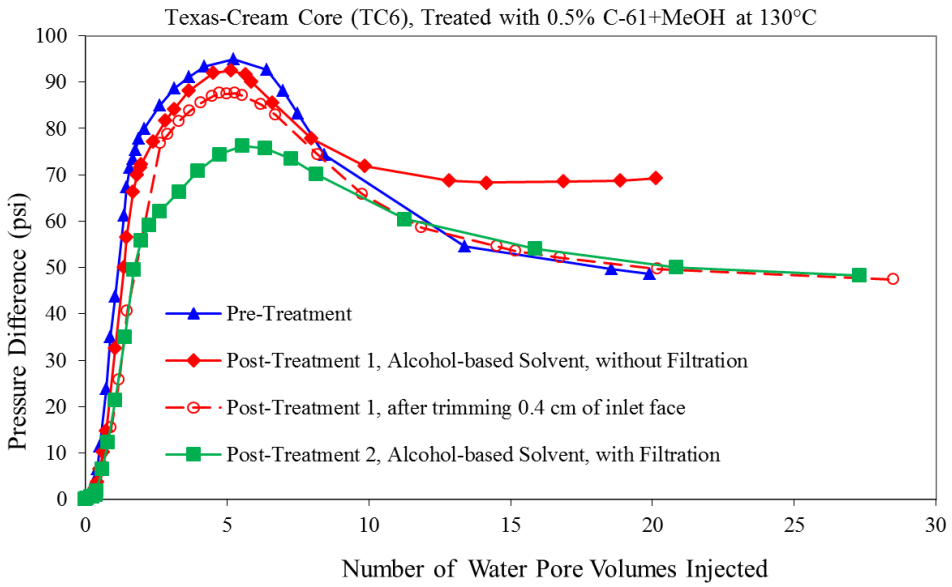

Figure 4.29: Differential pressures recorded during unsteady-state injection of DIW (not-equilibrated with resident N_2) at a flow rate of 100 cc/hr into the TC6 core sample saturated with N_2, outlet pressure=14.7 psia, core treated with the C-61 alcohol-based solution.

4.7.3 Filtration of Large Chemical Aggregates

Following the above observations demonstrating plugging of the core inlet face, apparently due to large chemical aggregates, it was decided to measure the size of the chemical C-61 particles dispersed in water-based (DIW) and alcohol-based (methanol) solvents. **Table 4.5** tabulates these results. It is noted that the average size of aggregates for 0.5 wt% chemical diluted in DIW is 262.6 nm. As noted in **Table 4.5,** no particles were detected when the chemical was diluted in methanol, demonstrating high solubility of C-61 in such an alcohol-based medium. As discussed before, about 30% of total pore volume in the Texas-Cream rock consists of pores with a radius less than 250 nm, based

on PSD extracted from the centrifuge Pc measurements (**Figure 4.20**). These data provide an explanation for severe plugging observed at the core inlet face, when a water-based solvent (DIW/IPA, 3:1) was used. In line with this, the degree of plugging was significantly mitigated when methanol (with no detectable particles in it) was employed as a carrier solvent.

Accordingly, it was decided to separate any possible large aggregates form the solution (0.5% C-61+ MeOH) by filtering it through a syringe filter with pore size of 0.2 µm. The filtered solution was then injected into the pre-treated TC6 core, after trimming its plugged inlet face. A low injection rate of 4cc/hr was also selected to provide a longer interaction period (retention time) between the chemical molecules and the rock surface. As **Figure 4.29** shows, the post-treatment DP across the core is to some extent lower than that of the before treatment case at the early stages of the test, whereas both trends become almost similar towards the end of the experiment (stabilized conditions). Here it should be mentioned that the pressure drops recorded for the tests conducted on trimmed core samples have been corrected according to the original length of the core (before trimming) to make the results comparable. The observations underline the positive effect of filtration technique on minimizing the negative impact of the large chemical particles on wettability alteration performance (compare the first treatment without filtration (red line) with the second treatment with filtration (green line) in **Figure 4.29**). However, even with the filtration method, the chemical treatment did not demonstrate a satisfactory performance, i.e. only a small decrease in DP was observed after the treatment. Here one may argue that because of low permeability of the Texas-Cream rock, adsorption of C-61 chemical particles on the rock surface, regardless of their size and filtration, damages the rock permeability and counteracts the positive impact of the rock's altered wettability. At this stage and to investigate the impact of the rock permeability, a high-permeability carbonate core (BD18) was treated with results to be discussed in the next section.

Table 4.5: Particle size and distribution, measured right after the preparation of the solution, for different concentrations of chemical C-61 diluted in DIW and methanol*, conducted at DuPont laboratory.

*With using the light scattering technique, no particles were detected when chemical diluted in methanol.

Concentration (Active ingredient) (%)	0.1		0.5		1.0		5.0	
Anionic Fluorosurfactant C-61	Average Size (nm)	Distribution	Average Size (nm)	Distribution	Average Size (nm)	Distribution	Average Size (nm)	Distribution
	310.2	0.192	250.2	0.059	280.5	0.278	262.6	0.227

4.7.4 Treatment of High-permeability Rock

The performance of the treatment solution optimized in the previous stages, i.e. 0.5 wt% C-61+MeOH filtered through 0.2µm, was evaluated for a high-permeability (k=122 md) Baker-Dolomite carbonate rock (BD18). Similar to the TC substrate, contact angle measurements were initially conducted on this rock to make sure essential level of wettability alteration is delivered to the BD rock surface using C-61 repellent agent. The results demonstrated that C-61 is capable of altering the wettability of BD carbonate samples to the same extent as that observed for TC. **Figure 4.30** depicts DIW and nC10 drops on treated TC and BD substrates (by using the optimized chemical solution mentioned above), showing almost the same level of water- and oil-repellency.

Following the promising contact angle measurements, 25 PVs of the optimized CS was injected at 4 cc/hr into the BD18 core sample with 18 hours soaking time. Pre- and post-treatment displacement tests by DIW and nC10 are shown in **Figure 4.31** and **Figure 4.32**, respectively. A significant reduction in DP during the post-treatment displacement test by water was observed, demonstrating the promising improvement of water mobility (second test in **Figure 4.31**). Nonetheless, the altered wettability was not sufficient to improve the oil mobility as almost similar DPs were obtained before and after the treatment (second test in **Figure 4.32**). Absolute permeability was also measured before and after the treatment by injecting single-phase decane through the core at 2000 psi. No detectable change in permeability was recorded after the treatment. It should be noted that the percentage of total pores with a radius less than 250 nm is about 17 % in Baker-Dolomite rock, whereas it was 30% in Texas-Cream samples according to PSD obtained from the conducted Pc centrifuge tests (**Figure 4.20**). The results highlight the importance of rock permeability in application of such chemicals, that is, possible permeability impairment in tight pores by chemical particles can

overshadow the positive impact of the improved fluids' mobility due to wettability alteration.

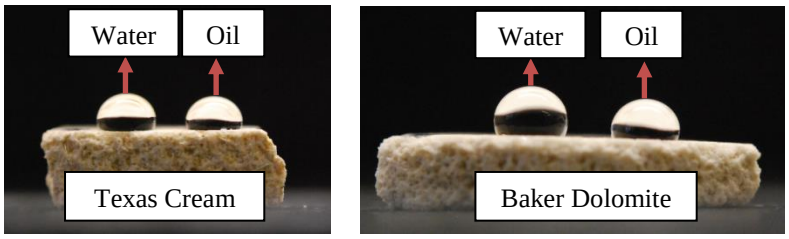

Figure 4.30: Water (left) and decane (right) drops on Texas-Cream (left picture) and Baker-Dolomite (right picture) carbonate substrates treated by 0.5 wt% C-61+MeOH, confirming that chemical imparts almost similar liquid-repellency to both carbonate minerals.

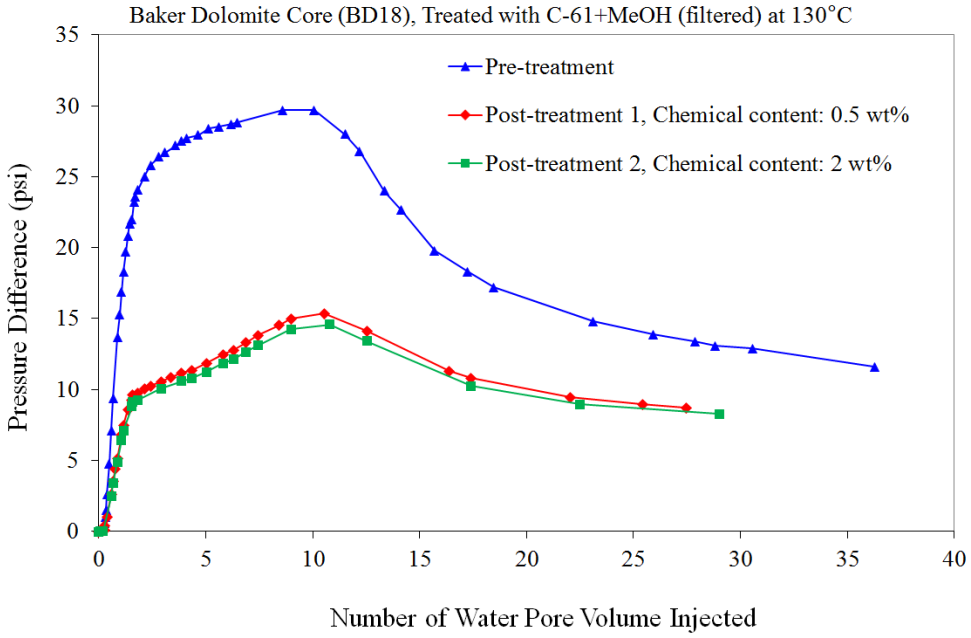

Figure 4.31: Differential pressures during unsteady-state injection of DIW (not-equilibrated with resident N_2) at a flow rate of 100 cc/hr into the BD18 core sample saturated with N_2, outlet pressure=14.7 psia, core treated at two concentrations of the C-61 alcohol-based solution.

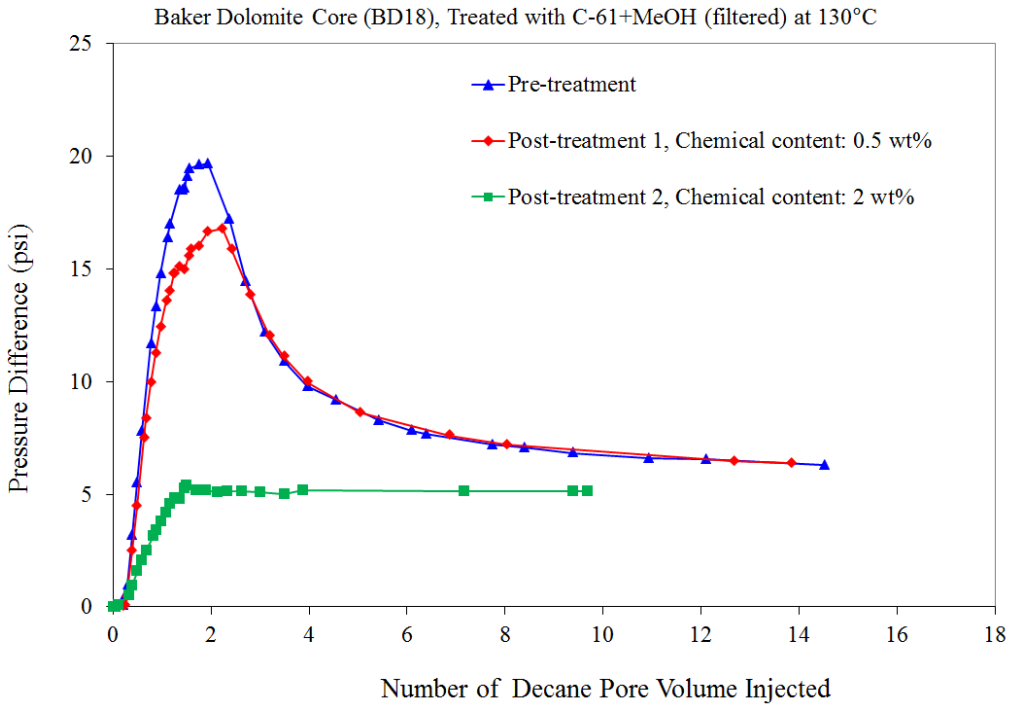

Figure 4.32: Differential pressures during unsteady-state injection of decane (not-equilibrated with resident N2) at a flow rate of 100 cc/hr into BD18 core sample saturated with N2, outlet pressure=14.7 psia, core treated at two concentrations of the C-61 alcohol-based solution.

4.7.5 Effect of Chemical Concentration

Considering the poor oil-repellency observed for the BD18 core sample treated with 0.5% C-61 concentrated solution, and considering the effective water-repellency achieved, it was hypothesized that boosting the fluorinated content of the solution by adding more chemical agent into it probably would enhance the oil-repellency strength of the treatment. This was according to the observations made through the course of contact angle measurements, i.e. comparison of the results of third series of tests in **Figure 4.25** with those in **Figure 4.26**.

After conducting series of contact angle measurements, it was revealed that 2 wt% C-61+MeOH can produce the same level of oil- and water-repellencies obtained for 0.5% concentrated solution, used in the previous treatment. Accordingly, 23 PVs of 2% concentrated solution (filtered through 0.2µm) was injected at a flow rate of 4 cc/hr into the BD18 core sample (previously treated by the 0.5% C-61 concentrated solution) at 130°C. Exposing the core sample to this higher concentration of the chemical agent, showed a pronounced improvement in oil mobility compared to the first treatment with the low-concentration solution (**Figure 4.32**). The water mobility did not improve any further (**Figure 4.31**), suggesting that the maximum level of water-repellency had been accomplished during the first course of treatment with 0.5% concentrated CS. Similar to

the first attempt, no permeability damage was also observed in the second treatment on this high-permeability rock.

In **Figure 4.32** it is noted that DP in the pre-treatment displacement test substantially increases and reaches a peak of about 20 psi just before the wetting oil phase breaks through the core outlet face, after which DP starts decreasing and reaches a plateau of about 6.4 psi after 10 PVs of oil is displaced. After performing an effective wettability alteration, i.e. second treatment, two main differences are evident in the post-treatment displacement test results: 1- the maximum value of DP before breakthrough time has drastically reduced from 20 to about 5 psi and 2- DP has quickly stabilised at its maximum value of 5 psi after breakthrough, instead of showing a peak behaviour trend like that of the pre-treatment case. As a matter of fact, since the porous rock becomes intermediate gas-wet after the treatment, oil phase occupies larger pores; hence less differential pressure (driving force) is required to pass the oil through the porous medium compared to when the wetting-oil phase travels through smaller and tighter pores of the untreated core. It should be mentioned that similar observations and explanations would apply to all other displacement tests performed in this work by unsteady-state method. It should also be highlighted that the ultimate impact of a wettability modifier on improving fluid mobilities is achievable by conducting steady-state relative permeability measurements using gas-condensate fluids, which is discussed in Chapter 6.

4.7.6 Effect of Resident Brine

Compatibility of injected chemical solutions with resident fluids around the wellbore, especially brine, is crucial to ensure a successful treatment process. All previous treatments on TC and BD cores were conducted on dry cores, i.e. chemical solution was injected into the core saturated with gas. Here, to examine the performance of the final optimized treatment solution (2% C-61+MeOH filtered through 0.2µm) in presence of brine, two additional tests on BD14a and BD14b core samples (see **Table 4.3** for rock properties) saturated with low-salinity (0.8% NaCl + 0.2% CaCl2) and high-salinity (12% NaCl + 10% CaCl2) brines, respectively, were conducted. These two extreme limits of brine salinity were selected to explore the chemical performance in the best and worst case scenarios. It should be noted that C-61 has an ionic functionality and as a result shows poor stability in brine media, i.e. chemical coagulates when contaminated with brine. However, the objective at this stage was to evaluate the capability of the

alcoholic carrier solvent, i.e. methanol, to displace the resident fluids with the minimum undesirable interactions between the chemical agents and brine components.

Prior to injection of the chemical solution, in both low- and high-salinity cases, about 10 PVs of brine was injected into the core saturated with N2. Approximately 65% brine saturation was established in both cases. This was followed by injection of about 20 PVs of chemical solution, at a flow rate of 4 cc/hr. The core was then dried and fully saturated with N2. This was followed by injection of C10 equilibrated with resident N2, at a flow rate of 100 cc/hr at 1000 psi. Similar displacement tests were also conducted using DIW. The results were finally compared with the corresponding pre-treatment tests under similar conditions.

Figure 4.33 and **Figure 4.34** show the pre- and post-treatment displacement tests conducted by DIW and C10, respectively, on the BD14a core sample saturated with the low-salinity brine during the treatment process. Noticeable reduction in DPs after the treatment for both water and oil displacement tests are evident, demonstrating an effective alteration of the rock wettability due to injection of C-61 alcohol-based CS. Absolute permeability of the core was also measured before and after the treatment using both decane and nitrogen fluids, showing no damage to the rock. These two observations confirmed that the CS was able to effectively displace the resident low-salinity brine and successfully alter the rock wettability. DPs recorded at the stabilized conditions before and after the treatment were used to calculate the end-point k_{ro} (at approximately So=0.8), showing an improvement factor of about 1.6.

Figure 4.35 and **Figure 4.36** show the pre- and post-treatment displacement tests conducted on the BD14b core sample saturated with the high-salinity brine during the treatment process. Whilst noticeable improvements in water and oil mobilities are noticed after the treatment during the early stages of the displacement tests, i.e. post-treatment DPs are considerably below the pre-treatment ones, DPs are almost similar, more evident for the oil (**Figure 4.36)**, when the stabilized condition is reached. The absolute permeability measurements also showed that some level of permeability damage, almost by 30%, has occurred. This implies that probably the positive effect of the wettability alteration has been overcome by the imposed damage on the rock permeability due to undesired interactions between the chemical and high salinity brine.

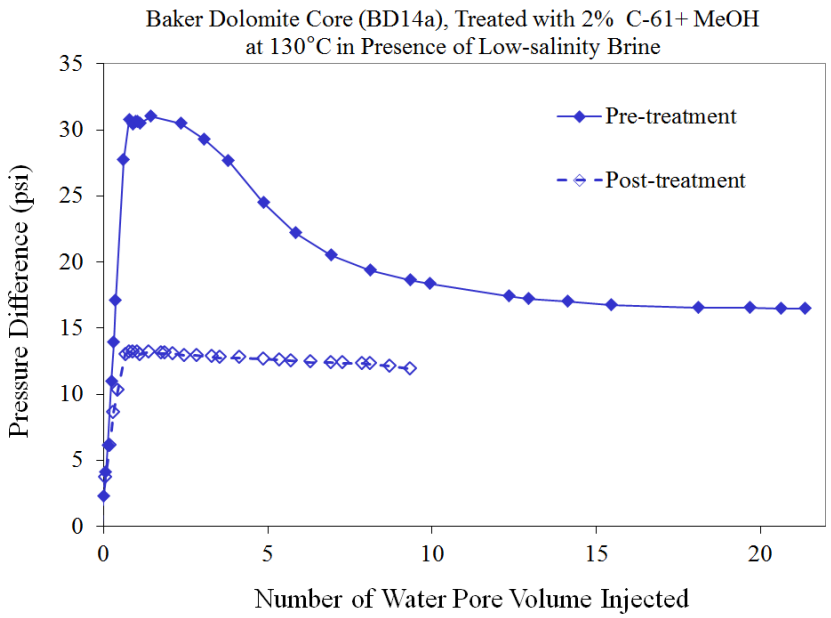

Figure 4.33: Differential pressures during unsteady-state injection of non-equilibrated water at 1000 psi at a flow rate of 100 cc/hr into the BD14a core sample saturated with N2, core treated with the C-61 alcohol-based solution in presence of low-salinity brine.

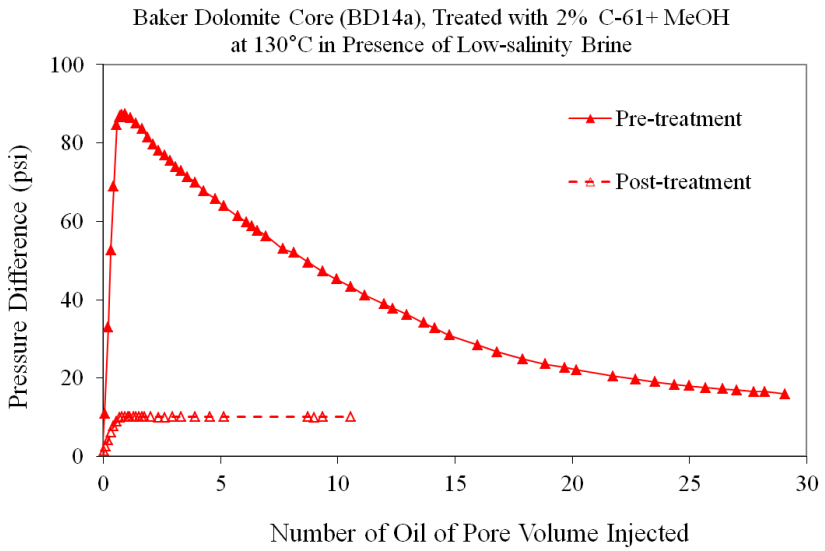

Figure 4.34: Differential pressures during unsteady-state injection of equilibrated nC10 (with N_2) at 1000 psi at a flow rate of 100 cc/hr into the BD14a core sample saturated with N_2, core treated with the C-61 alcohol-based solution in presence of low-salinity brine.

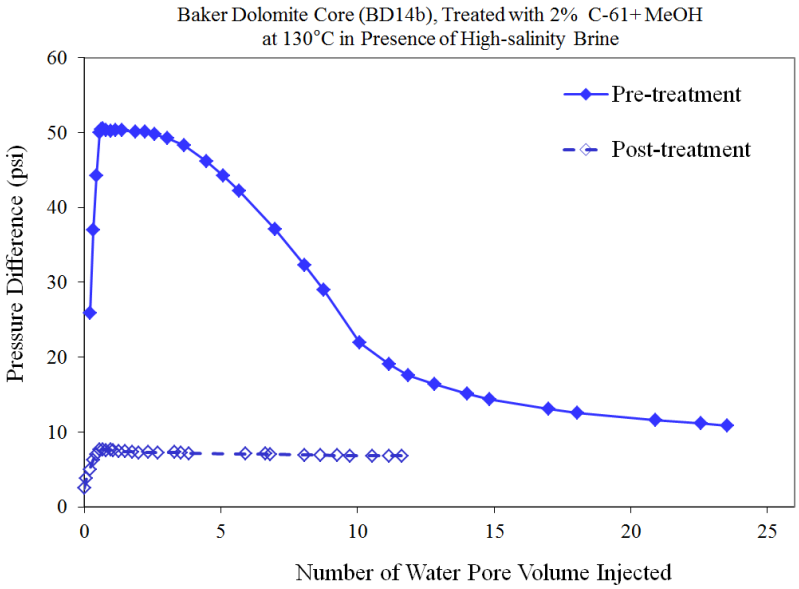

Figure 4.35: Differential pressures during unsteady-state injection of non-equilibrated water at 1000 psi at a flow rate of 100 cc/hr into the BD14b core sample saturated with N2, core treated with the C-61 alcohol-based solution in presence of high-salinity brine.

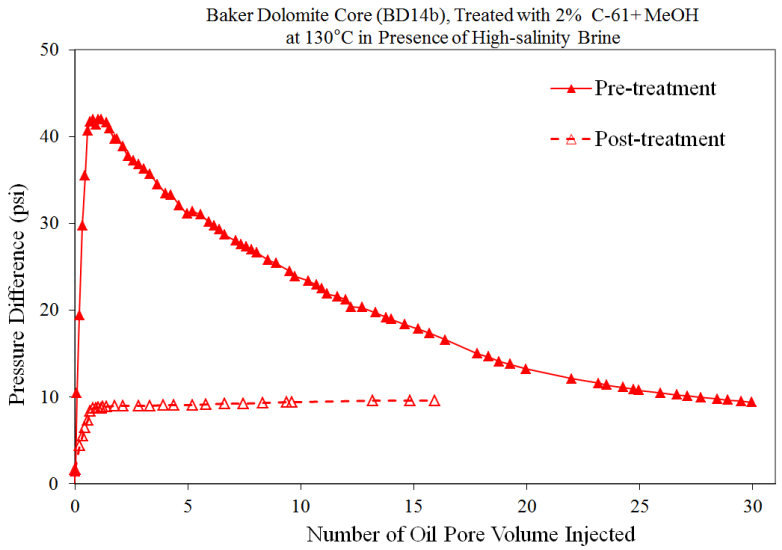

Figure 4.36: Differential pressures during unsteady-state injection of equilibrated nC10 (with N_2) at 1000 psi at a flow rate of 100 cc/hr into the BD14b core sample saturated with N_2, core treated with the C-61 alcohol-based solution in presence of high-salinity brine.

4.8 TREATMENT DURABILITY TEST

One of the key factors that a wettability-alteration process must have to make it a desirable technique for real field applications is its durability, i.e. flow of reservoir fluids, especially gas at extreme velocities and high temperatures may cause deterioration of the treatment. The durability of the treatment is an important factor favouring the application of wettability modifiers over other common methods used for

removing liquid blockages such as solvent injection and hydraulic fracturing with temporary and short-term effects. Strong and long-lasting adsorption of the chemical molecules on the rock surface can secure the durability of the treatment.

To examine the strength of the interactions between the C-61 chemical agent and carbonate surface, a durability test was performed on the BD14a core sample previously treated with 2% C-61 (the results were discussed in the previous section). This was achieved by flowing more than 1000 pore volumes of N_2 gas through the BD14a core sample at 130°C and actual pore velocity of 458 m/day to mimic the production of gas-condensate fluids after the treatment. Subsequently, an USS displacement test by water was carried out to explore any possible desorption and striping of the chemical molecules from the rock surface by the gas flowing at a high velocity.

Figure 4.37 shows DPs of the pre-treatment and post-treatment tests performed before and after the production period. It is noted that both DPs of the post-treatment periods follow very similar trends, with the small differences, which is within the range of the experimental errors. These observations underline the effective performance of the C-61 repellent agent on improving the liquid mobility in the carbonate rock on a reasonably permanent basis.

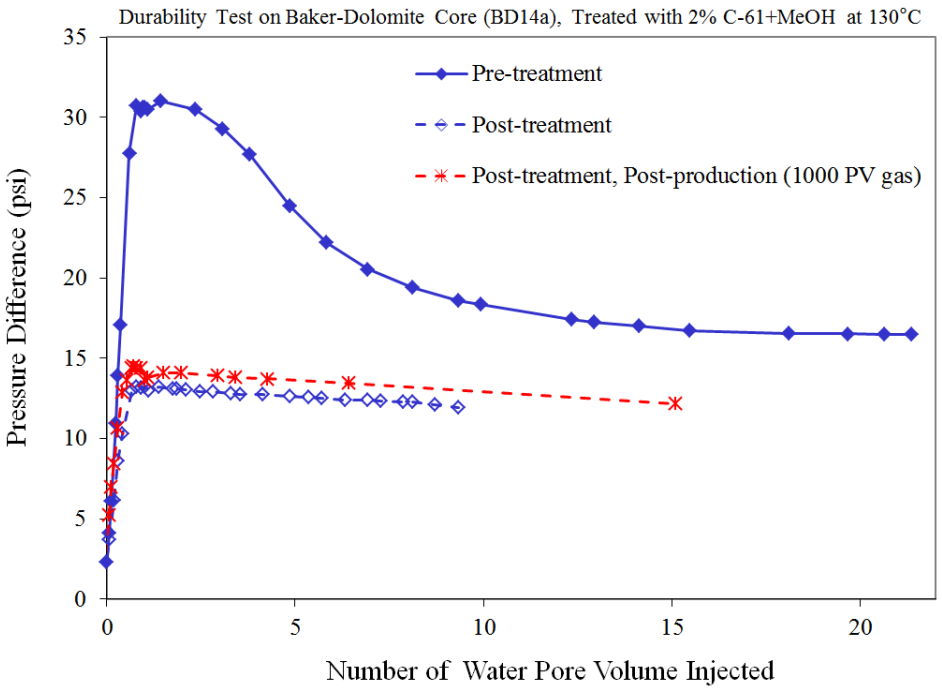

Figure 4.37: Durability test of the treatment by C-61, after injecting 1000 PVs N_2 at 130°C through the core with a velocity of 458 m/d, by comparing the differential pressures during unsteady-state injection of non-equilibrated water at 1000 psi at a flow rate of 100 cc/hr into BD14a core saturated with N_2.

4.9 PERFORMANCE OF COMBINED CHEMICALS

As discussed previously in section 4.7.6, injecting the treatment solution carrying C-61 fluorochemical into the carbonate rock saturated with high-salinity resident brine caused some degree of permeability damage. Anionic chemicals, e.g. C-61, intrinsically show poor stability in brine but are potentially good wettability modifiers for carbonate minerals. On the other hand, the non-ionic compounds benefit greatly from being compatible with brine solutions, but their chemical bonds with carbonate surfaces are not as effective as anionic ones. According to these, it was proposed to investigate the feasibility of application of a combined non-ionic and anionic chemical solution to alter the wettability of carbonate minerals in the presence of brine. In this application, the non-ionic part acts as a booster to enhance the stability of anionic part in the brine. However, as shown later, the mixing ratio of the selected anionic and non-ionic chemical agents in the solution should be optimized in a way that both chemicals preserve their favourable functionalities in the combined solution.

Following this approach, a wide range of investigations were conducted, searching for appropriate non-ionic chemicals that can be mixed with C-61 at appropriate proportions. Among all the chemicals screened, C-65 and C-30 (water-soluble fluorosurfactants listed in **Table 4.1**) showed excellent stability in both low and high-salinity environments.

Accordingly, stability of 0.5 wt% C-61/C-65 combined chemical (at different proportions) diluted in MeOH was investigated by mixing it with both low- and high-salinity brines with a weight ratio of 1:1 at the room temperature. The phase behaviour of the mixed solution was observed at three subsequent time steps of 30 seconds, 10 minutes and 1 hour. **Figure 4.38** illustrates the phase behaviour of the combined chemicals at these different time steps after contaminating with low-salinity brine. It is noted that as the proportion of non-ionic chemical C-65 in the solution increases, the size and amount of the chemical aggregates (corresponding to chemical C-61) decreases. For instance, in the cases of 20/80 and 10/90 combination ratios of C-61/C-65, the chemical solution becomes almost transparent with no aggregates after 1 hour. Similar observations were noticed for the chemical solutions contaminated with high-salinity brine as well.

Contact angles pertinent to carbonate substrates treated by each of these solutions are shown in **Figure 4.39**. It should be mentioned that the chemical solutions used for these treatments were not contaminated with brine. It is noted that by increasing the

percentage of the non-ionic part in the solution the treatment performance (liquid-repellency) decreases. That is, for the 90/10 to 50/50 combination ratios of C-61/C-65, the treatment is promising, i.e. $\theta_{C10\text{-}air}$=90°, whereas it becomes ineffective as C-65 proportion increases above 50%. The same behaviours in brine compatibility (**Figure 4.40**) and contact angles were also observed for C-61/C-30 combined chemicals.

In summary, these investigations confirmed the validity of the proposed approach of enhancing the stability of anionic chemicals against the brine by combining them with non-ionic agents. However, measured contact angles revealed that careful attention should be paid to selecting the optimum proportion of the non-ionic part in the solution to retain the good liquid-repellency performance of the anionic part. The viability of this method also needs to be further verified by performing displacement tests on cores initially saturated with brine. Moreover, it is also suggested that even for the chemicals with a reasonable level of compatibility with brine, to wash out the area around the wellbore region, prior to injecting the chemical solution, an appropriate alcohol blend compatible with brine can be used. This way, the alcohol blend that is injected in front of the chemical solution, would displace the resident brine accumulated around the wellbore and provide clean adsorption sites for the chemical agent interaction with the rock surface.

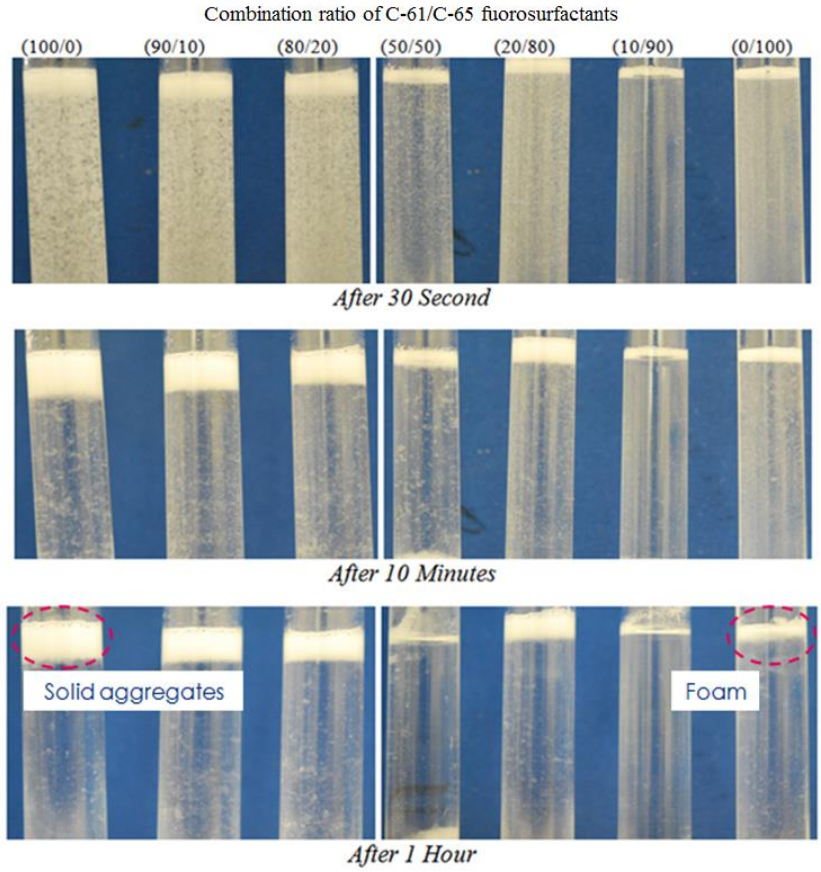

Figure 4.38: Phase behaviour of different composition of 0.5 wt% C-61/C-65 diluted in methanol at room temperature at three different time steps after mixing with low-salinity brine (1% NaCl+CaCl2) with a weight ratio of 1:1.
*Note: The same behaviour was observed after mixing with high-salinity brine, 20% NaCl+CaCl2.

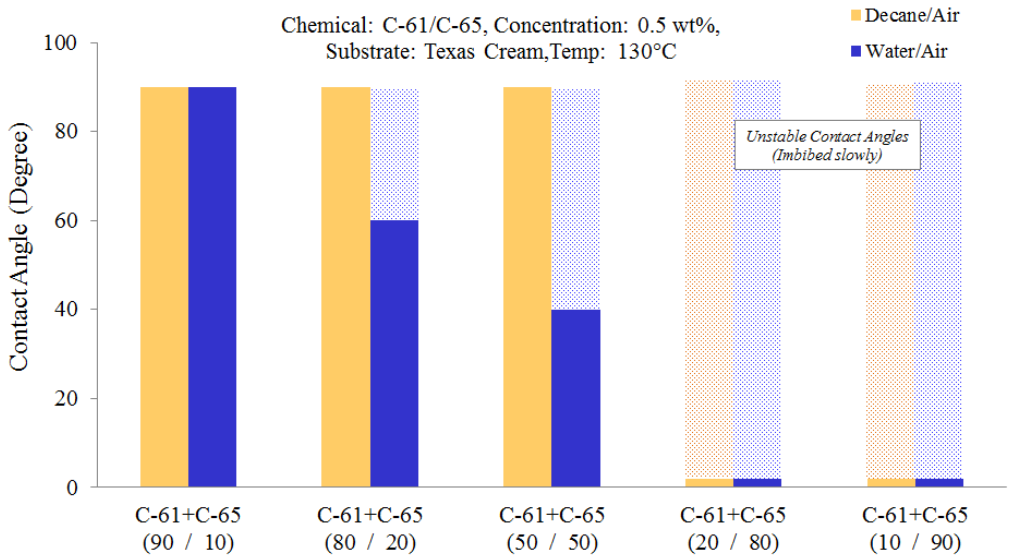

Figure 4.39: Measured contact angles on carbonate surfaces treated by combined treatment solution of C-61/C-65 (at different proportions) diluted in MeOH.

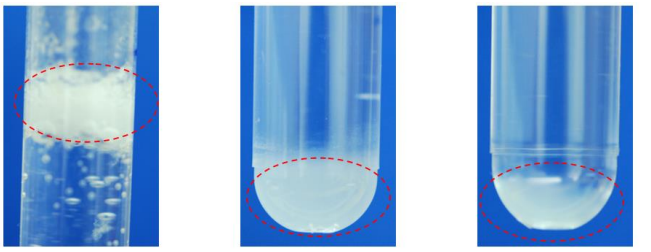

Figure 4.40: Phase behaviour of different composition of 1 wt% C-61/C-30 diluted in methanol after mixing with low-salinity brine (1% NaCl+CaCl2) with a weight ratio of 1:1 at room temperature.

4.10 EFFECT OF BRINE COMPOSITION ON CONTACT ANGLE DATA

In the previous contact angle tests, de-ionized water (DIW) was used. This was mainly to simplify the experiments and minimize the number of variables involved in the measurements. However, it should be noted that the formation brines contain a wide range of ionic components with various concentrations. It is believed that salinity (presence of ions in water) could have a major impact on the rock wettability for an oil/water/rock system where both liquid phases (i.e. oil and water) have comparable thermodynamic properties (Al-Aulaqi et al. 2013, AlShaikh and Mahadevan 2014). For gas/liquid/rock systems, however, there is a distinct contrast between two fluids' thermodynamic properties; hence wettability becomes less sensitive and less dependent on the salinity.

However here, to further explore the potential of wettability modifiers, e.g. C-61, for field applications, series of contact angle measurements on the treated BD and TC carbonate substrates (with 2 wt% C-61+MeOH) were performed using various brine compositions. **Table 4.6** lists all the brines and their corresponding ionic compositions used in this study. Here, it was considered to select a variety of brine compositions within the high and low salinity ranges. Accordingly, seven different brines in total were used, two of which are synthetic brines (LSB and HSB in **Table 4.6**) and five others with compositions identical to the formation brines (FB1 to FB5) found in the open literature. It should be noted that among these brines, FB1 and FB3 have a low-salinity of about 1,000 ppm, LSB and FB2 have a moderate-salinity of about 10,000 to 37,000 ppm and HSB, FB4 and FB5 have a high-salinity within 100,000 to 230,000 ppm.

Figure 4.41 illustrates the deposited sessile drops of these brine samples on the treated Texas-Cream substrate. All performed contact angle measurements on BD and TC substrates are also depicted in **Figure 4.42** and **Figure 4.43,** respectively. Here, it should also be mentioned that all these measurements were carried out at ambient conditions. An additional contact angle with DIW was also conducted on each substrate as the reference case. Accordingly, contact angles of 113° and 125° were observed on the BD and TC substrates, respectively, when DIW was used. Contact angle measurements on the BD substrate using different brines resulted in θ varying from 101° to 120° (**Figure 4.42**). The corresponding contact angles measured on the TC substrate were also in the range of 109° to 133° (**Figure 4.43**). Overall, both treated carbonate substrates showed an acceptable level of water-repellency with respect to all brines tested here albeit with slight variations in the measured contact angle data. It should be noted that it was not possible to find a meaningful correlation between the brines salinity and the recorded contact angles. In summary, and considering that both carbonate minerals were completely water-wet before the treatment (θ=0°) whilst contact angles of above 100° were achieved after the wettability alteration, it can be stated that this chemical can potentially alter the rock wettability and maintain its performance when contacted with a wide range of brine compositions. However, it should be mentioned that further investigations such as flow tests should be performed to confirm these preliminary findings.

Table 4.6: Ionic composition of different brines used for evaluating water-repellency on treated carbonate substrates.
* *LSB and HSB: Synthetic low- and high-salinity brines*
** *FB: Synthetic formation brines*

Ion *(ppm)*	*LSB	*HSB	**FB1	**FB2	**FB3	**FB4	**FB5
Na	3147	31470	475	11429	696	72272	59491
Ca	722	7220	-	430	66	11641	19040
Mg	-	-	-	1362	347	321	2439
K	-	-	15	351	-	3814	-
Ba	-	-	-	0.01	-	25	-
Sr	-	-	-	8	-	349	-
SO4	-	-	-	3500	96		350
Cl	6131	61310	700	20040	-	136489	132060
HCO3	-	-	5	48	5	243	354
S	-	-	-	-	-	17	-
TDS (Total Dissolved Solids)	10,000	100,000	1,195	37,168	1,210	225,221	213,749

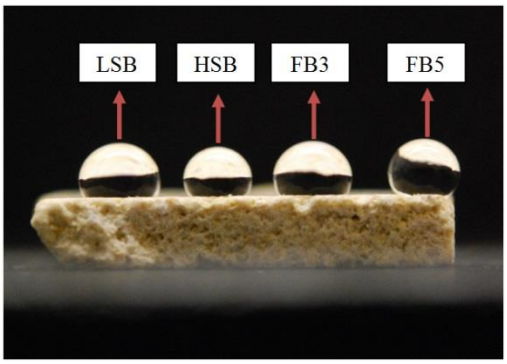

Figure 4.41: Brine contact angle tests performed on treated Texas-Cream substrate.

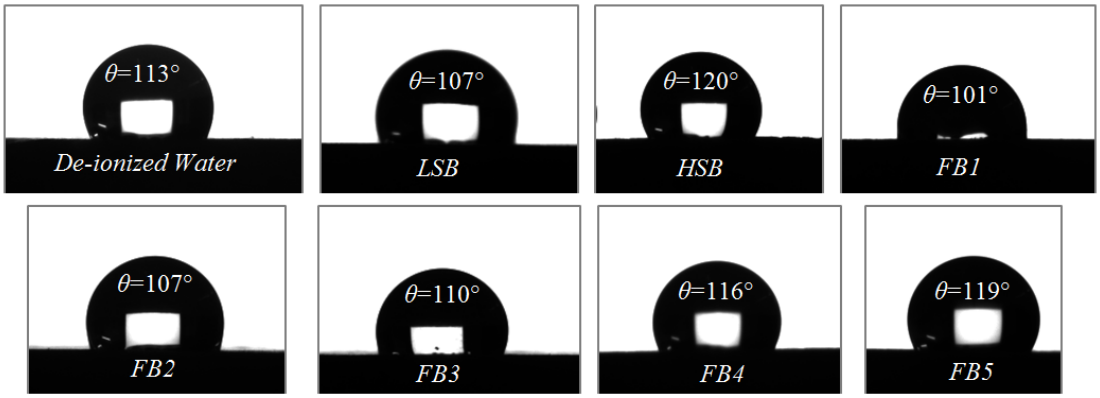

Figure 4.42: Contact angles measured on the treated BD carbonate substrate at ambient conditions using different brine compositions (*see Table 4.6*)

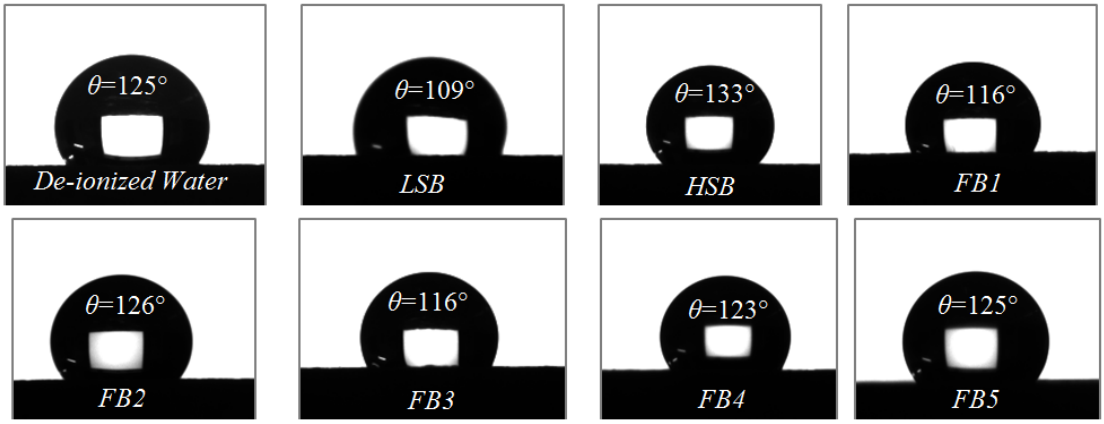

Figure 4.43: Contact angles measured on the treated TC carbonate substrate at ambient conditions using different brine compositions (*see Table 4.6*)

4.11 SUMMARY AND CONCLUSIONS

In this chapter results of series of screening tests performed on a number of fluorinated repellent agents were discussed. The investigations were mainly dedicated to finding appropriate wettability modifiers for carbonate rocks. Accordingly, fifteen chemicals were tested amongst which four were short listed based on the initial oil and water repellencies observed using contact angle measurement tests. The impact of chemical ionic group, chemical concentration, chemical delivery method, chemical particle size, solvent type, treatment duration, temperature, rock permeability and brine salinity on the chemical treatment performance were then investigated for the four selected chemicals. An optimized treatment solution for carbonate rocks was finally developed. The main conclusions from the experiments performed on these four chemicals are:

1- Anionic and to lesser extent non-ionic fluorochemicals, compared to cationic and amphoteric chemicals, showed the most promising wettability alterations on the carbonate minerals.

2- Non-ionic chemical (C-65) delivered an acceptable level of oil and water repellency ($\theta_{C10\text{-}air}$ =100° and $\theta_{DIW\text{-}air}$ =120°) when diluted in DIW, at both low (65°C) and high (130°C) temperatures. The chemical's water-repellency deteriorated as the chemical concentration and/or temperature increased. This was attributed to the formation of chemical bilayers at higher concentrations and/or temperatures. The formation of bilayers proved to be in favour of improving the chemical's oil-repellency.

3- C-65 showed a good compatibility with low- and high-salinity brines with an acceptable preserved level of oil-repellency. However, as brine reduced the chemical's solubility, possible formation of bilayers had an adverse impact on the chemical's water-repellency.

4- The existence of large chemical aggregates in the C-65 chemical solution caused the plugging of the core inlet face.

5- Anionic chemical (Z-610) demonstrated promising oil- and water-repellencies ($\theta_{C10\text{-}air}$=115° and $\theta_{DIW\text{-}air}$=139°) when delivered by water-based solvent, i.e. 0.5 wt% Z-610+DIW, at 130°C. However, the chemical performance in alcohol-based solvents was not encouraging.

6- At elevated temperatures, e.g. 160 and 190°C, excessive deposition of Z-610 on the carbonate substrate was observed.

7- Type and concentration of the brine ions (Na^+, Cl^- and Ca^{2+}) played an important role on the stability of Z-610 in the brine media. That is, salting-out of Z-610 observed only at high concentration (10 wt%) of NaCl brine, whereas it severely precipitated even at low concentration (1 wt%) of CaCl2.

8- Whilst soaking the TC rock substrate in 1 PV of 0.5% Z-610+DIW was insufficient to alter the rock wettability, a promising improvement in oil mobility by a factor of 1.6 was achieved by injecting 10 PVs of CS into the TC core sample with no noticeable permeability impairment.

9- Anionic chemical (C-61) resulted in promising wettability alteration of the carbonate substrate at 130°C when delivered with both DIW ($\theta_{C10\text{-}air}$=100° and $\theta_{DIW\text{-}air}$ =140°) and MeOH ($\theta_{C10\text{-}air}$=100° and $\theta_{DIW\text{-}air}$ =120°).

10- The possible existence of the C-61 large aggregates in the water-based solution caused a significant plugging issue at the core inlet face of the low-permeability Texas-Cream rock. Replacing the water-based solvent (DIW) with the alcohol-based one (MeOH) reduced the plugging issue to some extent.

11- A filtration method was proposed to separate the large chemical (C-61) aggregates before injecting into the core. This proved an effective method to reduce/eliminate the permeability impairment due to deposition of large chemical particles at the core inlet face.

12- During the Baker-Dolomite (BD18) carbonate rock treatment with C-61+MeOH, the chemical concentration demonstrated a crucial role in order to reach effective oil-repellency conditions. That is, 0.5% concentrated CS delivered only an acceptable water-repellency to the surface, whilst an effective oil-repellency achieved when high-concentration CS with 2% C-61 was used.

13- The alcohol-based CS of C-61 displaced the resident low-salinity brine effectively and improved the oil mobility in the BD14a carbonate rock by a factor of 1.6. However, in presence of high-salinity brine, the chemical instability and its precipitation impaired the rock permeability by 30%.

14- Core treatments with C-61 showed satisfactory level of durability during the high gas rate production, when more than 1000 PVs gas at 458 m/day was injected into the core at 130°C

15- Combining non-ionic fluorinated agents (compatible with brine) with the anionic chemical compounds (effective on carbonate minerals) proved an effective technique to improve the stability of the mixture in the brine media whilst

maintaining a favourable wettability alteration characteristic. However, it should be noted that the mixing ratio of two parts in the combined solution should be optimized in a way that both chemicals preserve their favourable functionalities.

16- Brine composition and its salinity proved to have minimal impact on the post-treatment contact angle measurements on the substrates treated by the C-61 wettability modifier.

4.12 REFERENCES

1. Al-Aulaqi, T., Q. Fisher, C. Grattoni and S. M. Al-Hinai (2013). Wettability Alteration by Brine Salinity and Temperature in Reservoir Cores. SPE Saudi Arabia Section Technical Symposium and Exhibition, 19-22 May, Al-Khobar, Saudi Arabia.

2. AlShaikh, M. and J. Mahadevan (2014). Impact of Brine Composition on Carbonate Wettability: A Sensitivity Study. SPE Saudi Arabia Section Technical Symposium and Exhibition, 21-24 April, Al-Khobar, Saudi Arabia.

3. Anderson, W. G. (1986). "Wettability Literature Survey- Part 1: Rock/Oil/Brine Interactions and the Effects of Core Handling on Wettability." Journal of Petroleum Technology 38(10): 1125-1144.

4. Araujo, Y. C., M. Araujo, H. Guzman and G. Moya (2001). Effect of the Spreading Coefficient on Two-Phase Relative Permeability. SPE International Symposium on Oilfield Chemistry. Houston, Texas, Copyright Society of Petroleum Engineers Inc.

5. Bonn, D., J. Eggers, J. Indekeu, J. Meunier and E. Rolley (2009). "Wetting and spreading." Reviews of Modern Physics 81(2): 739-805.

6. Bradford, S. A., L. M. Abriola and F. J. Leij (1997). "Wettability effects on two- and three-fluid relative permeabilities." Journal of Contaminant Hydrology 28: 171-191.

7. Danesh, A., G. D. Henderson, D. Krinis and J. M. Peden (1988). Experimental Investigation of Retrograde Condensation in Porous Media at Reservoir Conditions. SPE Annual Technical Conference and Exhibition. Houston, Texas, 1988.

8. Gennes, P. G. (1985). "Wetting: statics and dynamics." Reviews of Modern Physics 57(3): 827-863.

9. Fowkes, F. M. (1964). Contact Angle, Wettability, and Adhesion, . Contact Angle, Wettability, and Adhesion, AMERICAN CHEMICAL SOCIETY. 43: i-iii.

10. Hubbell, C. A. (2009). Surface Modification and Chromophore Attachment via Ionic Assembly and Covalent Fixation. PhD thesis, School of Polymer, Textile and Fiber Engineering, Georgia Institute of Technology

11. Jarvis, N. L. and W. A. Zisman (1965). "Surface Chemistry of Fluorochemicals." Interim rept, Naval Research Lab Washington DC(Accession Number : AD0624610).

12. Leja, J. (1982). Surface Chemistry of Froth Flotation, Plenum Press, New York

13. McCaffery, F. G. and D. W. Bennion (1974). "The Effect of Wettability on Two-Phase Relative Penneabilities." Journal of Canadian Petroleum Technology 13(4).

14. Owens, W. W. and D. L. Archer (1971). "The Effect of Rock Wettability on Oil-Water Relative Permeability Relationships." Journal of Petroleum Technology 23(7): 873-878.

15. Rowlinson, J. S. and B. Widom (1982). "Molecular Theory of Capillarity." Oxford University Press, New York.

16. Stumm, J. W. and J. J. Morgan (1970). " Aquatic Chemistry, An Introduction Emphasizing Chemical Equilibria in Natural Waters " New York, Wiley-Interscience, 583 P.

17. Whalen, J. W. (1973). Model Calculations for Wetting Studies: The Role of Contact Angle and Adsorption in Wetting Energetics. SPE Oilfield Chemistry Symposium. Denver, Colorado, 1973 Copyright 1973, American Institute of Mining, Metallurgical and Petroleum Engineers Inc.

18. Young, T. (1805). "An essay on the cohesion of fluids." Philos. Trans. R. Soc. London 95, 65.

19. Zisman, W. A. (1964). in Contact Angle, Wettability and Adhesion, Advances in Chemistry Series, vol. 43, ed. by R.F. Gould (ACS, Washington, 1964), p. 1.

5 PERFORMANCE OF WETTABILITY MODIFIERS IN GAS-CONDENSATE SYSTEMS

5.1 INTRODUCTION

Below the dew-point pressure of a gas-condensate system, particularly seen adjacent to the wellbore, condensate drops out of the gaseous phase (Danesh et al. 1991). At such conditions surface forces of the fluid/fluid and rock/fluid pairs govern the fluids' distribution and their flow characteristics within the porous media. High energy surfaces of the reservoir minerals in contrast to the low interfacial tension (IFT) of the gas/condensate system renders complete wetting of the rock surface by the condensate liquid whereby condensate exists as a thin film throughout the pores and non-wetting gas occupies the centre of them (Danesh et al. 1988, Haniff and Ali 1990, Jamiolahmady et al. 2000).

In condensing systems, as the reservoir depletion continues the interfacial tension between gas and condensate changes substantially, especially near the wellbore. Based on this, at the early stages of the two-phase flow in the reservoir ($P_{wbh}<P_{dew}$) the flow behaviour is principally dominated by the low-IFT effects. Nevertheless, high-IFT conditions eventually prevail as production continues ($P_{wbh}<<P_{dew}$).

It is well recognized that the wetting characteristics of a solid (rock) substrate with a certain surface energy is strictly influenced by thermodynamic properties of the fluids (e.g. gas and condensate) surrounding it. The pioneering work of Zisman (1964) indicated that when the contact angle (θ) of series of homologous liquids (such as n-alkanes) is measured on a given solid surface, the change of cos θ versus liquid surface tension (σ_{lg}) follows a linear trend (**Figure 5.1**). In addition, he introduced an important empirical parameter, known as critical surface tension (σ_c), obtained from the extrapolation of the linear curve to where cos θ=1 or θ=0° below which the liquid samples wet the solid surface completely. Fox and Zisman (1956) later realised that σ_c

varies between liquid types, i.e. the solid's wetting state alters with respect to each group of liquids. These facts, in spite being criticized for their empirical nature, underline the significance of fluid types and properties, e.g. composition and IFT, on wetting status of solid surfaces, which in particular for complex gas-condensate fluid systems necessitate careful consideration.

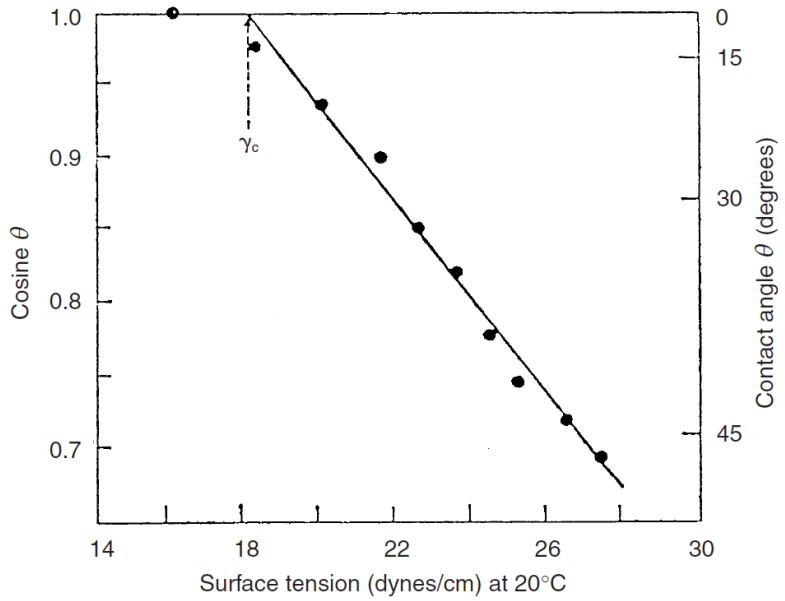

Figure 5.1: Zisman plot for determining critical surface energy of polytetrafluoroethylene using n-alkanes.

As discussed extensively in Chapters 3 and 4, treatment of the reservoir rocks with fluorinated chemicals have been proposed as a promising method for liquid-blockage issues in gas-condensate systems. These chemicals are able to reduce the surface energy of the rock minerals making them hydrophobic and lipophobic. This unique functionality has been attributed to the low-cohesive forces between the fluorinated chemical molecules, which creates low-energy surfaces against wetting. During the last decade, in spite of great deal of interest and effort into application of this technique, all previous reported studies in the literature lack an in-depth and comprehensive insight into the performance of such wettability modifiers in gas-condensate systems. That is, in all available investigations (see Chapter 2 for references) conventional oil and gas fluids, e.g. decane/nitrogen system, have been employed to assess the chemical's performance after the treatment (e.g. Fahes and Firoozabadi 2007). In other words, in all these studies conventional fluids at ambient conditions, e.g. decane/air or heptane/air, have been employed to carry out the contact angle measurements, as a (controversially) representative test for evaluation of the chemical's performance for gas-condensate

systems. Furthermore, whilst in few cases (e.g. Kumar et al. 2006) the treatment effectiveness have also been quantified through pseudo-steady state relative permeability measurements using gas-condensate fluids, the flow tests were performed at IFTs above 4 mN/m but not at lower IFT and under steady-state, which are more representative of these low-IFT fluid systems. Therefore, to the best knowledge of the author, there is no experimental evidence, reported on the alteration of contact angle data on the treated surfaces in presence of gas-condensate fluids.

This chapter is dedicated to this topic by performing a series of contact angle measurements on treated carbonate rock substrates, using various synthetic gas-condensate mixtures at high and low interfacial tension (IFT) values. In addition, according to the outcomes from these measurements, a number of unsteady-state flow tests, were performed to further understand the extension of the results of static contact angle measurements to the dynamic flow tests. These tests have been followed by the steady-state relative permeability measurements, which will be presented and discussed in the next Chapter.

5.2 SELECTION OF TREATMENT SOLUTION

Following the screening tests performed on a number of fluorinated chemicals, presented in Chapter 4, it was concluded that anionic chemical C-61 possesses the desired characteristics, i.e. it can effectively repel oil from the carbonate surfaces, when conventional fluid systems were used. The optimized chemical solution of C-61, determined through the core treatment experiments performed at 130°C, was 2 wt% chemical+MeOH. Accordingly, this CS was chosen for treating Texas-Cream (TC) and Baker-Dolomite (BD) carbonate substrates to be used for contact angle measurements and unsteady-state flow tests employing synthetic GC fluids. On the other hand, to validate the observations and generalize the findings from this study, a number of measurements were repeated on the carbonate substrates treated with another chemical, i.e. 0.5 wt% Z-610+DIW at 130°C, that also showed promising oil-repellency performance. In other words, the carbonate substrates treated with these two chemical solutions demonstrated effective oil-repellency characteristics (i.e. θ=95-100º was obtained) when conventional oil/gas fluid samples (e.g. nC10-air or nC10-N2) were employed at high-IFT conditions (**Figure 5.2**). Here, it should also be mentioned that all the results discussed in the following sections are for the Texas-Cream carbonate substrates treated with the optimised C-61 chemical solution, unless otherwise stated.

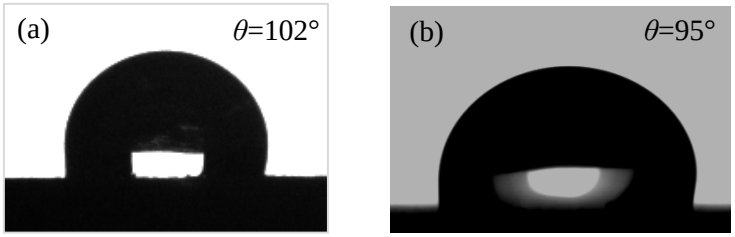

Figure 5.2: Contact angles measured on Texas-Cream substrate treated with 2 wt% C-61+MeOH at 130°C, using conventional oil/gas fluids, a) nC10 (in presence of air) contact angle (IFT=23.8 mN/m) at ambient pressure and b) nC10 (equilibrated with N2) contact angle at 1450 psig (IFT=17.6 mN/m).

5.3 FLUID MIXTURES AND TEST PROCEDURES

Three binary component mixtures of C1-nC4, C1-nC6 and C1-nC10 and two multi-component mixtures of C1-nC5-nC8-nC10 and C1-nC5-nC8-nC15 were used for these contact angle measurements. The PVTi module of the Eclipse commercial reservoir simulator was employed to model the thermodynamic phase behaviour of each hydrocarbon mixture. The 3-parameters Peng-Robinson equation of state was applied to estimate the corresponding physical properties of the fluids (gas and condensate). According to this, a CCE (constant composition expansion) experiment was simulated for each hydrocarbon mixture, providing the desired range of pressures and IFTs to carry out the contact angle measurements.

Our investigations were initially started with less-complicated binary-component mixtures, among which C1-nC10 was first employed at three different temperatures of 20, 50 and 100°C. This was to explore the dependency of the chemicals' oil-repellency strength to temperature. Considering that the impact of temperature was found to be minimal on the measured contact angle data, as will be discussed later, the rest of the measurements using other fluid mixtures were carried out at 20°C, i.e. room temperature, to simplify the experimental procedures.

Table 5.1 lists the total molar composition of all fluid mixtures tested at ambient temperature with their corresponding pressure and IFT ranges. The molar distribution of each hydrocarbon component in the corresponding condensate phase, representative of the liquid drop prevailing the contact angle behaviour, has also been shown in **Table 5.2**. **Table 5.3** also tabulates the composition of the C1-nC10 fluid mixtures and their corresponding properties used for high-temperature measurements. The reported IFT values in **Table 5.1** and **Table 5.3** correspond to values estimated by PVTi and measured during the course of the tests using the conventional pendant-drop technique

(for technical description of the IFT calculation by use of pendant-drop technique refer to Appendix A, at the end of this thesis).

Here, it should also be mentioned that the phase behaviour of C1-nC6 and C1-nC10 fluid mixtures at their selected compositions used in these studies mimics the phase envelope of volatile-oil, instead of gas-condensate, fluids. The pertinent compositions were selected in accord with producing adequate volume of oil, required for IFT and contact angle measurements, after mixing the fluids in the one-litre mixing-cell. It should be noted that this matter will not affect the conclusions drawn from this study for such binary-component mixtures. That is, based on the thermodynamic (Gibbs') phase rule, in a two-phase (P) system with two components (C) at equilibrium, the degrees of freedom (F) is two (F=C-P+2). According to this, for a two-component gas/oil system the thermodynamic properties of the fluids become only a function of pressure and temperature and thus independent of the components concentrations in the mixture (or phase behaviour). Considering these facts, hereafter the gas and condensate terms will be used for all hydrocarbon mixtures employed here, which is more relevant to the subject of this study.

Table 5.1: Total molar composition of hydrocarbon mixtures used in contact angle measurements and their corresponding pressures and IFTs (measured and estimated) at ambient (20°C) temperature.

Test Index	Gas-Condensate Mixture	Composition (mole percent) (%)	Test Pressure (psig)	IFT (Estimated by PVTi) (mN/m)	IFT (Measured) (mN/m)
1	C1-nC10	70-30	1500	10.8	10.02
2	C1-nC10	70-30	2800	3.15	3.86
3	C1-nC10	70-30	3900	0.85	1.42
4	C1-nC6	50-50	200	15.80	15.04
5	C1-nC4	74.4-25.6	400	8.8	10.57
6	C1-nC4	74.4-25.6	1450	1.16	1.18
7	C1-nC5-nC8-nC10	87-7-3-3	1100	10.40	9.71
8	C1-nC5-nC8-nC10	87-7-3-3	2800	0.89	1.12
9	C1-nC5-nC8-nC15	87-7-3-3	1100	10.16	9.68
10	C1-nC5-nC8-nC15	87-7-3-3	3000	0.96	1.90

Table 5.2: Molar distribution of hydrocarbon components in the condensate phase at different pressures (corresponding to the different IFT values, **Table 5.1**) based on the thermodynamic fluid models available in PVTi at ambient (20°C) temperature.

Test Index	Gas-Condensate Mixture	Composition (mole percent) (%)	Test Pressure (psig)	Molar Distribution (%) (of condensate phase)						
				C1	nC4	nC5	nC6	nC8	nC10	nC15
1	C1-nC10	70-30	1500	37.7	-	-	-	-	62.3	-
2	C1-nC10	70-30	2800	56.5	-	-	-	-	43.5	-
3	C1-nC10	70-30	3900	68.1	-	-	-	-	31.9	-
4	C1-nC6	50-50	200	7.6	-	-	92.4	-	-	-
5	C1-nC4	74.4-25.6	400	13.8	86.2	-	-	-	-	-
6	C1-nC4	74.4-25.6	1450	51.9	48.1	-	-	-	-	-
7	C1-nC5-nC8-nC10	87-7-3-3	1100	33.1	-	32.8	-	16.9	17.2	-
8	C1-nC5-nC8-nC10	87-7-3-3	2800	64.3	-	16.3	-	9.3	10.1	-
9	C1-nC5-nC8-nC15	87-7-3-3	1100	32.6	-	33.0	-	17.0	-	17.4
10	C1-nC5-nC8-nC15	87-7-3-3	3000	62.4	-	16.5	-	9.7	-	11.4

Table 5.3: Total molar composition of hydrocarbon mixtures used during contact angle measurements and their corresponding pressures and IFTs (measured and estimated).

Test Index	Fluid Mixture	Composition (mole percent) (%)	Test Pressure (psig)	Test Temperature (°C)	IFT (Estimated by PVTi) (mN/m)	IFT (Measured) (mN/m)
1	C1-nC10	80-20	1500	50	11.09	10.33
2	C1-nC10	80-20	4000	50	1.02	1.45
3	C1-nC10	80-20	1500	100	9.89	9.07
4	C1-nC10	80-20	4000	100	0.99	1.16

The general procedures to prepare the gas-condensate mixtures have been explained in Chapter 3, Section 3.2.4. In summary, the hydrocarbon components were initially combined in a mixing cell at a pressure slightly above the saturation pressure of the mixture for two to three days. The cell pressure was then depleted to the desired test pressure, whereby the condensate was dropped out from the primary gas phase. The equilibrated gas and condensate were finally transferred into two separate accumulators to be used for contact angle measurements.

The sequence of the steps taken to carry out the contact angle and IFT measurements have been discussed in detail in Chapter 3, Section 3.2.6. Accordingly, the measured

IFTs in these investigations have been calculated by fitting the Young-Laplace equation to the pendant drop of condensate created at the needle tip (see Appendix A for further details about Young-Laplace equation). The close agreement between the measured IFTs and those estimated by the fitted PVTi thermodynamic model (**Table 5.1** and **Table 5.3**) demonstrates the reliability and accuracy of the procedures used in this work to prepare and employ the gas-condensate mixtures. It should also be mentioned that the DSA polynomial (tangent-2) method was also used to calculate the corresponding contact angles at the three-phase contact point of condensate/gas/rock system.

5.4 BINARY-COMPONENT FLUID MIXTURES

To simplify the experimental procedures and minimize the number of variables involved in the tests, the corresponding investigations were initiated by employing binary-component mixtures. In the following the results for the C1-nC10 mixtures at 20, 50 and 100°C are discussed first, followed by presenting the results of the measurements performed with C1-nC6 and C1-nC4 fluid systems at 20°C.

5.4.1 C1-nC10 Mixture, 20°C

Contact angle measurements were performed on the treated Texas-Cream substrate at three different IFTs of 10.0, 3.9 and 1.4 mN/m, corresponding to test pressures of 1500, 2800 and 3900 psig, respectively. The pendant condensate drops pertinent to these IFTs are shown in **Figure 5.3**. **Figure 5.4** depicts the contact angles corresponding to IFT=10.0 mN/m, measured over a 12 hours period. Contact angles of 65°, 65°, 60° and 56° were recorded right after the first contact of the condensate drop with the substrate (θ_0) and then after 1, 6 and 12 hours, respectively. It is interesting to note that the condensate droplet remained almost stable, even after 12 hours, demonstrating the effective oil-repellency strength of the treated substrate, associated with the applied fluorinated chemical, with respect to this high-IFT hydrocarbon mixture. Moreover, it should be noted that in contrast to the high contact angle values of about 100° observed using conventional oil/gas systems (i.e. nC10-air or N2-nC10), the chemical's effectiveness is less pronounced for C1-nC10 hydrocarbon mixture as θ=65° was obtained. This trend can either be connected with the IFT reduction or fluid composition change when gas-condensate, instead of conventional, fluids were employed.

Figure 5.5 shows the contact angles measured at IFT=3.9 mN/m. Two differences between these contact angles and those measured at higher IFT=10.0 mN/m are noticed: (i) the contact angle at zero time has reduced by almost 20° (θ_0=44°) compared to that

measured at the higher IFT value (θ_0=65°) and (ii) the contact angle has significantly reduced (by 30°) to about 15° after 1 hour for this low-IFT system whilst it was quite stable at high-IFT conditions. The same trend was also noticed for the contact angles measured on the carbonate substrate treated by chemical Z-610, i.e. less stable and smaller contact angles were observed at low-IFT conditions.

The performance of chemical C-61 was further examined at the lower IFT value of 1.4 mN/m (P=3900 psig) as depicted in **Figure 5.6**. In line with the previous observations demonstrating the higher tendency of the condensate drop to wet the treated surface as IFT was reduced, a smaller contact angle of θ_0=30° was recorded at IFT=1.4 mN/m. This value reduced to 27° after 5 minutes, after which because more condensate travelled through the needle as a stream, recording the variation of contact angles with time failed.

The overall trend of the measured contact angles versus IFT for the C1-nC10 mixture is the monotonic increase in the condensate tendency to wet the treated rock surface with decreasing IFT.

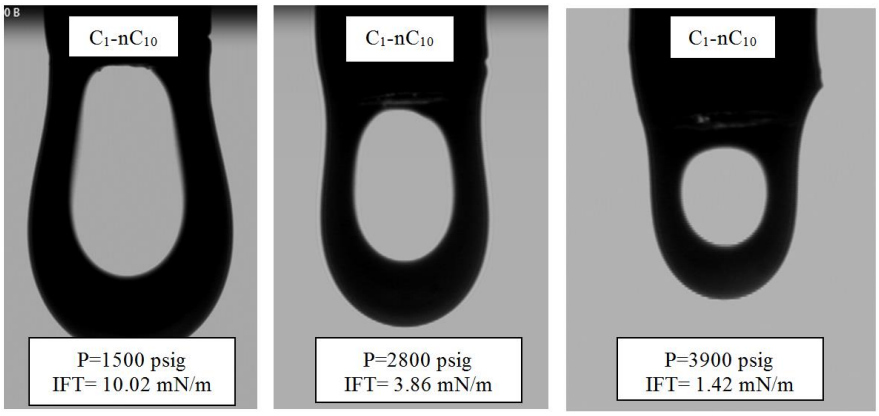

Figure 5.3: Pendant condensate drops of C1-nC10 used for IFT measurements at three different pressures and T=20°C.

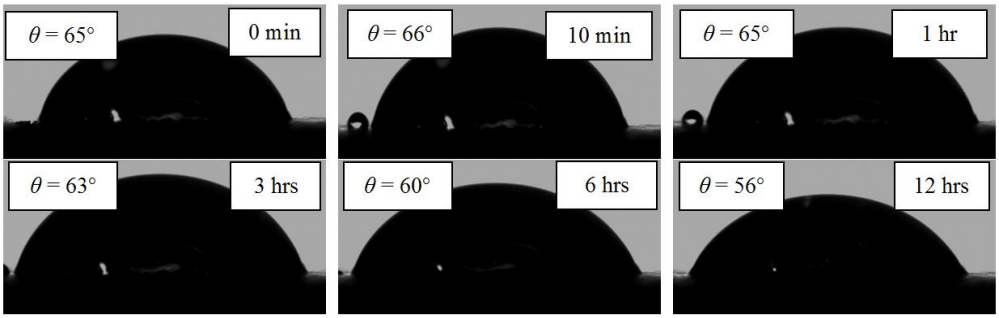

Figure 5.4: Status of a C1-nC10 condensate drop on the treated Texas-Cream substrate at T=20°C and IFT=10.02 mN/m, recorded versus time.

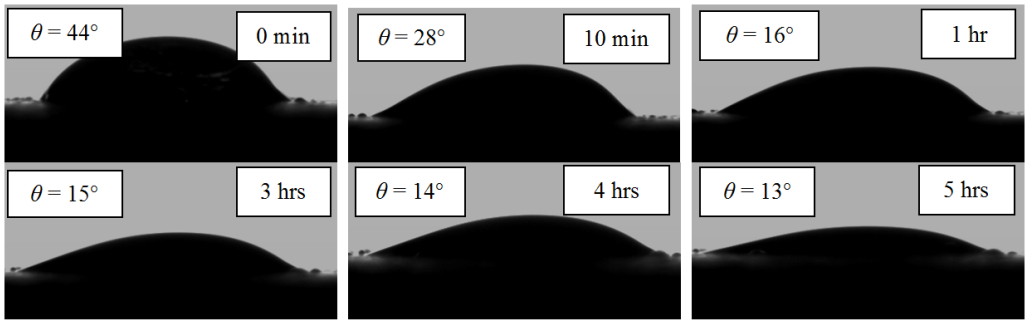

Figure 5.5: Status of a C1-nC10 condensate drop on the treated Texas-Cream substrate at T=20°C and IFT=3.86 mN/m, recorded versus time.

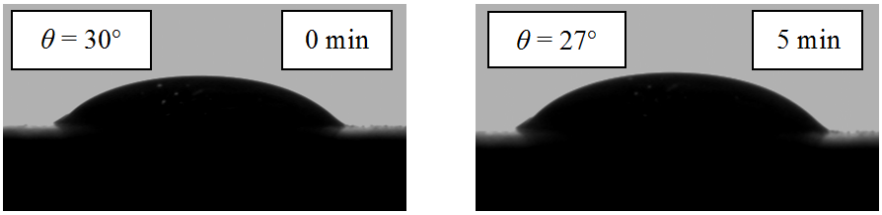

Figure 5.6: Status of a C1-nC10 condensate drop on the treated Texas-Cream substrate at T=20°C and IFT=1.42 mN/m, recorded versus time.

5.4.2 C1-nC10 Mixture, 50°C

Figure 5.7 depicts the C1-nC10 pendant oil drops at 1500 and 4000 psi used for measuring IFT of the system at 50°C. The calculated IFTs corresponding to these pressures were about 10.3 and 1.5 mNm^{-1}, respectively. **Figure 5.8** shows the observed contact angles on the treated BD and TC substrates measured at IFT of 10.3 mN/m. Promising contact angles of 77° and 71° were obtained on the treated BD and TC substrates, respectively. It should be noted that the difference between the contact angle observed here on the TC substrate at T=50°C and that obtained previously at T=20°C (**Figure 5.4**) are within the range of the experimental errors.

Figure 5.9 shows the measured contact angles on the BD and TC substrates at the low-IFT of 1.5 mN/m. Initial contact angles of 68° and 40° were recorded on these two treated substrates. It was noted that similar to the high-IFT case, increasing the temperature from 20°C (**Figure 5.6**) to 50°C had a minimal impact on the wetting tendency of the condensate drop on the treated (TC) surface at this low-IFT limit. The overall observations here is that the repellent-agent maintained its oil-repellency characteristics with increasing temperature (from 20 to 50°C) at both high and low-IFT conditions.

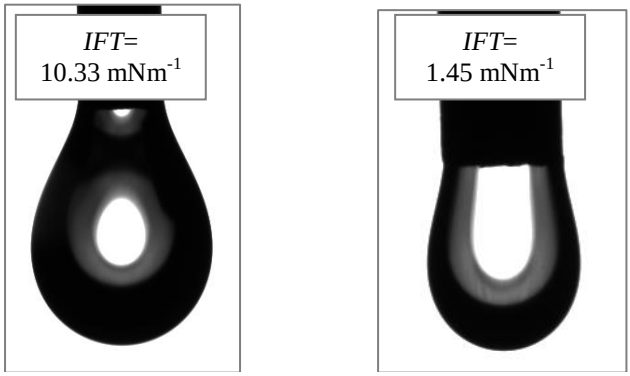

Figure 5.7: Pendant condensate drops of C1-nC10 used for IFT measurements at the test pressures of 1500 psi (left picture) and 4000 psi (right picture) and T=50°C.

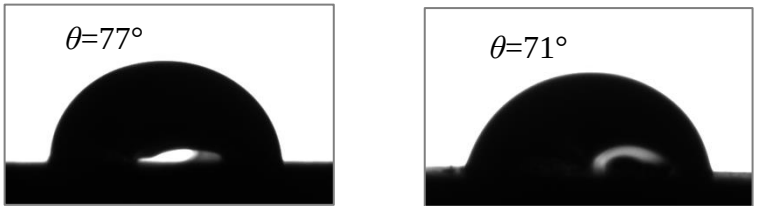

Figure 5.8: C1-nC10 condensate drops on the treated BD (left picture) and TC (right picture) substrates at T=50°C and IFT=10.3 mNm/m.

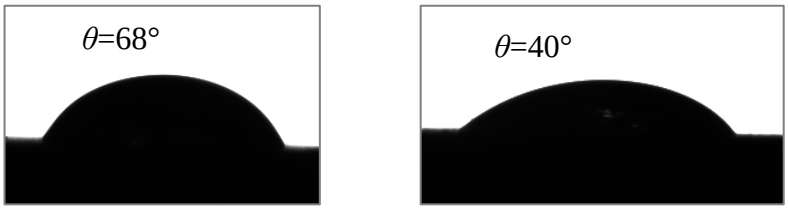

Figure 5.9: C1-nC10 condensate drops on the treated BD (left picture) and TC (right picture) substrates at T=50°C and IFT=1.5 mNm/m.

5.4.3 C1-nC10 Mixture, 100°C

Contact angle measurements similar to those performed at T=50°C were also carried out at a higher temperature of 100°C and two pressures of 1500 and 4000 psi. The measured IFT values corresponding to these two pressures, using the pendant drop method as shown in **Figure 5.10**, were about 9.1 and 1.2 mNm/m, respectively.

Figure 5.11 shows the measured contact angles at the high-IFT limit on the treated BD and TC surfaces. Recording high contact angles of θ_0=86° and 74° on these substrates, demonstrates that the chemical's oil-repellency strength has been preserved even at 100°C at the same level of those observed at 20°C and 50°C for similar IFT.

Figure 5.12 also shows the contact angles of θ_0=30° and 35° measured on the treated BD and TC substrates at the low IFT of 1.2 mNm/m. It should be mentioned that almost the same level of oil-repellency was also observed during the tests conducted at T=20°C (**Figure 5.6)** and 50°C (**Figure 5.9**). These observations, in line with previous findings, confirm the minimal effect of temperature on the chemicals' performance or condensate wetting tendency. According to these results, in order to eliminate the cumbersome and demanding procedures needed to deal with the high-pressure hydrocarbons at high temperatures, here the remaining investigations on the contact angle data using binary- and multicomponent GC mixtures were confined to the ambient temperature conditions, i.e. 20°C.

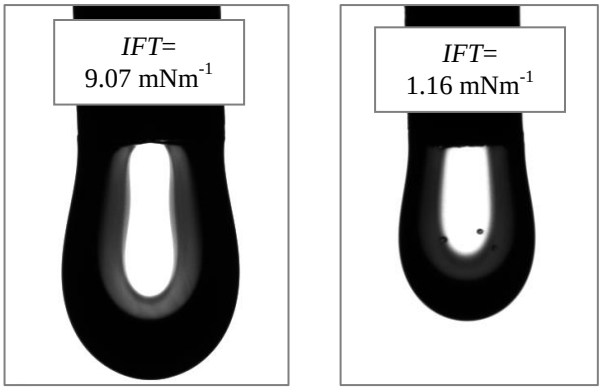

Figure 5.10: Pendant condensate drops of C1-nC10 used for IFT measurements at the test pressures of 1500 psi (left picture) and 4000 psi (right picture) and T=100°C.

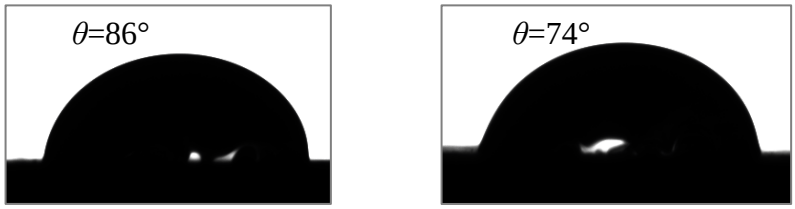

Figure 5.11: C1-nC10 condensate drops on the treated BD (left picture) and TC (right picture) substrates at T=100°C and IFT=9.1 mNm/m.

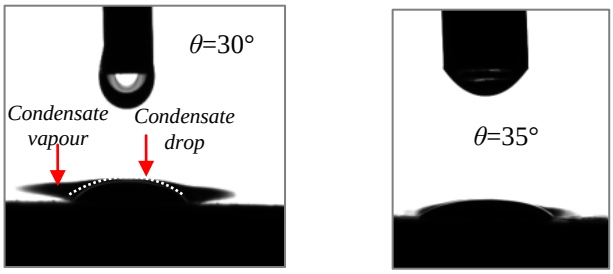

Figure 5.12: C1-nC10 condensate drops on the treated BD (left picture) and TC (right picture) substrates at T=100°C and IFT=1.2 mNm/m.

5.4.4 C1-nC6 Mixture, 20°C

The mixture of C1-nC6 was prepared at 200 psig corresponding to an IFT of 15.0 mN/m (**Figure 5.13**). **Figure 5.14** shows the observed contact angles at different time steps on the carbonate substrate treated with chemical C-61. Although θ_0=45° was recorded at the zero time step, the condensate drop imbibed very quickly into the rock surface within 10 seconds. The same trend, albeit with slightly longer period of stabilisation of the condensate drop, was also observed for the treated substrate by chemical Z-610. That is, condensate drop with θ_0=40° imbibed into the rock surface after 3 minutes (**Figure 5.15**).

It is interesting to note that compared to the first test conducted with C1-nC10 mixture at T=20°C and IFT=10 mN/m, here the tests were carried out at a higher IFT (i.e. 15 mN/m), whereas smaller contact angles were observed. Furthermore, contrary to the C1-nC10 case where stable oil-repellency was achieved, the C1-nC6 condensate drop rapidly spread on the carbonate substrate. These new observations underlined that in addition to the fluids interfacial effects, observed in the case of C1-nC10 mixture, the fluid mixture composition, i.e. the type of the hydrocarbon molecules present in the system, also has a crucial impact on the wetting characteristics of the treated surface.

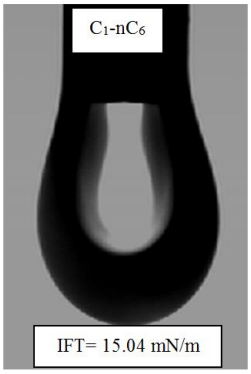

Figure 5.13: The pendant condensate drop of C1-nC6 used for IFT measurements at 200 psig.

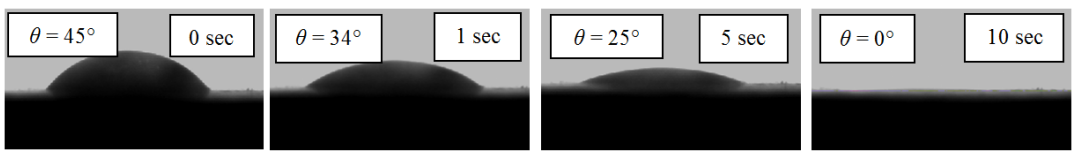

Figure 5.14: Status of a C1-nC6 condensate drop on the treated Texas-Cream substrate (using C-61 chemical solution) at T=20°C and IFT=15.04 mN/m, recorded versus time.

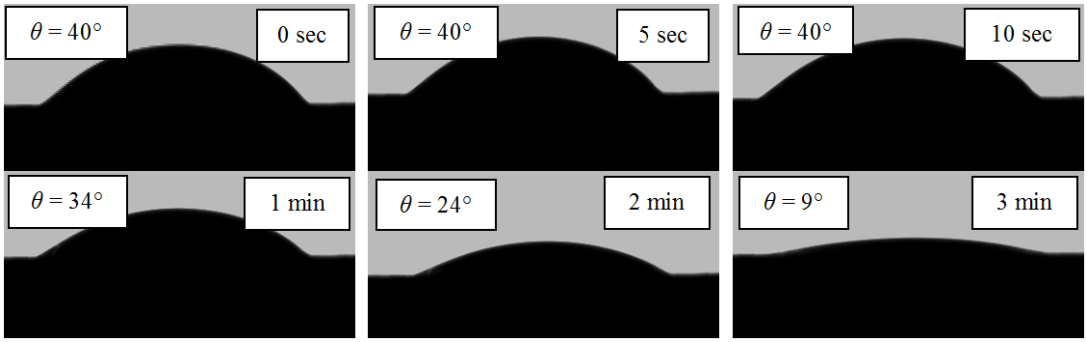

Figure 5.15: Status of a C1-nC6 condensate drop on the treated Texas-Cream substrate (using Z-610 chemical solution) at T=20°C and IFT=15.04 mN/m, recorded versus time.

5.4.5 C1-nC4 Mixture, 20°C

Contact angle measurements by C1-nC4 mixture were conducted on the treated carbonate substrates at two high- and low-IFT values of 10.6 and 1.2 mN/m, corresponding to the test pressures of 400 and 1450 psi, respectively. **Figure 5.16** illustrates the corresponding IFT measurements. **Figure 5.17** and **Figure 5.18** show the condensate behaviour on the treated substrate versus time at these two high- and low-IFT limits, respectively. It is observed that at both IFT conditions, the condensate drops imbibed into the rock surface very quickly, within 1 second. In other words, no evidence of the oil-repellency, even at the first contact of the condensate with the substrate at high-IFT conditions, was observed, i.e. θ_0=0°.

Comparison of the chemical performances at the high-IFT conditions above 10 mN/m for C1-nC10 (θ_0=65°), C1-nC6 (θ_0=45°) and C1-nC4 (θ_0=0°) mixtures provides more support to the previous findings from this study, expressing the reduced oil-repellency strength of the treated carbonate surface as the gas-condensate composition becomes lighter. In other words, the tendency of the condensate liquid phase to wet the treated solid surface increases, even at constant interfacial tensions, as the number of carbon atoms of the heavy-end component in the mixture decreases.

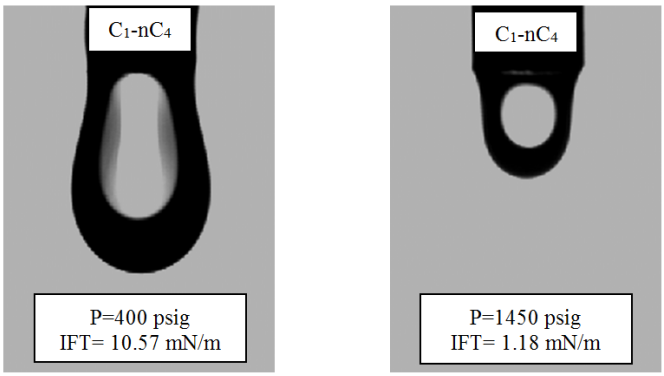

Figure 5.16: Pendant condensate drops of C1-nC4 used for IFT measurements at two different pressures.

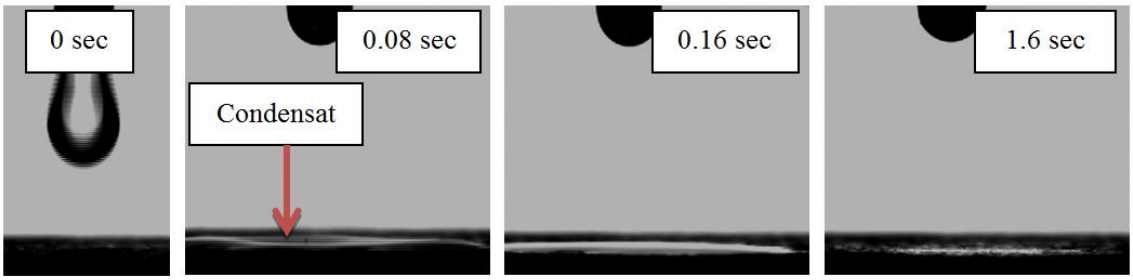

Figure 5.17: Quick spreading of the C1-nC4 condensate drop on the treated Texas-Cream substrate at T=20°C and IFT=10.57 mN/m.

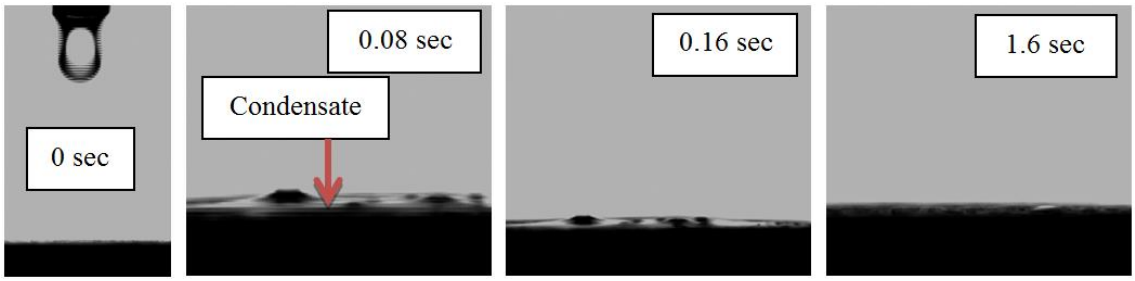

Figure 5.18: Quick spreading of the C1-nC4 condensate drop on the treated Texas-Cream substrate at T=20°C and IFT=1.18 mN/m.

5.5 MULTI-COMPONENT FLUID MIXTURES

The previous contact angle measurements, using binary-component mixtures, proved substantial dependency of the treated surface oil-wetting characteristics to the gas/condensate interfacial and composition. Following these interesting results it was decided to further investigate the impact of IFT and composition on the contact angles for more complex multi-component systems. Accordingly, two multi-component gas-condensate mixtures, composed of C1, nC5 (as the lighter proportions) and nC8 and

nC10/C15 (as the heavier proportions), were prepared at ambient temperature (20°C). The mole fraction of C1, nC5, nC8 and nC10 in the first fluid model was 87, 7, 3 and 3%, respectively. In the second mixture, the nC10 part (in the first model) was replaced by nC15 with similar proportion. Like binary-mixtures, two high- and low-IFT limits of about 10 and 1 mN/m (**Table 5.1**) were also considered for both these two multi-component systems.

5.5.1 C1-nC5-nC8-nC10 Mixture, 20°C

Contact angle measurements using the C1-nC5-nC8-nC10 mixture were conducted at two IFT values of 9.71 and 1.12 mN/m, corresponding to the test pressures of 1100 and 2800 psig, respectively. **Figure 5.19** depicts the pendant condensate drops used to measure the corresponding IFTs at these two pressures.

Figure 5.20 and **Figure 5.21** depict the contact angles of the condensate drop on the carbonate substrate treated with C-61 and Z-610 chemicals, respectively, at high-IFT of 9.7 mN/m. It is noted that the initial contact angle at the zero time step was θ_0=65° in both cases. The condensate drop, however, spread rapidly on the surface treated by C-61 within 1 minute. In the case of the treated substrate with Z-610, better oil-repellency was observed as contact angles of 44º and 28º were recorded after 1 and 4 hours, respectively. Comparing these results with those of the C1-nC10 binary-mixture at nearly similar IFT of 10.0 mN/m, where a stable $\theta_{\sim}$60º was obtained over a long 12-hours period (**Figure 5.4**), highlights the negative impact of the intermediate components, i.e. nC5 and nC8, in the gas-condensate composition increasing the wetting tendency of the condensate phase. It should be noted that the total molar distribution of the nC10 component in the condensate phase of the C1-nC10 binary mixture, i.e. 62%, was split between nC5 (33%), nC8 (17%) and nC10 (17%) in the corresponding liquid phase of the multi-component mixture (**Table 5.2**).

The treated surface showed even more oil-wetting characteristics when IFT of the system was reduced to 1.1 mN/m, as complete spreading of the condensate on both substrates treated by C-61 and Z-610 chemicals was observed. **Figure 5.22** demonstrates the rapid imbibition of the condensate drop occurred within 5 seconds. These observations, in line with the previous understandings from binary-mixtures, verify the reduced level of the treated surface oil-repellency strength with decreasing IFT.

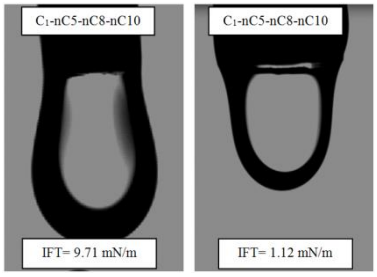

Figure 5.19: Pendant Condensate drops of C1-nC5-nC6-nC8-nC10 mixture used for IFT measurements at two different pressures of 1100 psi (left droplet) and 2800 psi (right droplet).

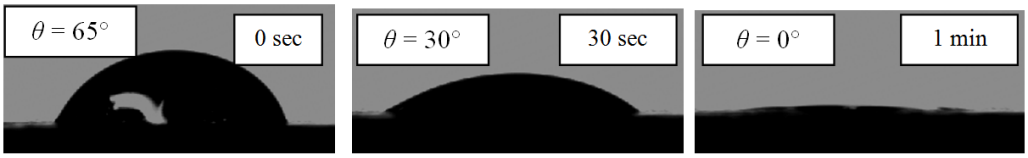

Figure 5.20: Status of a C1-nC5-nC8-nC10 condensate drop on the treated Texas-Cream substrate (using C-61 chemical solution) at T=20°C and IFT=9.71 mN/m, recorded versus time.

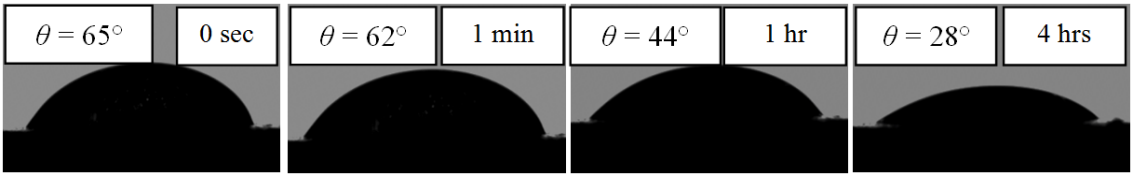

Figure 5.21: Status of a C1-nC5-nC8-nC10 condensate drop on the treated Texas-Cream substrate (using Z-610 chemical solution) at T=20°C and IFT=9.71 mN/m.

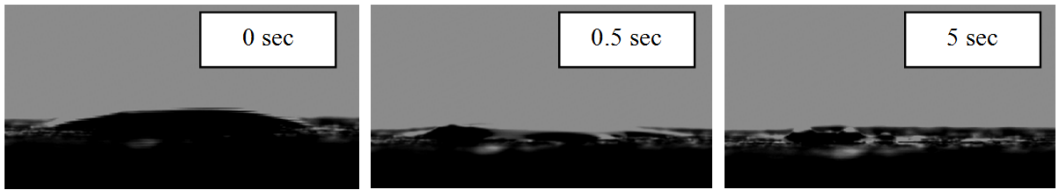

Figure 5.22: Quick spreading of the C1-nC5-nC8-nC10 condensate drop on the treated Texas-Cream substrate (using C-61 chemical solution) at T=20°C and IFT=1.12 mN/m, (similar trend was also observed on the substrate treated with Z-610).

5.5.2 C1-nC5-nC8-nC15 Mixture, 20°C

The impact of heavy-end components on the treated surface oil-repellency strength was further investigated using the C1-nC5-nC8-nC15 fluid system, whereby nC10 proportion in the first multi-component fluid model, discussed in the previous section, was replaced by nC15. The fluids were prepared at two pressures of 1100 and 3000 psig, corresponding to IFT values of 9.7 and 1.9 mN/m, respectively (**Figure 5.23**).

Figure 5.24 shows the contact angles of the condensate drop on the treated TC substrate measured at high IFT=9.7 mN/m. A promising contact angle of θ_0=75° was measured at zero time step. More importantly, the treated substrate showed sustainable oil-repellency for a long period, i.e. θ=62° was recorded after 5 hours. More promising results were also observed at the low-IFT of 1.9 mN/m, at which θ_0=79°. Furthermore, the condensate drop was almost stable over time as contact angles of 73º and 52º were observed after 1 and 5 hours, respectively (**Figure 5.25**). Very similar trends were also observed on the treated substrates by chemical Z-610 at both low- and high-IFT limits. These results at both IFTs, compared to those reported for the C1-nC5-nC8-nC10 mixture, highlight the dominant effect of the nC15 heavy-end component, overcoming the adverse impact of the nC5 and nC8 intermediate molecules. It should also be noted that none of the previous gas-condensate mixtures demonstrated such high and stable contact angles at low-IFT of about 1 mN/m observed here. These findings place more emphasis on the prevailing impact of the heavy-end components in gas-condensate compositions over negative low-interfacial effects on the oil-repellency strength of the treated substrate.

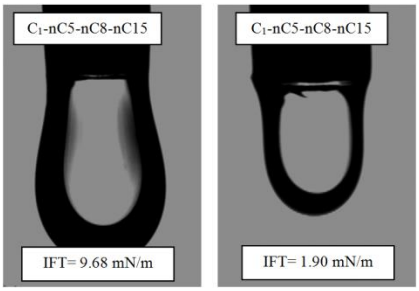

Figure 5.23: Pendent condensate drops of C1-nC5-nC8-nC15 used for IFT measurements at two different pressures of 1100 psi (left droplet) and 3000 psi (right droplet).

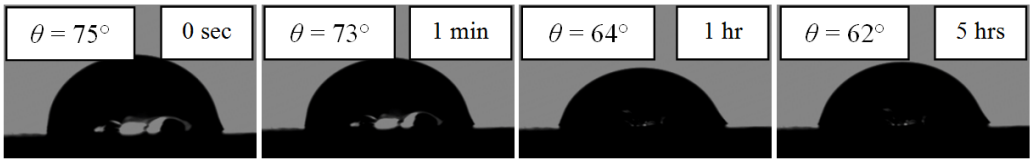

Figure 5.24: Status of a C1-nC5-nC8-nC15 condensate drop on the treated Texas-Cream substrate (using C-61 chemical solution) at T=20°C and IFT=9.68 mN/m, recorded versus time, (similar trend was also observed on the treated substrate by Z-610).

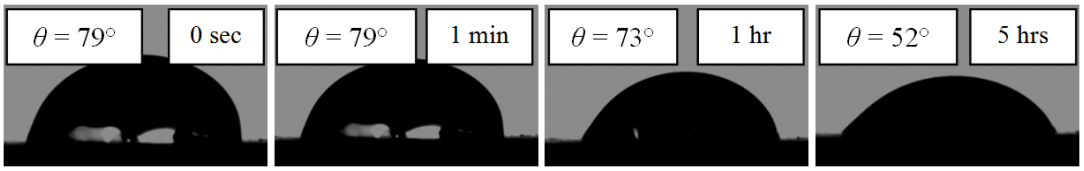

Figure 5.25: Status of a C1-nC5-nC8-nC15 condensate drop on the treated Texas-Cream substrate (using C-61 chemical solution) at T=20°C and IFT=1.90 mN/m, recorded versus time, (similar trend was also observed on the treated substrate by Z-610).

5.6 UNSTEADY-STATE DISPLACEMENT TESTS

Following the interesting results of the static contact angle measurements, demonstrating the significant dependency of the treated surface oil-repellency on the gas/condensate interfacial tension (IFT) and molecular composition, it was decided to verify whether these findings can be extended to the dynamic flow tests. For this purpose, series of unsteady-state (USS) displacement tests using different binary-mixtures of C1-nC10, C1-nC4 and N2-nC10 were carried out at ambient (20°C) temperature. In addition, another USS flow test was also conducted at 100°C using the C1-nC10 mixture to confirm the minimal impact of temperature on the results. **Table 4.3** lists the rock properties of the Baker-Dolomite carbonate core sample used to perform these displacement tests.

To perform the flow tests at 20°C, the binary-mixture of C1-nC10 that showed promising contact angles at high-IFT (of 10 mN/m) and to lesser extent at low-IFT (of 1 mN/m) values, i.e. θ_0 = 65º and 30º, respectively, was primarily selected as the main fluid mixture. In addition, two other binary mixtures of N2-nC10 and C1-nC4 were also used as the extreme limits showing the lowest and highest level of wetting tendency on the treated carbonate substrates. That is, the former one resulted in θ=95°, whereas the latter one resulted in complete wetting of the surface (θ=0°), both at high-IFT limits. The corresponding flow tests at 100°C, similar to the relevant contact angle measurements, were also carried out using binary-mixture of C1-nC10 at high-IFT limit of 10 mN/m. It should also be mentioned that the BD carbonate core sample used in the first case, i.e. flow tests at 20°C, was treated at 130°C using the optimized chemical solution of 2 wt% C-61+MeOH. In the second case, however, the core sample was treated at the same temperature of the flow tests, i.e. 100°C, using similar chemical solution mentioned earlier.

Table 5.4: Rock properties of Baker-Dolomite carbonate core samples used for unsteady-state displacement tests.

Core Sample Index	Length (cm)	Diameter (cm)	Permeability (mD)	Porosity (fraction)	Test Temp. (°C)
BD-13a	11.3	2.56	54	0.25	20
BD-20	8.4	3.78	56	0.24	100

5.6.1 Conditions of the Experiments Performed

The general procedures for performing the unsteady-state flow tests are available in Chapter 3. It should also be mentioned that the unsteady-state tests using gas-condensate mixtures were carried out at the pressures corresponding to the IFT condition of each fluid system listed in **Table 5.1** and **Table 5.3**. The conventional N2-nC10 mixture was also prepared at 4000 psi giving an IFT of about 10 mN/m.

To carry out the pre-treatment displacement tests, the dry core was initially saturated with dry methane gas at the test pressure. Subsequently, several pore-volume of the gas-mixture was injected into the core to displace the resident methane gas completely. Then the oil/condensate cell was opened to the core inlet and the oil was injected at a constant flow rate of 10 cc/hr. This injection rate corresponded to the actual pore velocities of 1.9 and 1 m/day in the BD-13a and BD-20 core samples, respectively. The differential pressure between the core inlet and outlet and produced volumes of the gas and oil at ambient conditions were recorded. After the displacement test performed on the BD-13a core sample, this core was dried inside the oven to be prepared for the next test using a different fluid mixture. It should be noted that this last stage was only repeated for the BD-13a core sample, as several fluid mixtures were employed.

Following the pre-treatment displacement tests, the carbonate rock was treated by injecting about 15 PVs of the chemical solution at a constant flow rate of 10 cc/hr through the core sample at 1000 psig, followed by 12 hours of soaking time. The treatment solution was then flushed with the methane gas, purging it from the remaining unreacted chemical particles. The core was then dried to be used for the post-treatment displacement tests. Here, it should be mentioned that the treatment stage of the BD-13a core sample was carried out on the dry rock, i.e. the core was only saturated with dry methane gas when the chemical injection commenced.

In the case of the BD-20 core sample, on the other hand, to evaluate the chemical performance at more realistic reservoir conditions, the treatment was performed in the presence of the residual oil and brine resident fluids. For this purpose, the 1 wt% (NaCl+CaCl2) low-salinity brine, which had shown a good level of compatibility with

chemical during the course of initial screening tests (i.e. Chapter 4, Section 4.7.6), was used to establish the connate water in the core before injecting the chemical solution. Accordingly, subsequent to the pre-treatment oil displacement the BD-20 core sample was flushed with about four PVs of the brine solution. This was followed by injecting approximately seven pore volumes of dry methane gas into the core after which the irreducible oil and water saturations were established at approximately 10% and 28%, respectively.

Following these treatments, the absolute permeability of the dry core samples to the methane gas was measured. The same permeability as the untreated rock was observed in both cases, demonstrating the effective adsorption of the chemical molecules on the rock surface without any adverse effect on its flow characteristics. Moreover, the procedure followed for the BD-20 core sample highlights the positive potential of the alcohol-based solvent in displacing the oil and brine and providing the solid surface for interaction with the active chemical agent.

5.6.2 USS Flow Tests at 20°C

The differential pressures (DP) recorded during the displacement tests before (BT) and after (AT) the wettability alteration treatment corresponding to each case are shown in **Figure 5.26** to **Figure 5.29.** Substantial decrease in DP is evident for N2-nC10 (**Figure 5.26**) and both C1-nC10 mixtures at high- and low-IFT values (**Figure 5.27** and **Figure 5.28**). This confirms the strong oil-repellency level of the treated rock surface with respect to these two fluid systems. It is also interesting to note that even for the C1-nC10 mixture at low-IFT of 1 mN/m a significant reduction in DP has happened owing to altered wettability. This mixture showed a contact angle of 30º on the treated carbonate substrate compared to 65º observed for the same mixture but at the higher IFT value of 10 mN/m.

Table 5.5 also shows the calculated trapped gas saturations (Sgtr) at the breakthrough time for each fluid system before and after the treatment. It is noted that the pre-treatment Sgtr at the breakthrough point for two cases of C1-nC10 (IFT~10 and 1 mN/m) and N2-nC10 is 43, 60 and 51%, respectively. These values have noticeably reduced to 30, 49 and 38% after the wettability alteration process respectively. The observed trends confirm that after the treatment the rock wettability has been altered to intermediate gas-wet conditions whereby the oil phase with less wetting characteristics occupies the intermediate and large pores and flows with less difficulty. As a result, the

smaller volume of gas is trapped and less viscous forces (DP) are needed to displace the oil.

The results of the experiments performed using the C1-nC4 mixture (**Figure 5.29**), contrary to those observed for the C1-nC10 and N2-nC10 systems, demonstrated the minimal impact of the wettability alteration on improving the oil mobility as almost similar DPs were observed before and after the treatment .

The overall trends observed in all unsteady-state displacement tests explained here, as shown in **Figure 5.30**, are in close agreement with the previous findings from the contact angle measurement tests. That is, in accordance with the ineffective oil-repellency trends observed during the course of contact angle measurements for the C1-nC4 mixture, the oil mobility did not improve after the core treatment. On the other hand, the oil-repellency strength of the treated surface increased promisingly with respect to the C1-nC10 fluid system, as observed during the contact angle measurements and further confirmed with the displacement tests. Furthermore, comparison of the results of displacement tests performed using C1-nC10 and C1-nC4, both at IFT=10 mN/m, strongly confirms the significant impact of the heavy-end components, e.g. nC10, reducing the wetting tendency of the condensate phase on the treated surface.

Table 5.5: Gas saturation calculated at the breakthrough time corresponding to the unsteady-state displacement tests before and after the treatment for three different fluid systems.

Test Conditions Mixture, Pressure (psi),IFT (mN/m)	Gas Saturation at Breakthrough (%)	
	Before Treatment	After Treatment
C1-nC10, 1500, 10	43 %	30 %
C1-nC10, 3900, 1	60 %	49 %
N2-nC10, 4000, 10	51 %	38 %

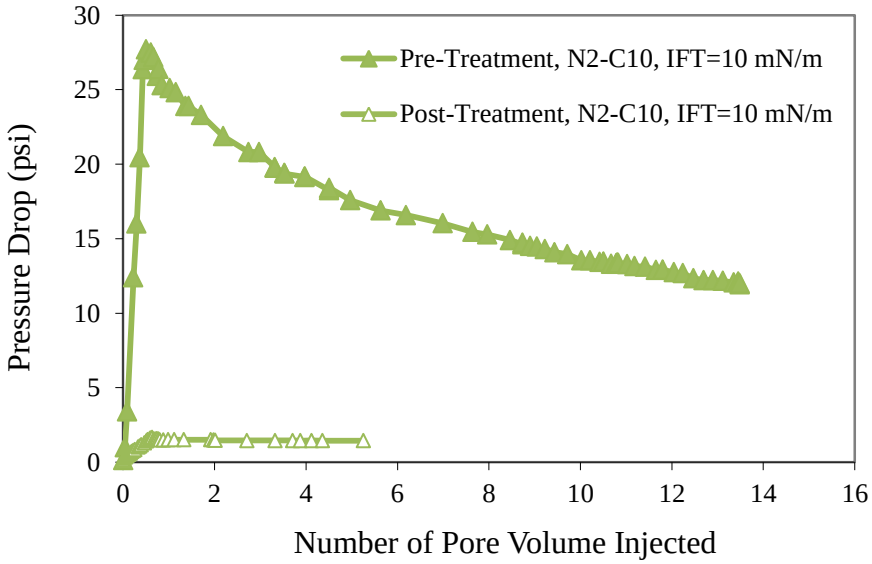

Figure 5.26: Pre- and post-treatment differential pressures measured across the BD-13a carbonate core sample during the unsteady-state injection of nC10 (equilibrated with N2) at a pore velocity of 1.9 m/day at 4000 psi (IFT~10 mN/m) and 20°C.

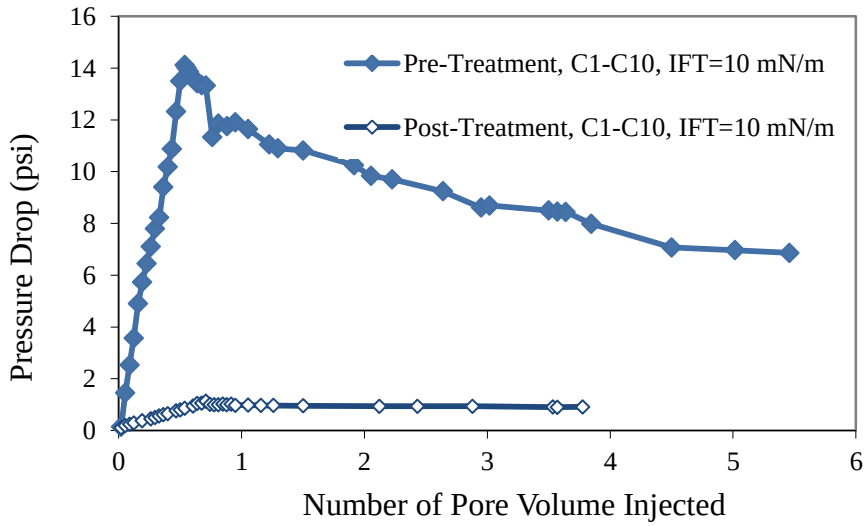

Figure 5.27: Pre- and post-treatment differential pressures measured across the BD-13a carbonate core sample during the unsteady-state injection of nC10 (equilibrated with C1) at a pore velocity of 1.9 m/day at 1500 psi (IFT~10 mN/m) and 20°C.

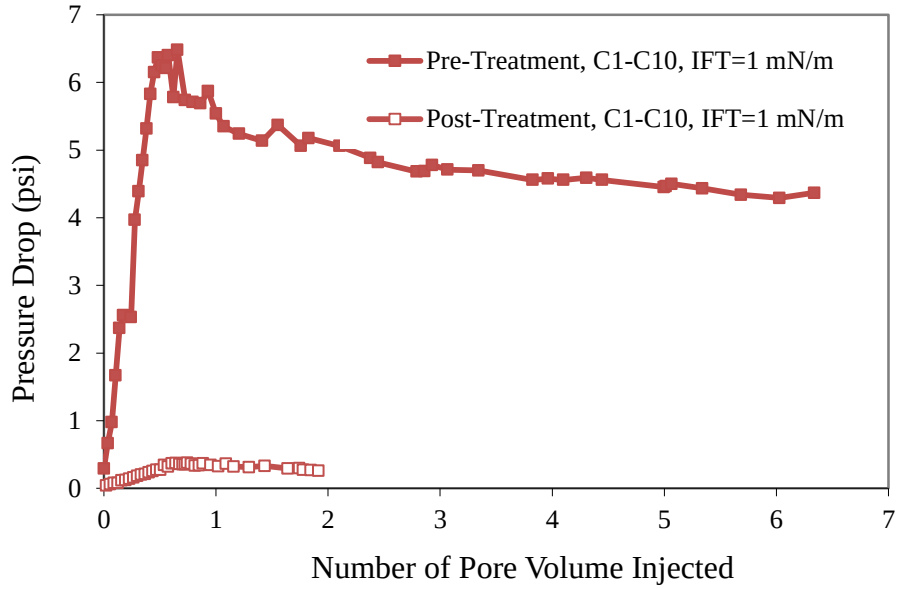

Figure 5.28: Pre- and post-treatment differential pressures measured across the BD-13a carbonate core sample during the unsteady-state injection of nC10 (equilibrated with C1) at a pore velocity of 1.9 m/day at 3900 psi (IFT~1 mN/m) and 20°C.

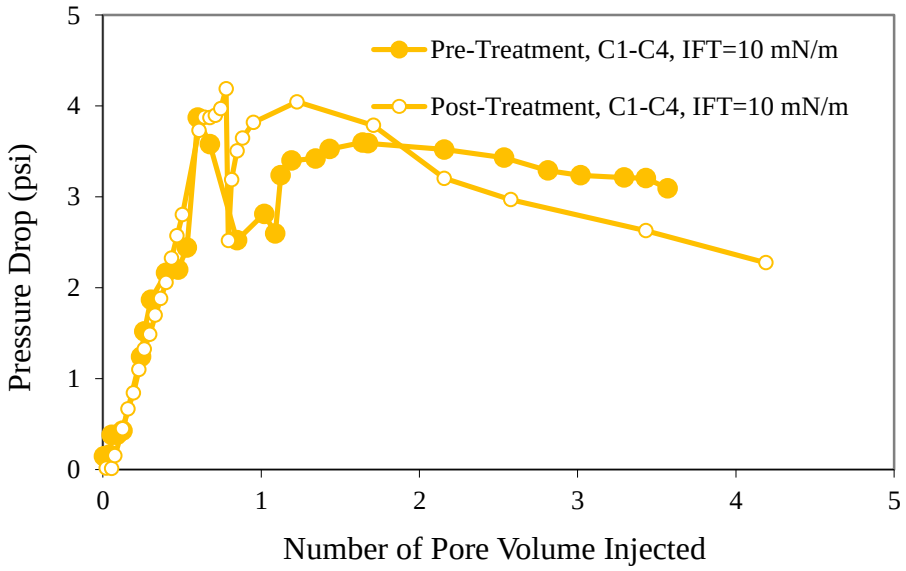

Figure 5.29: Pre- and post-treatment differential pressures measured across the BD-13a carbonate core sample during the unsteady-state injection of nC4 (equilibrated with C1) at a pore velocity of 1.9 m/day at 200 psi (IFT~10 mN/m) and 20°C.

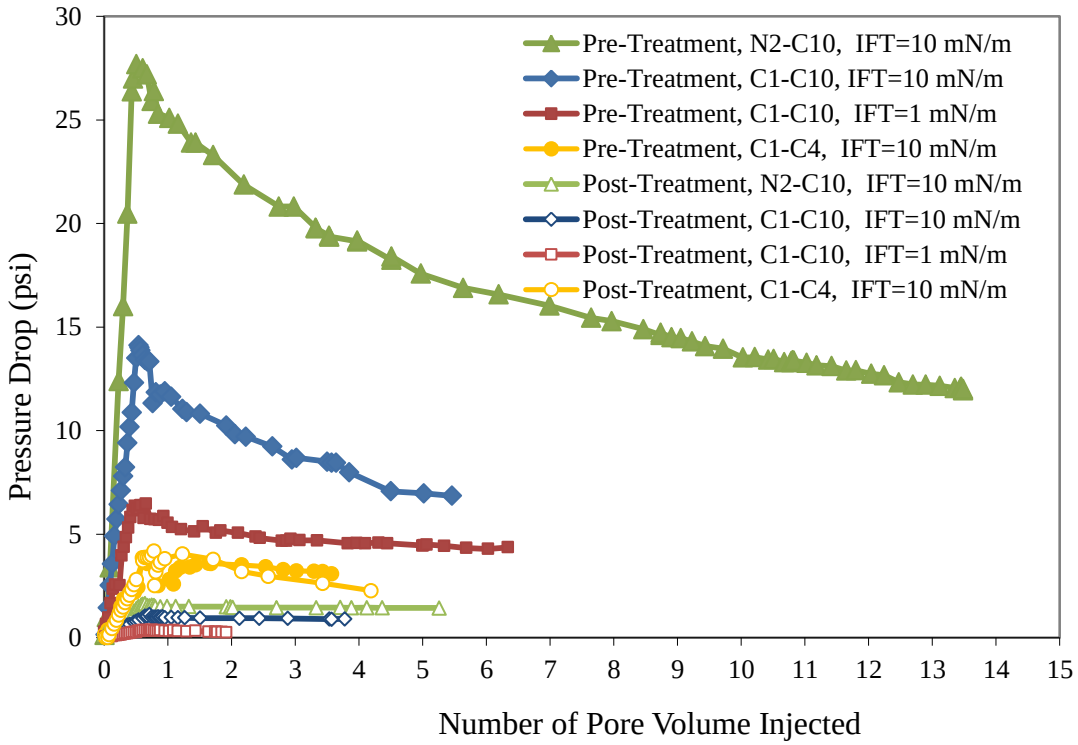

Figure 5.30: All pre- and post-treatment differential pressures measured across the BD-13a carbonate core sample during the unsteady-state injection of oil using different fluid mixtures of N2-nC10, C1-nC10 and C1-nC4 at 20°C.

Analysis of Kr Data

Differential pressures and oil and gas production data recorded during the USS displacement tests were used to estimate the level of improvement of relative permeability curves (k_{rg} and k_{ro}) after the treatment. For these unsteady-state tests the production and pressure data recorded during the displacement tests were history matched using the Sendra package to obtain the k_r data. The Chierici correlation available in Sendra optimizer was employed to estimate the corresponding k_{ro} and k_{rg} curves. Accordingly, Sgtr (trapped-gas saturation) and $k_{ro(Sgtr)}$ (end-point oil relative permeability) were used as the initial guess for the simulator. Capillary pressure (Pc) between oil and gas was also assumed to be zero for both before- and after-treatment conditions; hence the impact of wettability alteration was only reflected in k_r data. **Figure 5.31** depicts the estimated k_{ro} and k_{rg} curves for N2-nC10 and C1-nC10 fluid mixtures. It is noted that significant improvements in k_{ro} and to lesser extent in k_{rg} values have been achieved after the treatment in all cases. It should also be noted that both tests at IFT of 10 mN/m using N2-nC10 and C1-nC10 fluid systems show almost similar trends for k_{ro} and especially k_{rg} before and even after the treatment, which can in turn validate the reliability of the experiments performed in this study. Moreover, the

performed experiment at IFT of 1 mN/m using C1-nC10 mixture shows considerably higher k_{rg} values compared to two other cases at IFT of 10 mN/m. Such an observation is also consistent with general understandings for the near miscible (low-IFT) fluids showing higher relative permeabilities compared to conventional (high-IFT) fluid systems. It should be noted that as mentioned previously the final evaluation of the performance of any chemical should be done by conducting steady-state k_r measurements that are more representative of gas-condensate flow behaviour. The results of this last exercise will be presented in the next Chapter.

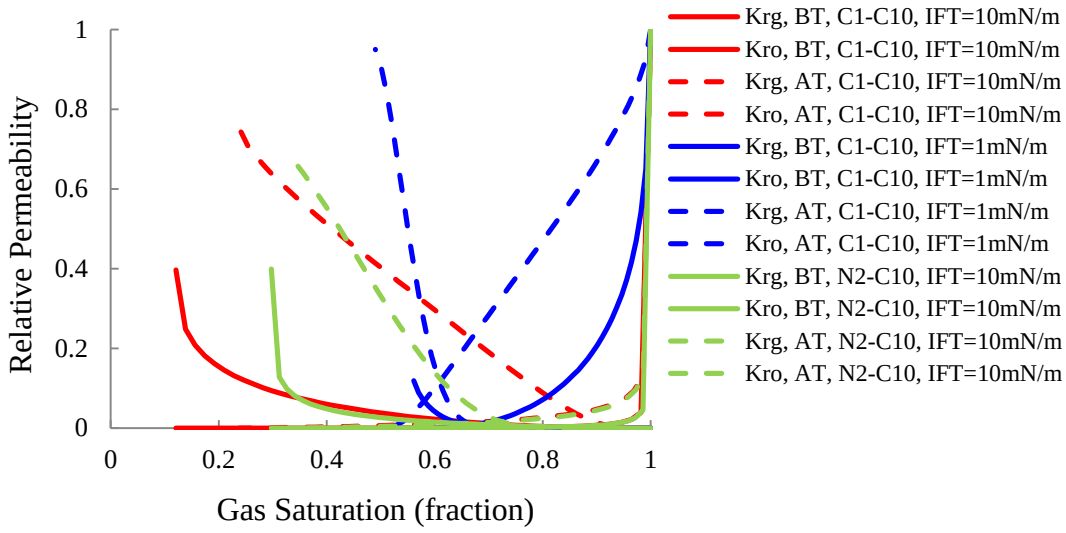

Figure 5.31: The oil and gas relative permeability curves for unsteady-state displacement tests performed on BD-13a carbonate core sample before (BT) and after treatment (AT) using different fluid mixtures.

5.6.3 USS Flow Tests at 100°C

For this part, the binary-component C1-nC10 mixture at 1500 psi, equivalent to IFT of 10 mN/m, was employed to perform the USS flow tests before and after the treatment on BD-20 carbonate core sample at 100°C.

Figure 5.32 compares the differential pressures recorded before and after the treatment during the USS displacement tests. A significant decrease in DP after the treatment is evident at the stabilized conditions, i.e. it has been reduced from about 2.6 psi to 0.5 psi after the wettability alteration process. According to this, there is a significant increase in the oil end-point relative permeability after the treatment by a factor of about 4.8 from 0.05 (before) to 0.24 (after the treatment). It should also be

noted that there is a pronounced decrease in the trapped gas saturation from 57% to 33% owing to the less oil-wetting state of the core occurred after the wettability alteration.

The production and pressure data recorded during the displacement tests were also history matched to obtain the relative permeability (k_r) data relevant to the pre- and post-treatment conditions. It should be mentioned that in this process, similar to the tests at 20°C, the capillary pressure was assumed to be negligible for both pre- and post-treated rocks, hence the wettability alteration effect is reflected in k_r. The history-matched k_r curves for oil and gas phases are plotted in **Figure 5.33**. As this Figure demonstrates a noticeable improvement in both oil and gas relative permeabilities by a factor of around 4 has been achieved after the chemical treatment. From the k_r data, it is also interesting to note that the critical oil saturation has decreased from 25% before to around 4% after that the treatment. **Table 5.6** summarizes these results. Having lower critical oil saturation, from the fluid flow point of view, implies easier oil displacement within the pores and as a result less liquid blockage around the wellbore against the gas production.

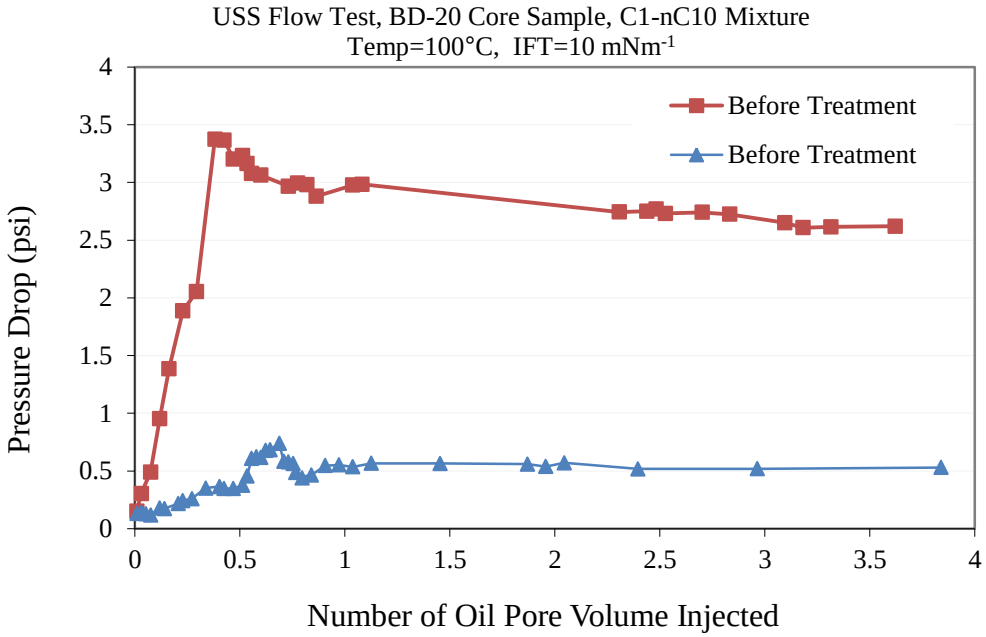

Figure 5.32: Pre- and post-treatment differential pressures measured across the BD-20 carbonate core sample during the unsteady-state injection of nC10 (equilibrated with C1) at a pore velocity of 1.0 m/day at 1500 psi (IFT~10 mN/m) and 100°C.

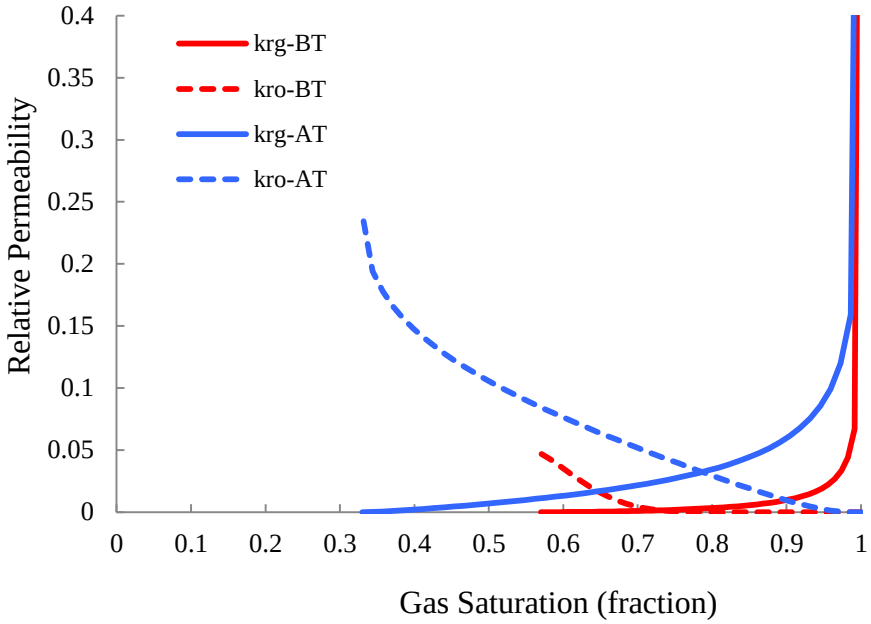

Figure 5.33: The oil and gas relative permeability curves for unsteady-state displacement tests performed on BD-20 carbonate core sample before (BT) and after the treatment (AT) using C1-nC10 mixture at 1500 psi and 100°C.

Table 5.6: The improvement of fluid flow properties as a result of wettability alteration observed during the USS displacement tests using C1-nC10 mixture at 1500 psi and100°C.

Parameter	Before Treatment	After Treatment
Sgtr	0.57	0.33
Socr	0.25	0.04
k_{ro}-endpoint	0.05	0.24

5.7 SUMMARY AND CONCLUSIONS

In this chapter the performance of the two optimised wettability modifiers for gas-condensate systems was investigated through conducting series of contact angle measurements and unsteady-state displacement tests using synthetic gas-condensate fluids. To the best knowledge of the author, this is the first time that such drop shape analysis (i.e. contact angle measurements) of the gas-condensate fluids on the treated rock surfaces are reported. The C-61 and Z-610 fluorochemicals were also used to treat the Texas-Cream and Baker-Dolomite carbonate rock samples and evaluate the generality of the contact angle finings under dynamic flow conditions. In both contact

angle measurements and displacement tests, the impact of the interfacial tensions (IFT) and molecular compositions of the gas/condensate fluid samples on the oil-wetting characteristics of the treated carbonate surface were thus evaluated using binary- and multi-component mixtures. The main experiments were conducted at ambient temperature (i.e. 20°C). In few cases the tests were repeated for 50 and 100°C as well. The following conclusions are drawn from this study:

1- Using the conventional oil/gas fluid systems of air-nC10 (at ambient pressure) and N2-nC10 (at 1450 psi, IFT~18 mN/m) showed a maximum oil-repellency achieved, i.e. θ=95°, on the treated carbonate substrates.

2- The wetting characteristics of the treated surface monotonically increased with lowering the interfacial tension of the C1-nC10 gas-condensate mixture. That is, the initial contact angles (θ_0 measured at the zero time step of condensate deposition on the substrate) of θ_0=65°, 44° and 30° were observed at IFT=10.0, 3.9 and 1.4 mN/m respectively. Moreover, the stability of the contact angles also deteriorated at low IFT values, e.g. at IFT=3.9 mN/m θ declined from 44° to 16° during 1-hour period, while at IFT=10.0 mN/m it was reasonably stable for a long time , e.g. 12 hours.

3- Promising levels of oil-repellency on the treated surface, comparable to those attained at ambient temperature (20°C), were also observed during the contact angle measurements at high temperatures of 50 and 100°C using C1-nC10 mixture at both high- and low-IFT values. This confirmed the preserved level of the chemical's effectiveness with temperature.

4- The molecular composition of the gas-condensate fluid, especially the type of the heavy-end components, showed a crucial impact on the treated surface oil-repellency strength. That is, replacing the nC10 heavy-end component in the C1-nC10 binary-mixture with nC6 or nC4 intermediate-components increased the wetting tendency of the condensate drop on the treated surface, even at high-IFT>10mN/m. The following individual observations were also made:

   a) Using binary-mixture of C1-nC6 (IFT=15.0 mN/m) instead of C1-nC10 (IFT=10.0 mN/m), reduced θ_0 from 65° to 45°. Furthermore, rapid imbibition of the condensate drop into the treated surface was observed.

   b) Complete spreading of the condensate drop on the treated substrate was observed when the C1-nC4 light hydrocarbon mixture was used at both IFT values of 10.6 and 1.9 mN/m, i.e. θ_0=0°.

5- Adding the nC5 and nC8 intermediate-components into the C1-nC10 mixture, i.e. resulting a C1-nC5-nC8-nC10 multi-component system, significantly increased the condensate wetting tendency (or decreased contact angles) on the treated surface at both high- and low-IFT limits.

6- The dominant positive impact of the nC15 heavy-end component over the negative effect of the intermediate ones in the C1-nC5-nC8-nC15 mixture enhanced the oil-repellency on the treated surface significantly. That is, high and almost stable θ_0=79° and 75° were observed at IFTs of 1.9 and 9.7 mN/m, respectively.

7- The overall trend of the contact angle measurements performed for the gas-condensate systems in this work demonstrated that (i) generally the condensate wetting tendency on the treated carbonate surface increases as IFT decreases and (ii) the condensate becomes less wetting with increasing the number of carbon atoms in the system for similar IFT conditions. The underlying mechanisms for the later behaviour, i.e. effect of molecular composition on oil-repellency strength of the treated surface, were not thoroughly understood. It is believed that the interaction of intermolecular forces is one of the main driving forces behind this effect. Such molecular interactions are partly captured by the measurable physical properties such as viscosity and surface tension. Further investigation on this subject is required.

8- The results of the unsteady-sate displacement tests at ambient temperature were in close agreement with the new findings from the contact angle measurements using gas-condensate fluid systems. That is, a significant decrease in differential pressure or increase in oil mobility was observed for binary-component mixtures with the nC10 as the heavy-end component, e.g. C1-nC10 and N2-nC10. On the other hand, the oil mobility after the treatment did not improve when the C1-nC4 light mixture was employed.

9- The unsteady-state displacement tests performed before and after the treatment using C1-nC10 binary-mixture at 100°C demonstrated promising improvement in fluid mobilities after the treatment. The extracted k_r data also showed that the trapped gas and critical condensate saturations decreased from 57% to 33% and from 25% to 4%, respectively. Furthermore, gas and condensate relative permeabilities increased by almost a factor of 4 as a result of the wettability alteration.

5.8 REFERENCES

1. Danesh, A., G. D. Henderson, D. Krinis and J. M. Peden (1988). Experimental Investigation of Retrograde Condensation in Porous Media at Reservoir Conditions. SPE Annual Technical Conference and Exhibition. Houston, Texas, 1988.

2. Danesh, A., G. D. Henderson and J. M. Peden (1991). "Experimental Investigation of Critical Condensate Saturation and Its Dependence on Interstitial Water Saturation in Water-Wet Rocks." SPE Reservoir Engineering 6(3): 336-342.

3. Fahes, M. M. and A. Firoozabadi (2007). "Wettability Alteration to Intermediate Gas-Wetting in Gas-Condensate Reservoirs at High Temperatures." SPE Journal 12(4): 397-407.

4. Fox, H. W. and W. A. Zisman (1956). Journal of Colloid Science 7: 109.

5. Haniff, M. S. and J. K. Ali (1990). Relative Permeability and Low Tension Fluid Flow in Gas Condensate Systems. European Petroleum Conference. The Hague, Netherlands, 1990 Copyright 1990, Society of Petroleum Engineers Inc.

6. Henderson, G. D., A. Danesh, D. H. Tehrani, S. Al-Shaidi and J. M. Peden (1998). "Measurement and Correlation of Gas Condensate Relative Permeability by the Steady-State Method." SPE Reservoir Evaluation & Engineering 1(2): 134-140.

7. Jamiolahmady, M., A. Danesh, D. H. Tehrani and D. B. Duncan (2000). "A Mechanistic Model of Gas-Condensate Flow in Pores." Transport in Porous Media 41(1): 17-46.

8. Kumar, V., G. A. Pope and M. M. Sharma (2006). Improving the Gas and Condensate Relative Permeability Using Chemical Treatments. SPE Gas Technology Symposium. Calgary, Alberta, Canada, Society of Petroleum Engineers.

9. Zisman, W. A. (1964). in Contact Angle, Wettability and Adhesion, Advances in Chemistry Series, vol. 43, ed. by R.F. Gould (ACS, Washington, 1964), p. 1.

6 STEADY-STATE RELATIVE PERMEABILITY MEASUREMENTS ON A TREATED CARBONATE ROCK

6.1 INTRODUCTION

The coupled flow of gas and condensate through the pores at low-IFT conditions is known to be fundamentally different from that of conventional gas-oil systems (Danesh et al. 1994, Jamiolahmady et al. 2000, Jamiolahmady et al. 2003). The positive coupling (increase of k_r as velocity increases and/or IFT decreases) and negative inertia (decrease of k_r as velocity increases) effects, which are governed by the competition between capillary (surface) and viscous forces, are the unique characteristics of such systems (Henderson et al. 1998, Jamiolahmady et al. 2009). These important phenomena were extensively discussed in Chapter 2. In there it was highlighted that such complex flow behaviours pertaining to condensing systems, i.e. k_r=f(velocity,IFT), can only be distinguished through unique and demanding core experiments, i.e. steady-state flow tests, whilst the unsteady-state methods can hardly capture these effects (Henderson et al. 1998, Henderson et al. 2000).

The main body of the available experimental investigations in the literature, exploring the application of wettability modifiers in gas-condensate reservoirs, correspond to tests carried out using conventional fluids (as discussed in Chapter 2). The results of few studies that have used the condensing fluids in their displacement tests are also open to criticisms from the standpoint of experimental conditions and procedures (Kumar et al. 2006, Bang et al. 2008). These measurements were only limited to displacement tests conducted at high gas/condensate IFT values in the range of 4 to 12 mN/m. Moreover, these tests were performed using the pseudo-steady state technique, which is less representative of near wellbore gas condensate flow behaviour but simpler than steady-state test performed at HW laboratories. Here it should be

mentioned that according to the comprehensive stead-state core experiments conducted at HW laboratories, the relative permeability rate-dependency associated with the condensing fluids becomes evident at IFTs below 3 mN/m (Jamiolahmady et al. 2009). Furthermore, the contact angle measurements using synthetic gas-condensate fluids, presented in Chapter 5, demonstrated the significant dependency of the wetting state of the treated substrates on the interfacial and molecular composition of the gas/condensate system, especially at low- IFT limits, which have been missed in other studies.

This chapter presents the results of the steady-state gas condensate relative permeabilities measured for a carbonate core sample before and after the wettability alteration. This was aimed to evaluate the ultimate performance of the effective wettability modifier identified in the previous chapters of this study (i.e. C-61 anionic fluorosurfactant) under more realistic conditions. The measurements were conducted using the binary mixture of C1-nC10 at varying IFT and velocity conditions. Here, it should be mentioned that because a new core was treated for these experiments and to ensure the rock wettability has been altered effectively after the chemical injection, a number of unsteady-state displacement tests were also conducted, prior to commencing the SS-k_r measurements. The experimental procedures and the corresponding results are discussed in the following sections.

6.2 ROCK, FLUID AND TEST PROCEDURES

The gas-condensate high-pressure core flood rig was deployed to measure the steady-state (SS) relative permeability (k_r) data. The main components of this rig and their corresponding key functionalities have been described in Chapter 3, Section 3.1.12. The general procedures followed to perform such SS flow tests have also been explained in Section 3.2.10 of Chapter 3. Here, more details about the rock and gas-condensate fluid properties and the specifications of the experiments performed are given.

6.2.1 Core Preparation, Before and After Treatment

The Baker-Dolomite, BD-12, outcrop carbonate core sample was used in these experiments. This core has a length of 27.3 and diameter of 2.54 cm. The absolute permeability of the dry core sample to the methane gas at confining stress of 2500 psi is 68 mD. It should be mentioned that this is an average value of all absolute permeabilities measured at the different stages of the test, which is subject to around 5% experimental error. The core has a porosity of 25% and contains zero initial water saturation. Here, it should also be noted that compared to the core samples used in

unsteady-state tests, a longer core was used here, ensuring more accurate estimation of flow properties especially the condensate saturation.

To prepare the core for pre-treatment tests, the virgin rock sample was initially washed by sequential injection of sufficient amounts of toluene and methanol until the core effluent turned clear and transparent. The core was subsequently dried inside an oven. The core was then loaded into the core holder and mounted inside the gas-condensate rig, where its pore volume, permeability and single-phase inertial factor were measured. Having calculated the basic rock properties, the SS-k_r measurements were commenced according to the procedures explained later.

In order to alter the rock wettability, the optimized treatment solution of 2 wt% C-61 diluted in methanol was employed. Having accomplished the pre-treatment SS-k_r tests, the core sample was loaded into the chemical treatment oven. Following this, approximately 15 pore volume of the aforementioned chemical solution was injected through the dry core primarily saturated with methane at a velocity of 1.5 m/day at 130°C. The chemical displacement was followed by an extra soaking time for 12 hours. The unabsorbed chemicals were eventually flushed out from the core by injecting methane. Finally, the core sample was dried to be used for post-treatment flow tests.

6.2.2 Binary Gas-Condensate Mixture

The steady-state k_r measurements in the gas-condensate rig at HW laboratory are routinely carried out using the binary mixture of C1-nC4 at 38°C. The operating systems are thus adjusted accordingly. That is, the setup has been leak-tight for pressures up to 4000 psi and the displacement pumps have been tuned for handling the C1-nC4 mixtures. During the course of screening tests, i.e. contact angle measurements and USS flow tests (discussed in Chapter 5), it was verified that the post-treatment liquid-wetting tendency of the carbonate rock when it came in contact with the light C1-nC4 mixture remained almost the same as the pre-treatment one. On the contrary, the treated carbonate surface showed noticeable oil-repellency when it came in contact with the C1-nC10 mixture. Based on these observations, it was decided to employ the C1-nC10, instead of C1-nC4, binary-mixture for conducting the k_r measurements at steady-state conditions. The gas-condensate setup was therefore first tested at higher pressures up to 7000 psi and the displacement pumps were also tuned to properly operate when using the C1-nC10 fluid system.

The binary-component gas-condensate fluid was prepared by mixing methane (C1) and n-decane (nC10) with a molar composition of 96.5% and 3.5%, respectively, at

38°C as the test temperature. The maximum liquid-drop-out corresponding to the CCE (constant composition expansion) test, calculated by the PVTi fluid module of Eclipse, is about 9% at pressure of 2200 psig, as shown in **Figure 6.1**. The dew-point pressure of this fluid mixture is estimated to be 4676 psi at 38°C, witnessed visually in the sight glass during the gradual depletion of the system pressure from above dew-point to the desired test pressure.

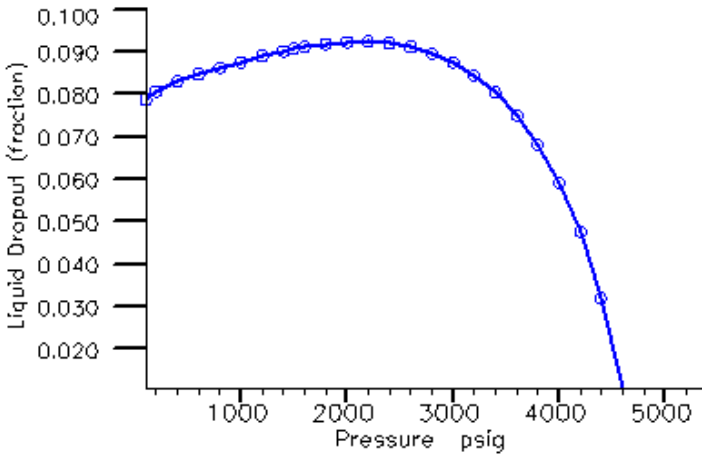

Figure 6.1: Liquid drop-out of the C1-nC10 fluid mixture in constant composition expansion (CCE) test at 38°C.

6.2.3 Single-phase Gas Inertial Factor Measurements

The dry methane gas was used to measure the core single-phase inertial factor. For this purpose, the core, under 2500 psi confining stress, was initially saturated with the methane at 2000 psi. The dry methane was then injected through the core at varying flow rates, increased from 100 to 7000 cc/hr incrementally, to measure the gas permeability reduction associated with the inertial resistance. The actual pore velocity of gas (v_{ag}) corresponding to these flow rates (Q_g) ranges from 19 to 1325 m/day, calculated by the following equation:

$$v_{ag} = \frac{Q_g}{A[\varphi(1-S_{wi})]} \qquad \text{Equation 6.1}$$

where A is the core cross section area, ϕ is the porosity and S_{wi} is the initial water saturation, i.e. zero for this case.

The Reynolds number (Re) for the flow in porous media is also calculated from the formulation below using the square root of permeability:

$$\mathrm{Re} = \frac{\rho_g \mathrm{v}_{ag} \sqrt{k}}{\mu_{\mathrm{g}}} \qquad \text{Equation 6.2}$$

where ρ is the density, k is the permeability, μ is the viscosity and the subscript (g) refers to gas phase.

To calculate the inertial factor (β), the modified form of the non-Darcy or Forchheimer equation (**Equation 2.1**, Chapter 2) for the gas compressibility using the real gas law is employed to give:

$$\frac{M_g (P_{in}^2 - P_{out}^2)}{2zRT\mu_g L(W_g / A)} = \frac{W_g}{A\mu_g}\beta + \frac{1}{k} \qquad \text{Equation 6.3}$$

where M is the molecular weight, P is the pressure, z is the gas compressibility factor, R is the gas constant, T is the temperature, W is the mass flow rate, L is the core length and the subscripts (in) and (out) refer to the core inlet and outlet.

Figure 6.2 shows the measured pressure difference and flow rate data included in **Equation 6.3** for the BD-12 core sample before wettability alteration. Based on the slope of the fitted straight line to these data, the core single-phase inertial factor is estimated as 3.56E8 1/m. The line intercept was also used to calculate the rock permeability as 71 mD, which compare well with the measured average value of 68 mD using methane.

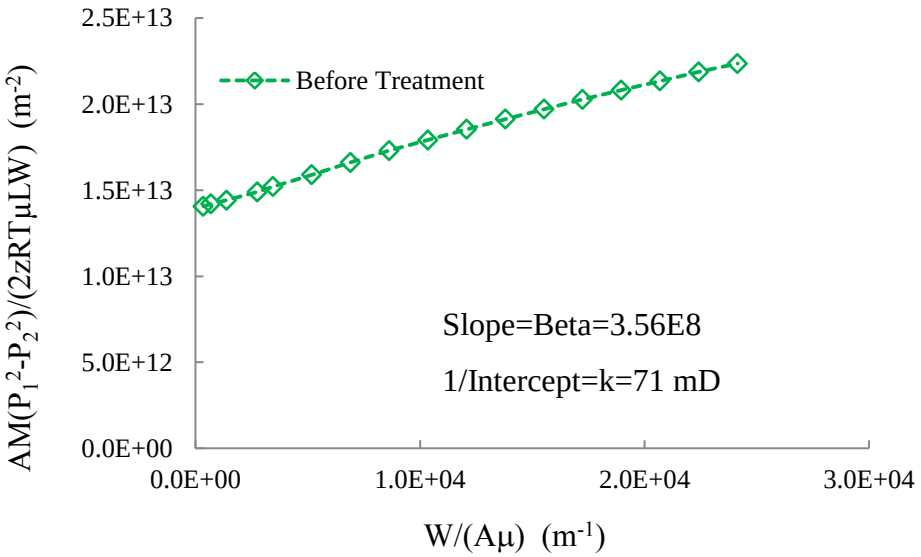

Figure 6.2: Single-phase inertial factor measurement using methane for the BD-12 core sample before chemical treatment.

6.2.4 Conditions of the Tests Performed

Our preliminary investigations on the oil-repellency strength of the treated surface in presence of condensing fluids (i.e. contact angle measurements discussed in Chapter 5), stressed the importance of IFT on wetting tendency of the liquid phase. That is, for C1-nC10 system, condensate contact angles monotonically decreased with IFT, i.e. θ=65°, 44° and 30° were observed at IFT=10, 3 and 1 mN/m, respectively. It was therefore decided to evaluate the chemical's performance at various thermodynamic equilibrium conditions corresponding to the same three IFT limits used previously in the contact angle tests. Accordingly, three pressures of 1500, 3000 and 4000 psi were chosen to measure the SS-k_r data. The IFT values corresponding to these pressures, calculated by PVTi, are 10.8, 2.7 and 0.77 mN/m, respectively. **Table 6.1** lists the fluid properties corresponding to the C1-nC10 binary mixture at these three pressures.

The steady-state k_r measurements before and after the wettability alteration were carried out in a stepwise manner from high- to low-IFT values, i.e. they commenced at a pressure of 1500 psi followed by 3000 and 4000 psi. It should also be noted, the whole system pressure including core and fluid accumulators raised to a pressure above the dew point, e.g. 5000 psi, in between each two successive stages. This was to dry the core and strip off all the condensate from the core to calculate the condensate saturation in the rock (more details are given in Chapter 3, Section 3.2.10).

As discussed previously in Chapter 2, Section 2.4, in retrograde gas systems, it is believed that the relative permeabilities become independent of IFT as interfacial tension between gas and condensate exceeds 3 mN/m. Moreover, the positive rate effect, i.e. increase of k_r with velocity, diminishes at such high-IFT conditions. Based on these facts, the k_r data for IFTs of 10 and 2.7 mN/m, were only measured for a single total pore velocity of about 20 m/day. The corresponding data provided the base relative permeability curves for the gas-condensate system considered here. At the lower IFT limit of 0.77 mN/m, on the other hand, the steady-state relative permeability points were measured at several flow rates, ranging from 20 to 636 m/day, providing the velocity-dependant relative permeability curves.

In order to complete the relative permeability data, several CGR (condensate to gas flow rate ratio) values were considered in all three IFT cases, providing the k_r data at different condensate saturation values. The fractional flow used here ranged from a CGR of 0.03 to 0.4. Here, it should be noted that at certain test conditions, especially at low-IFT values, the low initial CGR could reduce the condensate saturation in the core at the initial steady state conditions to a value lower than that initially established by condensation process. The condensate saturation in the core is subsequently increased with increasing CGR. As a result, a process of imbibition (during the initial condensation) followed by drainage (at low CGR) and continued by imbibition (at higher CGR), occurs as tests proceed.

Table 6.1: Estimated fluid properties by PVTi at three pressure levels for the C1-nC10 binary mixture used during steady-state relative permeability tests.

Pressure (psig)	ρ_g (kgm^{-3})	ρ_c (kgm^{-3})	μ_g (mPa.s)	μ_c (mPa.s)	IFT (mNm^{-1})
1500	76.0	693.7	0.0139	0.3555	10.77
3000	161.7	623.0	0.0203	0.2093	2.72
4000	221.3	570.8	0.0266	0.1461	0.77

6.3 PRELIMINARY EVALUATION OF TREATMENT

Considering the demanding and laborious procedures needed to perform the SS-k_r tests, it was decided to re-evaluate the treatment performance, before proceeding with the steady-state k_r measurements on the treated core. This was achieved by preforming a number of straightforward unsteady-state displacements, similar to those screening tests

discussed in Chapter 4, using the C1-nC10 binary-mixture employed in SS tests. Any distinct reduction in the differential pressures across the core during the displacement of gas by oil in these USS tests was attributed to alteration of rock wettability. The detailed procedures for conducting the unsteady-state tests have been explained in Sections 3.2.9 of Chapters 3. In general, during the unsteady-state test the core is fully saturated with single phase gas, while the single phase oil is injected into the core at a constant flow rate and displaces the resident gas. In steady-state test, however, the initial condensate saturation is primarily distributed across the core by dropping the pressure of the resident gas mixture saturating the core to a pressure below the dew-point, after which the gas and oil are injected into the core simultaneously at different fractional flow rates (more details are given in Chapter 3, Section 3.2.10). It will later be shown that employing the unsteady-state techniques for modelling the flow behaviour in gas-condensate systems will result in overestimating the performance of wettability modifiers.

6.3.1 Unsteady-state Displacement Tests

The unsteady-state displacement tests were carried out at ambient temperature (i.e. 20°C) and at two pressures of 1500 and 4000 psi, corresponding to two high and low-IFT values of 10.8 and 0.77 mN/m, respectively. The chemical treatment oven was employed to perform these tests before and after the treatment. Prior to the test, C1 and nC10 components were mixed at the test pressure to reach the equilibrium conditions. Subsequently, the oil and gas mixtures were transferred into two separate cells. Several pore volumes of gas were then injected into the core primarily saturated with dry methane gas to ensure it is fully saturated with the gas mixture. The oil cell was finally opened to the core to displace the resident gas at a constant actual pore velocity of about 2 m/day. The differential pressure (DP) across the core during the displacements were recorded before and after the treatment and used as a qualitative indication of the improvement in oil mobility owing to the altered rock wettability. **Figure 6.3** shows the results of USS displacement tests performed before and after the chemical treatment at high- and low-IFT conditions. As can be noted, there is a substantial reduction in differential pressures after the treatment in both high (**Figure 6.3a**) and low (**Figure 6.3b**) IFT limits, with almost same order of magnitude. These observations confirmed the rock surface is reasonably less oil-wet owing to an effective wettability alteration process. According to these results, the steady-state flow tests on the BD-12 core sample were then carried as discussed in the next section.

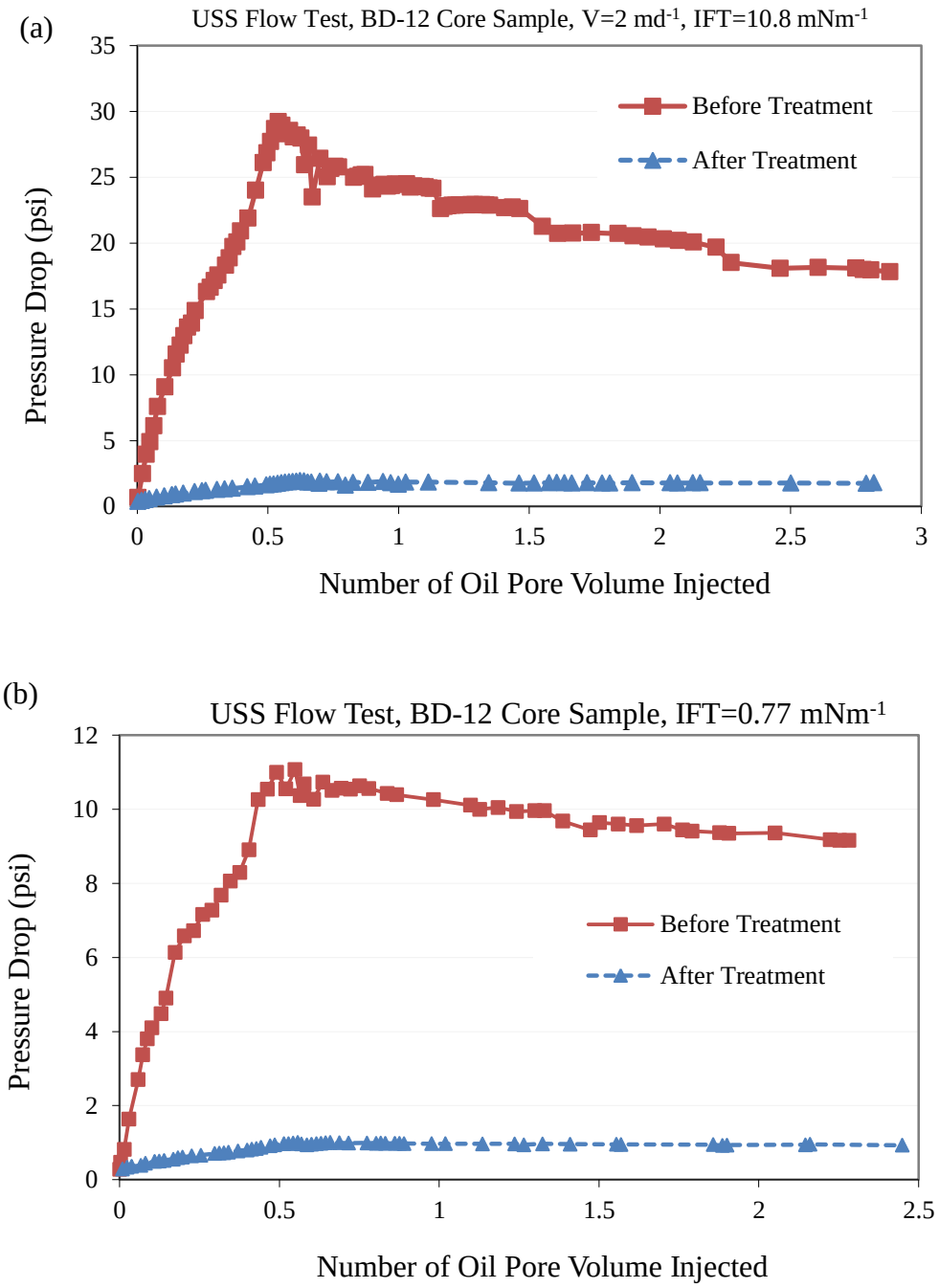

Figure 6.3: Pre- and post-treatment differential pressures measured across the core sample during the unsteady-state injection of the C1-nC10 oil into the core saturated with the gas at (a) 1500 psi (equivalent to IFT of 10.8 mNm^{-1}) and (b) 4000 psi (equivalent to IFT of 0.77 mNm^{-1}) both performed at ambient temperature.

6.4 STEADY-STATE RELATIVE PERMEABILITY MEASUREMENTS

The steady-state relative permeability measurements at high IFTs of 10.8 and 2.7 mN/m were carried out at three different CGR values of 0.05, 0.1 and 0.4 at upstream conditions. As mentioned earlier, only one injection rate of 105 cc/hr of total gas plus condensate, corresponding to the total actual pore velocity of about 20 m/d, was considered for these two tests. At the lower IFT value of 0.77 mN/m, apart from the CGRs mentioned above, an additional CGR of 0.03 was also considered. Moreover, the tests covered a wide range of velocities at each CGR.

At the beginning of each test, the system pressure, core plus all relevant gas and oil accumulators, was set at 5500 psi, well above the dew-point. The initial condensate saturation was distributed inside the core by lowering the pressure in the whole system gradually to the desired test pressure below the dew-point. The core was then isolated and the gas and condensate in the rest of the system were mixed for several times to reach the equilibrium state. The test at each pressure was commenced at the lowest CGR while the gas and condensate were injected simultaneously through the core at specified flow rates until steady-state was attained. As mentioned earlier, in the case of IFT=0.77 mN/m, the multiple-velocity k_r data were also obtained for each fractional flow ratio by increasing the gas and condensate injection rates simultaneously in such a way that the resulting CGR remained constant. Having accomplished the steady-state displacements at the first fractional flow ratio, CGR was increased to the next level in a stepwise manner by changing the gas and condensate injection rates whereby the total gas plus condensate flow rate remained constant. It should also be mentioned that after completion of each CGR, the fluids were thoroughly mixed and the condensate saturation in the core was calculated using material balance. The flow regime during injection is also defined in terms of the capillary number, which is calculated based on Equation 2.5 (Nc) and Equation 2.6 (Nc'), discussed in Chapter 2.

6.4.1 Single-rate Relative Permeability: IFT of 10.8 mN/m

Table 6.2 includes the flow conditions corresponding to the tests performed before and after the treatment at the pressure of 1500 psi equivalent to IFT of 10.8 mN/m. It is noted that during these measurements as CGR increased from 0.05 to 0.4, the Reynolds number decreased from 3.1E-4 to 2.3E-4. The Nc and Nc' capillary numbers also decreased from 2.8E-7 to 2.1E-7 and increased from 8.2E-6 to 3.4E-5, respectively.

Figure 6.4 plots the gas and condensate relative permeability curves versus condensate saturation and CGR measured on the pre- and post-treated BD-12 carbonate

rock sample. The corresponding test data have been included in **Table 6.3**. It is noticed that the condensate saturation established in the core has significantly reduced by approximately 39, 38 and 35% after the wettability alteration process at the selected CGRs of 0.05, 0.1 and 0.4, respectively. In other words, less condensate has been accumulated within the rock owing to the improved condensate mobility after the treatment. This, on the other hand, has resulted in substantial reductions in pressure drops during simultaneous displacement of gas and condensate through the core, which is more pronounced at higher CGR (or condensate saturation) values (**Table 6.3**). As a result, significant improvements in gas and condensate relative permeabilities by a factor of 2, 3.2 and 3.6, corresponding to the CGR values of 0.05, 0.1 and 0.4 respectively, have been achieved after the treatment, which is confirmed by the CGR-based kr data shown in **Figure 6.4b**.

Table 6.2: Flow conditions corresponding to the tests conducted on the BD-12 core sample at IFT of 10.8 mN/m.

Qg, cc/hr	Qc, cc/hr	CGR	Nc	Nc'	Re
100	5	0.05	2.819E-07	8.22E-06	3.12E-04
95.5	9.5	0.1	2.69E-07	1.43E-05	2.98E-04
75	30	0.4	2.11E-07	3.43E-05	2.34E-04

Table 6.3: Data corresponding to the SS-k_r measurements conducted on the BD-12 core samples before and after the treatment at IFT of 10.8 mNm/m.

CGR	Test	ΔP, psi	Sc	krg	krc	kr-IF
0.05	Before CT	12.98	0.75	0.034	0.044	2.0
	After CT	6.34	0.46	0.070	0.090	
0.1	Before CT	22.66	0.77	0.019	0.048	3.2
	After CT	7.00	0.48	0.061	0.154	
0.4	Before CT	54.17	0.85	0.006	0.063	3.6
	After CT	14.86	0.56	0.022	0.230	

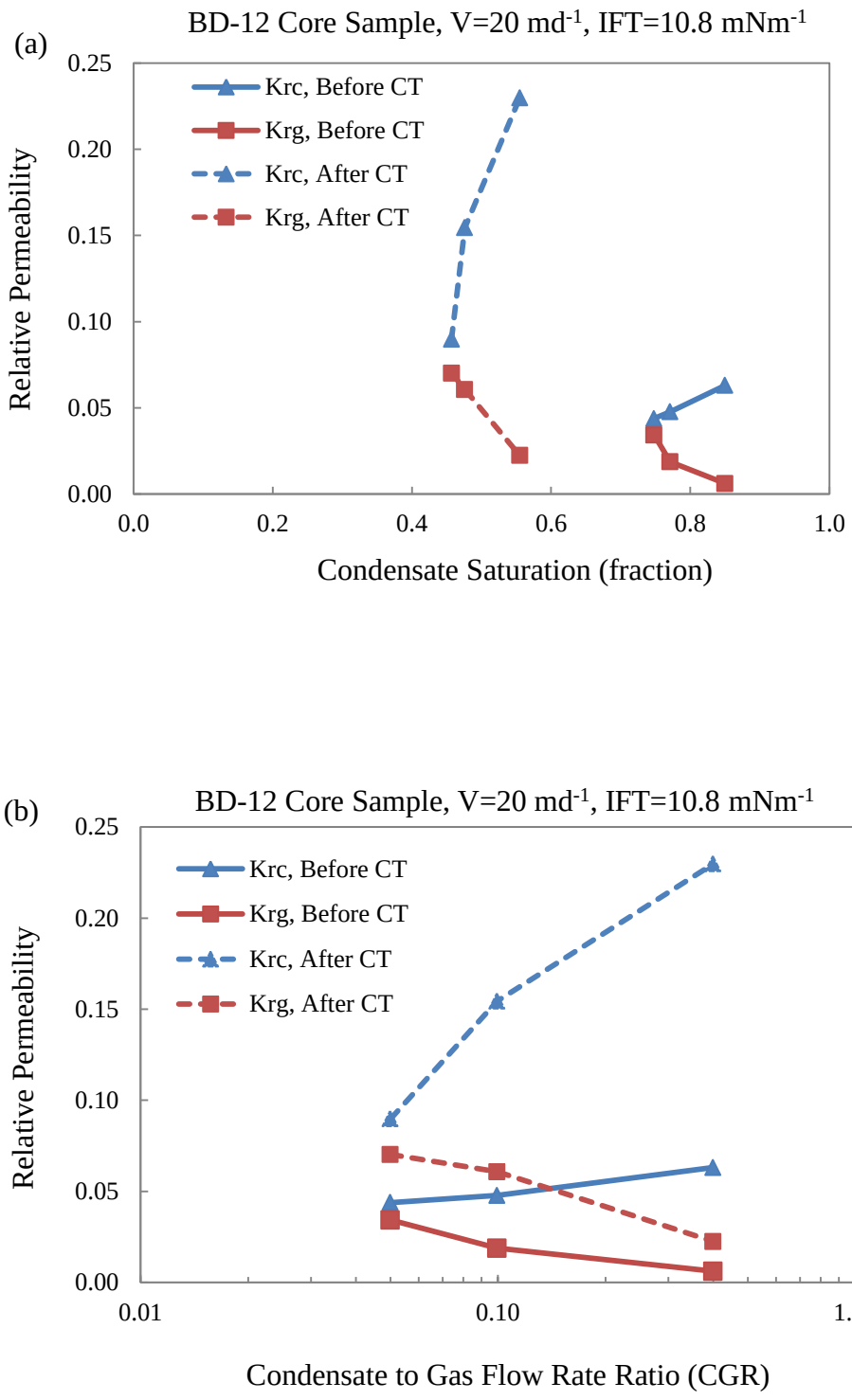

Figure 6.4: Pre- and post-treatment steady-state gas and condensate relative permeabilities of the BD-12 core sample versus (a) condensate saturation and (b) CGR at IFT of 10.8 mNm^{-1}.

6.4.2 Single-rate Relative Permeability: IFT of 2.7 mN/m

Table 6.4 includes the flow conditions corresponding to the tests performed before and after the treatment at the pressure of 3000 psi equivalent to IFT of 2.7 mN/m. It is noted that during these measurements as CGR increased from 0.05 to 0.4, the Reynolds number decreased from 4.6E-4 to 3.4E-4. The Nc and Nc' capillary numbers also decreased from 1.7E-6 to 1.2E-6 and increased from 2.2E-5 to 7.2E-5, respectively.

Figure 6.5 plots the gas and condensate relative permeability curves versus condensate saturation and CGR measured on the pre- and post-treated carbonate core sample. The corresponding test data have been included in **Table 6.5**. It should be mentioned that the condensate saturation obtained for the post-treatment measurements at CGR of 0.1 were considered not reliable and hence excluded from data reported here. As it is noted after the wettability alteration the condensate saturation corresponding to the CGRs of 0.05 and 0.4 has been favourably reduced by 54% and 32%, respectively, at this intermediate-IFT of 2.7 mN/m. However, the resulting reductions in pressure drops or equivalently increases in relative permeabilities are not as promising as those observed at the higher IFT value of 10.8 mN/m. As **Figure 6.5b** depicts, the gas and condensate relative permeabilities after the treatment have improved by a factor of 1.3 in all three CGR values.

Table 6.4: Flow conditions corresponding to the tests conducted on the BD-12 core sample at IFT of 2.7 mN/m.

Qg, cc/hr	Qc, cc/hr	CGR	Nc	Nc'	Re
100	5	0.05	1.65E-06	2.23E-05	4.55E-04
95.5	9.5	0.1	1.57E-06	3.32E-05	4.35E-04
75	30	0.4	1.23E-06	7.23E-05	3.41E-04

Table 6.5: Data corresponding to the SS-k_r measurements conducted on the BD-12 core sample before and after the treatment at IFT of 2.7 mNm/m.

CGR	Test	ΔP, psi	Sc	krg	krc	kr-IF
0.05	Before CT	8.82	0.72	0.074	0.038	1.3
	After CT	6.80	0.34	0.096	0.049	
0.1	Before CT	13.10	0.76	0.047	0.049	1.3
	After CT	10.05	-	0.062	0.063	
0.4	Before CT	28.55	0.81	0.017	0.070	1.3
	After CT	21.91	0.55	0.022	0.092	

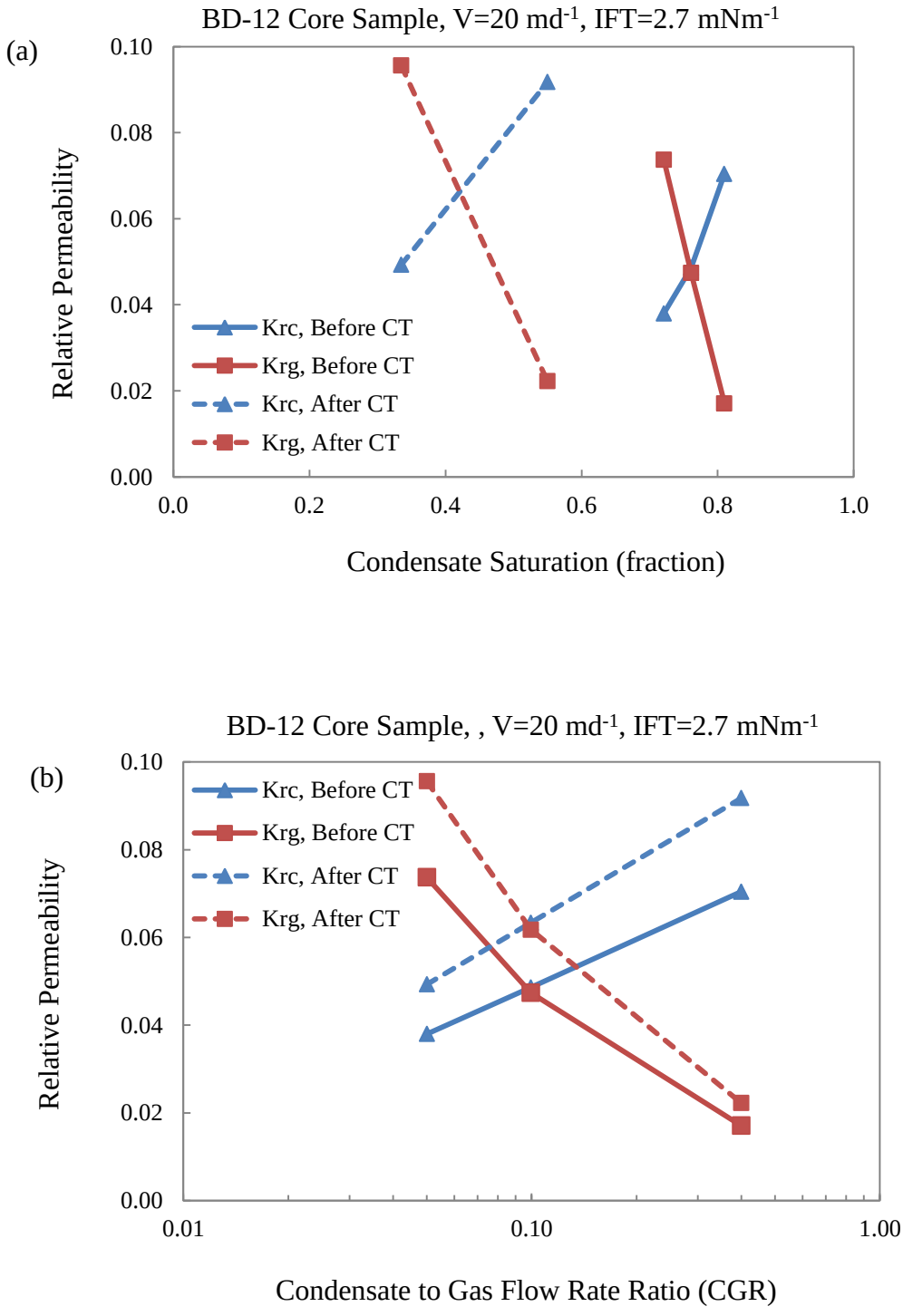

Figure 6.5: Pre- and post-treatment steady-state gas and condensate relative permeabilities of the BD-12 core sample versus (a) condensate saturation and (b) CGR at IFT of 2.7 mNm^{-1}.

6.4.3 Rate-dependent Relative Permeability: IFT of 0.77 mN/m

The steady-state relative permeability measurements corresponding to the low-IFT limit of 0.77 mN/m were carried out at a pressure of 4000 psi. The tests were conducted at four different CGR values of 0.03, 0.05, 0.1 and 0.4 at upstream conditions. Moreover, the rate-dependency of the relative permeabilities was also examined at each CGR value by injecting the fluids through the core at six actual total pore velocities of about 20, 40, 79, 159, 318 and 636 m/d. **Table 6.6** includes the flow conditions corresponding to the lowest and highest injection rates in this test. It is noted that during the tests at higher velocity of 636 m/day as CGR increased from 0.03 to 0.4, the Reynolds number decreased from 1.6E-2 to 1.1E-2. The Nc and Nc' capillary numbers also decreased from 2.5E-4 to 1.8E-4 and increased from 9.1E-4 to 1.5E-3, respectively.

The gas and condensate relative permeabilities versus CGR, measured on the untreated BD-12 core sample at IFT of 0.77 mN/m, are plotted in **Figure 6.6**. As noted from the gas k_r data in **Figure 6.6a**, the steady-state relative permeability increases with an increase in velocity at almost all CGR and velocity values. This implies more dominant effect of coupling over inertia for the range of CGRs and velocities considered here. One exception is however seen at the lowest CGR of 0.03 and highest rate of 636 m/d whereby the negative effect of inertia becomes slightly more dominant resulting in lower k_{rg} than that obtained at lower rate of 318 m/d. It seems that when CGR increases to 0.05 (i.e. condensate saturation increases) the negative inertia is compensated with the positive coupling and hence the change in k_{rg} becomes minimal when velocity increases from 318 to 636 m/d. Comparing the increase in relative permeability values at each CGR when velocity increases from the lowest to highest level demonstrates that the coupling effect becomes continuously more important as CGR increases. That is, k_{rg} corresponding to the CGR values of 0.03, 0.05, 0.1 and 0.4 has improved by 27, 59, 107 and 197%, respectively, when velocity has increased from 20 to 636 m/d. Similar trends are also observed for the recorded condensate relative permeability data (**Figure 6.6a**) in these steady-state measurements.

The measured relative permeability data on the BD-12 core sample after the treatment are plotted in **Figure 6.7**. Similar to the pre-treated core, the coupling effect dominantly governs the flow at all selected CGR values as there is an obvious increase in relative permeability values when velocity increases. More importantly, it is noted that the positive effect of coupling after the treatment, compared to that in pre-treated rock, has become more pronounced after the wettability alteration, especially at the

lower CGR values. That is, relative permeabilities corresponding to CGRs of 0.03, 0.05, 0.1 and 0.4 has improved by 91, 166, 161 and 208%, respectively, when the velocity has increased from lowest (20 m/d) to highest (636 m/d) value. These observations, compared to the pre-treated core data, demonstrate that the coupling effect after the treatment has improved by a factor of 3.4, 2.8, 1.5 and 1.1 at the corresponding CGR values mentioned earlier. In the same line, it can be argued that the negative effect of inertia has been reduced after the wettability alteration, resulting an increase in k_r due to the positive effect of coupling to become more evident. Further investigations are needed to better understand and distinguish between the impact of wettability alteration on coupling and inertial effects, e.g. performing steady-state k_r tests at lower CGR values (e.g. 0.005) where the flow is mainly dominated by inertia.

The condensate saturation in the core before and after the treatment was also measured for a number of CGRs at the lower velocity of 40 m/d (**Table 6.7**). In line with the previous observations obtained at two higher IFTs, the condensate saturation in the core in this low-IFT case was also reduced favourably after the wettability alteration, albeit to lesser extent. That is, the liquid saturation after the treatment has decreased by 26%, 29% and 22% corresponding to the CGR values of 0.03, 0.05 and 0.4, respectively. It is believed that the same trend can also be extended to the tests performed at high velocity conditions as based on the general understandings about condensing systems the condensate saturation does not change significantly when velocity increases. This was confirmed when a number of saturation points were measured at high velocity of 636 m/d before the treatment (**Table 6.9**) and subsequently minimal reduction in condensate saturation by about 2% was observed compared to those measured at low velocity of 40 m/d (**Table 6.7**) at similar CGR values. Accordingly and because laborious procedures are needed, the condensate saturations were not measured for the whole range of CGRs and velocities employed here.

Despite the observed improvement in coupling effect owing to chemical treatment and also favourable reduction in condensate saturation, the comparison between the measured k_r data before and after the treatment at identical CGR and velocity conditions demonstrates that the overall improvement in the relative permeability data after the wettability alteration is almost minimal.

Table 6.7 to **Table 6.9** compare the measured data before and after the treatment corresponding to the steady-state tests at three velocities of 40, 159 and 636 m/d, respectively. The corresponding relative permeability curves at these three velocities are plotted in **Figure 6.8**. The improvement in relative permeabilities at the lower CGR values is almost negligible, especially at lower velocities. At higher CGRs, the k_r improvement becomes more pronounced, but still not significant, as kr-IFs of about 1.1 have been attained.

Table 6.6: Flow conditions corresponding to the lowest and highest injection rates used during the SS-k_r tests conducted on the BD-12 core samples at IFT of 0.77 mN/m.

Velocity (m/day)	Qg (cc/hr)	Qc (cc/hr)	CGR	Nc	Nc'	Re
20	102	3	0.03	7.72E-06	3.61E-05	4.85E-04
	100	5	0.05	7.57E-06	5.06E-05	4.75E-04
	95.5	9.5	0.10	7.23E-06	7.51E-05	4.54E-04
	75	30	0.40	5.67E-06	1.42E-04	3.56E-04
636	3264	96	0.03	2.47E-04	9.11E-04	1.55E-02
	3200	160	0.05	2.42E-04	1.02E-03	1.52E-02
	3056	304	0.10	2.31E-04	1.16E-03	1.45E-02
	2400	960	0.40	1.82E-04	1.53E-03	1.14E-02

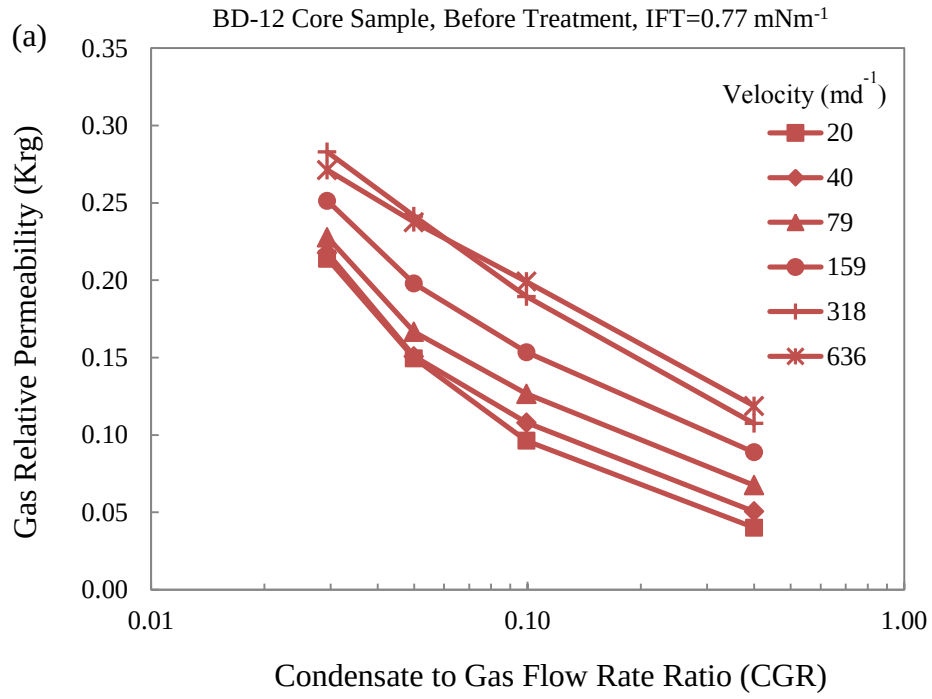

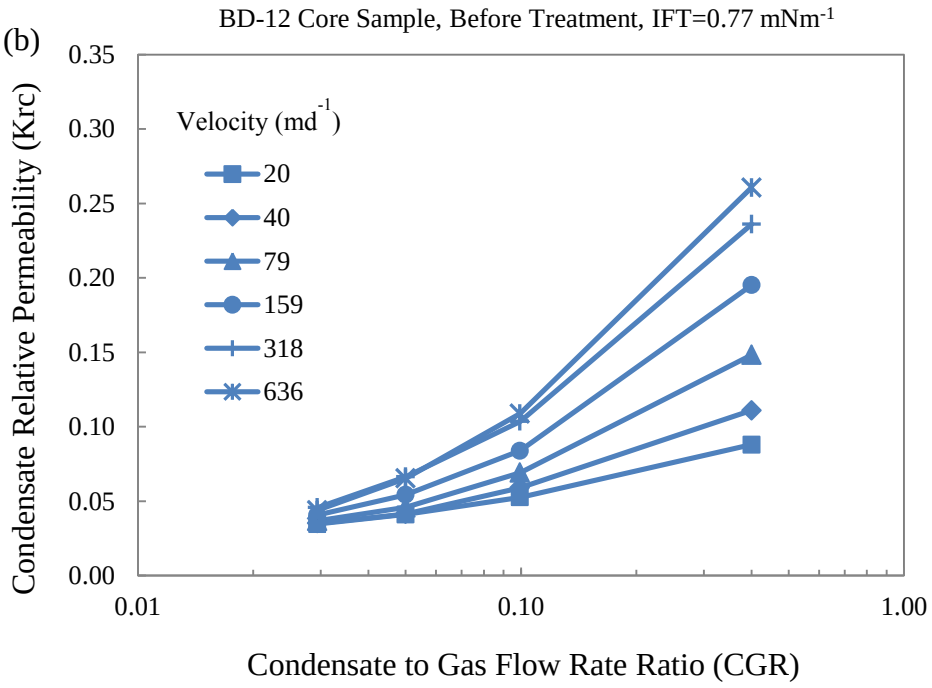

Figure 6.6: Gas (a) and condensate (b) relative permeability curves measured at IFT of 0.77 mNm^{-1} and six velocities versus CGR on the BD-12 core sample before the treatment.

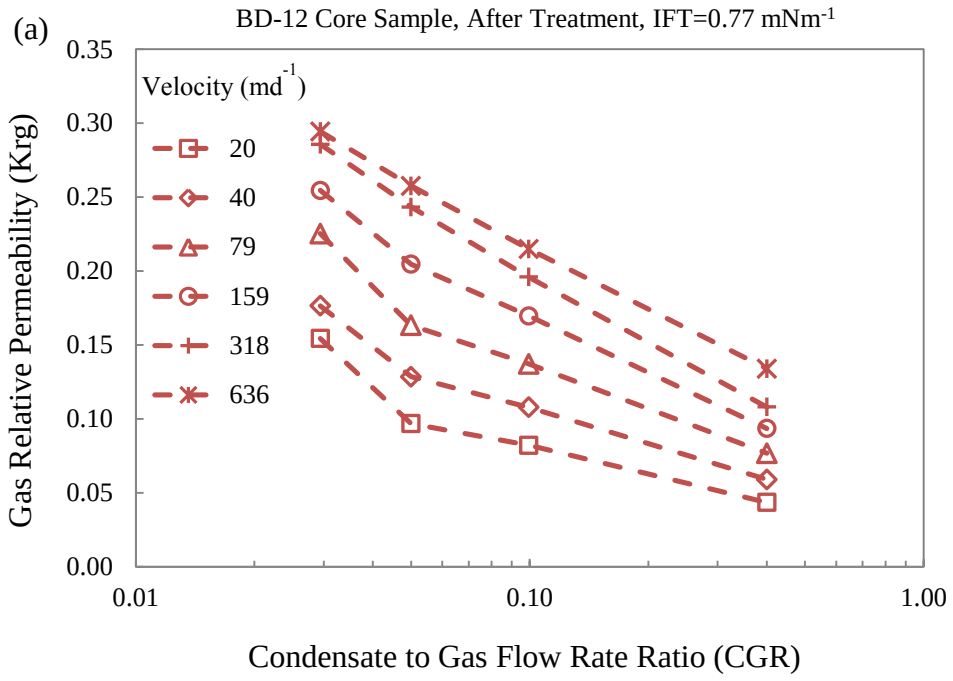

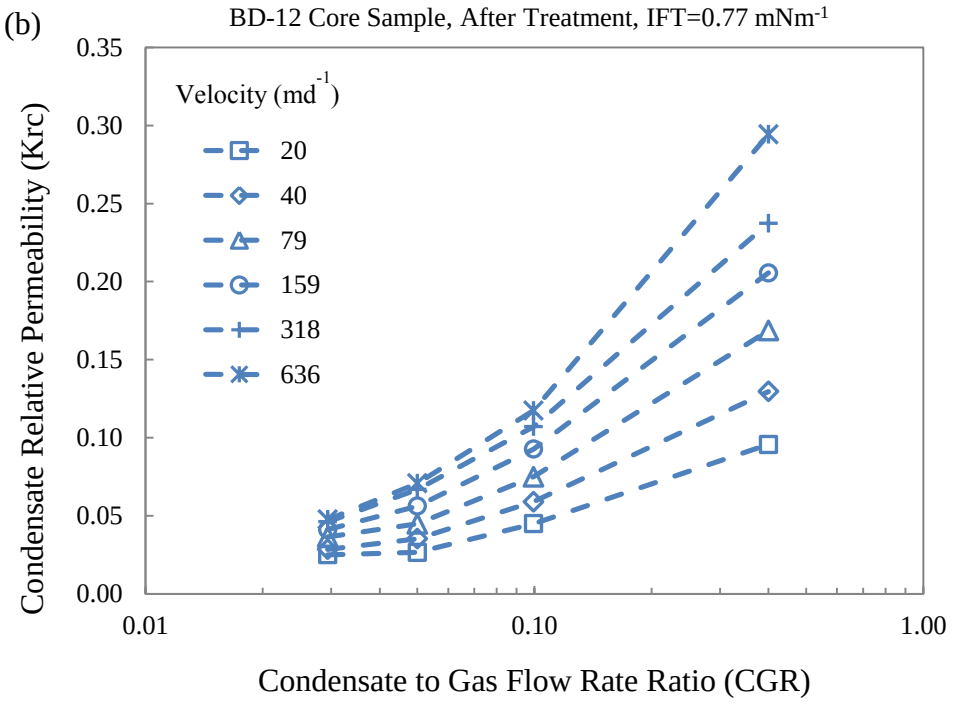

Figure 6.7: Gas (a) and condensate (b) relative permeability curves measured at IFT of 0.77 mNm^{-1} and six velocities versus CGR on the BD-12 core sample after the treatment.

Table 6.7: Data corresponding to the SS-k_r measurements conducted on the BD-12 core samples before and after the treatment at IFT of 0.77 mN/m and velocity of 40 md^{-1}.

CGR	Test	ΔP, psi	Sc	krg	krc	kr-IF
0.03	Before CT	7.98	0.68	0.218	0.035	0.81
	After CT	9.85	0.42	0.176	0.029	
0.05	Before CT	11.30	0.76	0.151	0.041	0.85
	After CT	13.26	0.47	0.128	0.035	
0.1	Before CT	15.07	-	0.108	0.059	1.00
	After CT	15.10	-	0.108	0.059	
0.4	Before CT	25.31	0.82	0.050	0.111	1.17
	After CT	21.67	0.60	0.059	0.130	

Table 6.8: Data corresponding to the SS-k_r measurements conducted on the BD-12 core samples before and after the treatment at IFT of 0.77 mN/m and velocity of 159 md^{-1}.

CGR	Test	ΔP, psi	Sc	krg	krc	kr-IF
0.03	Before CT	27.66	-	0.251	0.041	1.01
	After CT	27.32	-	0.254	0.041	
0.05	Before CT	34.45	-	0.198	0.054	1.03
	After CT	33.30	-	0.205	0.056	
0.1	Before CT	42.40	-	0.153	0.084	1.10
	After CT	38.38	-	0.170	0.093	
0.4	Before CT	57.54	-	0.089	0.195	1.05
	After CT	54.63	-	0.094	0.206	

Table 6.9: Data corresponding to the SS-k_r measurements conducted on the BD-12 core samples before and after the treatment at IFT of 0.77 mN/m and velocity of 636 md^{-1}.

CGR	Test	ΔP, psi	Sc	krg	krc	kr-IF
0.03	Before CT	102.52	0.66	0.271	0.044	1.09
	After CT	94.45	-	0.294	0.048	
0.05	Before CT	114.78	0.74	0.237	0.065	1.08
	After CT	105.84	-	0.258	0.071	
0.1	Before CT	130.76	-	0.199	0.109	1.08
	After CT	121.17	-	0.215	0.117	
0.4	Before CT	172.32	0.80	0.119	0.261	1.13
	After CT	152.62	-	0.134	0.294	

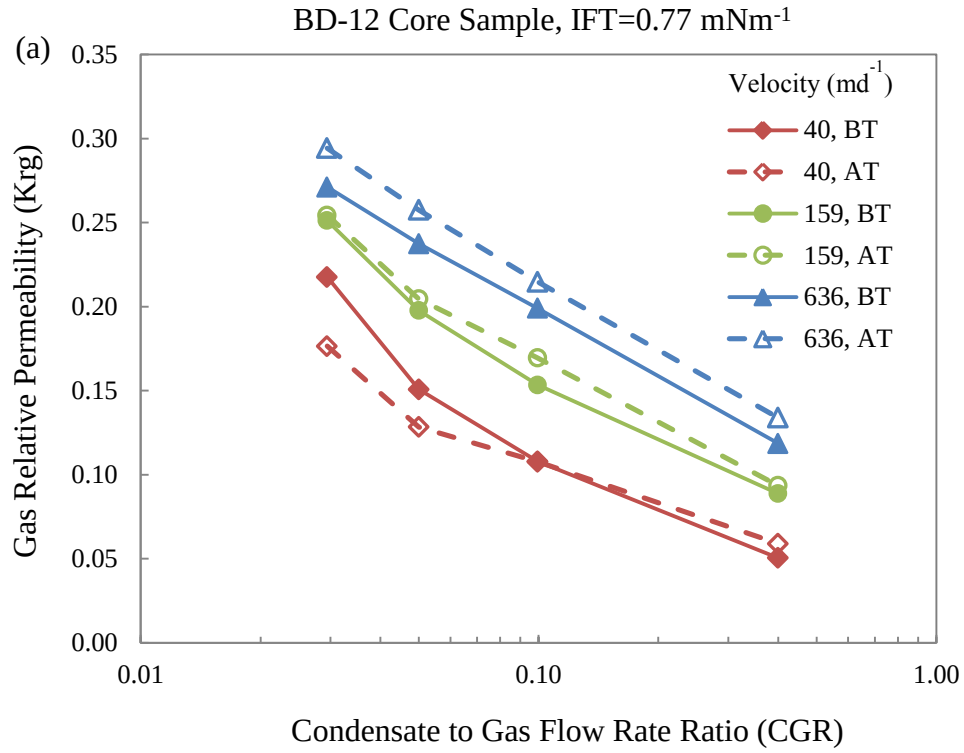

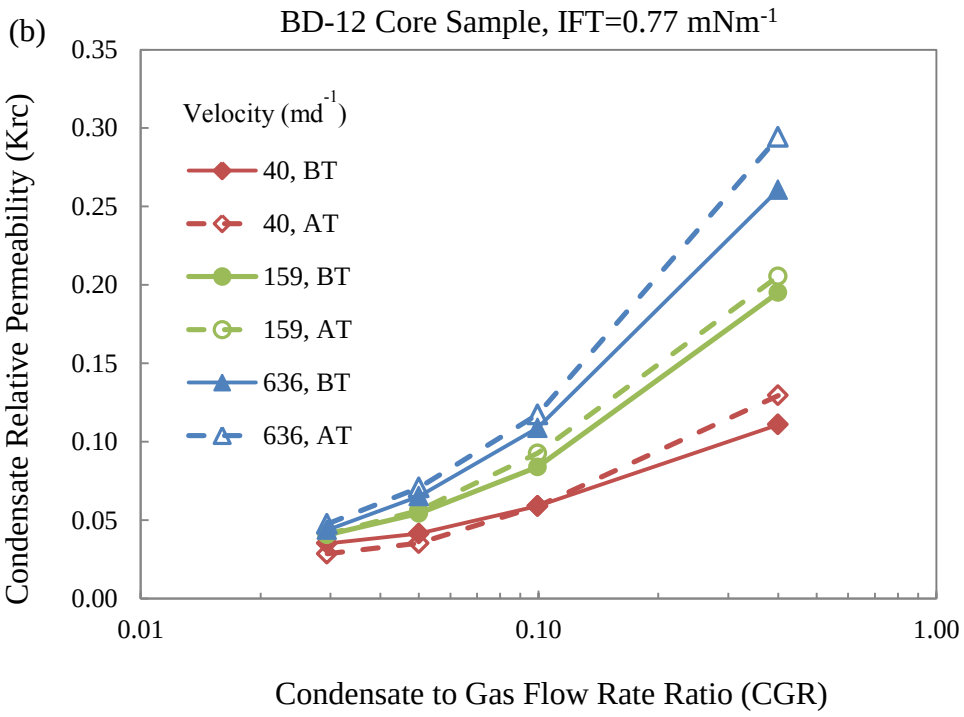

Figure 6.8: Pre- and post-treatment steady-state gas (a) and condensate (b) relative permeabilities of BD-12 core sample versus CGR at three selected velocities and IFT of 0.77 mNm^{-1}.

6.5 DISCUSSION ON RESULTS

The results of the steady-state relative permeability measurements discussed here demonstrated that the performance of the wettability alteration on improving the gas and condensate mobilities is highly dependent on the thermodynamic conditions of the condensing system. It was highlighted that at high interfacial tensions, where the base k_r data are measured, the treatment was able to effectively increase the relative permeabilities. However, at low interfacial tensions, although the positive coupling effect increased to some extent due to treatment, the resulting improvement in relative permeabilities were not promising. The observed trends are in close agreement with the general trends observed during the course of contact angle measurement tests, whereby a monotonic increase in the condensate wetting tendency with decreasing IFT was observed on the treated carbonate substrate.

The positive coupling effect in condensing systems has been attributed to the simultaneous coupled flow of gas and condensate within the pores where the gas passage is intermittently closed and opened by the condensate bridge formed at the pore throats (Jamiolahmady et al. 2000, Jamiolahmady et al. 2003). In this cyclic flow process and after formation of the liquid bridge, the pressure of the gas behind the condensate bridge gradually builds up until it overcomes the liquid hold-up and open its way through the pore. It is believed that at higher velocities this process becomes more efficient resulting in an increase in relative permeability. As mentioned above, after chemical treatment of the carbonate rock sample it seems that the positive effect of coupling has been increased. It is hypothesised that the alteration of the rock wettability has reduced the capillary pressure in the pores (i.e. reduced the wetting tendency of the condensate) and as a result the condensate bridge has become less stable and more fragile. In other words, after the treatment gas needs less pressure to break the liquid bridge and hence the coupling effect becomes evident even at lower velocities (compare **Figure 6.6a** with **Figure 6.7**a).

In order to confirm the results from the steady-state tests and more importantly evaluate the treatment durability versus time, a number of measurements at high and low IFT values of 10.8 and 0.77 mN/m were repeated after accomplishing the first series of experiments corresponding to all three selected IFTs. It should be noted that the first set of steady-state experiments (i.e. all three IFTs) after the treatment took about five months to be completed, during which the treated core was exposed to the gas and condensate fluid mixtures flowing at low and high velocities. This in fact

mimics the early production life of a gas well after the chemical stimulation. According to the new repeated data points, very consistent and comparable results compared to those measured first time (i.e. **Figure 6.4** and **Figure 6.8**) were obtained in both high- and low-IFT cases. This in turn, confirms the effective durability of the treatment versus production time and also reliability of the experiments performed here.

In this work, two methods of displacements, i.e. steady-state and unsteady-state, were employed to evaluate the improvement in liquid mobilities after the wettability alteration of the BD-12 carbonate core sample. Accordingly, the unsteady-state displacements conducted at IFTs of 10.8 and 0.77 mN/m, where the single phase oil displaced the resident gas, demonstrated significant reductions in pressure drops after the treatment, with almost comparable results at both high- and low-IFT limits. However, the steady-state tests showed a sharp contrast between the treatment performances at high- and low-IFT conditions, as discussed earlier. These observations underline the importance of using steady-state procedures in order to model the flow mechanisms in gas-condensate systems properly. Moreover, this implies that employing unsteady-state displacement tests for evaluating the treatment performance, would exaggerate the ultimate effect of the wettability alteration.

6.6 SUMMARY AND CONCLUSIONS

In this chapter the ultimate performance of the wettability alteration on improving the gas and condensate relative permeabilities were investigated through series of steady-state relative permeability measurements. To the best of the author's knowledge, such results have not been reported before for these applications. To perform these tests, the Baker-Dolomite, BD-12, carbonate core sample treated with 2 wt% C-61 anionic fluorosurfactant diluted in methanol was used. The C1-nC10 binary mixture was also employed to conduct the steady-state tests at 38°C. A number of unsteady-state displacements were also conducted to ensure the success of the treatment before commencing the post-treatment steady-state tests. The steady-state k_r measurements were carried out at three different IFT values of 10.8, 2.7 and 0.77mN/m. The tests at first two IFTs were performed at only one single rate of 20 m/d. On the other hand, the rate-dependency of the k_r data at the lower IFT limit of 0.77 mN/m was evaluated at six different velocities ranging from 20 to 636 m/d. CGRs (condensate to gas flow rate ratio) were varied between 0.03 and 0.4 during these steady-state test. The main conclusions from the experiments performed here are:

1- Significant improvement in relative permeabilities was obtained at the high-IFT value of 10.8 mN/m. That is, steady-state gas and condensate k_r increased promisingly by a factor of 2, 3.2 and 3.6 at corresponding CGR values of 0.05, 0.1 and 0.4. Furthermore, the condensate saturation or condensate blockage substantially reduced after the wettability alteration by approximately 35-39% in all fractional flow ratios considered.

2- The condensate saturations corresponding to the tests performed at IFT of 2.7 mN/m were considerably reduced almost with the same order of magnitude observed at higher IFT of 10.8 mN/m. However, the improvements in relative permeabilities were less pronounced compared to those obtained at IFT of 10.8 mN/m. That is, kr-IF of about 1.3 was achieved at all selected CGRs.

3- The overall results from the multiple-rate steady-state k_r measurements at IFT of 0.77 mN/m on the untreated rock sample demonstrated the dominant positive effect of coupling on relative permeability data for all CGR values ranging from 0.03 to 0.4 when velocity increased. After the wettability alteration process, the coupling effect became even more pronounced especially at the lower CGRs of 0.03 and 0.05 and moreover lower condensate saturations were obtained. However, the observed improvement in coupling and reduction in condensate saturation due to treatment were not effective as such to increase the relative permeabilities promisingly. That is, k_r over the entire range of CGRs and velocities considered here only improved by a factor of 1.1 or less at this low-IFT limit.

4- The overall trend of the steady-state relative permeabilities measured in this study, in line with the previous findings from the contact angle measurements, underlined the significant dependency of the treatment performance on the interfacial tension between gas and condensate. According to this, the resulting improvement in relative permeability because of wettability alteration gradually diminished when IFT decreased.

5- The comparison between the performance of chemical treatment evaluated by employing the steady-state and unsteady-state displacement techniques, demonstrated that whilst the former one provides the most reliable data for condensing systems, the unsteady-state flow tests can overestimate the benefits associated with the wettability alteration process especially at low IFT conditions.

6.7 REFERENCES

1. Bang, V. S. S., G. A. Pope, M. M. Sharma, J. Jimmie R. Baran and M. Ahmadi (2008). A New Solution to Restore Productivity of Gas Wells With Condensate and Water Blocks. SPE-116711-MS, SPE Annual Technical Conference and Exhibition. Denver, Colorado, USA, Society of Petroleum Engineers.

2. Danesh, A., M. Kahazam, G. D. Henderson, D. H. Tehrani and J. M. Peden (1994). Gas Condensate Recovery Studies. DTI Improved Oil Recovery and Research Dissemination Seminar, London.

3. Henderson, G. D., A. Danesh, B. Al-kharusi and D. Tehrani (2000). "Generating reliable gas condensate relative permeability data used to develop a correlation with capillary number." Journal of Petroleum Science and Engineering 25(1–2): 13.

4. Henderson, G. D., A. Danesh, D. H. Tehrani, S. Al-Shaidi and J. M. Peden (1998). "Measurement and Correlation of Gas Condensate Relative Permeability by the Steady-State Method." SPE Reservoir Evaluation & Engineering 1(2): 134-140.

5. Jamiolahmady, M., A. Danesh, D. H. Tehrani and D. B. Duncan (2000). "A Mechanistic Model of Gas-Condensate Flow in Pores." Transport in Porous Media 41(1): 17-46.

6. Jamiolahmady, M., A. Danesh, D. H. Tehrani and D. B. Duncan (2003). "Positive Effect of Flow Velocity on Gas–Condensate Relative Permeability: Network Modelling and Comparison with Experimental Results." Transport in Porous Media 52(2): 159-183.

7. Jamiolahmady, M., M. Sohrabi, S. Ireland and P. Ghahri (2009). "A generalized correlation for predicting gas–condensate relative permeability at near wellbore conditions." Journal of Petroleum Science and Engineering 66(3–4): 98-110.

8. Kumar, V., G. A. Pope and M. M. Sharma (2006). Improving the Gas and Condensate Relative Permeability Using Chemical Treatments. SPE-100529-MS, SPE Gas Technology Symposium, 15-17 May, Calgary, Alberta, Canada.

7 SIMULATION OF CHEMICAL TREATMENT

7.1 INTRODUCTION

Since the introduction of the wettability alteration technique in gas-condensate systems (Li and Firoozabadi 2000), there have been numerous experimental investigations carried out, assessing the feasibility of this method. Despite this, there are only few theoretical studies exploring the practical aspects of application of chemical treatment (CT) (Kumar et al. 2006, Bang et al. 2010). These studies have addressed only the overall performance of the treatment process (i.e. k_r improvement) on increasing the well productivity for an ideal case. Kumar et al. (2006), for instance, in a simulation exercise showed that gas and condensate production rate would increase by 80% when k_r corresponding to 20 ft treatment region improves by a factor of 2. Here, it should be mentioned that there are other important parameters, which from the reservoir engineering point of view, influence the performance of a well stimulation process. For instance, the treatment radius, recovery of the load fluids, unwanted impairment of the basic rock properties (k and φ) and sustainability of the treatment are a number of important parameters affecting the ultimate benefits from well stimulation operations.

In this chapter a comprehensive investigation on the effect of a number of important parameters, governing the performance of a chemically treated well, has been carried out. This has been achieved by performing a simulation exercise to scrutinize the individual and simultaneous effect of several parameters on treatment effectiveness. The first part relates to studying the impact of parameters such as permeability damage and solvent type individually. In the second part, the simultaneous impacts of a number of selected parameters on the treatment are investigated using statistical approaches.

7.2 RESERVOIR MODEL DESCRIPTION

7.2.1 Reservoir Properties

A cylindrical reservoir model, bearing a gas-condensate fluid, with uniform distribution of porosity and permeability was used in these investigations. Accordingly, the radial model consists of 39×1×1 grid blocks in the radial (r), angular (θ) and vertical (z) directions, respectively. The width of the radial grid blocks were distributed logarithmically starting from 0.25 ft for the adjacent grid to the wellbore to 698 ft for the boundary grid block, providing an outer reservoir radius of about 3490 ft. The reservoir was also assumed to be a single producing layer with a thickness of 150 ft to eliminate the gravity effect.

7.2.2 Single Well

The single-layer cylindrical reservoir model had a producing vertical well at its center penetrating the whole reservoir thickness. **Figure 7.1** illustrates the schematic of the reservoir model and its corresponding well. The wellbore had a diameter of 6 inches with no mechanical skin considered for it. The initial reservoir pressure was 6000 psia, which was well above the dew-point pressure of the reservoir fluid, i.e. 5089 psia. The well produced under constant bottom-hole pressure constraint of 4500 psia (which is 589 psi below the P_{dew}).

7.2.3 Rock Properties

The 150 ft thick reservoir layer contained a homogeneous rock with a uniform porosity and radial permeability of 18% and 14 mD respectively, unless otherwise stated. The rock compressibility factor was 4.25E-06 (1/psi) at the reference pressure of 6000 psia. The interstitial water saturation in the porous media was considered to be zero as well.

7.2.4 Fluid Properties

The reservoir bears a moderate retrograde gas-condensate fluid, which is a binary-mixture of C1 (91.8%) and nC10 (8.2%) with a dew-point pressure and maximum liquid dropout (in constant volume depletion, CVD, test) of 5089 psia and 15%, respectively, both at reservoir temperature of 250°F. **Figure 7.2** depicts the numerical CVD experiment corresponding to this fluid mixture, using the PVTi module of the Eclipse commercial reservoir simulator. The Lorentz-Bray-Clark viscosity correlation and 3-parameters Peng-Robinson equation of state (EOS) were used to design the appropriate compositional and black-oil fluid model corresponding to the C1-nC10 mixture.

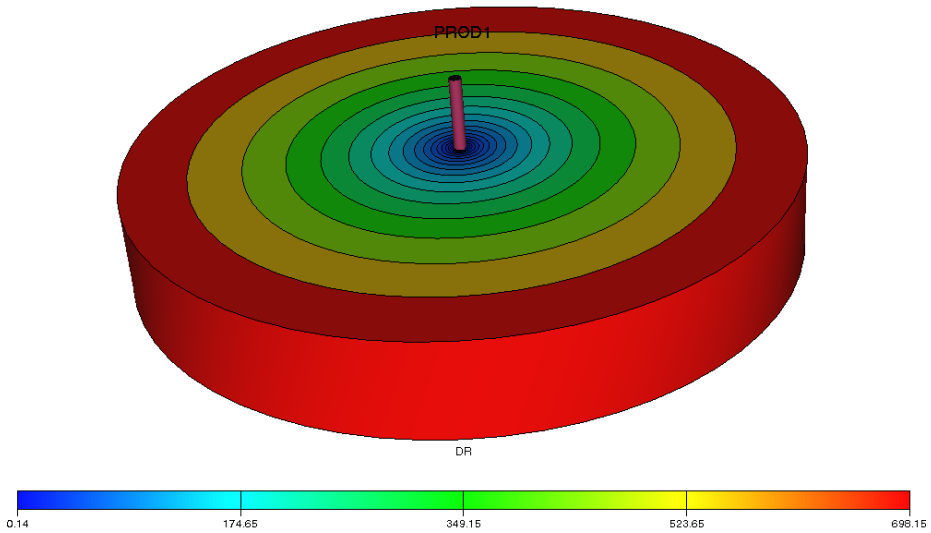

Figure 7.1: The single-layer cylindrical reservoir model, with its centered vertical production well, used in numerical simulations in this study (the colors illustrate the logarithmic distribution of grid blocks in the radial direction).

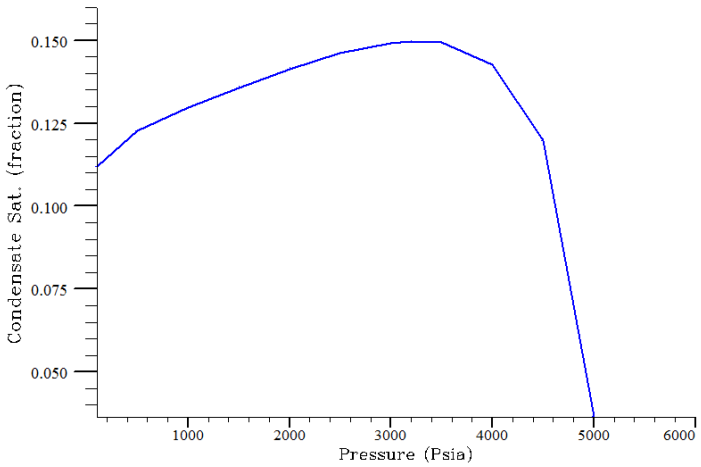

Figure 7.2: Condensate dropout versus pressure corresponding to CVD test on gas-condensate fluid used in numerical simulations in this study.

7.3 CHEMICAL TREATMENT PROCESS

Two types of chemical solutions (CS) including water-based and alcohol-based solutions were considered in these investigations. For the water-based solvent, the 3-component module of Eclipse (water, oil and gas) was implemented with the injected treatment solution to be the water phase with the viscosity and density of 1 cP and 62.4 lb/ft^3, respectively. For the alcohol-based solvent, on the other hand, the 4-component (water, oil, gas and injected solvent) extension of the Black-oil model of Eclipse was used, where the injected fluid is miscible with the hydrocarbons in the reservoir. This model implements the Todd and Longstaff empirical model for treating the effects of

physical dispersion between the miscible components in the hydrocarbon phase. The mixing parameter set in this model is used for calculating the viscosity and density of the miscible components. Moreover, the density and viscosity of isopropyl alcohol (IPA) was used here as the physical properties of the alcohol-based solvent.

Each treatment scenario consisted of three periods, 1- pre-treatment production, 2- chemical injection and 3- post-treatment production periods. For the reference case, the well initially produced for three years under constant BHP constraint of 4500 psia below the dew-point (stage-1), after which the condensate ring was stabilized around the wellbore. The production was then halted and the well was stimulated by injecting the required volume of the chemical solution (stage-2). The well came back on production again, following the treatment, and produced for an additional one year (stage-3), at the end of which the performance of the stimulation process was evaluated. It should also be mentioned that in the case of the untreated reservoir the well produced successively after the first production period (stage-1) without any interruption, using the original k_r curves.

The effect of the wettability alteration on improving the well productivity was considered as an increase in all three phases (gas, condensate and water) relative permeabilities in the stimulated region. Accordingly, an average k_r improvement factor (kr-IF) of 2.2 (**Figure 7.3**), unless otherwise specified, was assumed for all grid blocks invaded by the chemical solution, with a saturation above 10%, after the injection period. As a result, the kr-IF of 2.2 shown in **Figure 7.3** corresponds to the average of k_r improvements in the condensate saturation range between 0.27 and 0.37, occurring around the wellbore prior to the treatment (at the end of the third year of production). It should be mentioned that the levels of kr-IFs considered in this study have been selected according to the results of core experiments conducted in HW laboratory or those available in the literature. The gas/oil relative permeability data measured for a reservoir core sample at HW laboratory was also selected as the base-k_r curves used for the pre-treatment simulations. To produce the improved-k_r data for post-treatment conditions, the Corey correlation was employed. For this purpose, initially the relevant parameters to this correlation were tuned to match the measured base relative permeability curves. Accordingly, S_{gt} (trap-gas saturation), S_{ocr} (critical oil saturation), n_g (gas exponent), n_o (oil exponent), k_{rgmax} (gas end-point k_r) and k_{romax} (oil end-point k_r) were set at 0.35, 0, 4, 3.5, 1 and 0.065, respectively. To generate the post-treatment k_r data, the core exponents of the Corey correlation, fitted primarily for the base-k_r curves, were adjusted

based on the desired level of k_r improvement factor in a reasonable way whereby the general form of the k_r curvature was maintained. Here, for instance, to obtain kr-IF of 2.2, all core exponents of the base-k_r curves were maintained at their original levels, except n_g and k_{romax}, which were fixed at 2.85 and 0.146, respectively, as shown in **Figure 7.3**.

Figure 7.4 depicts the relative permeability curves of the water-based solvent used in this simulation exercise before and after the chemical treatment, where kr-IF of about 2.2 has been considered. The relative permeability curves for the alcohol-based solvent have also been assumed as straight lines, which is a reasonable assumption for such miscible fluids.

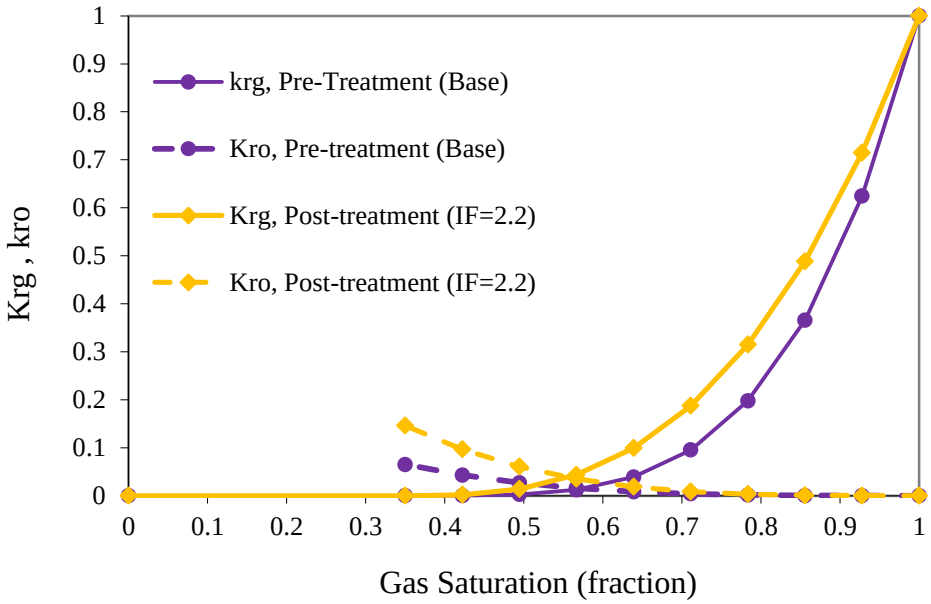

Figure 7.3: Base (untreated) and improved (treated) oil and gas relative permeability curves (k_{rg} and k_{ro}) with improvement factor (IF) of 2.2.

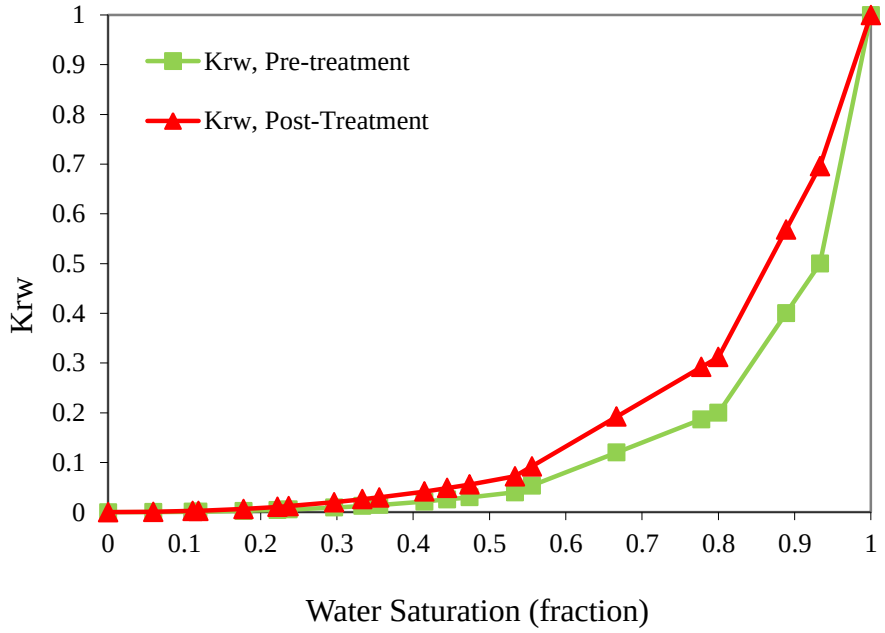

Figure 7.4: Relative permeability curves used for the water-based solvent in simulations before and after the wettability alteration process.

7.3.1 Treatment Performance; Gas Production Gain

To assess the effectiveness of the wettability alteration process, the total gas production gain (GPG) was used, which is the percentage increase in total gas produced from the treated reservoir over the first year of the second production period (stage-3 mentioned above) compared to that of the virgin (untreated) reservoir. It is also assumed that the treatment is completely uniform in the treated area and is durable over the post-treatment production period, unless otherwise specified. It should be mentioned that in these studies any CT operation resulting in GPG greater than 20%, is considered as a favorable and promising treatment.

7.4 IMPACT OF INDIVIDUAL PARAMETERS

A number of simulations were carried out to explore the impact of several parameters pertaining to the application of chemical treatment in gas-condensate systems, individually. These investigations were conducted on the base reservoir model described above, unless otherwise specified.

7.4.1 Alcohol-Based Versus Water-Based Solvents

The favorable application of alcohol-based solvents against the water-based ones, from a general practical point of view, was discussed in Chapter 4. One of the main desirable benefits of using alcohol- compared to water-based solvents was considered to be the minimal adverse effect of the injected chemical solution (CS) on the post-treatment

production period, i.e. better clean-up efficiency or recovery of the fluids carrying the chemicals. Here, to construct a better practical understanding of this subject, the performance of two types of treatment solutions including water-based and alcohol-based ones was compared through a simulation exercise. The effect of the solvent type on the CT performance was investigated on three reservoirs with different absolute permeabilities of 1.4, 14 and 140 mD, referred hereafter as low-, moderate- and high-permeability rocks. Subsequently, two treatment radii (TR) of 1.5 and 4.9 meters corresponding to the injection of 250 or 2500 STB chemical solution, respectively, were considered. Accordingly the corresponding results for water were compared with those of alcohol with the same injection volume. To have almost similar distribution of condensate phase around the wellbore before CT in all these cases, reservoirs with 1.4, 14 and 140 mD produced for 30 years, 3 years and 3.5 months, respectively, prior to the CS injection, creating a stabilized condensate ring with a radius of around 5 meters. **Figure 7.5** depicts the condensate distribution around the wellbore after 3 years (and also 15 and 30 years) for the reservoir with k=14 md.

The calculated GPGs corresponding to 250 and 2500 STB scenarios are shown in **Figure 7.6**. It is noted that at low injected volume of CS (250 STB) in low-permeability rock, the water-based carrier fluid has resulted in considerably lower increase in well productivity (GPG=21%) compared to that of the alcohol-based solution (GPG=55%). This is attributed to the poor back-flow of the water-based solvent, reducing the gas mobility during the post-treatment production period. For the cases of moderate- and high-permeability rocks, however, both types of solvents have approximately shown similar performances at lower injection volume of 250 STB, demonstrating the decreased negative impact of the water-based solvent back-flow on production in rocks with higher permeability. The same observations are also evident at higher injected volume of CS, i.e. 2500 STB, but for a different range of rock permeabilities. That is, the well productivity of the moderate-permeability rock has also suffered noticeably from the poor recovery of the water-based solution. The GPGs corresponding to water- and alcohol-based solvents in the case of k=14 mD are 23 and 70%, respectively. Furthermore, the poor clean-up of water from the low-permeability rock (k=1.4 mD) has resulted in a negative GPG of -57%, showing the well productivity impairment due to severe water blockage caused by the large volume of injected chemical solution. On the other hand, it is interesting to note that when 2500 STB of the alcohol-based, instead of water-based, CS has been injected into the low-permeability reservoir, a significant

increase in well productivity (GPG=148%) has been achieved. It is also noticed that as the rock permeability increases, lower GPGs (i.e. 70% and 26% for k=14 and 140 mD) have been achieved, demonstrating that the CT becomes less profitable. This underlines the more beneficial role of application of chemical stimulation in tighter rock systems, where the condensate blockage is more pronounced and has more detrimental effect on gas production.

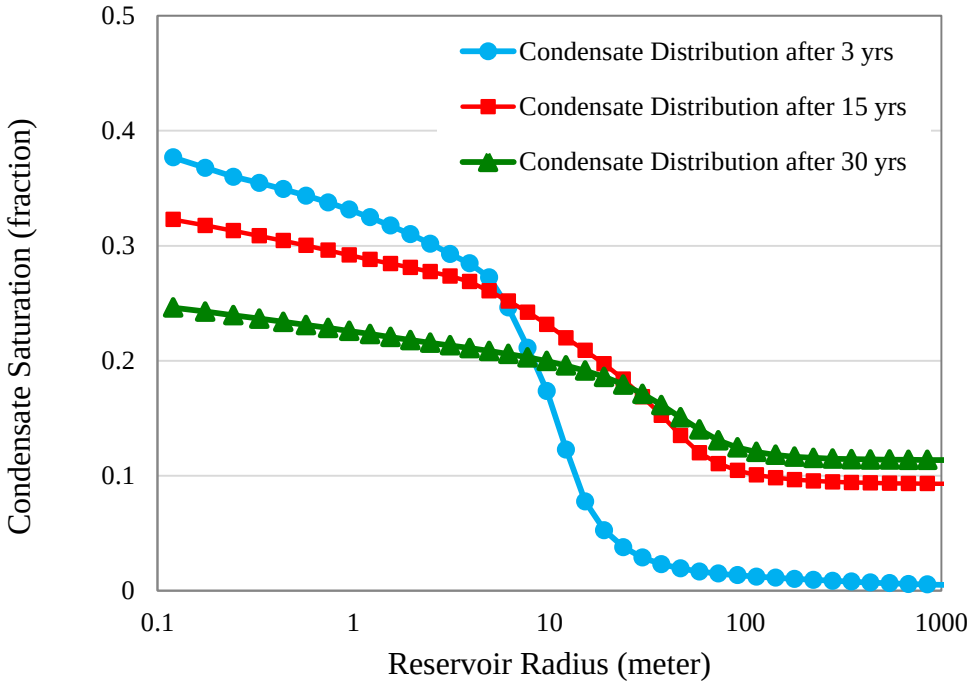

Figure 7.5: Distribution of the condensate phase along the reservoir with k=14 md after different production periods below the dew point pressure (5089 psia) prior to injection of chemical solution.

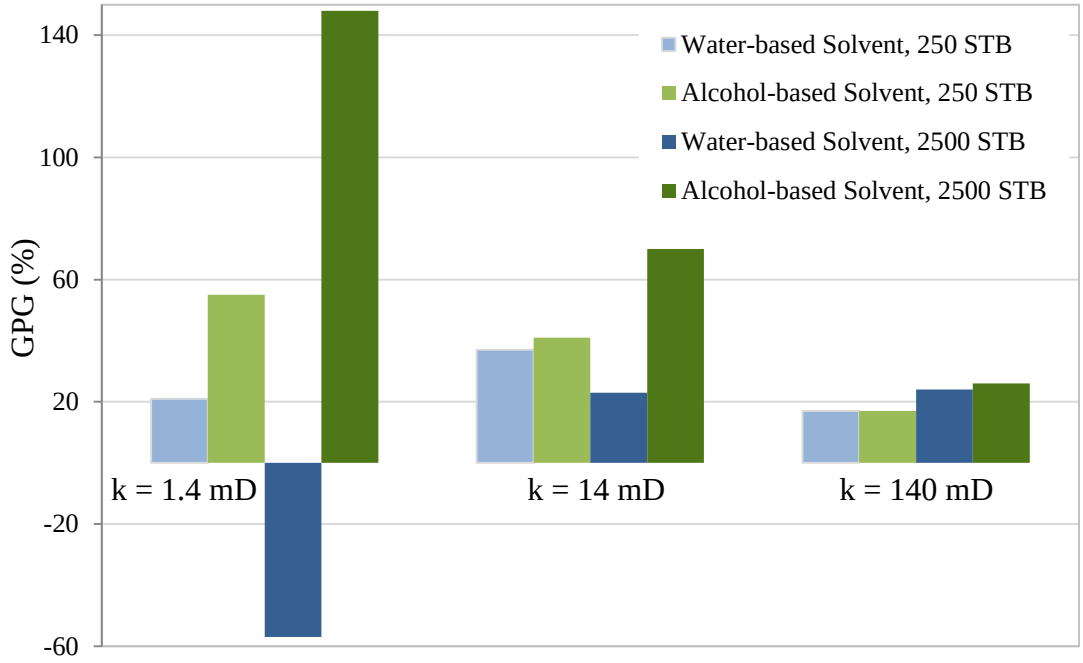

Figure 7.6: The performance of the alcohol-based against the water-based chemical solutions in low-, moderate- and high-permeability rocks.

7.4.2 Chemical Treatment versus Solvent Injection

Solvent injection (commonly composed of the alcohol blends) has been widely implemented as a practical solution to remedy the well productivity losses due to condensate/water blockages in gas and gas-condensate wells. The main purpose is that the injected solvents dissolve the accumulated liquids around the well and wash them out to restore the lost rock permeability. However the condensate and water can potentially return after a short time, restricting the production again. Naturally, applying wettability modifiers carried with the alcohol-based solvents can also provide such temporary advantages, inherent in solvent stimulations, in addition to those achieved by the more permanent wettability alteration process. Here, the performance of these two mechanisms, referred to hereafter as pure solvent injection (SI) and chemical treatment (CT), is separated and compared.

Figure 7.7 depicts the trend of GPGs obtained during one-year post-treatment production period, corresponding to the SI and CT scenarios for two loaded volumes of 250 and 2500 STB. It should be noted that, for each case, the calculated GPG at each time step is the percentage increase in total gas production from the beginning of the second production period until that particular time. It is noticed that at the early stages of the production right after the treatment there is a substantial increase in GPG in both

CT and SI scenarios. The duration of this peak, however, lasts only for few days and about one month for the small and large volumes of SI, respectively. This sharp increase of GPG is attributed to the removal of the condensate bank accumulated around the wellbore. However, after a short time, depending on the size of the stimulated region, the condensate ring evolves again through either dropping out from the gas phase or flowing from the blocks away from the wellbore. A sharp decrease in GPG (or gas mobility) was thus occurred in all these cases as production continued. This causes SI to become gradually ineffective, as GPGs reduces to below 20% after approximately two weeks and five months, for injected volumes of 250 and 2500 STB, respectively. In the corresponding CT cases, on the other hand, the well has favorably remained productive over the whole one-year production period, yielding average GPGs of 50% and 80% pertinent to small and large treatment radii, respectively. The results clarify the significant impact of the wettability alteration process on mitigating the condensate bank issues and improving the well productivity on a more permanent and long-lasing basis compared to the SI scenarios with temporary outcomes. It should be noted that here no deterioration of CT with time was assumed something that can have adverse effect on its performance as demonstrated in the following sections.

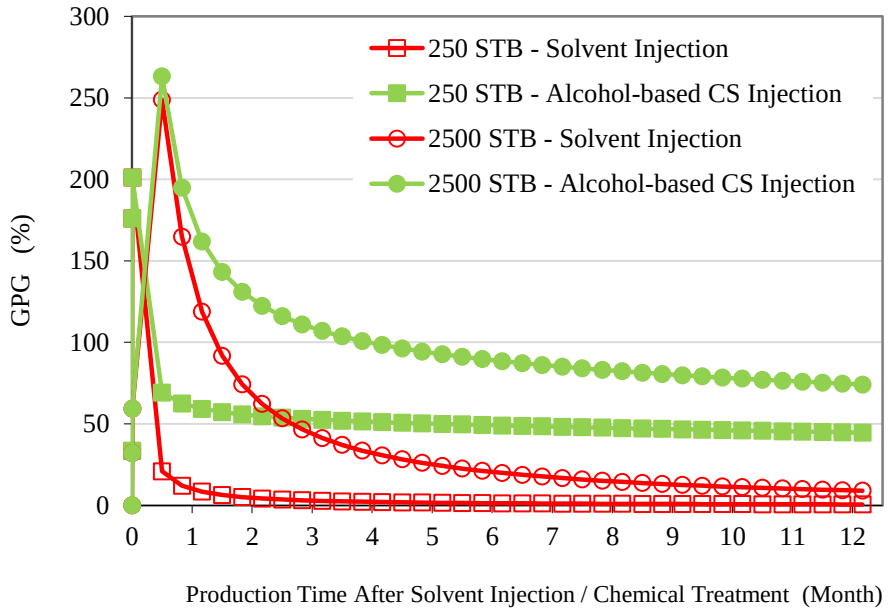

Figure 7.7: Comparing the gas production gain (GPG) from solvent injection and chemical treatment (using alcohol-based solution) versus time for two volumes of loaded fluids of 250 and 2500 STB.

7.4.3 Chemical Treatment in Mature Gas-condensate Reservoirs

Naturally the chemical treatment process would be more profitable if it is performed soon after the formation of the condensate phase around the wellbore (i.e. when the well bottom-hole pressure meets the dew-point). However, the performance of such treatments in mature gas-condensate reservoirs suffering from large condensate banks (or with average reservoir pressure below the dew-point) will remain open to question, especially when these treatments target only a small region around the wellbore.

This subject was investigated here for two reservoirs with long production periods of 15 and 30 years before being stimulated by injecting the chemical solution. The results were subsequently compared with the previous base case, in which the reservoir produced for 3 years prior to CT. It should be noted that in these two new cases the condensate phase saturation was around 10% away from the wellbore and above it near the wellbore (**Figure 7.5**).

Figure 7.8 depicts the total increase in GPG for each case when two different volumes of 250 and 2500 STB (equivalent to treatment radii of 1.5 and 4.9 meters) of an alcohol-based CS were injected. Although, at smaller treatment radius (250 STB), there is a reduction in the effectiveness of CT as condensate bank expands (longer production periods before the treatment), it is encouraging to note that there is still an acceptable level of improvement in the well productivity of reservoirs with large condensate banks. That is, GPGs of 41, 31 and 27% were achieved for the reservoirs with pre-treatment production times of 3, 15 and 30 years, respectively. Moreover, at larger treatment radius (2500 STB), GPG is relatively higher and the reduction in GPG with an increase in condensate radius is minimal and none-monotonic. Accordingly, GPGs of 70, 62 and 73% were obtained for three cases mentioned above. These results demonstrate that even in mature gas-condensate reservoirs the chemical treatment would be an effective remedial technique to mitigate the adverse effect of condensate blockage. More importantly, these observations underline the need for stimulating larger areas around the mature wells to gain the maximum benefits from the process.

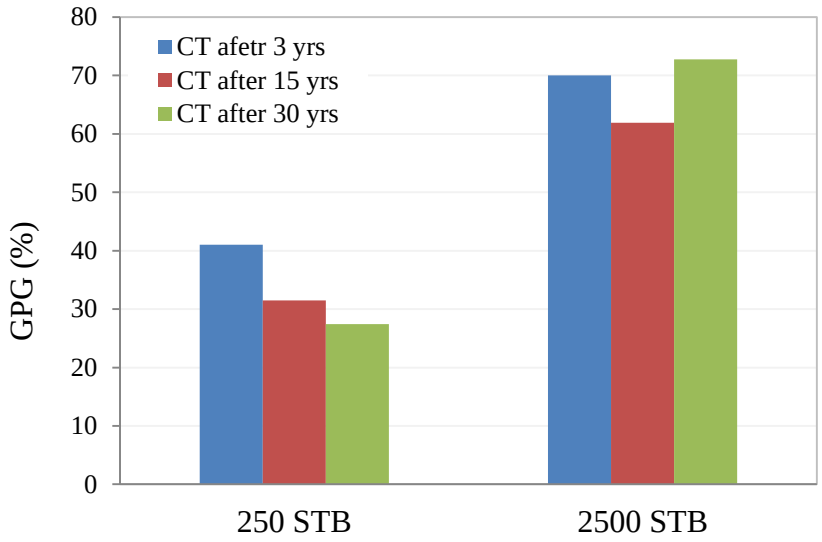

Figure 7.8: The performance of the alcohol-based chemical treatment in two mature gas-condensate reservoirs with 15 and 30 years production periods compared to that in the base case with 3 years production time.

7.4.4 Effect of kr Improvement Factor

As the ultimate objective of a wettability alteration process is to improve the mobility (k_r) of gas and liquid phases, the impact of k_r improvement factor (kr-IF) on the treatment performance, i.e. improving the well productivity, was investigated by considering five different levels of wettability alteration, resulting in kr-IFs of 1.4, 1.6, 1.8, 2.0 and 2.2. More details about the variation range of kr-IF considered here are discussed later in Section 7.5.1. As mentioned before, these IF values correspond to the average of k_r improvement in the condensate saturation range occurring around the wellbore prior to the treatment. The injection of 2500 STB alcohol-based CS was considered for this investigation, providing a treatment radius of 4.9 m.

Figure 7.9 shows all GPGs corresponding to each kr-IF case. The results demonstrate that there is nearly a linear relationship between the kr-IF and resulting GPGs. That is, GPGs of 24, 37, 48, 59 and 70% have been achieved for kr-IFs of 1.4, 1.6, 1.8, 2.0 and 2.2, respectively. From these data, it is evident that each incremental improvement in k_r by 0.2 has noticeably increased GPG by 11% on average. These observations highlight the significant impact of the level of wettability alteration (i.e. k_r improvement), delivered by the chemicals to the rock surface, on improving the well productivity.

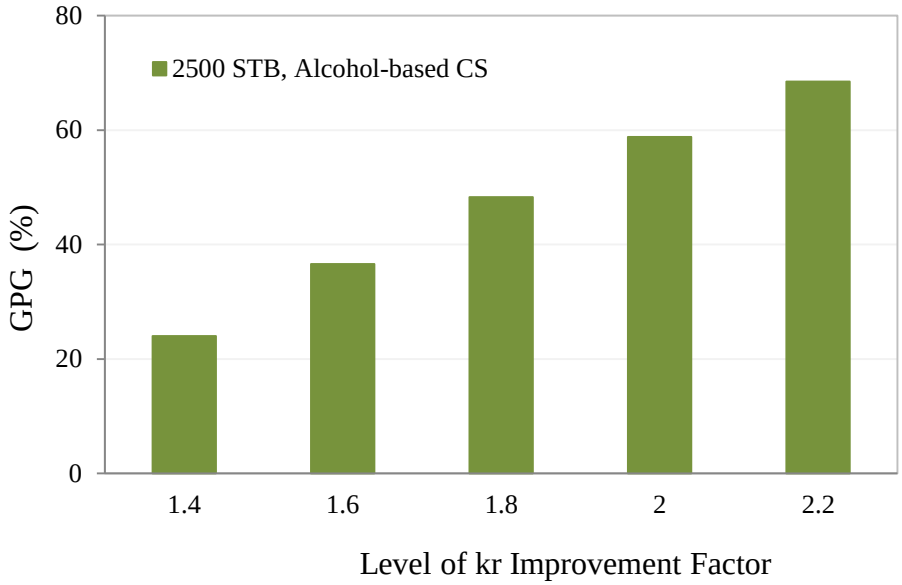

Figure 7.9: Effect of kr-IF on the chemical treatment performance for injection of 2500 STB alcohol-based chemical solution in the base reservoir model resulting in a treatment radius of 4.9 m.

7.4.5 Effect of Treatment Durability

Flowing large volumes of gas and condensate and possibly reservoir brine, particularly at high flow rates near the wellbore region, can potentially strip off chemical molecules from the rock surface. Other factors such as the chemical/physical bonding type between chemical molecules and charged surfaces of the minerals, salinity of the reservoir brine and reservoir temperature can also adversely affect the stability of chemicals at reservoir conditions, deteriorating the treatment effectiveness with time. Here, the durability of the treatment process, which is the time period that the chemical remains effective, was investigated by considering three cases of 50, 75 and 100% durable treatments corresponding to 6, 9 and 12 months periods, respectively. In the 50% durable case, for instance, the well produces under the prevailing conditions after the stimulation (i.e. improved k_r is used for the treated blocks) over the first half of the production period (i.e. six months), whereas the chemical loses its effectiveness in the second half of the production (i.e. base k_r is used). The injection of 2500 STB alcohol-based CS was also considered for these investigations.

Figure 7.10 depicts the variation of GPG with increasing the level of treatment durability. It is noted that there is a monotonic increase in GPG with durability, i.e., GPG is 40, 54 and 70% for 50, 75 and 100% durable cases respectively. In other words, improving the durability of the treatment by two times (e.g. from 6 to 12 months), increased the benefits from the wettability alteration (i.e. enhancement of the gas

productivity) by almost 30%. These results highlight the importance of the treatment durability on the wettability alteration performance.

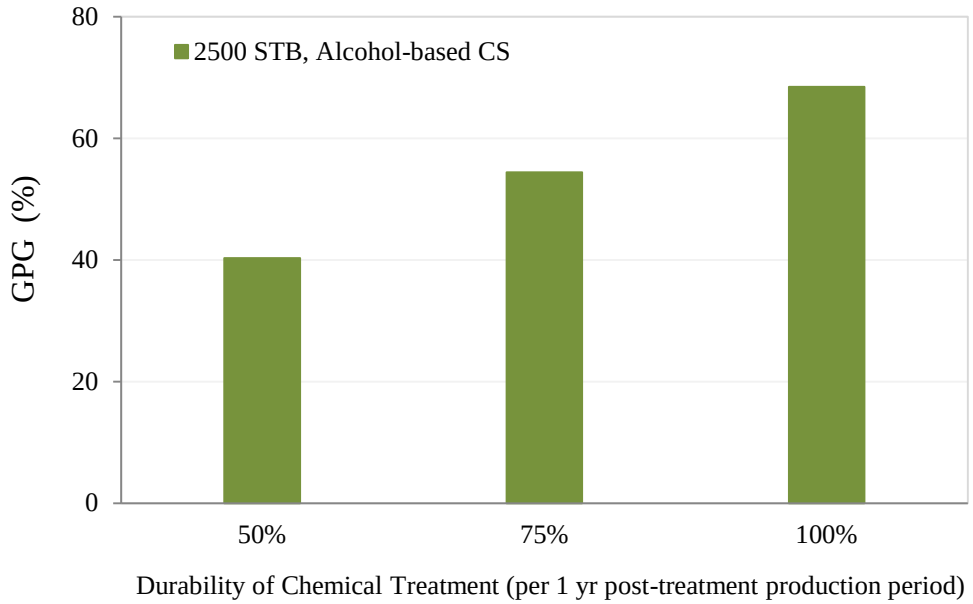

Figure 7.10: Effect of treatment durability over one-year production period on stimulation performance for injection of 2500 STB alcohol-based chemical solution in the base reservoir model.

7.4.6 Effect of Permeability Damage

Impairment of the rock permeability, due to excessive adsorption of the chemical molecules on the rock surface or precipitation of the chemical particles after contaminating with the reservoir resident fluids, e.g. brine, is one of the potential side effects pertaining to the chemical stimulations. In this exercise, six different levels of permeability damages (PD) ranging from 0% to 50%, associated with the chemically treated region, were assumed. More details about the range of permeability damages considered here are discussed later in Section 7.5.1

Figure 7.11 shows the impact of the magnitude of permeability damage on the treatment performance at two different treatment radii of 1.5 and 4.9 m, corresponding to both water- and alcohol-based chemical solutions. Overall, it is noted that by increasing the permeability damage, the performance of the treatment decreased in all cases, i.e. GPG deteriorated by about 40-60% when permeability damage increased from 0 to 50%. Moreover, the treatments by the water-based solvent at larger treatment radius (i.e. 2500 STB scenario), become unfavorable (GPG<20%) for rock permeability

impairments equal or above 10%. There are even negative GPGs noticed at such conditions, showing the loss of gas production after the treatment compared to the unstimulated case. The alcohol-based solution, however, remains desirable for wider range of permeability damages up to 40%. It is also noted that at smaller treatment radius (corresponding to 250 STB CS injected), water- and alcohol-based solvents show almost similar performances, i.e. both solutions have resulted in favorable treatments at permeability damage≤ 30%.

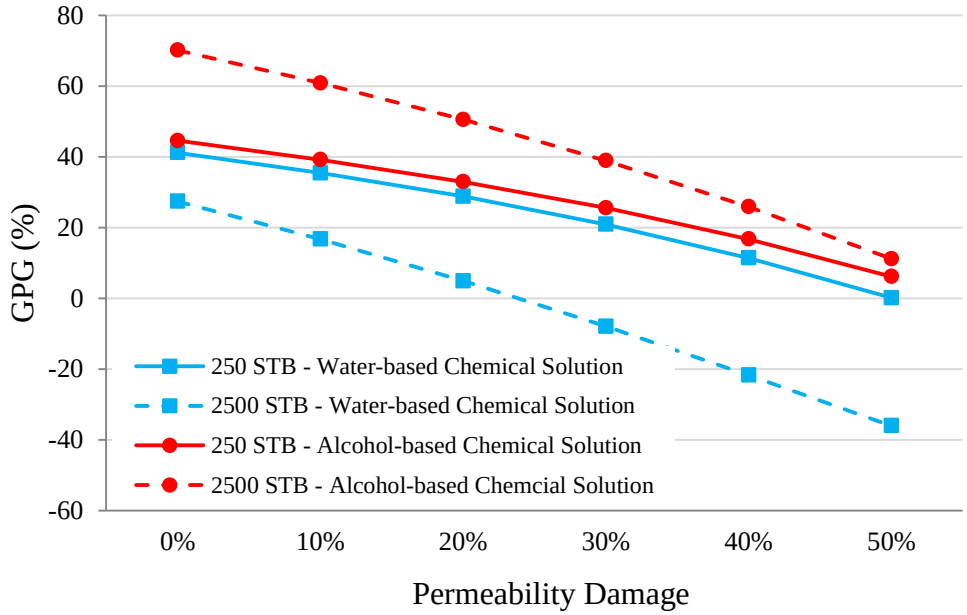

Figure 7.11: The performance of alcohol- and water-based solvents versus permeability damage at different treatment radii.

7.5 SIMULATANOUS IMPACT OF PARAMETERS USING STATISTICAL APPROACHES

In this section, five important parameters, which based on series of preliminary investigations are believed to play a significant role in the chemical treatment (CT) process, were selected to further explore their simultaneous impact on the productivity of a stimulated well. For this purpose, a statistical approach was employed. A MATLAB computer code was therefore developed to automate the simulations of numerous CT scenarios considered here and to further analyze the outcomes from these simulations. The rock and fluid properties of the base reservoir model and the alcohol-based treatment solution described in the previous section were used in all simulations

performed here. The selected parameters, their corresponding variation range and the applied statistical approach are discussed in the following sections.

7.5.1 Parameters and Their Variation Range

The five important parameters are: 1- treatment radius (TR) or the volume of injected chemical solution, 2- uniformity of treatment, 3- improvement factor of gas and condensate relative permeabilities (kr-IF), 4- permeability damage (PD) due to treatment and 5- durability of treatment. **Table 7.1** shows the variation ranges considered for these five parameters.

Looking into the condensate saturate profile across the reservoir at the end of the pre-treatment production period (i.e. after three years), demonstrates the stabilization of a condensate ring with a radius of about 5 meters around the well (**Figure 7.5**). According to this, four different TRs of 2, 3, 4 and 5 meters (corresponding to 500, 1000, 2000 and 3000 STB injected chemical solution, respectively) were considered in this simulation exercise.

Some experimental works reported in the literature have shown the capability of wettability modifiers to improve the liquid and gas relative permeabilities by a factor of about 2-3 under ideal conditions (Kumar et al. 2006, Bang et al. 2008). However, depending on the treatment conditions and also rock and chemical characteristics, less effective treatments (lower kr-IF), as seen in this work (Chapter 4), are likely to occur. Accordingly, in this exercise five levels of wettability alteration, resulting in kr-IFs of 1.2, 1.4, 1.6, 1.8 and 2, were assumed. The base-kr and kr-IFs of 1.4 and 2 are shown in **Figure 7.12**.

The excessive adsorption of chemicals on the rock surface or precipitation of chemical particles after interacting with formation resident fluids, e.g. brine, can potentially impair the permeability of the treated rock. The experimental works in this thesis (Chapter 4) showed some level of rock permeability impairment by about 30% in some cases due to incompatibility of the chemical with brine. There are also other experimental investigations in the literature (Panga et al. 2006, Fahes and Firoozabadi 2007) reported higher permeability damages, even above 50%. Based on these observations, six different levels of permeability damage, ranging from 0% to 50% were considered. That is, in the case of 50% PD, for instance, the original absolute permeability of the treated grid blocks, i.e. 14 md, reduced to 7 md after the chemical injection period.

During the screening tests performed on the fluorochemicals used in this work it was revealed that the volume of the chemical solution delivered to the rock is an important parameter to ensure an effective wettability alteration can be achieved. That is, whilst the injection of 1 pore volume (PV) of chemical solution was insufficient to alter the rock wettability, increasing the injection volume to 10 PVs resulted in a promising treatment (Chapter 4, Section 4.5.4). Based on this understanding, it is assumed that the regions close to the wellbore that are in more contact with the chemical would benefit from a more effective treatment, compared to those away from the well that are exposed to less amount of the wettability modifier agent. According to this, three levels of 50, 75 and 100% uniformity were considered. Here, in the case of 50% uniformity, for instance, when 500 STB (equivalent to 2 meters of invasion radius) chemical solution was injected, only the wettability (k_r) of the grid blocks within 1-meter radius around the wellbore was improved.

As mentioned earlier in Section 7.4.5, flowing large volumes of gas, condensate and brine at elevated temperatures, particularly at high flow rates near the wellbore region, would potentially cause desorption of the chemical molecules from the rock surface and consequently deterioration of the treatment effectiveness with production. Ahmadi et al. (2010), in their experiments, noticed a monotonic decrease in kr-IF from 1.8 to 1.6 during the flow of about 700 PVs of the gas-condensate fluid through the treated core. Here, the durability of the treatment process was investigated by considering three cases of 50, 75 and 100% effective treatments corresponding to 6, 9 and 12 months periods, respectively, during one-year post-treatment production period (see Section 7.4.5 for further details).

Table 7.1: The variation range of five parameters considered to investigate their simultaneous effect on the chemical treatment performance.

Indicator	Parameter	Level 1	Level 2	Level 3	Level 4	Level 5	Level 6
X_1	Treatment Radius (injected volume)	2 m (500 STB)	3m (1000 STB)	4m (2000 STB)	5m (3000STB)		
X_2	Uniformity	50%	75%	100%			
X_3	kr-Improvement Factor	1.2	1.4	1.6	1.8	2	
X_4	Permeability Damage	0%	10%	20%	30%	40%	50%
X_5	Durability	50% (6mths)	75% (9mths)	100% (12mths)			

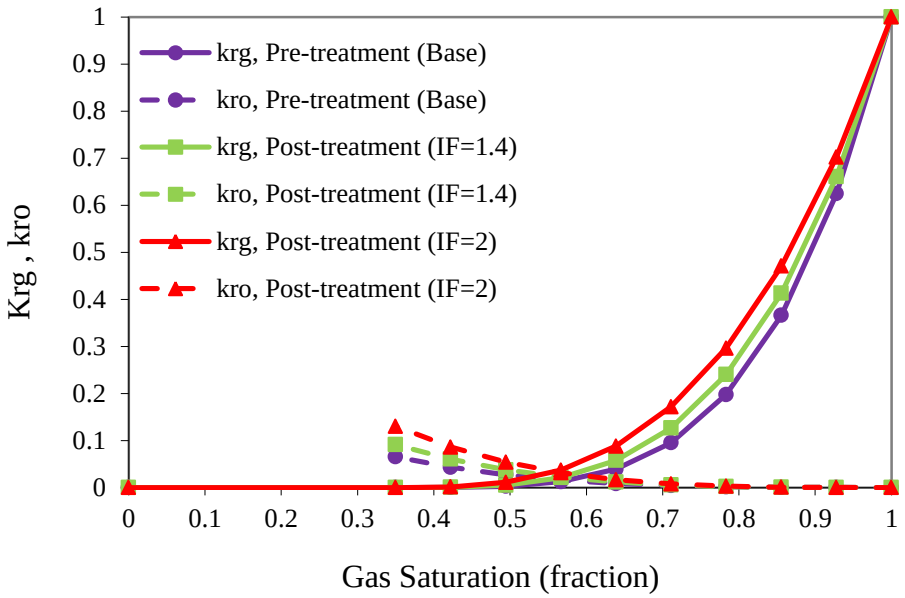

Figure 7.12: Base (untreated) and improved (treated) relative permeability curves (k_{rg} and k_{ro}) with improvement factors (IF) of 1.4 and 2 used in the performed numerical simulations.

7.5.2 Statistical Approach

To explore the relationship between the five parameters, a full-factorial experimental design was employed whereby all possible combinations of five parameters over their variation range (**Table 7.1**), were considered. A MATLAB computer code was therefore required and accordingly developed to facilitate conducting the 1080 designed simulations. That is, the developed program automatically reads the experimental design matrix and prepares the Eclipse input data-files using the appropriate include-files allocated to each parameter. The program then calls the Eclipse Black-oil simulator to run the model and subsequently reads the total produced gas at the end of the post-production period from the Eclipse RSM file. This data is used to calculate the pertinent GPG of each simulation. The statistical toolbox of MATLAB was finally employed to describe the relationship between GPG (response) and five independent parameters (predictors). For this purpose, the linear response surface model with (ILRSM) and without (LRSM) interaction parameters (**Equation 7.1**) was used to find the corresponding mathematical relationship expressing the dependency of GPG to each parameter.

$$\mathrm{GPG} = c_0 + \sum_{k=1}^{5} c_k x_k + \sum_{i=1}^{5}\sum_{j=1}^{5} c_i c_j x_i x_j \qquad \text{Equation 7.1}$$

The second and third terms on the right-hand side of **Equation 7.1** express the primary (c_k) and interaction ($c_i c_j$) coefficients, relevant to each parameter (x), respectively. The relative importance of each parameter is evaluated based on the magnitude of its primary coefficient, while the interaction coefficients demonstrate the mutual impact of each pair of variables on the CT performance, i.e. GPG. It should be mentioned that **Equation 7.1** in its current form shows the ILRSM model, while eliminating the third term from the right-hand side of it will construct the LRSM model.

7.5.3 Interpretation of Results

As mentioned earlier the LRSM and ILRSM models were fitted to the calculated GPGs pertinent to 1080 CT simulations. The corresponding RMSE (root mean square error) values were 4.90 and 1.56, respectively. Accordingly and naturally, ILRSM with more parameters provides a more reliable model compared to LRSM. It is also noted that the maximum and minimum differences between the estimated GPGs by ILRSM and the actual simulated ones are 3.8 and -7%, respectively, while the corresponding values for LRSM are 23 and -20%.

The primary and interaction coefficients assigned after employing the LRSM and ILRSM models are listed in **Table 7.2**. Accordingly, the LRSM primary coefficients allocated to x_1, x_2, x_3, x_4 and x_5 variables are 0.58, 1.89, 5.38, -5.97 and 1.87, respectively. Here, a positive coefficient reflects the positive impact of the relevant parameter on the CT performance, i.e. the higher the parameter's value, the higher the GPG, whilst the converse applies to parameters with a negative coefficient. Furthermore, the parameters corresponding to primary coefficients with larger magnitude have more dominant impacts on the well productivity. Accordingly, kr-IF shows the highest positive impact on the treatment performance. Subsequently, uniformity and durability of the treatment are at the next level of importance, with almost similar magnitudes, improving the treatment effectiveness. The radius of the chemical treatment also shows a positive effect on GPG, although to a lesser extent compared to the three other parameters mentioned earlier. It is also noted that among all parameters, permeability damage (PD) is the only parameter with a significant negative impact on the CT process whereby its adverse effect is as important as the positive effect of kr-IF.

Table 7.2: Primary and interaction coefficients estimated by linear response surface model without (LRSM) and with (ILRSM) interaction terms.

Coefficients	LRSM	ILRSM
C0	1.67	-1.94
C1	0.58	0.25
C2	1.89	1.56
C3	5.38	-1.91
C4	-5.97	2.75
C5	1.87	1.91
C12	-	0.20
C13	-	0.45
C14	-	-0.50
C15	-	0.18
C23	-	1.45
C24	-	-1.62
C25	-	0.57
C34	-	-0.08
C35	-	1.78
C45	-	-1.99

In order to provide more practical understanding of the effect of each parameter on the CT performance, a number of useful charts were created using the outcomes of the simulations performed. It should be mentioned that in these charts one parameter is varied whilst all other parameters are at their desirable levels, i.e. any parameter with a positive (negative) effect is at its highest (lowest) level to maximise GPG. The impact of kr-IF at different PD ranges, as two important parameters affecting the treatment performance, has been shown in **Figure 7.13**. In general, a monotonic increase in GPG is noticed with kr-IF for all values of PD. However, unpromising GPGs<20% has been obtained for PDs above 30%, even with the largest kr-IF of 2. Furthermore, it is noted that in the case of PDs of 20 and 30%, kr-IFs above 1.6 and 1.8 are required, respectively, to reach a favorable treatment with GPG>20%.

Figure 7.14 depicts the variation of GPG by increasing the level of kr-IF at three different cases of durability. It is noted that as kr-IF increases, the importance of durability on the CT performance becomes more pronounced. That is, for instance, at kr-IF=1.2, 1.6 and 2, increasing durability from 50% (6 months) to 100% (12 months)

improves GPG by almost 8% (from 7% to 15%), 19% (from 20% to 39%) and 28% (from 31% to 59%), respectively.

Figure 7.15 shows the variation of GPG by increasing the level of kr-IF at four different treatment radii and two levels of permeability damage of 0% and 30%. In the ideal case of 0% PD, treatment radius (TR) demonstrates minimal impact on the treatment performance at lower levels of kr-IF. That is, GPG at kr-IF=1.2 and 1.4 increased by almost 3% and 7%, respectively, when treatment radius was extended from 2 to 5 m. However, at the higher levels of kr-IF the impact of treatment radius is more appreciable, e.g. at kr-IF=2, GPG improved by 17% (from 43% to 59%) as a result of an increase in TR from 2 to 5 m. At the higher 30% permeability damage, on the other hand, the impact of treatment radius on GPG became negligible over all ranges of kr-IF. Even negative GPGs are noticed at lower kr-IF of 1.2 and 1.4, demonstrating the loss of gas production over the post-treatment period due to an ineffective wettability alteration process. This is attributed to the adverse impact of rock permeability reduction on well productivity, masking the positive effect of wettability alteration (kr-IF).

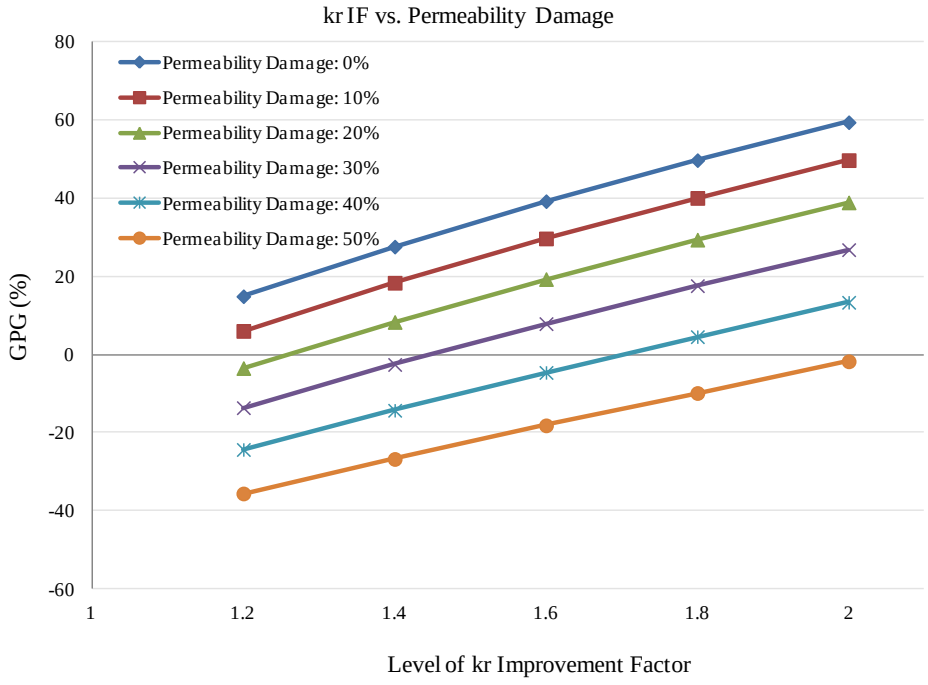

Figure 7.13: The effect of permeability damage on the chemical treatment performance at different k_r improvement factors (all other parameters are at their desirable levels).

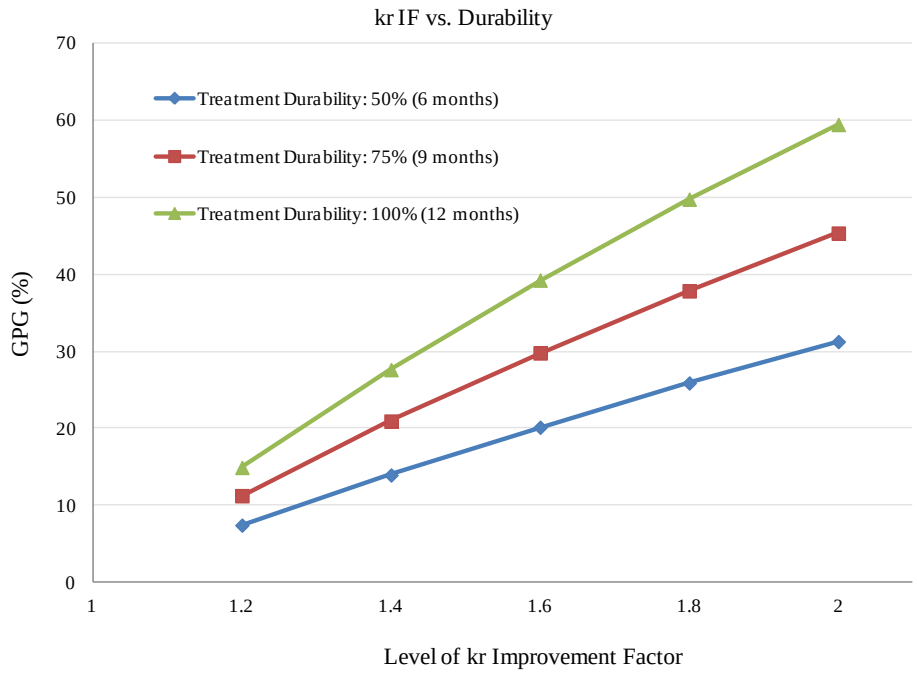

Figure 7.14: The effect of durability on the chemical treatment performance at different levels of k_r improvement factor (all other parameters are at their desirable levels).

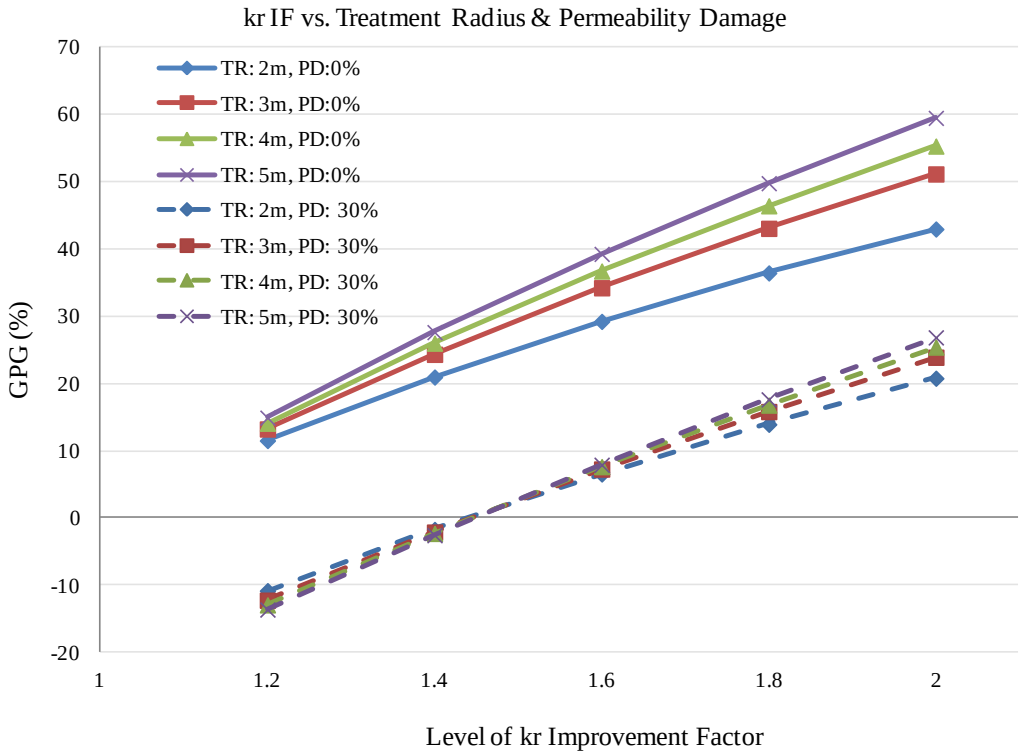

Figure 7.15: The effect of treatment radius (TR) on the chemical treatment performance, at different levels of k_r improvement factor and permeability damage (all other parameters are at their desirable levels).

In order to further scrutinize the impact of these five parameters, a number of informative charts were generated using the statistical toolbox of MATLAB employing the ILRSM fitted model. **Figure 7.16** to **Figure 7.22** depict the outcome of these charts. In these figures the impact of each individual parameter on improving or deteriorating the CT performance can be evaluated over its entire variation range when the other parameters are fixed at their desirable or undesirable levels (see footnotes of **Figure 7.16**).

Figure 7.16 corresponds to the most profitable treatment scenario for which all five parameters are set at their desirable level, i.e. TR=5m, Uniformity=100%, kr-IF=2, PD=0% and durability=100%. This case provides the highest level of GPG (59%) among all 1080 CT cases simulated. In this figure, the impact of each parameter on GPG when it is changed over its variation range whilst the other parameters are fixed at their desirable level, can be evaluated by following the green line allocated to each parameter. In fact, the slope of each line pertinent to a variable (and its ascending or descending trend) reflects the degree of importance and positive or negative impact of that parameter on GPG. Accordingly, increasing the level of kr-IF, durability, uniformity, and treatment radius from their minimum to maximum improves GPG by approximately 40, 25, 20 and 10%, respectively. On the other hand, increasing the permeability damage from 0 to 50% can drastically deteriorate the performance of CT (GPG) by more than 50%. **Figure 7.17** to **Figure 7.22** also show similar curves to **Figure 7.16** but at different conditions such that one parameter per each figure is set at its undesirable level.

In **Figure 7.17** it is noted that when kr-IF is at its minimum level, i.e. 1.2, the importance of other positive parameters, such as uniformity, durability and especially treatment radius, on CT performance becomes less pronounced compared to that observed in the previous case shown in **Figure 7.16**, where kr-IF was at its most desirable level. **Figure 7.18** and **Figure 7.19** depict the impact of parameters on GPG at two different levels of permeability damage of 20% and 50%, respectively. It is noted that in the 20% PD case, all other parameters show a noticeable positive impact on GPG. However, in the case of 50% PD, treatment radius, uniformity and durability are almost ineffective in improving the CT performance. Furthermore, very small and even negative GPGs are observed in the majority of cases with 50% PD, demonstrating the dominant impact of permeability reduction over other parameters.

The performance of the treatment at undesirable (minimum) level of uniformity and durability has also been shown in **Figure 7.20** and **Figure 7.21**, respectively. It is noted that in both cases kr-IF shows almost the same degree of importance over its variation range. That is, increasing kr-IF from 1.2 to 2 improves GPG from 10% to about 35%. Moreover, comparing the maximum GPG of 35% under conditions that all parameters except durability or uniformity are at their desirable levels with the maximum GPG of 59% in the ideal case of **Figure 7.16**, when all parameters are at their desirable level, demonstrates 24% reduction in GPG due to partial durability or uniformity conditions.

The impact of parameters on GPG for the shortest treatment radius has been shown in **Figure 7.22**. A promising GPG of 48% has been obtained for such small TR=2m when the other parameters are at their desirable levels. It is also noted that the degree of importance of other parameters, e.g. kr-IF and durability, on CT has been remained almost the same as those presented in **Figure 7.16** with longest TR=5m. That is, GPG, for instance, has been increased by 34% and 41% in **Figure 7.22** and **Figure 7.16**, respectively, when kr-IF has been improved from 1.2 to 2.

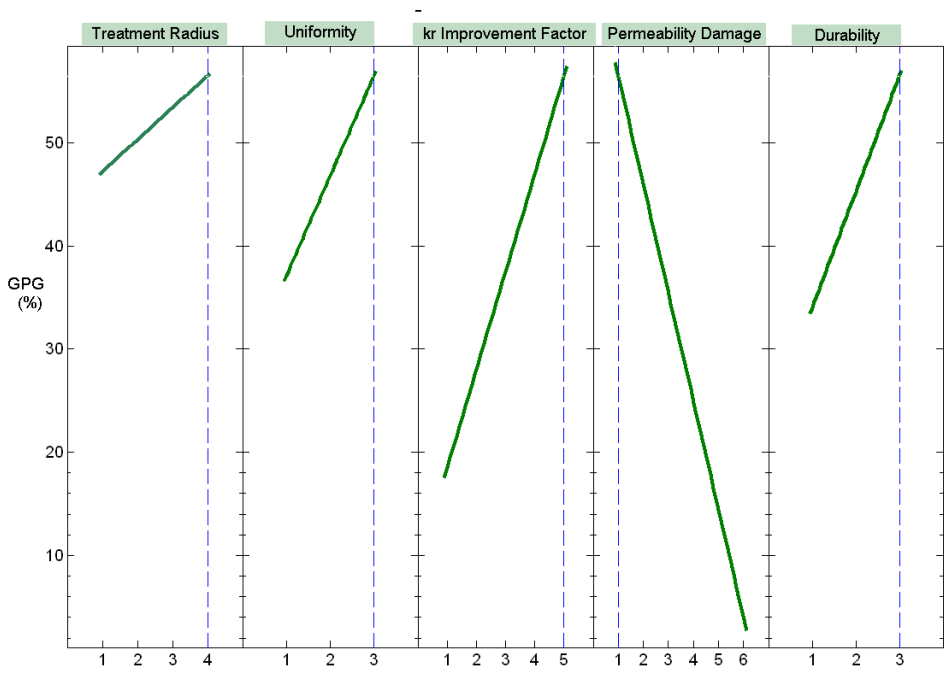

Figure 7.16: The impact of each of the five parameters on the chemical treatment performance when other parameters are at their desirable levels.

** The numbers on the x-axes correspond to the variation range of each individual parameter from its minimum to the maximum level according to Table 7.1.*

*** The parameters in the green boxes are at their desirable level, while the parameters in the yellow boxes are at their undesirable level.*

**** It should be noted that when a parameter is changing over its variation range and its impact on GPG is considered (green line), the other parameters are fixed at their mentioned (desirable or undesirable) levels.*

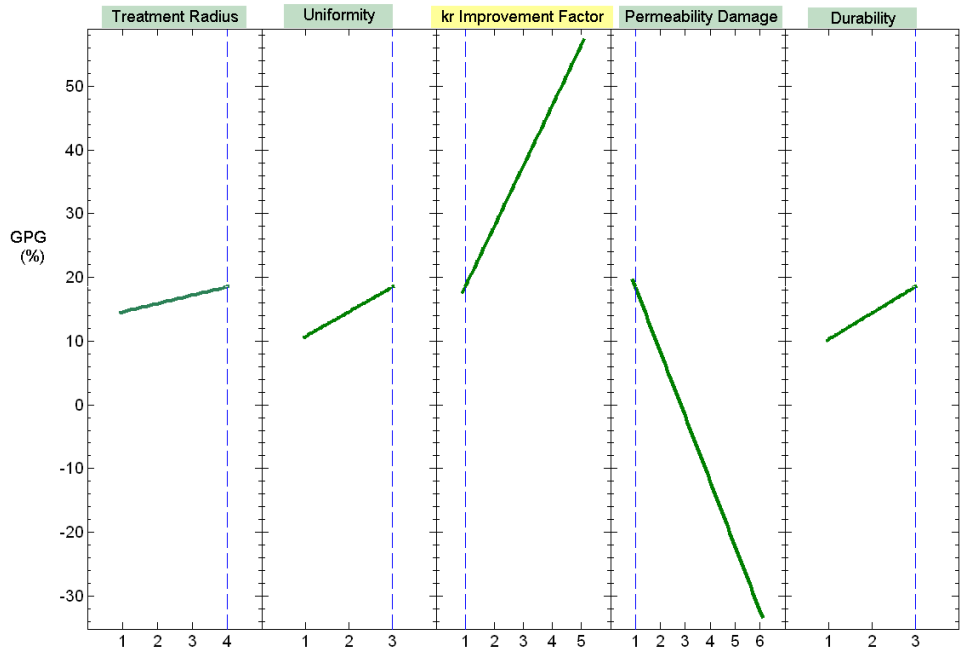

Figure 7.17: The impact of each of the five parameters on the chemical treatment performance when kr-IF (x_3) is at its undesirable (minimum) level and four other parameters are at their desirable levels.
See footnotes of Figure 7.16.

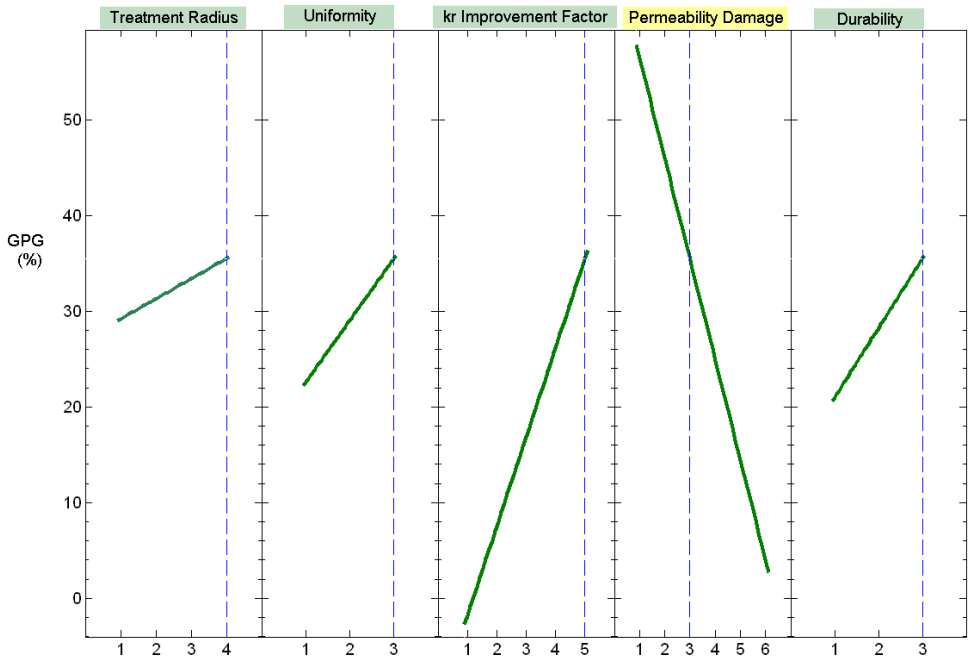

Figure 7.18: The impact of each of the five parameters on the chemical treatment performance when the Permeability Damage (x_4) is at its intermediate level (20%) and four other parameters are at their desirable levels.
See footnotes of Figure 7.16.

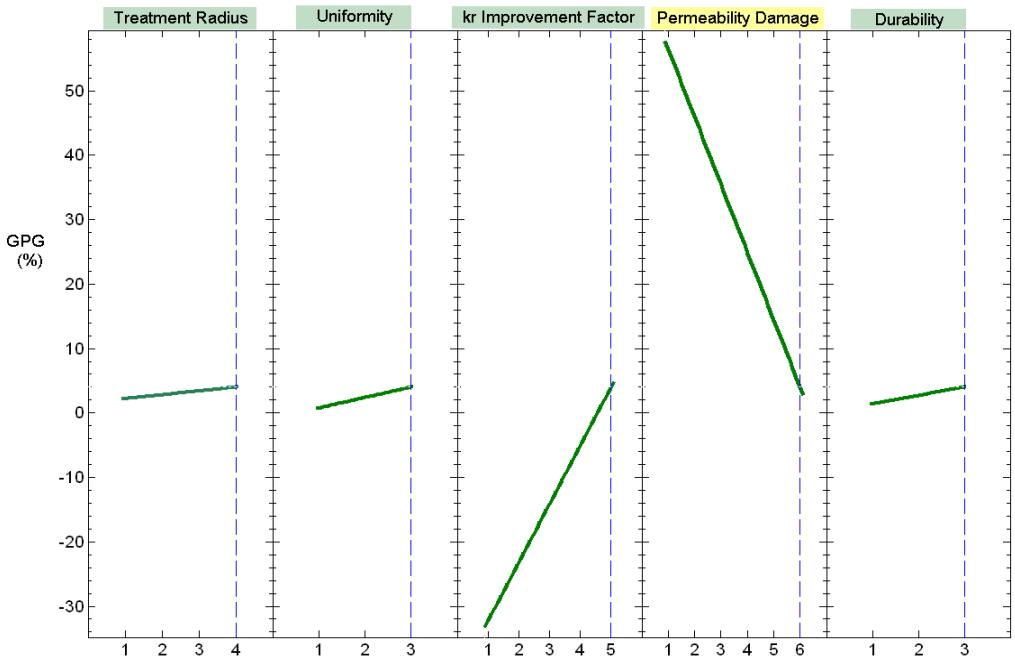

Figure 7.19: The impact of each of the five parameters on the chemical treatment performance when the Permeability Damage (x_4) is at its undesirable (maximum) level (50%) and four other parameters are at their desirable levels.
See footnotes of Figure 7.16.

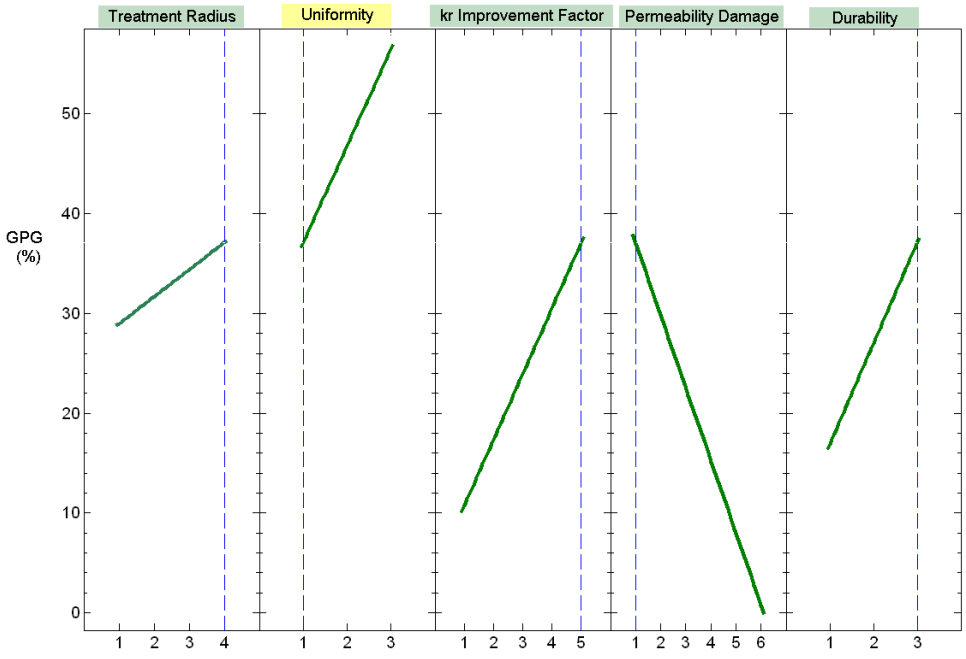

Figure 7.20: The impact of each of the five parameters on the chemical treatment performance when the Uniformity (x_2) is at its undesirable (minimum) level and four other parameters are at their desirable levels.
See footnotes of Figure 7.16.

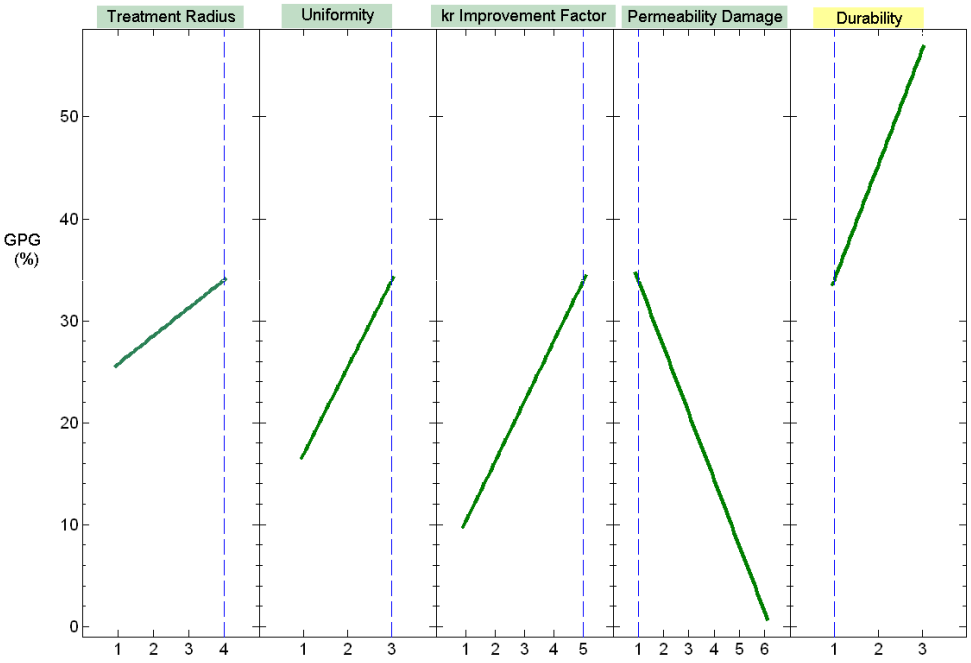

Figure 7.21: The impact of each of the five parameters on the chemical treatment performance when the Durability (x_5) is at its undesirable (minimum) level and four other parameters are at their desirable levels.
See footnotes of Figure 7.16.

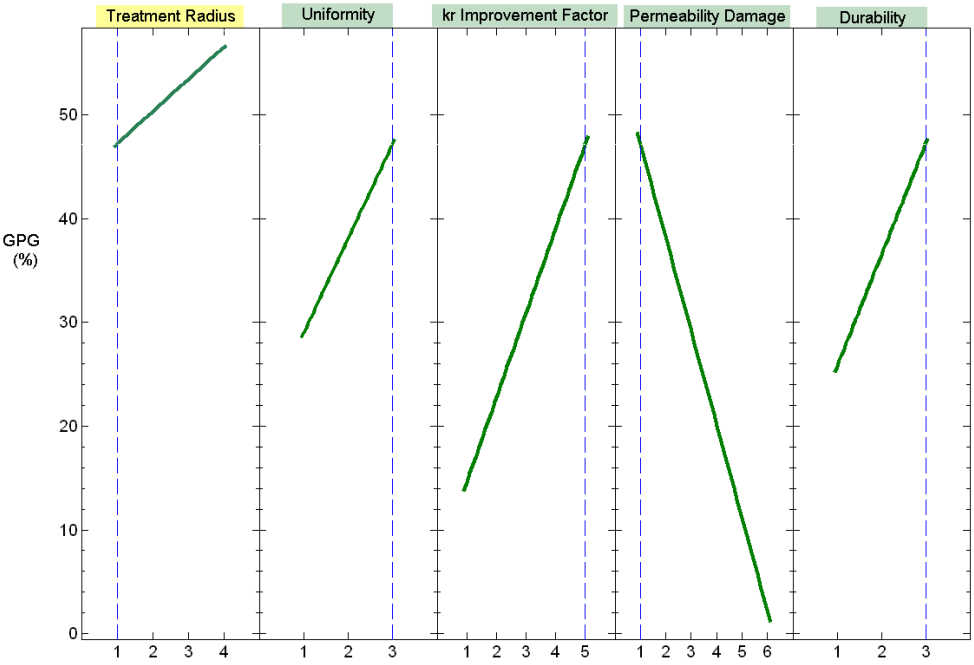

Figure 7.22: The impact of each of the five parameters on the chemical treatment performance when the Treatment Radius (x_1) is at its undesirable (minimum) level and four other parameters are at their desirable levels.
See footnotes of Figure 7.16.

7.6 SUMMARY AND CONCLUSIONS

In this chapter in order to explore the key parameters governing the effectiveness of chemical treatment thereby providing some practical understanding and guidelines on such a process, series of numerical simulations were conducted. The impacts of a number of important pertinent parameters on CT performance were studied individually and combined by performing either single-parameter simulations or multiple-parameters simulations based on statistical approaches. The main conclusions from this simulation exercise are:

Conclusions from single-parameter simulations

1- The adverse effect of the back-flow of the water-based chemical solution significantly reduced the CT performance compared to that of the alcohol-based solution in the low- and moderate-permeability (k=1.4 and 14 md, respectively) rocks, especially at higher volumes of CS injected, i.e. 2500 STB. That is, GPGs corresponding to the water- and alcohol-based solvents, in moderate-permeability rock, for instance, were 23% and 70%, respectively, when kr-IF=2.2. Both solvent types, however, showed almost similar performances in high-permeability rock, i.e. k=140 md.

2- Chemical treatment with wettability alteration demonstrated a better performance over the solvent injection. That is, the former one resulted in promising GPGs of about 50% and 80% corresponding to a treatment radius of 1.5 and 4.9 m over the one year post-treatment production period, whereas the latter one was only able to improve the well productivity (GPG>20%) for two weeks and five months for similar stimulated radius.

3- Chemical treatment proved an effective solution to improve the well productivity in mature gas-condensate reservoirs with large condensate banks ($P_{ave}<P_{dew}$) with almost the same level as that observed in slightly depleted gas condensate reservoir with a smaller condensate ring. Moreover, under such conditions stimulating a larger area around the wellbore becomes more important and sometimes necessary.

Conclusions from multi-parameter simulations using statistical approaches

4- The primary coefficients of the fitted LRSM model **Table 7.2 c**orresponding to the five parameters, demonstrated that the k_r improvement factor (kr-IF) has the largest positive impact on CT performance. In addition, uniformity and durability of the treatment, with almost similar degree of importance, and to a lesser extent treatment

radius (TR) were the next positive parameters improving GPG. On the other hand, permeability damage (PD) was the only negative parameter with a significant adverse impact on the CT performance.

5- The interaction coefficients estimated by the ILRSM model (**Table 7.2**) proved the uniformity/kr-IF and durability/kr-IF are the most important interactive factors dominating the performance of the chemical treatment.

6- In the case of PDs of 20 and 30% it was revealed that kr-IF should be above 1.6 and 1.8, respectively, to reach a favorable treatment (GPG>20%). Moreover, unpromising GPGs (<20%) were obtained for PDs above 30%, even with the highest kr-IF of 2. On the other hand, when the permeability damage increased, the uniformity and durability of the treatment played less favorable roles. That is, the undesired increase in negative effect of permeability damage with increasing uniformity and durability masked the potential positive impacts of these two latter parameters.

7- The positive impact of durability on the CT performance became more pronounced with increasing kr-IF. That is, increasing durability from 50% (6 months) to 100% (12 months) improved GPGs corresponding to kr-IF=1.2, 1.6 and 2 by almost 8, 19 and 28%, respectively.

8- In the case of PD=0%, although the treatment radius showed minimal impact on the CT performance at lower levels of kr-IF, its positive effect on GPG became more appreciable for kr-IF>1.6. That is, GPG corresponding to kr-IF=2, for instance, improved from 43% to 59%, when TR increased from 2 to 5m. Furthermore, the impact of TR became negligible over the whole range of kr-IFs at higher PDs (e.g. above 30%).

9- It was demonstrated that when kr-IF, durability, uniformity and TR increased from their minimum to maximum level independently (**Table 7.1**), and at the same time the other parameters are maintained at their desirable levels, GPG improved by approximately 40, 25, 20 and 10%, respectively (**Figure 7.16**). On the other hand, at the same conditions, increasing PD from 0 to 50% resulted in significant deterioration of the CT performance by more than 50%.

7.7 REFERENCES

1. Ahmadi, M., M. M. Sharma, G. A. Pope, D. E. Torres, C. Mcculley and H. Linnemeyer (2010). Chemical Treatment to Mitigate Condensate and Water Blocking in Gas Wells in Carbonate Reservoirs. SPE Western Regional Meeting. Anaheim, California, USA, Society of Petroleum Engineers.

2. Bang, V., G. A. Pope, M. M. Sharma, J. R. J. Baran and Ahmadi (2010). "A New Solution To Restore Productivity of Gas Wells With Condensate and Water Blocks." SPE Reservoir Evaluation & Engineering 13 (2): 323-331.

3. Bang, V. S. S., G. A. Pope, M. M. Sharma, J. Jimmie R. Baran and M. Ahmadi (2008). A New Solution to Restore Productivity of Gas Wells With Condensate and Water Blocks. SPE Annual Technical Conference and Exhibition. Denver, Colorado, USA, Society of Petroleum Engineers.

4. Fahes, M. M. and A. Firoozabadi (2007). "Wettability Alteration to Intermediate Gas-Wetting in Gas-Condensate Reservoirs at High Temperatures." SPE Journal 12(4): pp. 397-407.

5. Kumar, V., V. S. S. Bang, G. A. Pope, M. M. Sharma, P. S. Ayyalasomayajula and J. Kamath (2006). Chemical Stimulation of Gas/Condensate Reservoirs. SPE 102669, SPE Annual Technical Conference and Exhibition. San Antonio, Texas, USA, Society of Petroleum Engineers.

6. Kumar, V., G. A. Pope and M. M. Sharma (2006). Improving the Gas and Condensate Relative Permeability Using Chemical Treatments. SPE Gas Technology Symposium. Calgary, Alberta, Canada, Society of Petroleum Engineers.

7. Li, K. and A. Firoozabadi (2000). "Experimental Study of Wettability Alteration to Preferential Gas-Wetting in Porous Media and Its Effects." SPE Reservoir Evaluation & Engineering **3**(2): 139 - 149.

8. Panga, M. K. R., Y. S. Ooi, P. L. Koh, K. S. Chan, P. G. Enkababian, P. CHENEVIERE and M. M. Samuel (2006). Wettability Alteration for Water-Block Prevention in High-Temperature Gas Wells. SPE Europec/EAGE Annual Conference and Exhibition. Vienna, Austria, Society of Petroleum Engineers.

8 SUMMARY, CONCLUSIONS AND RECOMMENDATIONS

8.1 SUMMARY

Over the recent decades, production from gas and gas-condensate reservoirs has played a major role in the growing world's demand for more sustainable energy sources. Forecasting the hydrocarbons recovery from gas-condensate deposits has always been a challenging task due to unusual and complex phase behaviours and flow regimes of such fluid systems. The unique flow characteristics of condensing fluids necessitate appropriate and special procedures for modelling the fluids displacements within the reservoir. The decrease in relative permeability with increasing velocity (negative inertia) and increase in relative permeability with increasing velocity/decreasing IFT (positive coupling) are two competing effects that prevail the gas/condensate flow behaviour near the wellbore region.

Accumulation of liquid wetting phases, i.e. water and condensate, can adversely curtail the production from gas-condensate wells. Over the last several years, wettability alteration of the reservoir rocks from liquid- to intermediate-gas wet conditions, using appropriate repellent agents, has been proposed as a new solution to reduce the magnitude of the liquid hold-up around the wellbore on a relatively permanent basis compared with other common techniques. This chemical treatment method has attracted the attention of many investigators over the last two decades. However, despite the large number of theoretical and particularly experimental research works dedicated to application of this technique, as discussed extensively in Chapter 2 of this thesis, all published studies are open to serious criticism for ignoring or undervaluing the unique flow characteristics of gas-condensate systems (i.e. low-IFT and high-velocity effects) in their investigations. As a result, the employed approaches in these studies are mainly limited to using conventional gas/oil fluids, and more importantly, through incorrect and unreliable procedures. Therefore the idea behind this research work was to provide a

better understanding of the performance of wettability modifiers by use of reliable techniques that can properly predict the phase and flow behaviour of condensing systems.

The chemical solution developed in this work was optimized for wettability alteration of carbonate minerals, which compared with sandstones have received less attention. The main criteria considered in selection of the appropriate wettability modifier were: making the rock surface intermediate gas-wetness, e.g. $\theta_{liquid\text{-}gas}$>90°, being stable and effective at elevated temperatures, e.g. 130°C, having good back-flow or clean-up efficiency, e.g. alcohol-based solvents, being compatible with formation resident fluids, e.g. brine stability, causing minimal impairment to rock properties, e.g. zero permeability damage and having ecologically friendly characteristics, e.g. products with short-chain fluorinated carbon atoms. In order to optimize the treatment solution developed in this work and evaluate its ultimate performance for gas-condensate systems, a comprehensive set of experimental investigations was carried out through appropriate and systematic approaches. Accordingly, this study was initiated through employing conventional gas/oil (e.g. N2-nC10) fluids at ambient temperature, which compared with gas/condensate fluids are much easier and more straightforward to deal with. Subsequently, the contact angle measurement, spontaneous imbibition and unsteady-state displacement tests were carried out through which the composition of chemical solutions for the selected carbonate substrates was optimized. The experimental studies were then progressed to the next level; where the performance of the optimized treatment solutions was investigated under conditions more representative of the real reservoirs. For this purpose, various mixtures of synthetic gas-condensate fluids at high pressures and ambient/high temperatures were used. This stage was initially performed through a comprehensive set of contact-angle measurements, where the dependency of the chemicals' oil-repellency to the gas-condensate composition, IFT and temperature was investigated. The final stage of the experimental work conducted in this study was dedicated to evaluate the ultimate effect of the chemical treatment on gas and condensate flow properties in presence of low-IFT and high-velocity effects. This was achieved by performing a series of unique steady-state relative permeability measurements on a treated carbonate core sample. The results extracted from the laboratory measurements performed here were finally used as input data for a numerical simulation study. The aim of this simulation exercise was to scrutinize the importance

of different parameters pertaining to the reservoir and treatment process on the performance of the wettability alteration.

The overall outcomes from this research study demonstrate that underrating the crucial flow features associated with condensing fluids, would result in overestimating the performance of the chemical treatment. The new findings also provide valuable practical guidelines on design and application of such chemical stimulations for real field trials.

8.2 CONCLUSIONS

The technical content of this research work can be categorized into three main parts. First, Chapter 4 that has incorporated all the results corresponding to the preliminary screening tests using conventional fluids in order to find an optimum wettability modifier for the carbonate rock types. Second, Chapter 5 and 6, in which the performance of the treated carbonate substrates have been evaluated in presence of gas-condensate fluids through series of contact angle and steady-state relative permeability measurements. Third, Chapter 7, where the results from a simulation exercise investigating the impact of several pertinent parameters on the treatment performance have been discussed. The main findings from this thesis are discussed in the following sections.

8.2.1 Conventional Fluid Systems

In this part of the work, the conventional fluid systems, i.e. water-air and decane-nitrogen, were employed, providing quick and straightforward procedures to perform the experiments. The carbonate rock samples of Texas-Cream limestone and Baker-Dolomite outcrops were used. Series of screening tests, including contact angle measurements, free imbibition tests, unsteady-state displacements and brine compatibility tests, were conducted on four, out of fifteen, fluorinated liquid-repellent chemicals. The impact of a number of pertinent parameters was examined on the treatment performance. The most important parameters scrutinized were: chemical ionic functionality, chemical concentration, chemical delivery method, type of solvent, temperature, brine salinity and rock permeability. The corresponding investigations led to development of an optimized treatment solution for carbonate rock samples used in the rest of this study. The main conclusions drawn from the work carried out in this part are:

1. Among four different ionic groups of fluorinated chemicals tested, anionic and to lesser extent non-ionic repellent agents were the most effective wettability modifiers for the positively charged carbonate surfaces. On the contrary, cationic and amphoteric products showed week interactions with the carbonate minerals. The non-ionic compounds, compared to other fluorochemicals, demonstrated better stability in various brine salinities and compositions.
2. The likely formation of the chemical bilayers of the C-65 non-ionic fluorosurfactant at higher chemical concentrations and temperatures deteriorated the water-repellency strength of the chemical. The formation of bilayers, however, proved to be in favour of improving the chemical's oil-repellency characteristics.
3. Acceptable degree of stability in low- and high-salinity brines was observed for the C-65 non-ionic fluorosurfactant with a preserved level of oil-repellency. However, the increased level of chemical's free molecules activity due to presence of brine ions dissolved in the solution, accelerated the formation of the chemical's bilayers on the rock substrate, thereby the chemical's water-repellency strength was adversely reduced.
4. The injection of the water-based chemical solution of the C-65 non-ionic fluorosurfactant resulted in severe damage to the core permeability. The existence of the large chemical aggregates in the solution was accounted for such filtration and blocking observed at the core inlet face.
5. Promising oil- and water-repellencies (i.e. $\theta_{C10\text{-}air}$=115° and $\theta_{DIW\text{-}air}$=139°) were obtained on the carbonate surfaces treated by 0.5 wt% Z-610 anionic fluorosurfactant delivered by water at 130°C. The treatment, however, was not effective when alcohol-based carrier solvents were employed. Moreover, the excessive overreaction and deposition of the chemical molecules on the carbonate substrate was observed at elevated temperatures of 160 and 190°C.
6. The delivered amount of the chemical solution showed a crucial impact on the treatment effectiveness. That is, saturating the Texas-Cream carbonate core sample with one pore volume of Z-610 chemical solution was not sufficient to alter the rock wettability. On the other hand, a promising improvement in oil mobility by a factor of 1.6 was achieved when ten pore volume of the chemical was injected through the core.

7. The C-61 anionic fluorosurfactant was able to promisingly improve the wettability of the carbonate surfaces to intermediate gas-wetness at 130°C when delivered with both water ($\theta_{C10\text{-}air}$=100° and $\theta_{DIW\text{-}air}$=140°) and methanol ($\theta_{C10\text{-}air}$=100° and $\theta_{DIW\text{-}air}$ =120°) carrier solvents. However, the possible existence of the large chemical aggregates in the water-based solution caused a significant plugging issue at the core inlet face of the low-permeability Texas-Cream rock. The plugging became noticeably less pronounced when the alcohol-based solvent was employed. Furthermore, separating the large chemical particles from the solution prior to injection through a filtration method, proved an effective technique to reduce/eliminate the permeability impairment due to excessive chemical deposition at the core inlet face.
8. The chemical concentration played a crucial role to reach the desired level of oil-repellency within the pores. That is, the treatment with 0.5 wt% C-61 anionic fluorosurfactant delivered by methanol, improved only the water-repellency of the Baker-Dolomite (BD-18) rock, whilst an effective oil-repellency was also achieved when the treatment solution with 2 wt% of the C-61 repellent agent was employed. The corresponding treatment showed satisfactory level of durability during a long period of the high gas rate production, i.e. after more than 1000 PVs nitrogen gas at 458 m/day was injected trough the core at 130°C, the core liquid-repellency was preserved.
9. The methanol-based solvent carrying the C-61 repellent agent was able to displace the resident low-salinity brine promisingly during the BD-14a carbonate rock treatment at 130°C. This treatment resulted in the oil mobility increase by a factor of 1.6. The instability and precipitation of the chemical particles in presence of high-salinity brine resulted in rock permeability impairment by 30%; but some levels of wettability alteration were still observed.
10. Preliminary investigations on the proposed method of combining anionic and non-ionic chemicals to integrate the effectiveness of the former on carbonate surfaces with the stability of the latter in brine showed encouraging results if their concentrations or mixing ratios were selected correctly.
11. Brine composition and its salinity proved to have minimal impact on the post-treatment contact angle data (water-repellency) measured on the carbonate substrates treated by the C-61 anionic wettability modifier.

8.2.2 Gas-condensate Fluid Systems

All previously reported studies in the literature lack correct and reliable approaches to evaluate the performance of the wettability modifiers in presence of gas-condensate fluids. In this research work accurate experimental procedures were sought to characterize the flow features of the treated carbonate rocks under conditions prevailing near the gas-condensate wells. For this purpose, for the first time, static contact angle measurements using synthetic gas-condensate fluid mixtures at high pressure and in few cases high temperature were performed. The impact of the hydrocarbon molecular composition and interfacial tension on the wetting tendency of the liquid condensate was scrutinized using binary- and multi-component mixtures. The C-61 and Z-610 anionic fluorosurfactants were used to treat the Texas-Cream and Baker-Dolomite carbonate rock samples. The generality of the new findings based on the static contact angle data was further evaluated under dynamic flow conditions by performing a number of unsteady-state displacement tests. The ultimate effect of the wettability alteration was finally quantified by measuring a number of steady-state relative permeability points under varying IFT and velocity conditions. For this purpose, the BD-12 Baker-Dolomite carbonate core sample and C1-nC10 fluid mixture were employed. The main findings from these unique experimental investigations are:

Contact Angle Measurements

1. The general trend of the performed contact angle measurements on the treated carbonate substrates using binary mixtures of C1-nC10, C1-nC6 and C1-nC4 at ambient temperature (i.e. 20°C) demonstrated that the condensate wetting tendency increases as IFT decreases and/or the hydrocarbon mixture becomes lighter (i.e. the number of carbon atoms decreases). That is, the first contact of the C1-nC10 condensate drop with the treated surface resulted in θ_0=65°, 44° and 30° at IFT=10.0, 3.9 and 1.4 mN/m respectively. However, the contact angle values versus time deteriorated at lower IFT values. On the other hand, replacing the nC10 heavy-end component in the C1-nC10 binary-mixture with the nC6 and nC4 intermediate-components at almost similar IFT conditions (i.e. IFT≥10 mN/m) reduced the initial contact angle from 65° to 45° and 0°, respectively. In other words, rapid spreading of the condensate droplet on the rock surface was evident in both cases.

2. The chemical's oil-repellency characteristics were promisingly preserved at high temperatures. That is, contact angle values comparable to those attained at ambient temperature (20°C) were observed at 50 and 100°C using C1-nC10 binary-mixture at both high- and low-IFT values.
3. The type of the intermediate and heavy-end parts in the multi-component mixtures played a crucial role on the condensate wetting tendency. That is, the presence of the nC5 and nC8 intermediate components in the C1-nC5-nC8-nC10 multi-component system drastically decreased the contact angles at both high- and low-IFT limits compared to those observed for the C1-nC10 binary-mixture. Furthermore, the dominant positive impact of the nC15 heavy-end component in the C1-nC5-nC8-nC15 mixture was evident as it markedly enhanced the oil-repellency of the treated surface, i.e. high and almost stable θ_0=79° and 75° were obtained at IFTs of 1.9 and 9.7 mN/m, respectively.

Unsteady-state Displacement Tests

4. The overall results from the dynamic unsteady-sate flow tests at ambient temperature confirmed the validity of the new findings from the contact angle measurements using gas-condensate fluids. That is, for instance, whilst the oil mobility corresponding to the C1-nC4 mixture (IFT=10 mN/m) did not change after the treatment, noticeable improvement in the oil mobility (or decrease in differential pressure) was achieved when heavier hydrocarbon mixture of C1-nC10 was employed at the similar IFT conditions.
5. The unsteady-state displacement tests performed on the pre- and post-treated carbonate rock using C1-nC10 binary-mixture at 100°C demonstrated promising improvement in flow performance owing to the wettability alteration. According to the extracted relative permeability data the gas and condensate relative permeabilities increased by almost a factor of four and the trapped gas and critical condensate saturations decreased from 57% to 33% and from 25% to 4%, respectively.

Steady-state Relative Permeability Measurements

6. Following the treatment, the gas and condensate steady-state relative permeabilities at IFT of 10.8 mN/m increased considerably by a factor of 2, 3.2 and 3.6 at corresponding CGR values of 0.05, 0.1 and 0.4, respectively. The

condensate saturation or condensate blockage also substantially reduced by approximately 35-39%.

7. The reduction in condensate saturation due to treatment corresponding to the tests performed at IFT of 2.7 mN/m were almost within the same range of those observed at the higher IFT of 10.8 mN/m. Nevertheless, the improvement in relative permeability was less pronounced, i.e. kr-IF of about 1.3 was achieved at all selected CGRs.
8. The velocity-dependent relative permeability curves measured at the low IFT of 0.77 mN/m on the untreated rock sample demonstrated the dominant positive effect of coupling over inertia for a wide range of CGR from 0.03 to 0.4. Following the treatment, the effect of coupling became more evident compared to that observed in the untreated rock sample, especially at the lower CGRs of 0.03 and 0.05. Moreover, the condensate saturation in the core was also reduced favourably. However, the overall improvement in relative permeabilities was not promising as kr-IFs of 1.1 or less were obtained over the entire range of CGRs and velocities considered.
9. The overall trend of the steady-state relative permeabilities measured here, in line with the new findings from the contact angle measurements, highlighted the significant dependency of the treatment performance on the gas/condensate interfacial tension. That is, the resulting improvement in k_r due to wettability alteration gradually diminished when IFT decreased.
10. The steady-state flow tests demonstrated the most reliable technique to measure the gas/condensate relative permeabilities and accordingly to evaluate the ultimate effect of the treatment. On the other hand, it was revealed that employing the unsteady-state displacement tests can overestimate the performance of the wettability alteration, especially at low IFT conditions.

8.2.3 Simulation of Chemical Treatment

A simulation exercise on the application of chemical treatment (CT) in gas-condensate wells was carried out in this part of the work. The simulations were conducted on a synthetic single-well one dimensional radial model bearing a moderate gas-condensate fluid with 15% maximum liquid drop-out. The percentage increase in cumulative gas produced from the treated compared to the virgin untreated case, over a one-year production period, known as gas production gain (GPG), was used to evaluate the

treatment performance. A wettability alteration process with a GPG above 20% was considered as an effective treatment. First, the impact of a number of parameters pertinent to the chemical stimulation was investigated individually through single-parameter simulations. Next, the simultaneous impacts of five important parameters on well productivity were further scrutinized employing statistical approaches. For this purpose a MATLAB-based computer programme was developed employing a full-factorial experimental design in order to facilitate the design and implementation of total of 1080 multi-parameter simulation cases. The linear response surface model with (ILRSM) and without (LRSM) interaction terms was then fitted to the resulting GPGs expressing the relationship between the parameters and their level of importance in the treatment performance. The main conclusions from this simulation exercise are:

Single-parameter Simulations

1. Generally, during the post-treatment production period, the poor clean-up of the water-based treatment solution, compared to the efficient recovery of the alcohol-based solvent, adversely reduced the CT performance. The rock permeability was however an important parameter controlling the extent of the water-based solution poor recovery. That is, GPGs corresponding to the water- and alcohol-based solvents in moderate-permeability rock (k=14 mD) were 23% and 70%, respectively, whereas almost similar GPGs were obtained in the case of high-permeability rock (k=140 mD).
2. Chemical treatment (using alcohol-based carrier solvent carrying wettability modifier agents) demonstrated considerably better performance compared to that of the solvent stimulation (using only alcohol). That is, approximately stable GPGs of 50% and 80% were achieved after wettability alteration of about 1.5 and 4.9 meters around the wellbore, whereas the solvent stimulations maintained the GPG above 20% for only two weeks and five months, respectively, for almost similar stimulated radii.
3. The application of chemical treatment in mature gas-condensate wells ($P_{wbh}<<P_{dew}$) suffering from large condensate banks proved to be an effective remedial solution to improve the well productivity. Moreover, compared to the slightly depleted reservoirs with small condensate rings, stimulating a larger area around the wellbore became more crucial and sometimes necessary to gain the maximum benefit from the wettability alteration process.

Multi-parameter Simulations

4. The fitted LRSM model demonstrated that the k_r improvement factor (kr-IF) has the largest positive impact improving the productivity of the treated well (i.e. GPG). In addition, uniformity and durability of the treatment, with almost similar degree of importance, and to a lesser extent treatment radius (TR) were the next positive parameters increasing GPG. On the other hand, the permeability damage (PD) was the only negative parameter that adversely reduced the CT performance.
5. The fitted ILRSM model showed that the uniformity/kr-IF and durability/kr-IF interaction parameters were the most important interactive factors dominating the performance of the chemical treatment.
6. In the case of PDs of 20 and 30%, kr-IFs above 1.6 and 1.8 were required, respectively, to reach desirable GPGs above 20%. Moreover, the treatment, even for the highest level of kr-IF (i.e. 2), was always ineffective (i.e. GPG<20%) when PD increased above 30%.
7. At higher permeability damages, the uniformity and durability of the treatment were less important factors to improve GPG. The positive impact of these two parameters was in fact masked with the undesired increase in negative effect of permeability damage when the magnitude of two aforementioned parameters increased.
8. The positive impact of durability on the treatment performance was more pronounced at higher kr-IFs. That is, an increase in the durability from 50% (6 months) to 100% (12 months) improved GPGs corresponding to kr-IF=1.2, 1.6 and 2 by almost 8, 19 and 28%, respectively.
9. The treatment radius showed minimal impact on GPG at lower levels of kr-IFs, whereas its positive effect became appreciable for kr-IFs>1.6. Furthermore, the extent of the permeability damage when increased above 30% minimized the impact of TR over the entire range of kr-IFs.
10. When kr-IF, durability, uniformity and TR increased from their minimum to maximum levels independently, whilst other parameters were maintained at their desirable levels, GPG improved by approximately 40, 25, 20 and 10%, respectively. On the other hand, increasing PD from 0 to 50% reduced GPG by more than 50%.

8.3 RECOMMENDATIONS FOR FUTURE WORK

The work presented in this research thesis covered some important areas concerning the application of wettability alteration in carbonate gas-condensate reservoirs. The new findings from this study provide valuable insights into the practical application of chemical treatment and useful guidelines on designing more effective wettability modifiers. The author recommends that the following subjects to be further investigated in completion of the results from this research thesis:

1. The contact angle data reported in this work were measured on treated carbonate rocks with non-uniform rough surfaces, which can be subject to significant changes from one rock type to another. To better understand the impact of surface roughness on the wetting characteristics of a treated substrate it is recommended to repeat similar measurements on smooth carbonate minerals, e.g. polished calcite and marble crystals, and those with a known uniform roughness. Some primary results pertaining to this effect have been presented in Appendix B of the thesis; however wider range of experiments with different fluids and solid surfaces is required.
2. Both experimental and simulation results here highlighted more efficient performance of the alcohol-based carrier solvents compared to water-based ones. The final treatment solution developed in this work employed a methanol-based solvent. However, from the safety and environmental standpoints, it is highly recommended to investigate the potential of using more favourable alcohol solvents (e.g. isopropyl alcohol) for field applications.
3. The developed treatment solution here was effective for carbonate rocks with a permeability range between 50 to 100 mD (e.g. Baker-Dolomite rock samples), as a considerable level of permeability damages was observed for tighter rocks (e.g. Texas-Cream rock samples, k~10mD). New chemicals with more desirable molecular formulations (e.g. optimum fluorine content and lower molecular weight) should be sought for effective treatment of tighter rock samples. This would probably require modification of the solvent composition. The undesirable need for filtration of the large chemical particles used in this work can also be relaxed accordingly.
4. Here, limited numbers of binary- and multi-component synthetic gas condensate mixtures were employed during the course of contact angle measurements. It is recommended that wider range of fluid compositions and

thermodynamic conditions to be considered to further generalize the new findings of this work.

5. The steady-state relative permeability tests performed here on a treated Baker-Dolomite rock sample using C1-nC10 binary mixture are advised to be extended to a number of different fluid mixtures.
6. In this study, the steady-state flow tests when the inertia and coupling effects are competing were performed only at one IFT and selected number of velocities. To better understand the impact of wettability alteration on these two effects it is recommended to perform more steady-state flow tests at a wider range of velocities and IFTs. The impact of altered wettability on the two-phase inertia can also be further investigated during these new tests.
7. In this study, the chemical treatment simulation was conducted for a synthetic reservoir model with varying reservoir pressure using a constant improvement factor for relative permeabilities after the treatment. The inertial and coupling effects were also inactive in all conducted simulations. The experimental results of this work, however, proved the dependency of the chemical treatment performance on IFT (i.e. reservoir thermodynamic conditions). It is highly advised to evaluate the impact of chemical treatment on well productivity more reliably using the measured steady-state core data (e.g. similar to those obtained in this work). The inertia and coupling effects can also be activated accordingly.

The following subjects are also suggested for future works in this research area:

1. The clean-up of the fluids pumped into the formation during hydraulic fracturing stimulations is a challenging issue affecting the well productivity. The application of the wettability alteration technique for better clean-up of the liquids hold-up within the fracture medium can be investigated in two directions: (i) appropriate chemicals can be designed to be dissolved and carried with the fracturing fluid, altering the wettability of the stimulated regions and (ii) the propping agents can be coated with the liquid-repellent products before pumping into the fracture.
2. The chemicals used in this work were delivered into the porous medium using liquid-based carrier solvents, e.g. water or methanol. The injection of the liquid-repellent agents dispersed into the gas can also be considered as well. The gas,

compared to liquid, can penetrate longer distances across the reservoir, hence larger contact area is treated. The gas injection at high pressures and rates also favours the condensate revaporization and furthermore the negative effect associated with the solution backflow on production becomes minimal when gas is employed as a carrier fluid.

APPENDIX A

AN INTRODUCTION TO IFT AND CONTACT ANGLE PHENOMENA

A.1 PHENOMENA OF SURFACE TENSION AND CONTACT ANGLE

The molecules present in the bulk of a pure liquid medium are pulled equally in every direction by neighbouring liquid molecules, and hence experience a net force of zero. Conversely, the molecules exposed at the surface do not have neighbouring liquid molecules in all directions, resulting in a net internal force (pressure), pulling the surface molecules inward (**Figure A.1**) (Yuan and Lee, 2013). This intermolecular force, tending to contract the liquid surface area to maintain the lowest surface free energy, is called the surface tension (Erbil, 2006). Surface tension is one of the readily accessible experimental parameters corresponding to the thermodynamic state and structure of an interface (Atae-Allah, 2001).

Unlike liquids, the mobility of the surface molecules in solids is exceedingly low and hence the surface of the solids is not usually capable of adjusting to ideal equilibrium conformation manifested by the minimizing of surface free energy. This is why in practice the surface structure of most solids is largely a frozen-in record of an arbitrary past history (Erbil, 2006). According to this, to measure the surface tension of solids, the use of indirect methods is necessitated (Ebril, 2006). In this respect, the study of interaction between a solid surface and different liquids with known surface tensions provides a rather empirical method, where the phenomenon of contact angle is employed. Qualitatively, contact angle is the macroscopic representation of some microscopic characteristics such as surface roughness, surface energy and surface coatings (Stacy, 2009). Quantitatively, the contact angle, θ, is the angle between the tangent plane to the surface of the liquid and the tangent plane to the surface of the solid, at the three-phase contact point where the liquid, gas and solid intersect. Generally speaking, the contact angle is a quantitative measure of the wetting of a solid by a liquid. That is, low contact angles indicate strong liquid-solid interactions resulting

in spreading of the liquid on the solid surface, while high contact angle values indicate weak interactions at the interface and poor wetting.

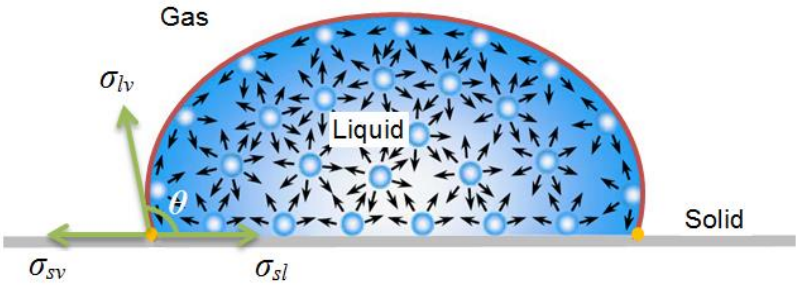

Figure A.1: 2-D schematic of a sessile liquid drop resting on a solid substrate surrounded by gas; the unbalanced forces of liquid molecules at the surface create the surface tension (red line) and the interaction between three phases at the triple contact point (yellow mark) results in contact angle.

In system of a static liquid drop resting on an ideal solid surface, the drop is in equilibrium by balancing three forces of interfacial tensions between solid-liquid (σ_{sl}), solid-vapor (σ_{sv}) and liquid-vapor (σ_{lv}) (**Figure A.1**). In such condition, the mechanical equilibrium at the three-phase intersection point, as was first derived by Young (1805), is:

$$\sigma_{sv} = \sigma_{sl} + \sigma_{lv} \cos\theta \qquad \text{(A1)}$$

Here, it should be noted that the contact angle (θ) appeared in Young's equation belongs to an ideal solid surface that is chemically homogenous, rigid, flat at an atomic scale and not perturbed by chemical interaction or by vapor or liquid adsorption. However, in reality, all solids have surface imperfections and are heterogeneous to a degree. This results in existence of many metastable states of a droplet on a solid, whereas interpreting the contact angle data in terms of Young's equation can be misleading (Ebril, 2006; Schwartz and Garoff, 1985; Gao and McCarthy, 2006). In such cases, the study of dynamic contact angles or (contact angle hysteresis) is a more appropriate approach and provides more practical information. In practice, the dynamic contact angle is measured through a contact angle test when the three-phase contact line is in actual motion by expanding or contracting the liquid, whereby the advancing (θ_a) and receding contact angles (θ_r) are produced, respectively. As a result, θ_a approaches a

maximum value and θ_r approaches a minimum value ($\theta_a > \theta_r$). The equilibrium contact angle (θ_e) also corresponds to the observed angle of a free-standing drop on the substrate under a static state. Practically, the value of θ_e is between θ_a and θ_r, but often nearer to θ_a. The static contact angle tests are generally more straightforward and less demanding to perform in comparison with dynamic contact angle tests and therefore are more commonly practiced. The contact angle data presented in this work also represent the equilibrium contact angles of a static sessile drop resting on the solid surface.

A.2 MEASUREMENT OF STATIC CONTACT ANGLE AND IFT

A.2.1 Contact Angle Measurement

The most conventional methods used for measuring the contact angles are Wilhelmy Plate, Capillary Rise and Goniometry, among which the later one is more widely employed. Goniometry uses a profile image of a drop on the surface, obtained optically, to find the contact angle parameters. There are therefore various mathematical models developed that are used for analysing the shape and geometry of the drop. These models either consider the complete drop shape, part of the drop shape or only the area of phase contact. The contact angle is then determined using the tangent to the drop interface at the 3-phase contact point, which is defined as the slope of the fitted mathematical expression to the drop profile. The most commonly used models for curve fitting purposes are general conic (ellipse) and circular section equations, which are fitted to the whole drop contour, and a polynomial function, which only models a part of the drop profile in the region of the baseline (phases contact area). In this work, the third technique, i.e. polynomial curve fitting, which is also called Tangent-2, was employed. In order to calculate the contact angle, a number of points from the contour of the drop near to the contact points are extracted, using DSA image processor software, and fitted by a quadratic polynomial equation using least square method. From the slope of the polynomial equation at the contact point of 3-phase the contact angle is determined.

Tangent-2 method can typically model the drop interface without constraints on drop volume or contact angle magnitude. Furthermore, as this technique only adapts a curve to the contact region, irrespective of the drop shape symmetry, the explicit contact angles at the left and right hand side of the contact line can be estimated (**Figure A.2**). For the same reason, this method is also suitable for dynamic contact angles, where the needle must be kept in the middle of the drop during measurement.

It should also be mentioned that the rock samples used in this work had relatively rough surfaces and moreover it is presumed that the chemical treatment of the rock surfaces is not usually performed uniformly, i.e. the chemical molecules are not proportionally bonded with the mineral particles. The presence of such surface roughness and chemical heterogeneity causes the liquid drops not to usually represent a symmetric distribution on the treated surface. From this perspective, the polynomial models, in comparison with other models, can provide a more representative value for the contact angle at the phases contact point. The disadvantage of this method is this function is just the result of numerous theoretical simulations; it is sensitive to disturbing in the contact section of drop profile that caused by contaminants or surface irregularities; and it requires an excellent image quality, especially in the region of contact section.

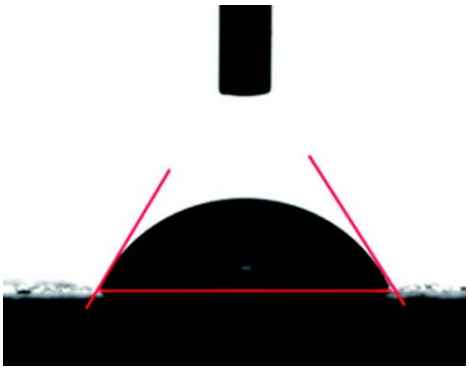

Figure A.2: Magnified snapshot of a liquid drop on the treated Texas-Cream limestone used for calculation of contact angle by use of Polynomial (Tangent-2) technique employing DSA software.

A.2.2 Calculation of IFT

The traditional methods for measuring interfacial tension between two immiscible fluids are du Noüy ring, Wilhelmy plate, capillary rise and maximum bubble pressure. The dynamic spinning drop tensiometer is also a widely used method, particularly suitable for ultra-low interfacial tension measurements. These techniques can provide accurate results but they are difficult to use and much care should be taken during the measurement process. In the recent decades, a new technique, called the drop-shape method, has been significantly developed and extensively used, taking advantages of new advances in computer systems, mathematical science and image processing. The drop shape analysis (DSA) technique is principally based on the solution of the Young-Laplace equation of capillarity. The DSA method operates by adjusting a theoretical

contour to the drop profile, from which the IFT, contact angle, drop volume, and surface area can be computed. Commonly used drops used in DSA method are the sessile drop (formed on a solid surface) and the pendant drop (hanging from a capillary tube). The DSA technique in comparison to other traditional methods only needs small quantities of liquid; it can be applied to liquid-vapour and liquid-liquid interfaces; it can be used in extreme conditions of temperature and pressure; and, moreover, the interface is not contaminated or interfered with by the system.

The Young-Laplace equation expresses the pressure difference, ΔP, across a curved interface between two homogeneous fluids under mechanical equilibrium, as a function of curvature of the surface and the surface tension. This equation, which is known as the fundamental equation of capillarity, has the following form:

$$\Delta P = \sigma \left(\frac{1}{R_1} + \frac{1}{R_2} \right) \qquad (A2)$$

where ΔP is the difference between the pressure inside and outside the interface, σ is the surface tension and R_1 and R_2 are the two principal radii of the curvature of the drop surface. The Young-Laplace equation can be applied to a sessile or pendant drop if the radii of curvature are sufficiently larger than the thickness of the interface separating two bulk phases.

The first solutions to the Young-Laplace equation were initially published in the form of tables containing the shape parameters from known values of the interfacial tension and contact angle for sessile and pendant drops (Bashforth and Adams, 1883; Fordham, 1948; Hartland and Hartley, 1976). Later, a new technique introduced by Rotenberg et al. (1983), which was relied on a numerical integration of the Young-Laplace equation in presence of gravity forces, led to considerable development of drop shape analysis for surface science without use of pre-generated tables. This method, called axisymmetric drop shape analysis (ADSA), is based on two principle assumptions: 1- the experimental drop is Laplacian and axisymmetric, and 2- gravity is the only external force. Based on this technique, surface tension is used as an adjustable parameter, whereby the best theoretical profile that fits the experimental drop profile is obtained.

Consider a sessile or pendent drop, as shown in **Figure A.3**, under equilibrium conditions. As it is noticed, the X axis is tangent to the curved interface and normal to

the axis of symmetry (Z) and the origin is placed at the apex of the drop. R_1 turns in the plane of the paper and R_2 rotates in a plane perpendicular to the plane of the paper and about the axis of symmetry. Φ is also defined as the turning angle measured between the tangent to the interface at point P(x,z) and the datum plane.

Because of the axial symmetry of the drop, the principal curvatures at the apex of the drop are the same in all directions, that is, $R_1=R_2=R_0$. Thus, the pressure difference in the apex of the drop ΔP_a can be calculated from equation A2:

$$\Delta P_a = \frac{2\sigma}{R_0} \qquad (A3)$$

From the fundamentals of hydrostatics, the following relationship applies to the pressure difference at point P(x,z) across the drop interface with respect to the pressure difference at the apex (ΔP_a):

$$\Delta P = \Delta P_a \pm \Delta\rho \mathrm{gz} = \frac{2\sigma}{R_0} \pm \Delta\rho \mathrm{gz} \qquad (A4)$$

where $\Delta\rho$ is the density difference between the drop and surrounding, g is the gravitational acceleration and z is the height above (or below) the apex. Furthermore, in above formulation, plus (+) and minus (-) operators are used for analysis of the sessile and pendant drops, respectively.

Equating Equation A4 for ΔP and the Young-Laplace equation for a curved interface (i.e. Equation A2), the following expression is obtained:

$$\sigma\left(\frac{1}{R_1}+\frac{1}{R_2}\right) = \frac{2\sigma}{R_0} \pm \Delta\rho \mathrm{gz} \qquad (A5)$$

From the geometry of the drops shown in **Figure A.3**, the local curvatures, $1/R_1$ and $1/R_2$, can be expressed in spherical coordinates by:

$$\frac{1}{R_1} = \frac{d\Phi}{ds} \qquad (A6)$$

$$\frac{1}{R_2} = \frac{\sin\Phi}{x} \qquad (A7)$$

Combining Equations A6 and A7 with Equation A5 and after some rearrangements, the following equation can be obtained:

$$\frac{d\Phi}{ds} = \frac{2}{R_0} \pm \frac{\Delta\rho g z}{\sigma} - \frac{\sin\Phi}{x} \qquad (A8)$$

Because of the symmetry in the drop shape, the interface surface can be expressed in a parametric form in the X-Z plane given by:

$$x = x(s) \quad , \quad z = z(s) \qquad (A9)$$

where the parameter s is the arc length of the drop interface measured from the origin. In this parametric representation, both x and z are only function of s. The variation of s in the differential form, from geometrical considerations, can be described as:

$$\frac{dx}{ds} = \cos\Phi \qquad (A10)$$

$$\frac{dz}{ds} = \sin\Phi \qquad (A11)$$

Equations A8, A10 and A11 form a system of first-order differential equations that define *x*, *z*, and Φ as functions of the argument *s*. For given R_0 and $\Delta\rho g/\sigma$ the complete shape of the curve for the drop interface is obtained by integrating simultaneously the differential equations under following boundary conditions existing at the apex of the drop:

$$x(0) = z(0) = \phi(0) = 0 \qquad (A12)$$

In the DSA software used to perform the IFT and contact angle measurements in this work, the following dimensionless variables are defined:

$$x_D = \frac{x}{R_0} \quad , \quad z_D = \frac{z}{R_0} \quad , \quad s_D = \frac{s}{R_0} \tag{A13}$$

This transforms the previous derived differential equations to the following dimensionless form:

$$\frac{dx_D}{ds_D} = \cos \Phi \tag{A14}$$

$$\frac{dz_D}{ds_D} = \sin \Phi \tag{A15}$$

$$\frac{d\Phi}{ds_D} = 2 \pm \beta z_D - \frac{\sin\Phi}{x_D} \quad , \quad \beta = \frac{\Delta\rho g R_0^2}{\sigma} \tag{A16}$$

Equations A14 to A16 form the fundamental equations for a pendant (or sessile) drop. The parameter β describes the shape of the drop profile and is therefore called the shape parameter. There are several optimization methods developed to fit the theoretical drop profile to the experimental measured points. In the DSA software, the robust shape comparison technique is used. This technique is a statistical method which is characterized by its stability against outliers. In this way, even low-quality drop images can still be evaluated. In this method, the comparison is not made directly via profile points, but via their vectors. An advantage of this method is that it is possible to optimize the individual parameters used independently. Following the optimization process, the interfacial tension is finally computed from the optimum values of R_0 and β.

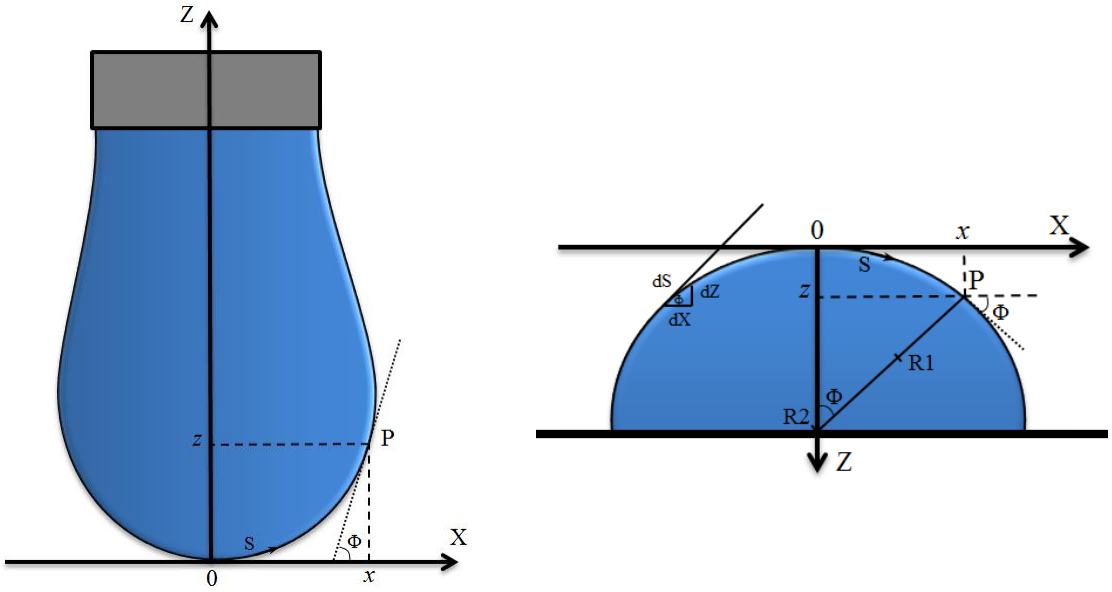

Figure A.3: Definition of co-ordinate systems for pendant (left) and sessile (right) drops using for drop shape analysis method.

A.3 REFERENCES

1. Yuan, Y. and Lee, T.R. 2013. Contact Angle and Wetting Properties. *Springer Series in Surface Sciences* 51, DOI 10.1007/978-3-642-34243-1_1.

2. Atae-Allah1, C., Cabrerizo-V´ılchez1, M., G´omez-Lopera1, J.F., Holgado-Terriza1, J.A., R. Rom´an-Rold´an1 and Luque-Escamilla, P.L. 2001. Measurement of surface tension and contact angle using entropic edge detection. *Measurement Science and Technology Journal*, 12 (2001) 288–298.

3. Erbil, H. Y. (2006). Surface Chemistry of Solid and Liquid Interfaces. Wiley-Blackwell.

4. Stacy, R. (2009). Contact Angle Measurement Technique for Rough Surfaces. MSc. thesis, Michigan Technological University.

5. Young, T. 1805. An Essay on the Cohesion of Fluids. Philos. Trans. Roy. Soc. London. 95:65-87.

6. Schwartz, L.W. and Garoff, S. (1985). Contact Angle Hysteresis on Heterogeneous Surfaces Langmuir 1 (2), 219-230.

7. Gao, L., McCarthy, T.J. (2006). Contact Angle Hysteresis Explained. Langmuir 22 (14), 6234–6237.

8. Adamson, A.W. (1997). Physical Chemistry of Surfaces. Wiley.

9. Bashforth, F. and Adams, J.C.(1883). An Attempt to Test the Theories of Capillary Action by Comparing the Theoretical and Measured Forms of Drops of Fluid. Cambridge Univ. Press, London.

10. Hartland, S. and Hartley, R.W. (1976). Axisymmetric Fluid Liquid Interfaces. Elsevier Scientific, Amsterdam/Oxford/New York.

11. Rotenberg, Y., Boruvka, L. and Neumann, A.W. (1983). Determination of surface tension and contact angle from the shapes of axisymmetric fluid interfaces. Journal of Colloid Interface Sci. 93 169-83.

12. Anderson, W.G. (1986). Wettability Literature Survey- Part 1: Rock/Oil/Brine Interactions and the Effects of Core Handling on Wettability. Journal of Petroleum Technology, 38 (10), 1125-1144.

APPENDIX B

PARAMETERS AFFECTING CONTACT ANGLE DATA

B.1 INTRODUCTION

Wettability determines the distribution of the reservoir fluids within the rock medium and therefore directly affects the flow characteristics of fluids. Contact angle measurement is used as a primary test determining the basic wetting properties of the reservoir fluids with respect to selected mineral surfaces. Reproducibility of contact angle data is significantly relied on preparation of a smooth and homogenous solid surface. However, the surfaces of pores of the reservoir rocks are generally rough and extremely complex in character because of cementation and other digenetic effects. Mixed mineral composition, pore geometry, surface roughness, adsorption effects and rearrangement or alteration of the surface by the solvent can all be considered as effective parameters controlling the wetting characteristics of the reservoir fluids (Morrow, 1975; Adamson, 1997). In the following subsections, the importance of some parameters affecting the wetting characteristics of the carbonate rock substrates and their significance for the results presented in this work are discussed.

B.2 INITIAL WETTABILITY STATE OF RESERVOIR ROCKS

Solid surfaces are usually contaminated with foreign substances during their manufacture or formation and so are the reservoir rocks. In this respect, the mineralogy of the rock surface and the chemical composition of the reservoir fluids are two important parameters that influence the rock wettability.

Shallow gas reservoirs usually contain methane gas produced by the degradation of organic matter or by the destruction of liquid hydrocarbons during the intermediate stage of the thermal history of the formations (Rice, 1980). These gases usually migrate into initially water-saturated (i.e. water-wet) formations. Because gases normally do not contain substances potential to change the hydrophilic affinity of the grain surfaces, the reservoir rocks remains water-wet after gas invasion. In deep reservoirs with a high-

temperature profile, gas could have possibly formed within the reservoir rock by the degradation of trapped liquid hydrocarbons. Furthermore, the thermal cracking of crude oil results in the formation C1 through C4 gases, hydrogen sulfide, and bitumens in carbonate reservoir rocks. If heavier oil extractions coat the pores partially or totally, the formation is rendered oil-wet (Sassen, 1988). Here it should be mentioned that the two above mentioned wettability state of gas reservoirs, i.e. water-wet and oil-wet conditions, are referred to the conventional definition for wettability where the oil and water phases are competing to wet the rock surface. However, it should be noted that these two liquid phases (i.e. water and oil) are always acting as the wetting phase with respect to the embedding gas phase. That is, because of the high surface energy of the rock surface, the liquids (in presence of gas) tend to spread on the rock substrate in order to minimize the free energy of the surface. In this respect, all rock samples used in this work are considered strongly liquid-wet in their virgin state (i.e. before chemical treatment).

B.3 EFFECT OF SURFACE ROUGHNESS

Surface roughness is defined as the ratio of real surface area to the plan (flat) area. All real solid surfaces, as discussed in Appendix A, represent some degree of surface roughness. Strictly speaking, surface roughness is also an inherent characteristic of the reservoir pores. The two common spectroscopic methods used to determine the surface roughness are Atomic Force Microscopy (AFM) and Scanning Electron Microscopy (SEM). In the field of surface science, it is believed that in addition to the surface energy, surface roughness is also an important parameter controlling the wetting characteristics of solid substrates (Wenzel, 1936; Tamai and Aratani, 1972; Anderson, 1987). For a given drop volume, the total liquid-solid interaction on a rough surface is greater than that on a flat surface. If the smooth material produces a contact angle (θ) above 90° with respect to a liquid drop, i.e. the surface shows a non-wetting state, the presence of surface roughness makes the surface more non-wet (i.e. θ increases), but if θ is less than 90°, increasing the surface roughness increases the surface wetting characteristics (i.e. θ decreases), (Wenzel, 1936; Cassie and Baxter, 1944; Johnson and Dettre, 1963).

The main body of contact angle tests performed in this work (as presented in Chapters 4 and 5) were conducted on treated substrates of carbonate rocks with non-uniform rough surfaces. Here, to provide a preliminary understanding of the impact of

surface roughness on the performance of wettability modifiers, a few contact angle tests were carried out on smooth surfaces of calcite and the results were compared with those obtained for rough surfaces of Texas-Cream (TC) limestone. For this purpose, highly smoothed single-crystals of calcite (CaCO3) were sourced from MTI Corp. The rhombus shape crystals were supremely polished bringing them to an average roughness (Ra) less than 5 Angstroms. **Figure B.1** compares the smoothed surface of a CaCO3 crystal used here with the rough surface of a TC substrate. Similar to the TC samples used in contact-angle tests discussed in Chapter 5, the calcite crystals were also treated by use of, 2 wt% C-61+MeOH anionic chemical solution at 130°C. The C1-nC10 and C1-nC4 binary gas-condensate mixtures were employed to repeat two contact angle measurement tests previously performed on TC surfaces (presented in Chapter 5) at ambient temperature (20°C) and IFT of 10 mN/m. Here, it should be noted that the smooth calcite surface like the rough surface of the carbonate rocks (Figure 3.7, Chapter 3) was strongly oil-wet before the wettability alteration, i.e. a contact angle of about 5° was measured through the decane drop deposited on the untreated calcite at ambient conditions.

Figure B.2 and **Figure B.3** depict the oil-wetting state of the treated smooth and rough surfaces with respect to two condensing systems of C1-nC10 and C1-nC4, respectively. Comparison between the contact angles of C1-nC10 drop (**Figure B.2**) on the treated smooth surface of calcite (θ=50°) and rough surface of TC limestone (θ=65°), demonstrates that lower level of oil-repellency has been achieved on the smooth surface after the wettability alteration. In other words, the surface roughness inherent in the TC rock surface has promoted the wetting tendency of the treated surface towards less oil-wet conditions. This is also in agreement with the general understanding of the impact of roughness on surface wettability, i.e. when a surface is roughened, its wetting state is increased. On the other hand, the C1-nC4 condensate drop has almost wetted both treated surfaces of smooth Calcite (θ=7°) and rough TC limestone (θ=0°), as shown in **Figure B.3**. This observation, compared with that observed for the C1-nC10 mixture, further supports and extends the generality of our new findings from the contact angle tests on the rough rock surfaces (discussed in Chapter 5), where the fluid composition showed a significant impact on the condensate wetting tendency, i.e. the lighter molecular composition the more oil-wetting characteristics.

Here, it should be mentioned that the carbonate surfaces used for measurement of contact angles in this work were those that trimmed off the outcrop samples by use of a slitting saw. Smoothing of these surfaces was then carried out by use of mechanical polishing. The overall finish of these cuts is usually flat surfaces at the macroscale (Figure 3.6, Chapter 3). However, the existence of micro pores, inherent in a deposited rock structure (Figure B.), produces some degree of roughness at the mineral surface. As discussed above, this surface roughness gives a rise to the magnitude of the measured contact angle on the treated rock surface. Furthermore, performing contact angles on such macro-flat rough surfaces of rock samples rather than very smooth surfaces of synthetic materials (e.g. calcite crystals) have more practical application, and are more representative of the actual performance of the fluorochemicals in real reservoirs.

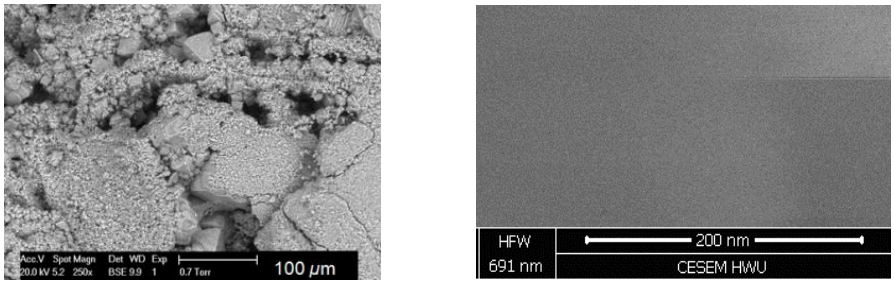

Figure B.1: ESEM images of the rough surface of the Texas-Cream limestone (left) and uniform smooth surface of the CaCO3 calcite crystal (right).

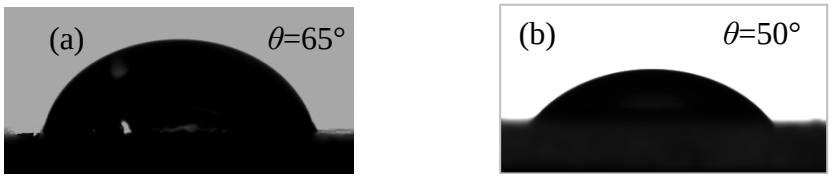

Figure B.2: C1-nC10 condensate drops on treated surfaces of the rough TC limestone (a) and smooth Calcite (b) at 20°C and IFT of 10 mN/m.

Figure B.3: C1-nC4 condensate drops on treated surfaces of the rough TC limestone (a) and smooth Calcite (b) at 20°C and IFT of 10 mN/m.

B.4 PRE-TREATMENT PREPARATION OF ROCK SUBSTRATES

Proper cleaning of the solid surfaces is essential before measurement of contact angle or dynamic flow tests. The rock surfaces should be washed with solvents, which do not dissolve the minerals but dissolve the possible contaminating materials. In this work, the outcrop carbonate samples of Texas-Cream limestone and Baker-Dolomite were employed. Generally, the outcrop samples compared with the reservoir core samples are considerably less contaminated with impurities from drilling and completion fluids and hence require less rigorous cleaning. It has been shown that mixtures or series of solvents are generally much more effective than single solvents (Grist et al., 1975; Gant and Anderson, 1988). Whilst toluene used alone is one of the least effective solvents, it becomes often very effective when combined with other solvents such as methanol or ethanol. The toluene is more effective in removing hydrocarbon residuals and weakly polar compounds, while the more strongly polar methanol or ethanol can remove brines and some other strongly adsorbed polar compounds on the rock surface. In this work, methanol or a mixture of toluene/methanol were used for washing the outcrop samples.

B.5 DECOMPOSITION AND HYDRATION OF THE CARBONATE MINERALS

The carbonate rock samples used in this work (i.e. Texas-Cream limestone and Baker Dolomite) were exposed to high temperatures at different stages of the experiments performed. That is, after each cleaning process using solvents (e.g. methanol or toluene/methanol) or wettability alteration process using chemical solutions (e.g. fluorosurfactant agents diluted in methanol or water) the rock samples were dried out inside an oven. The oven temperature during this drying stage was set between 65-100 °C. Furthermore, the chemical treatment stage (i.e. impregnating rock samples with chemical solution) was also performed at temperatures ranging between 65-190 °C. One important argument here is that whether heating up the carbonate minerals (saturated with other solutions) at the range of selected temperatures would have any influence on the molecular structure of the rock sample, for instance decomposition or hydration of the minerals; and what impact it would have on the treatment performance from a wettability perspective.

B.5.1 Decomposition

Limestone and dolomite are two common types of sedimentary carbonate rocks, which are composed predominately of the mineral calcite (CaCo3) and mineral dolomite $CaMg(CO3)_2$, respectively. The thermal decomposition of these two compounds can occur under high temperatures, where they are broken down into simpler form of substances. The corresponding reaction for the calcite follows the equation, $CaCO3(s) \rightarrow CaO(s)+CO2(g)$, while the reaction for the dolomite takes place in two distinct stages: the first is associated with the formation of magnesia (MgO) and calcite (CaCO3), and the second with the decomposition of calcite. Differential thermal analysis (DTA) curves, described in various studies, have shown that generally the thermal decomposition (or decarbonation) of dolomite and calcite minerals occur at extreme temperatures ranging between 700-950 °C (McIntosh et al., 1990; Gunasekaran and Anbalagan 2007; Rodriguez-Navarro et al., 2009). Accordingly, with respect to the range of temperatures employed in this work (i.e. 65-190 °C), it is convincing that the decomposition and structural transformation of the carbonate rock samples during heating-up or drying-out stages has not occurred.

B.5.2 Hydration

Mineral hydration is an inorganic chemical reaction where water is added to the crystal structure of a mineral. In this process, it is likely that water molecules get directly incorporated into the mineral structure. This adsorbed water (bound-water) is tightly tied to the mineral, whereby considered part of it, and hence is not free to move with the ordinary liquid pore water (free-water). The chemically bound-water is assumed not to be lost at heating up to 105 °C, whereas the free-water can be removed at much lower temperatures (Fagerlund, 2009). The presence of bound-water would have an impact on rock properties, e.g. porosity, permeability and wetting characteristics (Bush and Jenkins, 1970). During injection of a water-based chemical solution through the core or drying-out stage, both performed at high temperatures, the possible hydration of the carbonate minerals would have an undesired impact on the wetting characteristics of the treated rock. One simple, though not quite conclusive, way to understand whether such hydration process for the carbonate rocks used in this work has occurred or not is the weighing method. That is, the adsorbed water to the mineral structure after the heating process can result in an increase in the weight of the carbonate rock sample. This weighing technique was carried out for a number of carbonate rock samples treated at

different temperatures, between 65 and 130°C, using a high-precision digital balance with an accuracy of 0.0001 g. The samples were weighed before and after the chemical treatment when they were completely dry. The results showed almost negligible change in the weight of the samples, demonstrating presumably no hydration has occurred during the treatment or drying-out of the carbonate rock samples.

B.6 REFERENCES

1. Erbil, H. Y. (2006). Surface Chemistry of Solid and Liquid Interfaces. Wiley-Blackwell.
2. Adamson, A.W. (1997). Physical Chemistry of Surfaces. Wiley.
3. Anderson, W.G. (1986). Wettability Literature Survey- Part 1: Rock/Oil/Brine Interactions and the Effects of Core Handling on Wettability. Journal of Petroleum Technology, 38 (10), 1125-1144.
4. Morrow, N.R. (1975). The Effects of Surface Roughness on Contact Angle with Special Reference to Petroleum Recovery. Journal of Canadian Petroleum Technology, 14 (4), 42-53.
5. Wenzel, R. N. (1936). Resistance of slid surfaces to wetting by water. Ind. Eng. Chem., 28 (8), 988-994.
6. Tamai, Y. and Aratani, K. (1972). Experimental study of the relation between contact angle and surface roughness. J. Phys. Chem. 76 (22), 3267-3271.
7. Cassie, ABD; Baxter, S. (1944). Wettability of Porous Surfaces. Trans. Faraday Soc. 40. 546-551.
8. Johnson, R.E., and Dettre, R.H. (1963). Contact Angle Hysteresis I. Study of an Idealized Rough Surface. Adv. Chem. Ser. 43, 112-135.
9. Anderson, W. G. (1987). Wettability Literature Survey Part 4: Effects of Wettability on Capillary Pressure. J. Pet. Technol. 39 (10), 1283-1300.
10. Gant, P.L. and Anderson, W.G. (1988). Core Cleaning for Restoration of Native Wettability. SPE Formation Evaluation, 3 (1), 131-138.
11. Grist, D.M., Langley, G.O., and Neustadter, E.L. (1975). The Dependence of Water Permeability on the Core Cleaning Method in the Case of Some Sandstone Samples. Journal of Canadian Petroleum Technology, 14 (2),48-52.
12. Rice, D.D. (1980). Chemical and Isotopic Evidence of the Origins of Natural Gases in Offshore Gulf of Mexico. Trans . Gulf Coast Assn. of GSA (1980) 203-13.
13. Sassen, R. (1988). Geochemical and Carbon Isotopic Studies of Crude Oil Destruction, Bitumen Precipitation, and Sulfate Reduction in the Deep Smackover Formation. Organic Geochemistry 12 (4), 351-61.
14. Rodriguez-Navarro, C., Ruiz-Agudo E., Luque, A., Rodriguez-Navarro, and Ortega-Huertas A.B.M. (2009). Thermal decomposition of calcite: Mechanisms of formation and textural evolution of CaO nanocrystals. American Mineralogist, Volume 94, pages 578-593.
15. McIntosh, R.M., Sharp, J.H., Wilburn, F.W. (1990).The thermal decomposition of dolomite. Thermochimica Acta, 165 (2), 281-296.
16. Gunasekaran, S., and Anbalagan, G. (2007). Thermal decomposition of natural dolomite. Bull. Mater. Sci., 30 (4), 339-344.

17. Bush, D.C. and Jenkins, R.E. (1970). Proper Hydration of Clays for Rock Property Determinations. Journal of Petroleum Technology, 22 (7), 800-804.

18. Fagerlund, G. (2009). Chemically Bound Water as Measure of Degree of Hydration; Method and Potential Errors. Lund Institute of Technology, Lund University, Report TVBM-3150.